Development and evaluation of harvesting and lipid extraction processes for biodiesel production from microalgae

WANG QUAN

2020

Supervised by Prof. Masaki Takaoka

Department of Environmental Engineering, Graduate School of Engineering, Kyoto University

Abstract

Microalgae have a high growth and substance accumulating rate, and can grow 10 ~ 50 times faster than terrestrial plants. The cultivating microalgae will not occupy arable land, and has less effect on agriculture. Thus, biodiesel production from microalgae has a potential to resolve fossil fuel depletion and greenhouse gas emission by its combustion. A series of steps will be conducted from microalgae to biodiesel, such as microalgae cultivation, harvesting, drying and lipids extraction with refining, sequentially. During the process, the key is to lower energy and material cost with a positive net energy ratio. The waste water and solid produced by the process can be recovered and transferred to nutrients and energy for cultivation, which can increase the energy and material utilization efficiency. In addition, by-product (high-value products) from the biodiesel production can also improve economic benefit. In this study, we mainly focused on microalgae harvesting and lipids extraction.

Chapter 1 summarized references about the complete process of biodiesel production from microalgae including microalgae species screen, cultivation, thickening, dewatering, drying, products extraction and waste disposal. By analysing these references, the bottleneck of biodiesel production from microalgae is considered as energy and material consumption.

Chapter 2 presented flocculation of four fresh microalgae and marine microalgae by $AlCl_3$, Chitosan, ACPAM (acrylamide-methacrylic acid ester-acrylic acid copolymer) and NaOH, which represents inorganic flocculant, organic flocculant, amphoteric flocculant and auto-flocculation. The results show $AlCl_3$ can be widely applied on both fresh and marine species, while NaOH only works for marine microalgae, and chitosan is successfully applied to fresh species. As for ACPAM, just 3 fresh species can be flocculated by it. Among them, the dosage demand of chitosan is least, and demand of NaOH is highest, since pH of medium should be adjusted to > 10 for inducing auto-flocculation. Other than flocculation efficiency, settle time, CF and CST were measured for evaluating flocculation performance. The relationship between CST and PAM dosage for adjusting floc dewaterability was built up. At last, according to data from this experiment and references, LCA was utilized to screen optimal harvesting methods for the 8 species and the potential environmental effect from harvesting each specie is analysed.

Chapter 3 investigates the influence from pH, salinity, and cell density on flocculation of *Nannochloropsis oculata* by using $AlCl_3$ and chitosan as flocculants. Both independent factor experiments and response surface methodology (RSM) were designed. Results from the independent factor experiments showed $AlCl_3$ performed better under alkaline conditions, whereas chitosan had better performance at acidic condition. Salinity inhibited chitosan much more obviously than $AlCl_3$. Microalgae with higher cell density can be harvested by $AlCl_3$ without increasing dosage. But the optimal dosage of chitosan increased linearly within the cell density. RSM identified [pH][cell density] and [salinity][cell density] were interaction effects for $AlCl_3$ and [salinity][cell density] was interaction effect for chitosan. Finally, it's proved that the dual flocculant ($AlCl_3$+chitosan) achieved better FE then using of the two flocculants

individually.
Chapter 4 investigates whether or not amphoteric flocculant can be used for harvesting microalgae. Three potential influencing factors (pH, dosage, and stirring speed of intensive mixing step) are screened to mainly affect flocculation process. By RSM, significant factors including interaction effects are identified. This model from RSM was optimized by removing nonsignificant factors and applying Box–Cox transformation to significantly improve the adequacy. Thermal stability analyses by TG/DTA and XRD showed the ACPAM's stability below 100°C. However, crosslinking of ACPAM by imidization and condensation started to occur at 120°C, resulting in a lower flocculation performance. Finally, the applicability of the ACPAM for other two microalgal species was studied by comparing with $AlCl_3$ and chitosan.
Chapter 5 shows lipids extraction from sewage sludge by DME method. The influence of sludge ball size, extraction time and DME dosage on extraction was studied. By comparing with B&D method for 5 kinds sludges (3 undigested and 2 anaerobically digested sludges), the results showed B&D method could extract more raw lipids but the proportion of FAMEs by DME is twice more than B&D. Characteristic of treated sludge shows the LHV by DME are much higher than by B&D, which indicated MDE treated sludge can be used as solid fuel. And experiment of recovering and reusing DME were conducted to testify its reusability. Finally, an economic analysis was used to evaluate and compare DME, conventional solvent extraction and heating dry method.
Chapter 6 investigates a modified DME method to reduce energy consumption during lipids extraction. To extract lipids from thickened microalgae was achieved by using ethanol and acetone as entrainer to adjust miscibility of DME with water. To optimize extraction condition (extraction time, DME dosage, additive agent dosage and ratio of ethanol to acetone), the raw lipids yield, FAMEs and dewater rate were examined. Then the modified DME method was compared with B&D method and Soxhlet extraction method. The TG/DTA, FTIR and CHN was used to analysis the difference of lipids extracted by these methods. Considering the influence of trace metals in biodiesel on its utilization, ICP/MS and ICP/AES were used to qualify and quantify it in extracted raw lipids.
Chapter 7 presented the inhabitation of water content in microalgae on lipids extraction. Centrifuged and totally dried microalgae is added with pure water to make samples with certain water content. Extraction by DME for these samples were compared. We investigated improvement of cell disruption method (heating, homogenization, ultrasonic, microwave, acidification) on lipids extraction by measuring raw lipid yield, FAMEs yield, bound/free water content (by using DSC), release of intracellular components (by 3D-EEM), floc size distribution, cell wall rupture degree (by SEM), and C/H/N of residuals for evaluating LHV. The results showed heating, ultrasonic and microwave could strengthen lipids extraction but acidification and homogenization did not.
Chapter 8 summarizes conclusion from these studies, elaborates technical prospects of biodiesel production from microalgae with DEM extraction, and further works.

CONTENTS

Chapter 1 Introduction and Literature Review

1.1 Background

Microalgae is the groups of simple microscopic eukaryotic or prokaryotic photosynthetic organisms, which can be found in various body of water [1], such as fresh water (salinity < 0.05%), brackish water (salinity of 0.05 ~ 3%), Saline water (salinity of 3 ~ 5%) and brine (salinity > 5% up to 26 ~ 28% max). They are unicellular species which exist individually, or in form of multi-cellular. The cell size of the microalgae varied with species with a ranging of 5 ~ 50 μm [2]. Microalgae have a high growth rate and substance accumulating rate, and can grow 10 ~ 50 times faster than terrestrial plants [3]. These features invoke studies mainly on their application for biodiesel and high-value product.

On the one hand, energy consumption has gradually increased with the global population growing and industrial development, and it's estimated the consumption will increased from 550 EJ/a to 865 EJ/a in 2040 [4]. Since the energy consumption mainly comes from fossil fuels (petroleum, coal, and natural gas), it leads to fossil fuel depletion, greenhouse gas emission, ecological deterioration and environmental pollution [5][6][7]. The combustion of the fossil fuel emits carbon oxides, nitrogen oxides, and sulphur oxides, which cause not only global warming but also acidification and air pollution. The CO_2 concentration in atmosphere has recently exceed 400ppm (Figure 1.1) and is still increasing. If the value reaches to 450ppm, serious consequences (marine life losses by ocean acidification, great ice loss and overall surface temperature increasing) will occur [8]. Therefore, to meet the growing energy demand with less CO_2 discharge, renewable, sustainable and alternative energy is urgent to be explored for resolving the global crisis. Biodiesel is exactly one such carbon-neutral and renewable energy and has a potential to meet the increasing demand of energy consumption [9]. Initially, edible feedstock (first-generation biofuels), such as wheat, palm, corn, soya beans, sugarcane, rapeseed, oil crops, sugar beet, maize etc., are studied for the biodiesel production [10], but biodiesel from edible feedstock will compete with food supply by occupy arable land and bring about a risk of famine. Thus, the second-generation biofuels are produced from woody crops, agricultural waste, non-food crops grown on marginal land unsuitable for food production [11]. Since the process do not use arable land, it has an advantage than the first-generation biofuels. However, the biodiesel is rather difficult to be extracted, and a series of physical and chemical treatments (energy or material consumption process) are necessary [12]. Biofuels production from the microalgae is third generation. The feature of microalgae described above makes the third-generation biofuel a research hotspot. Especially, lipids in microalgae have the highest conversion efficiency of 91%, compared with oil palm of 3%, coconut of 1.5%, avocado of 1.4%, jatropha of 1.2% and rapeseed of just 1% [13].

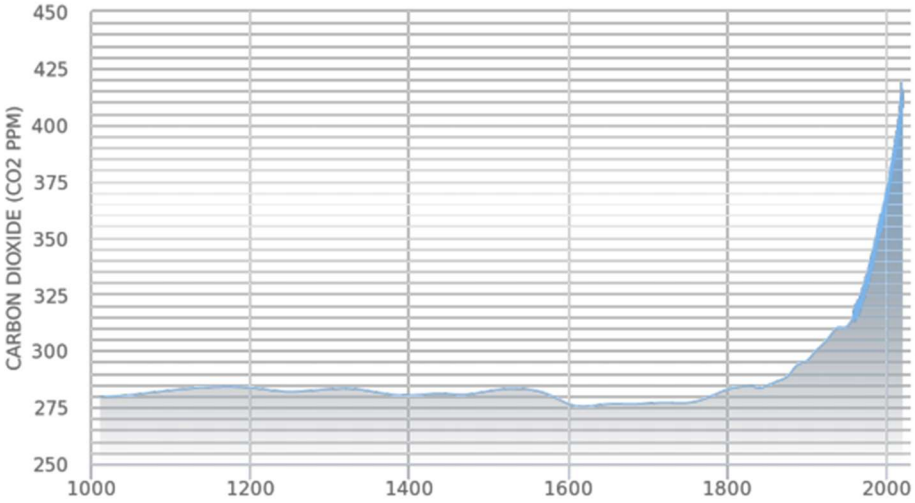

Figure 1.1 Global CO_2 Levels [8].

On the other hand, apart from a large amount of lipid, microalgae contain several high-value biomolecules. Microalgae bioreactor integrating with genetic engineering can be an attractive utilization for producing pharmaceuticals, such as hormones, enzymes, anticancer agent, vaccines, and immune regulators [14]. It's also reported that various by-product of microalgae, Carotenoids, Polyunsaturated fatty acids and food pigment, can be used as food additives, even as a high-protein supplement in human nutrition [15][16]. In addition, researches show the potential utility of microalgae in hydrating, anti-aging, sunscreen, and whitening cosmetics [17]. These multiple metabolites can be extracted from microalgae by advanced techniques, such as three-phase partitioning [18], ionic-liquid-based aqueous biphasic systems [19], membrane technologies [20], supercritical fluid extraction [21] and pressurized liquid extraction [22]. Since the high-value products are obtained along with lipid, the processes possess an economic merit. And the mixture of products needs to be separated or fractionated. Among them, proteins and polysaccharides can be precipitated and separated by using trichloro acetic acid and cold ethanol, respectively [23]. It is reported that proteins can also be separated by chromatographic methods (ion-exchange chromatography, size exclusion chromatography) [24][25]. As for pigments and lipids can be fractionated by solvent extraction [26].

Biodiesel and high value products from microalgae are composed of a series of processes as shown in the Figure 1.2. In view of different target products, microalgae species are firstly screened for high accumulation. The screened species will be cultivated in a raceway pond or photobioreactor with input of carbon dioxide, water, nutrients and light. Usually, when growth of microalgae steps into stationary phase, the microalgae enters into concentration process. Since microalgae's small cell size and low density in medium, the concentration process to pre-condense biomass concentration is necessary. Sedimentation, filtration and centrifugation are three common methods used in the microalgae concentration, and among them sedimentation is considered as the most economical one [27]. Even though a small part of microalgae can be sedimented merely by gravity, for most of microalgae flocculants are needed to

induce the sedimentation [28]. The biomass concentration of the concentrated microalgae can reach to ~2%, but it is still not enough for product extraction. Thus, a dewatering process, such as centrifugation or press filter, can be utilized to increase biomass concentration to ~ 20%. During microalgae concentration and dewatering process, separated water containing nutrients and un-harvested microalgae cells, can be recycled and reused for microalgae cultivation for cost saving. The dewatered microalgae can be directly applied to products extraction or firstly totally dried with subsequently products extracting, which is determined by extraction crafts. For some of extraction crafts, solvents used have a potential to be recovered and reused. Virous products can be extracted during this step, and refining of products is often conducted. Waste produced during the process can also be utilized. Semi-solid waste with organic components will be treated by anaerobic digestion, and obtained biogas can be used for electricity generation. Solid waste can be combusted directly, the heat generated can also be used to generate electricity. In addition, carbon dioxide emitted by the electricity generation can be considered as a carbon source for microalgae cultivation, by which reducing greenhouse gas emissions can be achieved. The above process will be explained in detail below.

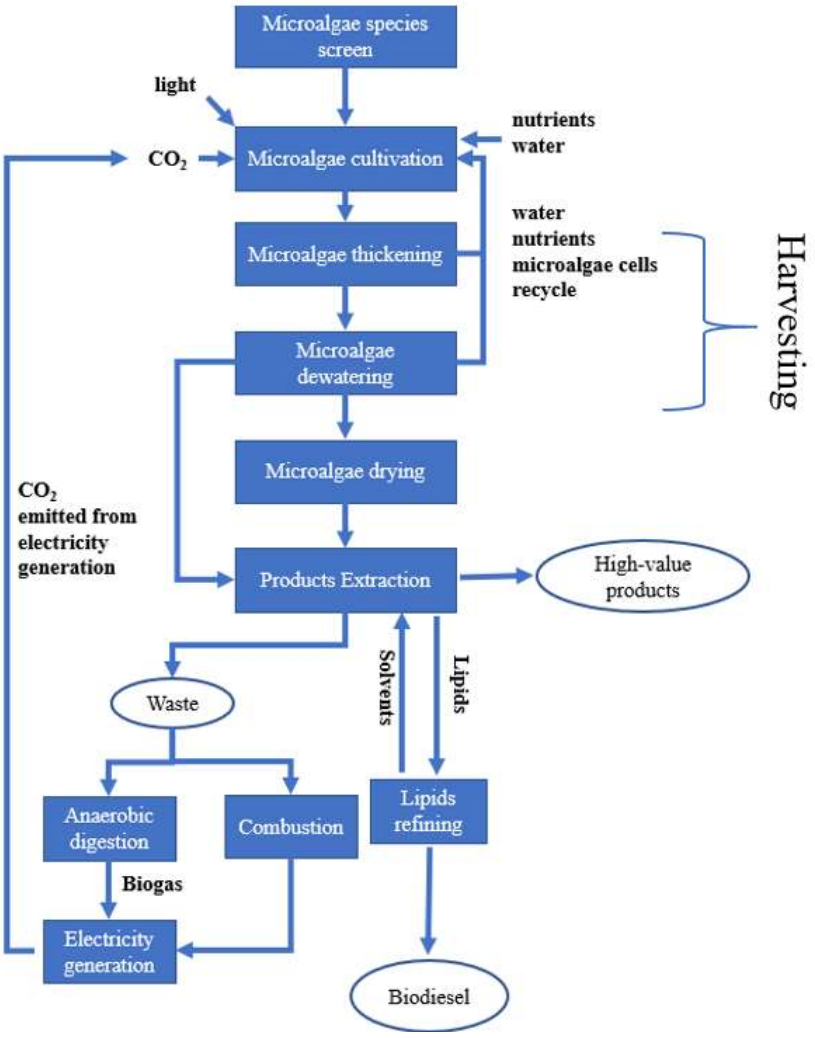

Figure 1.2 Process flow of biodiesel and high-value products production.

1.2 Microalgae species screen

Microalgae exists with various species and forms. As shown in the Figure 1.3, microalgae can be generally divided into several Phylums (green algae, brown algae, dinoflagellates, diatoms, red algae, euglenoids…), and each Phylum are further divided into several Classes, and so on. Microalgae is a huge group, morphological characteristics varied with species, and the common morphological characteristics includes Colonial, Capsoid, Coccoid, Palmelloid, Filamentous, Parenchymatous [29]. There is a big difference of accumulated products in microalgae among species. The target product content and biomass productivity are two key factors for screening microalgal species [30]. Besides, some of other factors should be considered. The species with high robustness can be easily cultivated; relatively higher CO_2 uptake and tolerance indicates the species cultivation can be improved by CO_2 aeration; capacity to be cultivated in outdoor is also important for utilization of sunlight; tolerance to a wide range of temperature determines represents the species can be cultivated in a wide range of regions and seasons; the species with higher photo conversion efficiency often have higher biomass productivity; and response to growth medium also affect the accumulation efficiency [31].

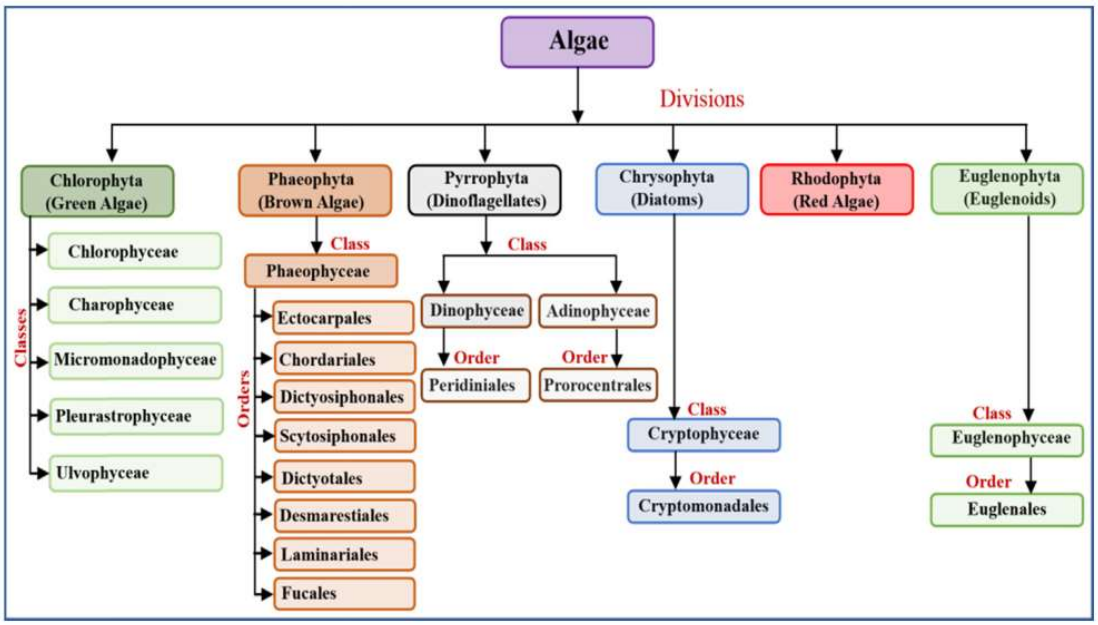

Figure 1.3 Classification of microalgae [29].

In the Table 1.1, biomass and lipids productivity of 65 microalgae species were sumarized by M.K. Enamala et al. (2018) [29]. The biomass productivity is ranged from 0.013 to 8.7 g/L*d, while most of them distributed within 0.1~0.4 g/L*d. Some species with highest biomass productivity are identified as *Chlorella protothecoides*, *Chlorella sp.*, *Chlorella emersonii*, *Botrycoccus braunii*, *Chlamydomonas reinhardtii*, *Chlorella vulgaris*, *Chlorella protothecoides*, and *Aurantiochytrium sp.*, which have a value more than 2 g/L*d. Total lipids extracted are also varied with species. *Chla. Pitschmannii*, *Chlorella vulgaris*, *Scenedesmus obliquus* and *Phaeodactylum tricornutum* are four

species with total lipids extracted more than 50% (dry base). It should be noticed that even for same specices, biomass productivity may vary with cultivation condition and lipid extraction yield may vary with extraction methods.
As for high-value products, they can be obtained from various specices. For example, phycocyanin, protein, and vitamin B_{12} can be extracted from *Arthrospira* or *Spirulina sp.*; *Chlorella sp.* can produce carbohydrate in addition to lipids; *Dunaliella salina* can produce Carotenoids and β-carotene; Carotenoids with astaxanthin can be extracted from *Haematococcus pluvialis*; *Nannochloropsis sp.*, *Phaeodactylum tricornutum* and *Nitzchia* are used to generate EPA; and polysaccharides is successfully extracted from *Porphyridium cruentum*.

1.3 Microalgae cultivation

Microalgae is naturally growth in lakes, rivers and oceans, but the biomass concentration in such place is too low to be used for production of biodiesel and other high-value products [32]. Thus, addition of nutrient into cultivation medium is required to increase the biomass concentration. Considering the high cost of chemical nutrient and its risk on the environment, organic fertilizers from solid waste and wastewater from domestic or industry effluent can be used as a substitute. In addition, cultivating microalgae in wastewater is able to remove C/N/P and improve effluent quality. As it was reported [33], 78% of soluble organic C, 89% of total nitrogen and 70% of total phosphate were removed from wastewater of soybean processing by cultivating *Chlorella pyrenoidosa* in it. It should be noticed that even though lack of some of nutrient could reduce biomass productivity, N-deprived medium had been proved to enhance accumulation of carbohydrates and lipid in microalgae cells [34]. Besides, light, temperature and pH was found to affect microalgae production [35]. The intensity of light determines the rate of microalgae growth because of its directly effect on photosynthesis rate. Cultivation of microalgae in non-optimal temperaure can result in low biomass concentration since the unsuitable temperature changes biochemical processes in cell [36]. Genrally, temperature of 20 ~ 30 °C is suitable for most of microalgae species, some thermophile species (*Anacystis nidulans* and *Chaetoceros*) can tolerate temperatures up to 40 °C, even few species grow in hot spring with a temperatures of 80 °C [36]. Different cultivation medium have different pH values, which can also affect microalgae growth, and the suitable pH range is 6 ~ 8.76 for most of species [36]. Some commonly used cultivation systems are described as following.
Open pond system. It is considered as simplest method to cultivate microalgae in the large scale as shown in the Picture 1.1 (a). Circular and raceway ponds are two typical open pond system. The circular pond is the most primitive one, and it is composed of circular-shaped tank with a diameter of ~ 45m and depth of 0.3 ~ 0.7 m, and rotating agitator was installed to mix water with microalgae [37]. The utilization of this type is very limited, since bigger pond for larger scale have stronger water resistance, and therefore causes strain on the mechanical parts of agitator, and construction cost with energy consumption is very high during the process [38][39]. Recently, raceway pond,

another open pond system which consists of several closed loop channels (depth of 0.3 m) and paddlewheel (mxing water with cells), is most frequently used. As reported, a single paddlewheel is enough for agitating 50,000 m^2 of raceway pond, which indicated its higher energy efficiency than the circular pond [40]. Sum up, the advantage of open ponds is energy and cost saving, and its disadvantages include large occupation, relatively lower biomass concentration, which is not conducive to following harvest [41]. In addition, open ponds outdoor is easily affect by rainwater casued fluctuation of water quality (turbidity, salinity and pH), and protozoa/bacteria may contaminate the medium, which is harmful to microalgae.

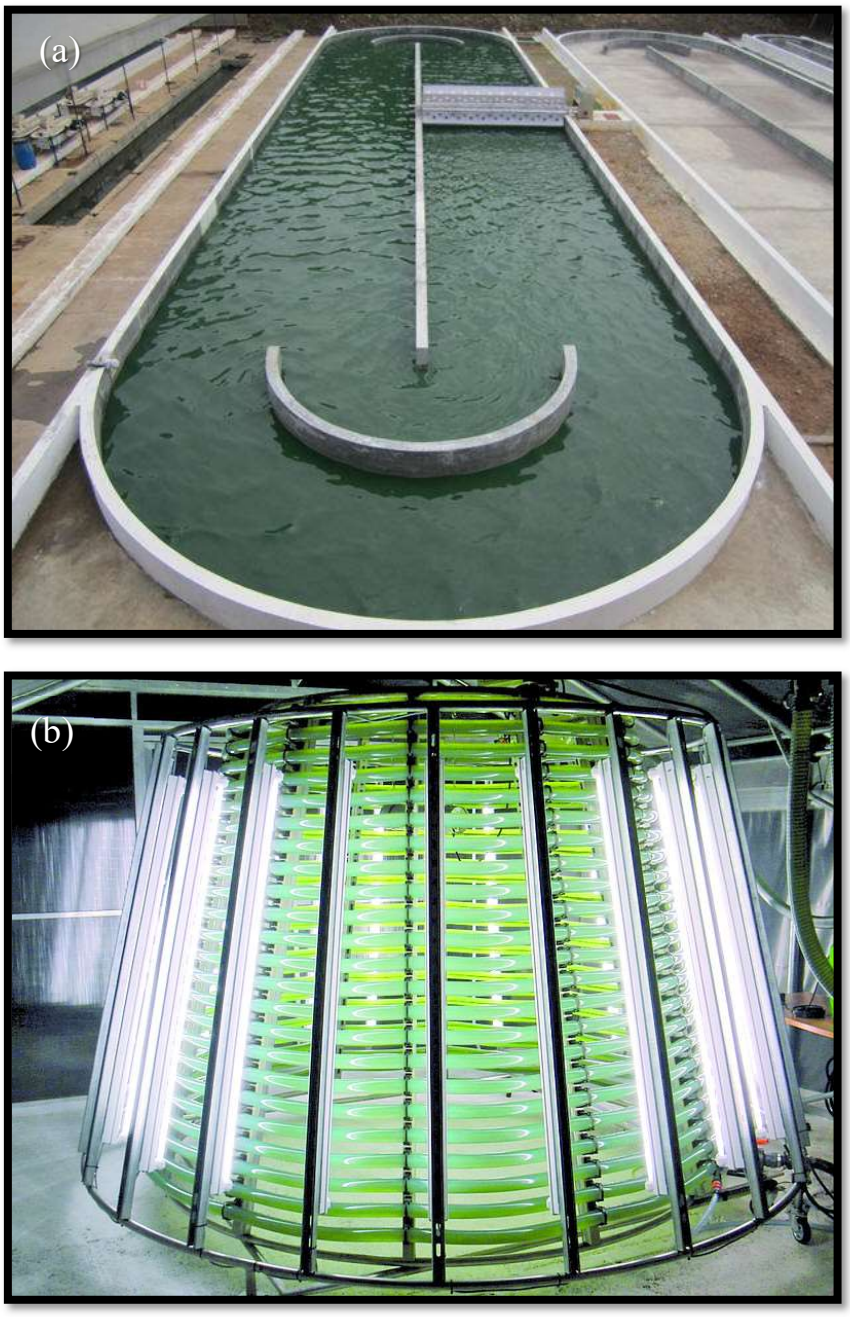

Picture 1.1 a) open pond system, b) Photobioreactor (*Aban Infrastructure Pvt. Ltd*).

Table 1.1 Biomass and lipids productivity of microalgaes [29].

Strain	Habitat	Nutrients	Biomass		Lipid	
			Biomass production (g/L/day)	yield (g/L)	Lipid production (g/L/day)	Total lipid extracted (wt% of biomass
P. carterae	Marine water	Modified f/2 medium	0.22	n.a	0.072	n.a
D. salina	Marine water	j/2 medium	n.a	n.a	0.116	n.a
Porphyridium cruentum	Marine water	n.a	0.37	n.a	0.034	9.5
Tetraselmis suecica (F&M-M33)	Marine water	n.a	0.32	n.a	0.027	8.5
Tetraselmis sp. *(F&M-M34)*	Marine water	n.a	0.3	n.a	0.043	14.7
Tetraselmis. Suecica (F&M-M35)	Marine water	n.a	0.28	n.a	0.036	12.9
Phaeodactylum tricornutum (F&M-M40)	Marine water	n.a	0.24	n.a	0.044	18.7
Nannochloropsis sp. *(F&M-M26)*	Marine water	n.a	0.21	n.a	0.061	29.6
Nannochloropsis sp. *(F&M-M27)*	Marine water	n.a	0.2	n.a	0.048	24.4
Nannochloropsis sp. *(F&M-M24)*	Marine water	n.a	0.18	n.a	0.548	30.9
Nannochloropsis sp. *(F&M-M29)*	Marine water	n.a	0.17	n.a	0.037	21.6
Ellipsoidion sp. *(F&M-M31)*	Marine water	n.a	0.17	n.a	0.047	27.4
Nannochloropsis sp. *(F&M-M28)*	Marine water	n.a	0.17	n.a	0.06	35.7
Nannochloropsis (CS 246)	Marine water	n.a	0.17	n.a	0.049	29.2
Isochrysis sp.*(CS 177)*	Marine water	n.a	0.17	n.a	0.037	22.4
Pavlova salina (CS 49)	Marine water	n.a	0.16	n.a	0.049	30.9
Pavlova lutheri (CS 182)	Marine water	n.a	0.14	n.a	0.052	35.5
Isochrysis sp. *(F&M-M37)*	Marine water	n.a	0.14	n.a	0.037	27.4
Skeletonema sp. *(CS 252)*	Marine water	n.a	0.09	n.a	0.027	31.8
Thalassiosira pseudonana (CS 173)	Marine water	n.a	0.08	n.a	0.017	20.6
Skeletonema costatum (CS 181)	Marine water	n.a	0.08	n.a	0.017	21.1
Chaetoceros muelleri (F&M-M43)	Marine water	–	0.07	n.a	0.021	33.6
Chaetoceros calcitrans (CS 178)	Marine water	n.a	0.04	n.a	0.017	39.8
Chlorococcum sp. *(UMACC 112)*	Fresh water	n.a	0.28	n.a	0.053	19.3
Scenedesmus sp.	Fresh water	n.a	0.26	n.a	0.053	21.1
Chlorella sorokiniana (IAM-212)	Fresh water	n.a	0.23	n.a	0.044	19.3
Chlorella sp. *(F&M-M48)*	Fresh water	n.a	0.23	n.a	0.042	18.7
Scenedesmus sp. *(F&M-M19)*	Fresh water	n.a	0.21	n.a	0.04	19.6
Chlorella vulgaris (F&M-M49)	Fresh water	n.a	0.20	n.a	0.369	18.4
Scenedesmus quadricauda	Fresh water	n.a	0.19	n.a	0.351	18.4

Monodus subterraneus (UTEX 151)	Fresh water	n.a	0.19	n.a	0.03	16.1
Chlorella vulgaris (CCAP 211/11b)	Fresh water	n.a	0.17	n.a	0.032	19.2
Porphyridium cruentum	Marine water	n.a	1.5	1.90	n.a	n.a
Chlorella vulgaris	Fresh water	BBM	0.020	3.2	0.002	27
Aphanothece	Fresh water	BGN	0.031	5.0	0.005	8
Dunaliella	Marine water	ESAW	0.015	2.4	0.002	17.1
Phaeodactylum	Marine water	Ukeles	0.0003	0.150	0.000	6.1
Phormidium		BGN	0.017	2.8	0.002	11.7
Scenedesmus	Fresh water	BBM	0.027	4.3	0.003	14.1
Neochloris oleabundans	Fresh water	Bristol medium	0.15	0.09	0.038	56
Chlorella sp.	Marine water	Walne's nutrient medium	n.a	1.42	0.139	26
Chlorella vulgaris	Fresh water	Basal medium	0.254	1.69	0.054	38
B. braunii	Fresh water	modified chu13 medium	0.026	n.a	0.005	25.7
C. vulgaris	Fresh water	BG11 medium	0.104	n.a	0.006	11.9
Scenedesmus sp.	Fresh water	BG11 medium	0.217	n.a	0.020	11.9
Scenedesmus obliquus	Fresh water	N-deficient culture medium	0.09	2.0	n.a	35
Chlorella vulgaris	Fresh water	N-deficient culture medium	0.18	3.0	n.a	40
Neochloris oleoabundans	Fresh water	N-deficient culture medium,	0.09	2.1	n.a	35
Spirulina maxima	Fresh water	N-deficient culture nedium	0.21	3.1	n.a	9
N. oculata (NCTU-3)	Marine water	modified f/2 medium	0.48	n.a	0.142	29.7
N. oleoabundans	Fresh water	Bristol medium	0.19	1.96	0.004	16.5
S. obliquus	Fresh water	Bristol medium	0.26	1.87	0.03	12.5
Chaetoceros muelleri (F&M-M43)	Marine water	n.a	0.07	n.a	0.021	33.6
Chaetoceros calcitrans (CS 178)	Marine water	n.a	0.04	n.a	0.017	39.8
P. tricornutum (F&M-M 40)	Marine water	n.a	0.24	n.a	0.044	18.7
Skeletonomacostatum (CS 181)	Marine water	n.a	0.08	n.a	0.017	21
Skeletonoma sp.*(CS 252)*	Marine water	n.a	0.09	n.a	0.027	31.8
Thalassioria pseudonana (CS 173)	Marine water	n.a	0.08	n.a	0.017	20.6
Chlorella sp. *(F&M-M48)*	Fresh water	n.a	0.23	n.a	0.042	18.7
Chlorella sorokiniana (IAM-212)	Fresh water	n.a	0.23	n.a	0.044	19.3
Chlorella vulgaris (CCAP 211/11b)	Fresh water	n.a	0.17	n.a	0.032	19.2
C. vulgaris (F&M-M49)	Fresh water	n.a	0.20	n.a	0.036	18.4
Chlorococcum sp. *(UMACC 112)*	Fresh water	n.a	0.28	n.a	0.053	19.3
Scenedemus quadricauda	n.a	n.a	0.19	n.a	0.035	18.4
Scenedemus (F&M-M19)	Fresh water	n.a	0.21	n.a	0.040	19.6
Scenedemus sp. *DM*	Fresh water	n.a	0.26	n.a	0.053	21.1
T. suecica (F&M-M33)	Marine water	n.a	0.32	n.a	0.027	8.5
Tetraselmis sp. *(F&M-M34)*	Marine water	n.a	0.30	n.a	0.043	14.7

T. suecica (F&M-M35)	Marine water	n.a	0.28	n.a	0.036	12.9
Ellipsoidion sp. *(F&M-M31)*	Marine water	n.a	0.17	n.a	0.047	27.4
Monodus subterraneus (UTEX 151)	Freshwater	n.a	0.19	n.a	0.030	16.1
Nannochloropsis sp. *(CS 246)*	Marine water	n.a	0.17	n.a	0.049	29.2
Nannochloropsis sp. *(F&M-M26)*	Marine water	n.a	0.21	n.a	0.061	29.6
Nannochloropsis sp. *(F&M-M27)*	Marine water	n.a	0.20	n.a	0.048	24.4
Nannochloropsis sp. *(F&M-M24)*	Marine water	n.a	0.18	n.a	0.054	30.9
Nannochloropsis sp. *(F&M-M29)*	Marine water	n.a	0.17	n.a	0.037	21.6
Nannochloropsis sp. *(F&M-M28)*	Marine water	n.a	0.17	n.a	0.060	35.7
Isochrysissp. ((T-ISO) CS 177)	Marine water	n.a	0.17	n.a	0.037	22.4
Isochrysissp. (F&M-M37)	Marine water	n.a	0.14	n.a	0.037	27.4
Pavlova salina (CS 49)	Marine water	n.a	0.16	n.a	0.049	30.9
Pavlova lutheri (CS 182)	Marine water	n.a	0.14	n.a	0.050	35.5
Porphyridium cruentum	Marine water	n.a	0.37	n.a	0.034	9.5
Chaetoceros muelleri	Marine water	n.a	0.07	n.a	0.021	33.6
Chaetoceros calcitrans	Marine water	n.a	0.04	n.a	0.017	16.4
Chlorella emersonii	Fresh water	n.a	0.041	n.a	0.050	25
Chlorella protothecoides	Fresh water	n.a	7	n.a	1.24	57
Chlorella sorokiniana	Fresh water	n.a	1.47	n.a	0.044	22
Chlorella vulgaris	Fresh water	n.a	0.20	n.a	0.04	58
Chlorella sp.	Fresh water	n.a	2.5	n.a	0.042	48
Chlorococcum sp.	Fresh water	n.a	0.28	n.a	0.53	19.3
Dunaliella salina	Marine water	n.a	0.34	n.a	0.116	25
Ellipsoidion sp.	n.a	n.a	0.17	n.a	0.047	27.4
Isochrysis sp.	Marine water	n.a	0.17	n.a	0.037	33
Monodus subterraneus	Fresh water	n.a	0.19	n.a	0.030	16
Nannochloris sp.	Marine/fresh Water/brackish	n.a	0.51	n.a	0.076	56
Nannochloropsis oculata	Brackish water	n.a	0.48	n.a	0.142	29.7
Nannochloropsis sp.	Marine/fresh Water/brackish	n.a	1.43	n.a	0.090	53
Pavlova salina	Marine water	n.a	0.16	n.a	0.049	30.9
Pavlova lutheri	Marine water	n.a	0.14	n.a	0.040	35.5
Phaeodactylum tricornutum	Marine water	n.a	1.9	n.a	0.044	57
Porphyridium cruentum	Marine water	n.a	1.50	n.a	0.034	60
Scenedesmus quadricauda	Fresh water	n.a	0.19	n.a	0.035	18.4
Scenedesmus sp.	Fresh water	n.a	0.26	n.a	0.053	21.1
Skeletonema sp	Marine water	n.a	0.09	n.a	0.027	31.8
Skeletonema costatum	Marine water	n.a	0.08	n.a	0.017	51.3

Thalassiosira pseudonana	Marine water	n.a	0.08	n.a	0.017	20.6
Tetraselmis suecica	Marine water	n.a	0.32	n.a	0.036	23
Tetraselmis sp.	Marine water	n.a	0.30	n.a	0.043	14.7
Scenedesmus sp.	Fresh water	BG 11	0.217	0.003	0.002	n.a
Botryococcus braunii	Fresh water	Modified chu13	0.026	n.a	0.005	0.005
Chlorella vulgaris	Fresh water	BG 11	0.104	n.a	n.a	0.020
Botryococcus sp.	Fresh water	n.a	0.035	n.a	0.011	n.a
Chlorella vulgaris	Fresh water	n.a	0.074	n.a	0.011	n.a
Scenedesmus sp	Fresh water	n.a	0.071	n.a	0.009	n.a
Scenedesmus sp.	Fresh water	50% BG 11	0.11	n.a	0.008	31–33
Botryococcus braunii	Fresh water	BG 11	n.a	0.037	n.a	13.5
Chlorella saccharophila	Fresh water	BG 11	n.a	0.002	n.a	18.10
Dunaliella tertiolecta	Marine water	Modified BG 11	n.a	0.038	n.a	15.20
Pleurochrysis carterae	Marine water	Modified BG 11	n.a	0.037	n.a	12
Consortium	Fresh water	BG 11	n.a	0.041	n.a	12.20
Chlorella Vulgaris	Fresh water	Artificial wastewater medium	n.a	0.69	0.147	42
Chlorella sp	Fresh water	Tris–acetate–phosphorus	0.92	1.07	0.200	n.a
Botryococcus braunii	Fresh water	Secondary domestic wastewater	0.034	0.48	n.a	36.14
T. suecica	Marine water	f/2 media	0.064	0.58	n.a	n.a
P. tricornutum	Marine water	f/2 media	0.018	0.26	n.a	n.a
C. calcitrans	Marine water	f/2 media	0.044	0.48	n.a	n.a
I. galbana	Marine water	f/2 media	0.024	0.57	n.a	n.a
N. oculata	Marine water	f/2 media	0.020	0.57	n.a	n.a
Chaetoceros muelleri (F&M-M43)	Marine water	n.a	0.07	n.a	0.021	33.6
Chaetoceros calcitrans	Marine water	n.a	0.04	n.a	0.017	39.8
P. tricornutum (F&M-M40)	Marine water	n.a	0.24	n.a	0.044	18.7
Skeletonema costatum (CS 181)	Marine water	n.a	0.08	n.a	0.017	21.0
Skeletonema sp. *(CS 252)*	Marine water	n.a	0.09	n.a	0.027	31.8
Thalassiosira pseudonana (CS 173)	Marine water	n.a	0.08	n.a	0.017	20.6
Chlorella sp. *(F&M-M48)*	Fresh water	n.a	0.23	n.a	0.042	18.7

Chlorella sorokiniana (IAM-212)	Fresh water	n.a	0.23	n.a	0.044	19.3
Chlorella vulgaris (CCAP 211/11b)	Fresh water	n.a	0.17	n.a	0.032	19.2
C. vulgaris (F&M-M49)	Fresh water	n.a	0.20	n.a	0.036	18.4
Chlorococcum sp. *(UMACC 112)*	Fresh water	n.a	0.28	n.a	0.053	19.3
Scenedesmus quadricauda	Fresh water	n.a	0.19	n.a	0.035	18.4
Scenedesmus (F&M-M19)	Fresh water	n.a	0.21	n.a	0.040	19.6
Scenedesmus sp. *DM*	Fresh water	n.a	0.26	n.a	0.053	21.1
Tetraselmis suecica (F&M-M33)	Marine water	n.a	0.32	n.a	0.027	8.5
Tetraselmis sp. *(F&M-M34)*	Marine water	n.a	0.30	n.a	0.043	14.7
T. suecica (F&M-M35)	Marine water	n.a	0.28	n.a	0.036	12.9
Ellipsoidion sp. *(F&M-M31)*	Marine water	n.a	0.17	n.a	0.047	27.4
Monodus subterraneus	Fresh water	n.a	0.19	n.a	0.030	16.1
Nannochloropsis sp. *(CS 246)*	Marine water	n.a	0.17	n.a	0.049	29.2
Nannochloropsis sp. *(F&M-M26)*	Marine water	n.a	0.21	n.a	0.061	29.6
Nannochloropsis sp. *(F&M-M27)*	Marine water	n.a	0.20	n.a	0.048	24.4
Nannochloropsis sp. *(F&M-M24)*	Marine water	n.a	0.18	n.a	0.054	30.9
Nannochloropsis sp. *(F&M-M29)*	Marine water	n.a	0.17	n.a	0.376	21.6
Nannochloropsis sp. *(F&M-M280*	Marine water	n.a	0.17	n.a	0.060	35.7
Isochrysis sp. *(T-ISO) CS 177)*	Marine water	n.a	0.17	n.a	0.037	22.4
Isochrysis sp. *(F&M-M37)*	Marine water	n.a	0.14	n.a	0.037	27.4
Pavlova salina (CS 49)	Marine water	n.a	0.16	n.a	0.049	30.9
Pavlova lutheri (CS 182)	Marine water	n.a	0.14	n.a	0.050	35.5
Porphyridium cruentum	Marine water	n.a	0.37	n.a	0.034	9.5
Scenedesmus sp. *(LX1)*	Fresh water	BG11 medium	n.a	313[a]	112[b]	n.a
Chlorella emersonii	Terrestrial	M7 medium	3.7	37.4	n.a	n.a
Botrycoccus braunii	Fresh water	M7 medium	4.6	36.1	n.a	n.a
S. obliquus (YSL02)	Fresh water	Bold basal medium	1.84	n.a	0.53	29
Chla. Pitschmannii (YSL03)	Fresh water	Bold basal medium	1.04	n.a	0.54	51
C. vulgaris (YSL04)	Fresh water	Bold basal medium	1.65	n.a	0.44	26
S. obliquus (YSL05)	Fresh water	Bold basal medium	1.71	n.a	0.48	28
Chla. Mexicana (YSL07)	Fresh water	Bold basal medium	1.53	n.a	0.45	29
C. vulgaris (2714)	Fresh water	Modified culture medium	0.39	1.17	0.16	40
Chlorella vulgaris	Fresh water	N11 medium	n.a	0.31	0.171	55
Chlamydomonas reinhardtii	Fresh water	n.a	2.0	n.a	0.505	25.25
Scenedesmus obliquus	Fresh water	n.a	0.026	n.a	0.008	31.14
Botryococcus braunii	Fresh water	n.a	0.345	n.a	0.062	17
Chlorella vulgaris	Fresh water	Kessler and czygan	0.16	n.a	0.034	30
Scenedesmus obliquus	Fresh water	Kessler and czygan	0.25	n.a	0.041	60
Ellipsoidion Parvum	Fresh water	Kessler and czygan	0.09	n.a	0.111	n.a
C. oleofaciens	n.a	BG11 medium	0.20	n.a	0.035	n.a

H. pluvialis	Fresh water	BG11 medium	0.06	n.a	0.020	n.a
B. braunii	Fresh water	BG11 medium	0.03	n.a	0.43	40
Scenedesmussp	Fresh water	TAP media	0.080	n.a	0.030	n.a
Chlamydomonas debaryana	Fresh water/ Terrestrial	B3NV media	0.051	n.a	0.005	n.a
Chlorella sorokiniana-(FGP5)	Fresh water	n.a	0.030	n.a	0.003	n.a
Nannochloropsis sp	Marine/ Freshwater	n.a	0.21	n.a	0.061	29.6
Chlorella vulgaris	Fresh water	Thin stillage (TS)	2.5	9.8	1.1	43
Chlorella vulgaris	Fresh water	Soy whey (SW)	1.6	6.3	0.2	11
Chlorella vulgaris	Fresh water	Modified basal medium	2.0	8.0	0.6	27
B. braunii (AP103)	Fresh water	Modified chu13 medium	0.114	1.8	n.a	19
T. variabilis	Brackish water	BG110	0.040	0.020	n.a	12.1
A. augstumalis	n.a	BG110	0.017	0.008	n.a	3.2
P. autumnale	n.a	Modified BG11	0.055	0.027	n.a	2.4
Nannochloropsis Oculata	Marine water	n.a	0.004	0.002	n.a	15.1
Spirulina sp	Fresh water	Zarrouk's medium	1.37	n.a	0.66	20
Chlorella sp.	Fresh water	BBM medium	1.65	n.a	0.74	26
Amphora sp.	Marine water	n.a	0.16	n.a	0.037	24
Chlorella vulgaris	Fresh water	n.a	0.46	n.a	0.079	17.3
Chlorella salina	Marine water	n.a	0.17	n.a	0.0182	11
Chlorella protothecoides	Terrestrial	n.a	0.25	n.a	0.045	18
Chlorella emersonii	Terrestrial	n.a	0.29	n.a	0.054	18.6
Scenedesmus sp.	Fresh water	n.a	0.10	n.a	0.015	16
Ankistrodesmus sp.	n.a	n.a	0.09	n.a	0.015	17.5
Chlamydomonas reinhardtii	Fresh water	n.a	0.05	n.a	0.009	18.9
D. salina (Shariati)	Marine water	n.a	0.05	n.a	0.010	18.9
Dunaliellasp	Marine water	n.a	0.12	n.a	0.025	22
D. salina (UTEX 200)	Marine water	n.a	0.15	n.a	0.036	24
Chlorella pyrenoidosa	Fresh water	Bold's basal medium	0.106	n.a	0.019	29.68

Isochrysis galbana	Marine	Enriched artificial seawater with f/2 medium	0.51	1.51	0.070	16.47
Kirchneriella lunaris	Fresh water	BG11 medium	0.293	n.a	0.008	n.a
Selenastrum capricornutum	Fresh water	BG11 medium	0.097	n.a	0.006	n.a
Staursatrum sp.	Fresh water	BG11 medium	0.078	n.a	0.000	n.a
Chlorella vulgaris	Fresh water	BG11 medium	0.225	n.a	0.007	n.a
Scenedesmus obliqnus	Fresh water	BG11 medium	0.206	n.a	0.006	n.a
Navicula sp.	Fresh water	D1 medium	0.071	n.a	0.003	n.a
Phaeodactylum tricornutum	Fresh water	f/2 medium	0.256	n.a	0.026	61.43
Batrachospermum Sirodotia	Fresh water	BG11 medium	0.049	n.a	0.001	n.a
Lyngbya kuetzingii	Fresh water	BG11 medium	0.234	n.a	0.007	n.a
Isochrysis sphacrica	Fresh water	f/2 medium	0.255	n.a	0.008	n.a
Microcystis aeruginosa (NPCD-1)	Fresh water	n.a	0.046	13.1	0.013	28
Synechococcus sp. *(PCC7942)*	Marine water	n.a	0.052	n.a	0.014	26.9
Trichormus sp. *(CENA77)*	Soil, subglacial	n.a	0.030	n.a	0.007	23.7
Chlorella protothecoides	Terrestrial	Bristol's and Wu's Media culture medium	8.7	43.3	4.32	42.3
Ettlia sp. *(YC001)*	Fresh water	BG11 Agar medium	0.19	3.10	0.080	42
Aurantiochytrium sp. *(KRS101)*	Marine water	Defined medium	6.69	31.8	n.a	38.1
Chlorella protothecoides	Terrestrial	Basal culture medium		0.5	0.015	27
Endogenous Chlorella sp	n.a	Brewery wastewater	n.a	2.7	0.052	23
Chlorella vulgaris (UTEX-265)	Fresh water	TAP medium	n.a	3.5	0.108	42
Ettliatexensis	Fresh water	Bold's basal medium	0.92	0.459	0.322	35
Synechococcus sp. *(PCC7942)*	Marine water	BG-11 liquid medium	0.124	n.a	0.35	29
Chlorella sp. *(KMN1)*	Marine water	Bold's basal medium	0.022	0.96	0.26	27.11
Chlorella sp. *(KMN2)*	Marine water	Bold's basal medium	0.016	0.79	0.24	31.52
Chlorella sp. *(KMN3)*	Marine water	Bold's basal medium	0.043	1.59	0.31	20.27
Scenedesmus sp. *(KMN4)*	Marine water	Bold's basal medium	0.023	0.92	0.25	28.63
Monoraphidium sp. *(KMN5)*	Marine water	Bold's basal medium	0.013	0.65	0.23	34.93
Chlorococcum sp. *(IMMTCC-1)*	Fresh water	Bold basal medium	n.a	n.a	2.095	8.7
Chlorella sp. *(IMMTCC-2)*	Fresh water	Bold basal medium	n.a	n.a	4.071	22.7
Scenedesmus sp. *(IMMTCC-3)*	Fresh water	Bold basal medium	n.a	n.a	2.429	11.04
Scenedesmus sp. *(IMMTCC-7)*	Fresh water	Bold basal medium	n.a	n.a	2.786	14.6
Chlorella sp. *(IMMTCC-8)*	Fresh water	Bold basal medium	n.a	n.a	1.167	6.1
Chlorella sp. *(IMMTCC-9)*	Fresh water	Bold basal medium	n.a	n.a	0.857	4.9
Micractinium sp. *(ME05)*	Fresh water	BG-11 medium	0.47	0.93	0.05	10.7
H. tetrachotoma (ME03)	n.a	BG-11 medium	0.04	0.31	0.01	8.7
Scenedesmus sp. *(ME02)*	Fresh water	BG-11 medium	0.06	0.12	0.004	12.3
Ettlia sp.	Fresh water	Sugar factory wastewater	n.a	8.02	0.96	42
I. galbana	Marine water	f/2 medium	n.a	0.001	0.013	21
P. tricornutum	Marine water	f/2 medium	n.a	0.001	0.017	28

Photobioreactor. To resolve these problem of open ponds, the photobioreactor (Picture 1.1.b) was developed to control cultivation condition for higher biomass concentration. For photobioreactor, microalgae is cultivated in an enclosed system, and the medium will not be affected by external environment. Photobioreactor has smaller size and uses less land comparing with open pond, and the enclosed structure prevents contamination. Light intensity, nutrient, temperature, pH and CO_2 can be controled, and therefore higher biomass concentration can be achieved. However, the scale of Photobioreactor is limited and its high operating costs ought to be considered [42]. Tubular, vertical column and flat-plate are three type of photobioreactors. Tubular photobioreactor [43] is a long transparent loop tubes made of glass or plastic. The microalgae is circulating in the tube with pump or air lift as power. Since mass transfer is poor in the long tube, substrate and product concentration may vary with different place. Vertical column bioreactor [44] is a series of thick cylindrical tubes with aeration for supplying carbon source and homogenization. Highly gas-liquid transfer efficiency can be obtained by this method because of large surface area of numrous small bubbles by the aeration, and its operation cost (energy) is lower than the tubular photobioreactor. But the cylindrical-shaped container is not conducive to light enters the inner layer and is harder to clean. Flat-plate photobioreactor got its name from its rectangular-shaped transparent container with depth of 1 ~ 5 cm [45]. The homogenization is realized by recirculating airlift system. The structure with largest total surface is beneficial to llumination and low oxygen condition for highest photosynthetic efficiency [46]. What needs to be improved is the aeration design to reduce its stress damage on cells.

1.4 Microalgae harvesting (thickening and dewatering)

Generally, microalgae harvesting include two steps: thickening and dewatering. Microalgae thickening is the primary step of microalgae harvesting. After the thickening, the biomass concentration of microalgae slurry can be increased to 20 ~ 70 g/L from 0.2~0.5 g/L, and the thickened microalgae is suitable for dewatering to a biomass concentration of 150 ~ 250 g/L. The harvesting methods can be divided into mechanical, chemical, biological and electrical based methods [47].

1.4.1 Centrifugation

Centrifugation using centrifugal force to displace gravity for condensing microalgae. The thickening efficiency is affected by microalgae cell size, density difference between cell with medium, centrifugation time and centrifugal speed [48]. Centrifuge can be continuous mode or batch mode, and disk stack centrifuges, decanters, hydro-cyclones, perforated basket centrifuges and imperforated basket centrifuges are common types of centrifuges. By high energy consumption, high harvesting efficiency (>90%) can be obtained. However, it was indicated that scarifying high biomass harvesting efficiency (28.5%) can save 82% of energy consumption [49]. Disc stack centrifuges can be used for harvesting microalgae without pre-concentration

(thickening) by consumption of huge amount of energy. It was estimated the energy consumed in the process accounted for 14 ~ 20% of total production cost [47]. Thus, it is usually applied to high value products other than biodiesel production because of its poor net energy ratio. Yet instead of using disc stack centrifuges for cultivated microalgae directly, using for preconcentrated ones (thickened) can improve the net energy ratio. Decanter centrifuges and solid bowl centrifuges are similar to disc stack centrifuges, by which high concentration factor can be achieved but with high energy consumption. In comparison, hydrocyclone type centrifuge can continuously harvest large amounts of microalgae with low maintenance demands. Since the concentration factor by it is relatively low, it was suggested hydrocyclone type centrifuge was suitable for preconcentrating microalgae prior to another harvesting method [50]. Even so, the energy cost by hydrocyclone is considerable, and need to be evaluated for checking net energy ratio.

1.4.2 Filtration

Filtration is a method to use membrane to separate microalgae cell from medium. Under gravity, press pressure or vacuum force, medium (water) is allowed to pass through membrane while cells are held back. Compared to centrifuge, the harvested microalgae cells are less disrupted, which prevents the loss of target products. Filtration also can be divided into continuous mode or batch mode. Some of filtration types include: according to classification of membrane pore size, ultrafiltration (0.02 ~ 0.2 μm), microfiltration (0.1~10 μm) and macrofiltration (10 μm); according to classification of hydrodynamic conditions, dead end filtration and cross-flow filtration; according to classification of source of power, vacuum filtration and pressure filtration [50][51]. The ultrafiltration and microfiltration have an ability to harvest microalgae with low cell density (cultivated microalgae), but the fouling problem caused by captured cells hindered its utilization. To solve this problem, the cross-flow filtration was explored to instead the dead-end type. In the cross-flow filtration, the microalgae liquid flows through metallic membrane at an angle parallel to it, and the water in microalgae is allowed through the porous membrane while microalgae cells are retained. Microalgae biomass concentration gradually increases with less energy input, as the it flows through the membrane [52]. The biomass concentration can reach to 50 ~ 370 g/L by cross-flow filtration. Press filtration is widely used for sludge dewatering in an industrial scale, and it was proved to successfully harvest microalgae [53]. Press filtration has the potential to dewater thickened microalgae rather than apply to the cultivated ones.

1.4.3 Coagulation and flocculation

The microalgae disperse and keep stable in the cultivation medium because of their negative charge of cell surface. The flocculants can break this stability by double layer compression, charge neutralization, sweep and adsorption and bridging, and induce aggregation with sedimentation of microalgae cells, and this process is called coagulation and flocculation. The flocculants can be inorganic or organic. The inorganic

flocculants are the agents with multivalent cations, such as aluminium sulphate, polyaluminum, ferric chloride and ferric sulphate. Generally, high multivalent salt has better flocculation performance than low multivalent salt [47]. Even though flocculation of microalgae can be easily achieved by the inorganic flocculants, some researches indicated they are not environment friendly and remnants in biomass are harmful to be as animal feed stock, and remnants in recycled cultivation medium inhibited microalgae's growth [47]. As for organic flocculants, according to carried charge of functional group, they can be divided into cationic, anionic, non-ionic and amphoteric types. Considering the negative surface charge of microalgae cell in natural conditions, cationic organic flocculant (Chitosan, cationic starch…) has been proved to successfully flocculate microalgae [54], since cationic organic flocculant can absorb on the negative surface by electrostatic force. Cationic flocculants' high charge density makes it more effective to harvest microalgae and less dosage is required than inorganic ones [55]. Several factors can affect the flocculation performance of flocculants, such as pH and salinity of medium, cell density, different microalgae species and flocculants type [47]. In general, coagulation and flocculation are mainly a microalgae thickening method for condensing biomass concentration to a value of 20 ~ 70 g/L, and usually is combined with dewatering process (centrifuge and filtration). Except flocculation induced by chemical flocculants, other coagulation/flocculation methods include auto-flocculation, electrolytic process and bio-flocculation.

Auto-flocculation. Certain microalgae can be sedimented spontaneously without any operation or just changing in nitrogen, pH and dissolved oxygen [56]. The marine microalgae can be flocculated by pH adjustment of above 10 since precipitate formation of Ca and Mg hydroxides, which can be considered as auto flocculation [47]. The flocculation efficiency by pH adjustment to alkalinity can reach to 95 ~ 98%, while decreasing the pH to 4 also can result flocculation with a flocculation efficiency of 90 ~ 95% [47]. Auto-flocculation is non-toxic, but sometimes (pH adjustment for flocculation and neutralization of the liquid) may cost a lot.

Electrolytic process. It shares the same mechanism with flocculation by flocculants. The difference is the flocculants in this method is generated by electrolytic oxidation, and then microalgae aggregates to form flocs and moves towards anode [57]. The flocculation efficiency (80 ~ 95%) of the process is affected by electrode material, current intensity, process time, medium pH and composition of medium [58][59]. The advantage includes widely application on different species, low chemical cost, no left-over anions (Cl^-, SO_4^{2-}), low energy cost than centrifugation and easy to control [60]. The disadvantages are replacement and maintenance of electrode, increase in temperature of medium, changes of medium pH and metals remnants in harvested microalgae [61].

Bio-flocculation. The process uses bio-flocculant extracted from some micro-organisms. Extracellular Polymeric Substances (EPS) from bacteria, microalgae, and fungi is type of the bio-flocculant. Extraction of EPS and addition of it for flocculation is not economic. It's better to cultivate the micro-organisms with microalgae needed to be harvested [62], if the micro-organisms are bacteria or fungi the addition of organic carbon source in medium is required. Some research has proved its flocculation

efficiency (FE) for various species, for example, 88% of FE for *Nannochloropsis oceanica*, 90~94% of FE for *Pleurochrysis carterae*, 91~95% of FE for *B. braunii*, *S. quadricauda* and *S. capricornutum*, but just 38~49% of FE for *A. flosaquae* and *M. aeruginosa* [47]. Thus, the applicability of Bio-flocculation should be investigated for other microalgae species.

1.4.4 Flotation process

The flotation used air bubbles to absorb and carry microalgae cells from bottom to top of liquid, and then the microalgae cells are collected by skimming process [63]. The method is especially suitable for the species with low specific gravity of cell to water and self-float characteristics. Its advantages include short operation time, low occupation, possible to large scale harvest and high flexibility with low initial cost. Flocculants and surfactants can improve its efficiency [47], and they make microalgae cells hydrophobic with high molecular weight and easy to adhere on the bubbles. In addition, the efficiency was affected by type of surfactant or flocculants, medium pH and salinity, type of bubble formation, recycling rate, hydraulic retention time, air tank pressure and particle floating rate [64]. It's reported that micro sized bubble with high surface area and low-rise velocity resulted high harvesting efficiency [65]. Flotation are mainly classified, depending on how to produce bubble, as 4 types as following.

Dissolved air flotation. In the method, high pressure air is dissolved in water to generate small bubbles with a size of 10 ~100 μm. The size of bubbles is important and should be controlled, since oversized bubbles will break up microalgae floc [66]. In the study of Henderson et al. (2009) [67], recover efficiency of 60, 63 and 95% were obtained by dissolved air flotation with aluminium sulphate, cationic surfactant (CTAB) and cationic polymer added respectively. The method is an energy intensive process, but energy demands and flocculant dosage can be reduced 80 and 95%, if use modified dissolved Air Flotation (Ballasted DAF).

Dispersed air flotation. The method can generate much bigger size of bubbles (700~1500 μm) by high speed mechanical agitator or passing air through porous materials [47]. Compared with DAF, this method uses less energy but more equipment investment. Among several chemicals, such as sodium dodecylsulfate (SDS), N-cetyl-N-N-N-trimethylammonium bromide (CTAB), saponin and chitosan, to improve performance of Dispersed air flotation, the CTAB is the most promising one [47]. It's reported that harvesting efficiency increases from 65.1 to 83.1% with increasing of CTAB dosage from 20 to 60 mg/L [68]. In addition, the CTAB as a surfactant can capture lipid dispersed in liquid, thus lipid recover rate by dispersed air flotation with CTAB is higher than centrifugation [69]. Therefore, the method is suitable for biodiesel from microalgae.

Electrophoresis technique. Chen et al., (2011) [57] described this method. In the process, anode produce multivalent metal ion, which flocculates the microalgae, and cathode generates hydrogen bubbles, which adsorb the formed floc and take them to the surface of water. This method can widely used on different microalgae species without addition of chemicals, but cathodes fouling and high energy consumption should be resolved.

Ozonation-dispersed flotation. Ozone can displace air to generate bubbles, and since

ozone is strong oxidizing agent, it can break up microalgae cells, then released substance from the cell lysis is able to enhance harvesting efficiency with a mechanism same as flocculant. In another hand, oxidizing of ozone bubbles oxidise and absorb soluble organic compounds in medium and make the bubbles positive charged, which is beneficial for enhancing harvesting efficiency [47]. In researches, *Chlorella vulgaris* and *Scenedesmus obliquus* has been harvested by this method with a FE of 98 and 95% [70]. In despite of these merits, the high cost and possible contamination problems of ozonation-dispersed flotation indicate it should be further investigated and ameliorated.

1.5 Microalgae drying

The microalgae drying can further reduce the water content in dewatered samples, but this process usually is not a necessary step for products extraction, since extraction can be directly conducted for the dewatered microalgae. However, drying process can provide better condition of microalgae for extraction [71], despite its extremely high energy consumption. Solar drying, oven drying, freeze drying, spray drying and fluidized bed drying are commonly used methods. During the drying, high temperature with high pressure, such as oven drying, should be taken into consideration, to prevent degradation of target products under the condition. In comparison, freeze drying using negative pressure sublimation to remove water can ensure stability of the target products [72]. The disadvantage of freeze drying is that the energy cost is higher than the oven drying. Thus, to maintain stability of products with relatively less energy a spray dryer (low-heat treatments) is often applied. Spray dryer has been widely used in pharmaceutical processing and feed processing industry. For microalgae, spray dryer has a potential to dry for high-value products, but for biodiesel production is not uneconomical. It was evaluated that energy consumption varied from 3 to 20 GJ per ton water removed with evaporation rates ranging from 0.1to 12 t/h [73]. Therefore, the biodiesel production from microalgae should give priority to extraction from dewatered samples.

1.6 Products extraction

Extraction process is the very important step to obtain products, and different extraction methods can be applied to wet microalgae (dewatered) or dry microalgae (dried). For the wet microalgae, a cell disruption to release intracellular material after dewatering process is a common step before extraction [74]. As for dry microalgae, since cell disruption has been accomplished in drying process by high temperature and water content of samples has been reduced to below 15%, sometimes additional cell disruption can be omitted [75]. Some extraction methods with cell disruption are summarized as follows.

1.6.1 Solvent Extraction

Solvent extraction is a series of traditional organic solvent-based methods used in

laboratory scale, such as Folch, Soxhlet, and Blight&Dyer method. By contacting organic solvent with microalgae, organic components in it can transfer into the solvent while residual of microalgae as waste can be separated. The polarity, lipid solubility, water miscibility, and low toxicity of solvent are research focus [76].

The Folch method [77] use chloroform and methanol as solvent with a ratio of 2:1. After solvent addition, 10 min of homogenate (by homogenizer) is conducted for mixing and cell disruption. Then 25% volume of saline solution is added with stirring, and mixture is centrifuged for layering. Lipids can be recovered by collecting solvent layer and evaporating solvent.

Soxhlet extractor [77] was designed to extract organic components from solid samples. Soxhlet extractor is composed of upper and lower two chambers, the sample is located at upper chamber while solvent in lower chamber. Then the solvent is heated to evaporation and condensation (cool water) refluxed into the upper chamber, so the solvent can contact with sample for extraction. With more and more solvent get into upper chamber, these solvent with extracted substance return lower chamber from siphon. So back and forth, the extract is enriched in the solvent of lower chamber, and the process will last for 12 ~ 24h. Generally, nonpolar solvent of hexane is used, yet some of polar solvent (ethanol, methanol, acetone...) can mix with hexane to adjust polarity of mixture for extracting different products with different polarity [78].

Blight&Dyer method [79] is similar to Folch method and usually used for lipids extraction as a benchmark for total lipid in sample. In the method, methanol, chloroform and pure water with a ratio of 2:1:0.8 are added and mixed with the dried sample. The mixture is crushed by the homogenizer for 5 min and mixed by the vortex genie for 5min. Then, chloroform and pure water of 1:1 are added into the mixture with 2 min of mixing. By centrifugation, the mixture is divided into 3 layers from top to bottom: water-methanol, microalgae and lipid-chloroform layer. After the chloroform layer was recovered, the solvent is removed and lipid can be recovered.

DME method using liquefied dimethyl ether as solvent has been proved to successfully extract lipid from various type of biomass, such as sludge, cattle manure and microalgae [95-97]. DME can be easily liquefied at 0.51~0.59 MPa at room temperature (20~25 ℃). The liquefied DME not only has a partial miscibility with water but also a high affinity to organic compounds, which makes the DME suitable for lipid extraction and simultaneous dewatering. It is hence considered as an energy saving procedure. In addition, DME (boiling point of -25 ℃) can evaporate from final product at room temperature and be recycled/reused efficiently.

1.6.2 Mechanical Methods

Milling and pressing [77] are two common methods used in industrial scale extraction without solvent addition. In the milling method, microalgae cells are disrupted by collided beads with size of 0.3 ~ 0.5 mm through shaking or agitating, and released intracellular material can be collected. Biomass concentration, flow rate, agitator movement type and speed, and temperature affect this process. The bead milling has been successfully applied on microalgae with a lipid yield of 11~ 40% [77]. Pressing is a classical method to extract various products from sources. The method uses

mechanical pressure to crush and break microalgae cells, and lipids and other products can be squeezed. For example, 91% of proteins was extracted from *Nannochloropsis sp*, 82% of phycocyanin from *Spirulina platensis*, 3.4% of astaxanthin from *Haematococcus pluvialis* and 96.2 % of lipids from *Chlorococcum infusarium* [77].

1.6.3 Freeze thaw Method

This method can freeze biomass to -80 ℃, intracellular water of microalgae cell crystallized, and expansion of the ice crystals lyses the cells after thawed. The process can decrease the loss of volatile components in biomass. To improve extraction efficiency, freeze thaw method is usually combined with ultrasonication, microwave-assisted extraction, or bead milling [80].

1.6.4 Enzymatic Methods

Enzymes can be used to disrupt microalgae cell as an alternative to mechanical disruption [81]. Since microalgae cell is consisted of polysaccharides and sac containing lipids is made of phospholipids, two enzymes (cellulase and lipase) are selected for microalgae [80]. Enzymes as a cell lysing agent to assist extraction has been reported [81], and the extraction was conducted under neutral pH and mild temperature (25 ~ 37 ℃) without drying process (energy intensive). In addition, enzymatic digestion is a method to treat and utilize the organic waste after lipids extracted for bioethanol production [82].

1.6.5 Supercritical fluid extraction

Supercritical fluid extraction (SFE) can be achieved by increasing pressure and temperature above the critical point of the solvent. Recently, using CO_2 as solvent for SFE has been studied, since its low critical point (30.9 ℃ and 73.9 bar) and non-toxicity of CO_2 [83]. Moreover, by depressurization CO_2 gasified and separated from extracts, while the CO_2 gas can be recovered for reuse, which is economic and environmental-friendly. SFE-CO_2 can selectively extract nonpolar lipids rather than phospholipids due to its non-polarity [84]. Hexane, pentane, butane, nitrous oxide, sulphur hexafluoride, and fluorinated hydrocarbons are also used as solvent for SFE.

1.6.6 Microwave-Assisted Extraction

Microwave can efficiently disrupt microalgae cells through vaporizing moisture in cells by heat combined with an electroporation effect, which results a release of intracellular materials [85]. Microwave-assisted extraction can be applied to dewatered sample without drying [86]. It's also reported that microwave can be utilized for transesterification of lipids into biodiesel [77]. It is a rapid, simple and efficient extraction method, yet high maintenance cost in industrial scale is a drawback.

1.6.7 Ultrasonic-Assisted Extraction

Ultrasound [77] can generate dense small bubbles in liquid, and these bubbles will burst violently, which results high pressures and high-speed liquid jets. And this shear forces by bubble burst disrupts the microalgae cells. Moreover, ultrasound helps solvent penetrate cell wall into internal to extract products by produced high pressure. Ultrasonic-assisted extraction can be conducted under low temperature, which is beneficial to extraction of thermally sensitive components.

1.6.8 Other methods

Hydrothermal liquefaction is a method to convert biomass into lipids rather than lipids extraction by hot compressed water within its subcritical region (200 ~ 350 ℃ with pressures of 15 ~ 20 MPa). Under the condition, biomass break down and repolymerize to lipids compounds. The method is suitable for biomass with high water content [87][88]. Osmotic pressure method is more applicable for marine microalgae, and by it suddenly changed osmotic pressure alters the movement of water passing through cell wall, then causes release of intracellular substance [89]. Pulsed electric field method uses brief pulses of a strong electric field to expand cell membrane pore size and improve their permeability, and hence the intracellular substance is released [90].

1.7 Treatment of waste from products extraction process

Waste biomass from the lipids extracted microalgae can be anaerobic digested for biogas production and nutrient remineralisation [91][92]. The produced biogas (methane) is further utilized for electricity generation, and it's estimated 9,360 MJ energy can be recovered from 1-ton lipids extracted microalgae [93]. The factors influencing biogas production includes microalgae species, waste biomass compositions and anaerobic digestion condition. The different species has different composition, and some of them can secrete some extracellular substances which can inhibit activity of anaerobic bacterial; the upstream process, especially lipids extraction with cell disruption, can improve digestion efficiency [94]. In addition, after lipids extraction, the C/N ration of residual biomass will decrease, since lipids extraction take away carbon while leave nitrogen. The low C/N ration may cause ammonia production during the anaerobic digestion, which will in turn inhibit digestion. Thus, before anaerobic digestion the C/N ration of waste microalgae should be checked and high carbon organics could be added to adjust the C/N ration. The residuals from anaerobic digestion containing phosphorus and nitrogen can also be used as fertilizer.
Fermentation [94] is another approach to utilize the lipids extracted microalgae. The main product from the fermentation is bioethanol (ethanol and methane), and fermentation treated waste can be further degraded by anaerobic digestion as described above. In the fermentation, the cell way should be firstly disrupted to release polysaccharides and carbohydrates, and lipid extraction process usually involve such cell disruption step, which make the lipids extracted microalgae to be employed without

additional pre-treatment or little pre-treatment.
Combustion of the waste microalgae from lipids extraction of dimethyl ether (DME) [95] method is possible. Since the DME method can extract lipid with simultaneous dewatering, the water content of waste microalgae is reduced from ~ 80% to ~ 50% with a positive value of LHV, which indicated the waste has a potential to be incinerated for electricity generation.
The biodiesel production process consumes considerable energy and material, and the waste treatment process is not only for waste disposal but also for recovering energy and nutrients, which is important section to minimize cost and maximize net energy ratio.

1.8 Research Objectives

In this study, to solve the problem of CO_2 emission and fossil fuel depletion, biodiesel production from microalgae were studied. Considering the majority of consumption during the process is occurred in microalgae harvesting/drying and lipid extraction, this study focused on flocculation of microalgae and lipid extraction by the DME method. The consumption should be minimized and net energy ratio should be improved. Besides, the lipid extraction from microalgae by DME was seldom studied, so we started from lipid extraction by DME using sludge as biomass, and the obtained results can guide the microalgae as biomass. With an objective of low energy and material consumption, the details of this study are as follows.

1) To evaluate flocculation performance of different flocculants on various microalgae species. Four fresh water microalgae and four marine water microalgae were flocculated by aluminium chloride, Chitosan, amphoteric Polyacrylamide and pH adjustment (by HCl and NaOH). According to the flocculation experiments, LCA was used to compare the different microalgae species with different harvesting methods. The LCA mainly examined energy consumption, greenhouse gas and eutrophication emission potential on environment.
2) To evaluate the effects of three key factors, pH, cell density, and salinity, on the FE of two common flocculants ($AlCl_3$ and chitosan). The independent influences of each variable were investigated using single-factor experiments, and RSM) was then applied to explore their interactions. Finally, the flocculation performance of a combination of chitosan and $AlCl_3$ under different conditions was investigated.
3) To investigate whether or not the amphoteric flocculant can be used for microalgae flocculation. A typical amphoteric flocculant (ACPAM) was chosen to harvest the common freshwater microalgae *Coccomyxa sp. KJ*. The RSM was utilized to optimize operation condition of ACPAM.
4) To compare with lipids extraction form microalgae and swedge sludge, swedge sludge by DME method was firstly investigated. A fixed-bed extraction apparatus was used to determine the optimal sludge ball size, extraction time, and DME to sludge ratio. And the DME method was compared with traditional Bligh and Dyer (B&D) methods. Based on experimental data, an economic analysis was conducted.
5) To reduce energy cost during lipid extraction, a novel extraction method (modified

DME method) without requirement of sample dewatering was explored. Entrainer for DME was screened from several solvents. The effect of extraction time, dosage of DME, proportion of entrainer in DME and ratio of two screened entrainer on extraction performance were investigated. The method was then compared with Bligh&Dyer and Soxhlet extraction methods.

6) To study effect of microalgae property on lipids extraction, samples with different water content were tested for DME method. To improve lipids yield, cell disruption methods were conducted on flocculated microalgae, and their enhancement on lipids yield was confirmed.

1.9 Structure of the dissertation

This dissertation consists of eight chapters. The main analysis is from chapter 2 to chapter 7, which contain microalgae harvesting (flocculation and dewatering) and lipids extraction from it. The chapter 2 was firstly studied, and big difference of FE among flocculants and species was observed, thus studying mechanism to clarify it in chapter 3 was necessary and helped to instruct the use of flocculants under different condition. In addition, in chapter 2 showed flocculation performance of amphoteric flocculant, which was not reported by others. So, further research in chapter 4 was conducted to confirm its application and the method to optimize flocculation condition. The lipid extraction part was stared from chapter 5, in which lipid extraction from sludge by DME was studied to compare and instruct research on microalgae (chapter 6 and 7). The two chapters investigated lipid extraction from liquid microalgae and improvement of cell disruption on the DME method. Totally, the structure of this dissertation is illustrated in the Figure 1.4.

Chapter 1 summarized literature relating to biodiesel production from microalgae. It consists of microalgae species screen, cultivation, thickening, dewatering, drying, products extraction and waste treatment. For each step, several techniques are illustrated and compared. By analysing these references, my study mainly focuses on how to reduce energy and material cost during the process.

Chapter 2 presents flocculation performance of $AlCl_3$, Chitosan, ACPAM and NaOH for 8 microalgae species. $AlCl_3$ showed a wide application for both fresh and marine microalgae. Addition NaOH can only flocculate marine microalgae and chitosan successfully applied to fresh species with lest dosage demand. As for ACPAM, it flocculated 3 fresh species. The settle time, CF and CST were measured. And the CST was used to evaluate PAM demand in dewatering (press filter) by a model. At last, LCA was utilized to screen optimal harvesting methods for the 8 species.

Chapter 3 investigates the effects of pH, salinity, and cell density on harvesting of *Nannochloropsis oculata* cells by using $AlCl_3$ and chitosan through independent factor experiments and response surface methodology (RSM). And $AlCl_3$ performed better under alkaline conditions, whereas chitosan showed better performance at acidic pH. Salinity had little influence on t $AlCl_3$, by contrast, increasing salinity reduced the FE of chitosan. As cell density increased, the optimal dosage of $AlCl_3$ increased to a constant. But the optimal dosage of chitosan increased linearly within the studied cell

density range. RSM showed interaction effects of [pH][cell density] and [salinity][cell density] for $AlCl_3$ and [salinity][cell density] for chitosan. Finally, higher FE could be achieved with lower dosages of the dual flocculant compared with use of the two flocculants individually.

Chapter 4 uses RSM to investigate the flocculation performance of an amphoteric flocculant for harvesting microalgae. Three potential influencing factors (pH, dosage, and the stirring speed of an intensive mixing step, ω1) are screened. By RSM, ω_1, dosage, [ω_1][ω_1], [dosage][dosage], and [ω_1][dosage] are identified as significant factors. This model was optimized by removing nonsignificant factors and applying Box–Cox transformation, both of which significantly improved the adequacy of the model. Thermal stability analyses showed that the ACPAM was generally stable below 100°C with some weight loss caused by moisture evaporation. However, crosslinking of its molecules by imidization and condensation started to occur at 120°C, resulting in a lower flocculation performance. Finally, the applicability of the ACPAM was studied by comparing its FE to other flocculants ($AlCl_3$ and chitosan) for harvesting other two microalgal species.

Chapter 5 shows Liquefied DME can extract lipid from sewage sludge. The influence of different variables on extraction is studied. The DME method was compared with Bligh and Dyer method (B&D) for 5 kinds of dewatered sludges from 3 undigested and 2 anaerobically digested sludges. Bligh-dyer method averagely extracted more raw lipids than DME, yet the proportion of FAMEs by DME is twice as much as B&D. Characteristic of treated sludge shows the LHV by DME are much higher than by B&D. And recovery and reuse of DME experiment are conducted to testify reusability of DME. Finally, an economic analysis was used to evaluate DME, conventional solvent extraction and heating dry method.

Chapter 6 investigates a modified DME method to reduce energy consumption during lipids extraction. It was achieved through using DME as solvent with entrainer (ethanol and acetone). The extraction condition (extraction time, DME dosage, additive agent dosage and ratio of ethanol to acetone) are investigated. Then the raw lipids yield and FAMEs by the DME method was compared with B&D method and Soxhlet extraction method. The TG/DTA, FTIR and CHN was used to analysis the difference of lipids extracted by these methods. Considering the influence of trace metals in biodiesel on its utilization, ICP/MS and ICP/AES were used to qualify and quantify the trace metals in the extracted raw lipids.

Chapter 7 studies the inhabitation of water content in microalgae on its lipids extraction. Microalgae is firstly harvested by centrifugation and dried in oven; the dry samples are then added with pure water to certain water content. Extraction performance (DME) of these samples with different water content are evaluated. The improvement of cell disruption method (heating, homogenization, ultrasonic, microwave, acidification) on lipids extraction is investigated referring to a comparison of raw lipid yield, FAMEs yield, bound/free water content (by using DSC), release of intracellular components (by 3D-EEM), floc size distribution, cell wall rupture (SEM), C/H/N for calculating LHV of combustion. Among these 5 cell disruption methods, heating, ultrasonic and microwave shows the obvious enhancement on DME method.

Chapter 8 summarizes conclusion from these studies, elaborates technical prospects of biodiesel production from microalgae with DEM extraction, and further works.

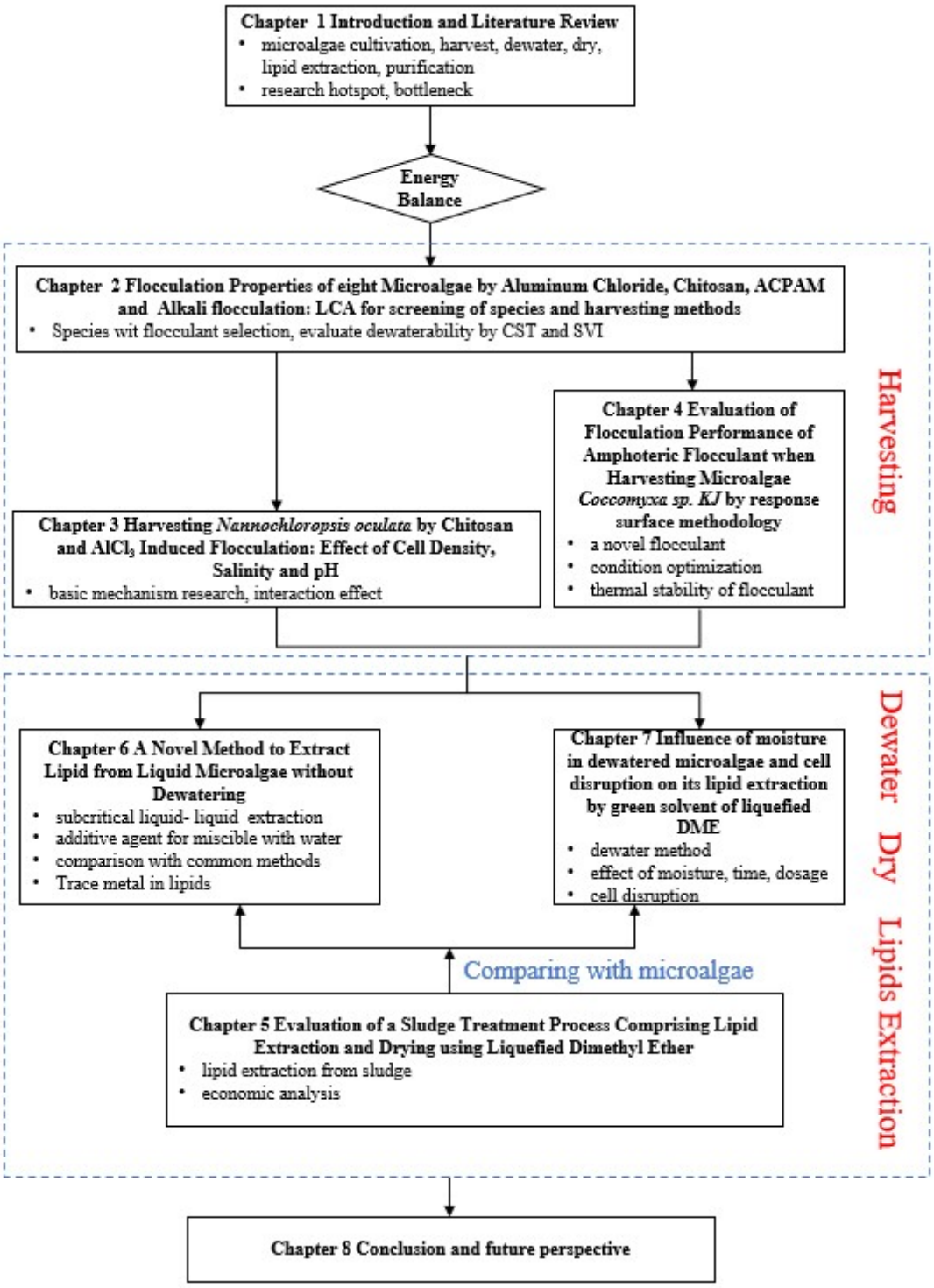

Figure 1.4 The structure of the doctoral dissertation.

References

[1] Thurman, H. V., & Burton, E. A. (1997). Introductory oceanography. New York: Prentice Hall.

[2] Zhu, L., Li, Z., & Hiltunen, E. (2018). Microalgae Chlorella vulgaris biomass harvesting by natural flocculant: effects on biomass sedimentation, spent medium recycling and lipid extraction. Biotechnology for biofuels, 11(1), 183.

[3] Ho, S. H., Kondo, A., Hasunuma, T., & Chang, J. S. (2013). Engineering strategies for improving the CO_2 fixation and carbohydrate productivity of Scenedesmus obliquus CNW-N used for bioethanol fermentation. Bioresource technology, 143, 163-171.

[4] Creasey, J. J., Chieregato, A., Manayil, J. C., Parlett, C. M., Wilson, K., & Lee, A. F. (2014). Alkali-and nitrate-free synthesis of highly active Mg–Al hydrotalcite-coated alumina for FAME production. Catalysis Science & Technology, 4(3), 861-870.

[5] Yin, Z., Zhu, L., Li, S., Hu, T., Chu, R., Mo, F., ... & Li, B. (2020). A comprehensive review on cultivation and harvesting of microalgae for biodiesel production: environmental pollution control and future directions. Bioresource Technology, 122804.

[6] Okoro, V., Azimov, U., Munoz, J., Hernandez, H. H., & Phan, A. N. (2019). Microalgae cultivation and harvesting: Growth performance and use of flocculants-A review. Renewable and Sustainable Energy Reviews, 115, 109364.

[7] Mathimani, T., & Mallick, N. (2018). A comprehensive review on harvesting of microalgae for biodiesel–Key challenges and future directions. Renewable and Sustainable Energy Reviews, 91, 1103-1120.

[8] Cameron, G., Aguirre, E., Mutnuri, M., & Liu, A. (2019). Multiple Regression Analysis: Atmospheric CO_2 Concentration. researchgate.net.

[9] Zhu, L., Nugroho, Y. K., Shakeel, S. R., Li, Z., Martinkauppi, B., & Hiltunen, E. (2017). Using microalgae to produce liquid transportation biodiesel: what is next?. Renewable and Sustainable Energy Reviews, 78, 391-400.

[10] Maity, J. P., Bundschuh, J., Chen, C. Y., & Bhattacharya, P. (2014). Microalgae for third generation biofuel production, mitigation of greenhouse gas emissions and wastewater treatment: Present and future perspectives–A mini review. Energy, 78, 104-113.

[11] Naik, S. N., Goud, V. V., Rout, P. K., & Dalai, A. K. (2010). Production of first and second generation biofuels: a comprehensive review. Renewable and sustainable energy reviews, 14(2), 578-597.

[12] Bindra, S., Sharma, R., Khan, A., & Kulshrestha, S. (2017). Renewable energy Sources in different Generations of Bio-fuels with special Emphasis on Microalgae Derived Biodiesel as Sustainable industrial fuel Model. Biosciences Biotechnology Research Asia, 14(1), 259-274.

[13] Mata, T. M., Martins, A. A., & Caetano, N. S. (2010). Microalgae for biodiesel production and other applications: a review. Renewable and sustainable energy reviews, 14(1), 217-232.

[14] Yan, N., Fan, C., Chen, Y., & Hu, Z. (2016). The potential for microalgae as

bioreactors to produce pharmaceuticals. International journal of molecular sciences, 17(6), 962.
[15] Sathasivam, R., Radhakrishnan, R., Hashem, A., & Abd_Allah, E. F. (2019). Microalgae metabolites: A rich source for food and medicine. Saudi journal of biological sciences, 26(4), 709-722.
[16] Begum, H., Yusoff, F. M., Banerjee, S., Khatoon, H., & Shariff, M. (2016). Availability and utilization of pigments from microalgae. Critical reviews in food science and nutrition, 56(13), 2209-2222.
[17] Couteau, C., & Coiffard, L. (2018). Microalgal application in cosmetics. In Microalgae in health and disease prevention (pp. 317-323). Academic Press.
[18] Zhao, W., Duan, M., Zhang, X., & Tan, T. (2018). A mild extraction and separation procedure of polysaccharide, lipid, chlorophyll and protein from Chlorella spp. Renewable Energy, 118, 701-708.
[19] Santos, J. H., Trigo, J. P., Maricato, E., Nunes, C., Coimbra, M. A., & Ventura, S. P. (2018). Fractionation of Isochrysis galbana Proteins, Arabinans, and Glucans Using Ionic-Liquid-Based Aqueous Biphasic Systems. ACS Sustainable Chemistry & Engineering, 6(11), 14042-14053.
[20] Giorno, F., Mazzei, R., & Giorno, L. (2013). Purification of triacylglycerols for biodiesel production from Nannochloropsis microalgae by membrane technology. Bioresource technology, 140, 172-178.
[21] Canela, A. P. R., Rosa, P. T., Marques, M. O., & Meireles, M. A. A. (2002). Supercritical fluid extraction of fatty acids and carotenoids from the microalgae Spirulina maxima. Industrial & engineering chemistry research, 41(12), 3012-3018.
[22] Herrero, M., del Pilar Sánchez-Camargo, A., Cifuentes, A., & Ibáñez, E. (2015). Plants, seaweeds, microalgae and food by-products as natural sources of functional ingredients obtained using pressurized liquid extraction and supercritical fluid extraction. TrAC Trends in Analytical Chemistry, 71, 26-38.
[23] Sarkar, S., Manna, M. S., Bhowmick, T. K., & Gayen, K. (2020). Priority-based multiple products from microalgae: review on techniques and strategies. Critical Reviews in Biotechnology, 1-18.
[24] Schwenzfeier, A., Wierenga, P. A., Eppink, M. H., & Gruppen, H. (2014). Effect of charged polysaccharides on the techno-functional properties of fractions obtained from algae soluble protein isolate. Food hydrocolloids, 35, 9-18.
[25] Cuellar-Bermudez, S. P., Aguilar-Hernandez, I., Cardenas-Chavez, D. L., Ornelas-Soto, N., Romero-Ogawa, M. A., & Parra-Saldivar, R. (2015). Extraction and purification of high-value metabolites from microalgae: essential lipids, astaxanthin and phycobiliproteins. Microbial biotechnology, 8(2), 190-209.
[26] Gilbert-López, B., Mendiola, J. A., Fontecha, J., van den Broek, L. A., Sijtsma, L., Cifuentes, A., ... & Ibáñez, E. (2015). Downstream processing of Isochrysis galbana: a step towards microalgal biorefinery. Green Chemistry, 17(9), 4599-4609.
[27] Jankowska, E., Sahu, A. K., & Oleskowicz-Popiel, P. (2017). Biogas from microalgae: Review on microalgae's cultivation, harvesting and pretreatment for

anaerobic digestion. Renewable and Sustainable Energy Reviews, 75, 692-709.
[28] Menegazzo, M. L., & Fonseca, G. G. (2019). Biomass recovery and lipid extraction processes for microalgae biofuels production: a review. Renewable and Sustainable Energy Reviews, 107, 87-107.
[29] Enamala, M. K., Enamala, S., Chavali, M., Donepudi, J., Yadavalli, R., Kolapalli, B.,et al. (2018). Production of biofuels from microalgae-A review on cultivation, harvesting, lipid extraction, and numerous applications of microalgae. Renewable and Sustainable Energy Reviews, 94, 49-68.
[30] Singh, K., Kaloni, D., Gaur, S., Kushwaha, S., & Mathur, G. (2020). Current research and perspectives on microalgae-derived biodiesel. Biofuels, 11(1), 1-18.
[31] Veillette, M., Chamoumi, M., Nikiema, J., Faucheux, N., & Heitz, M. (2012). Production of biodiesel from microalgae. Advances in Chemical Engineering, 10, 245-260.
[32] Vandamme, D., Foubert, I., & Muylaert, K. (2013). Flocculation as a low-cost method for harvesting microalgae for bulk biomass production. Trends in biotechnology, 31(4), 233-239.
[33] Lam, T. P., Lee, T. M., Chen, C. Y., & Chang, J. S. (2018). Strategies to control biological contaminants during microalgal cultivation in open ponds. Bioresource technology, 252, 180-187.
[34] Jorquera, O., Kiperstok, A., Sales, E. A., Embirucu, M., & Ghirardi, M. L. (2010). Comparative energy life-cycle analyses of microalgal biomass production in open ponds and photobioreactors. Bioresource technology, 101(4), 1406-1413.
[35] Dassey, A. J., & Theegala, C. S. (2013). Harvesting economics and strategies using centrifugation for cost effective separation of microalgae cells for biodiesel applications. Bioresource technology, 128, 241-245.
[36] Khan, M. I., Shin, J. H., & Kim, J. D. (2018). The promising future of microalgae: current status, challenges, and optimization of a sustainable and renewable industry for biofuels, feed, and other products. Microbial cell factories, 17(1), 36.
[37] Shen, Y., Yuan, W., Pei, Z. J., Wu, Q., & Mao, E. (2009). Microalgae mass production methods. Transactions of the ASABE, 52(4), 1275-1287.
[38] Lee, Y. K. (2001). Microalgal mass culture systems and methods: their limitation and potential. Journal of applied phycology, 13(4), 307-315.
[39] Hamed, I. (2016). The evolution and versatility of microalgal biotechnology: a review. Comprehensive Reviews in Food Science and Food Safety, 15(6), 1104-1123.
[40] Rogers, J. N., Rosenberg, J. N., Guzman, B. J., Oh, V. H., Mimbela, L. E., Ghassemi, A., ... & Donohue, M. D. (2014). A critical analysis of paddlewheel-driven raceway ponds for algal biofuel production at commercial scales. Algal research, 4, 76-88.
[41] Tredici, M. R. (2004). Mass production of microalgae: photobioreactors. Handbook of microalgal culture: Biotechnology and applied phycology, 1, 178-214.
[42] Posten, C. (2009). Design principles of photo-bioreactors for cultivation of

microalgae. Engineering in Life Sciences, 9(3), 165-177.
[43] Torzillo, G., & Zittelli, G. C. (2015). Tubular photobioreactors. In Algal biorefineries (pp. 187-212). Springer, Cham.
[44] Huo, S., Wang, Z., Zhu, S., Shu, Q., Zhu, L., Qin, L., ... & Dong, R. (2018). Biomass accumulation of Chlorella zofingiensis G1 cultures grown outdoors in photobioreactors. Frontiers in Energy Research, 6, 49.
[45] Tamburic, B., Zemichael, F. W., Crudge, P., Maitland, G. C., & Hellgardt, K. (2011). Design of a novel flat-plate photobioreactor system for green algal hydrogen production. International journal of hydrogen energy, 36(11), 6578-6591.
[46] Tan, J. S., Lee, S. Y., Chew, K. W., Lam, M. K., Lim, J. W., Ho, S. H., & Show, P. L. (2020). A review on microalgae cultivation and harvesting, and their biomass extraction processing using ionic liquids. Bioengineered, 11(1), 116-129.
[47] Singh, G., & Patidar, S. K. (2018). Microalgae harvesting techniques: A review. Journal of environmental management, 217, 499-508.
[48] Heasman, M., Diemar, J., O'connor, W., Sushames, T., & Foulkes, L. (2000). Development of extended shelf-life microalgae concentrate diets harvested by centrifugation for bivalve molluscs–a summary. Aquaculture Research, 31(8-9), 637-659.
[49] Dassey, A. J., & Theegala, C. S. (2013). Harvesting economics and strategies using centrifugation for cost effective separation of microalgae cells for biodiesel applications. Bioresource technology, 128, 241-245.
[50] Milledge, J. J., & Heaven, S. (2013). A review of the harvesting of micro-algae for biofuel production. Reviews in Environmental Science and Bio/Technology, 12(2), 165-178.
[51] Pragya, N., Pandey, K. K., & Sahoo, P. K. (2013). A review on harvesting, oil extraction and biofuels production technologies from microalgae. Renewable and Sustainable Energy Reviews, 24, 159-171.
[52] Liu, W., & Canfield, N. (2012). Development of thin porous metal sheet as micro-filtration membrane and inorganic membrane support. Journal of membrane science, 409, 113-126.
[53] Alam, M. A., Wang, Z., & Yuan, Z. (2017). Generation and harvesting of microalgae biomass for biofuel production. In Prospects and challenges in algal biotechnology (pp. 89-111). Springer, Singapore.
[54] Vu, H. P., Nguyen, L. N., Lesage, G., & Nghiem, L. D. (2020). Synergistic effect of dual flocculation between inorganic salts and chitosan on harvesting microalgae Chlorella vulgaris. Environmental Technology & Innovation, 100622.
[55] Granados, M. R., Acién, F. G., Gomez, C., Fernández-Sevilla, J. M., & Grima, E. M. (2012). Evaluation of flocculants for the recovery of freshwater microalgae. Bioresource technology, 118, 102-110.
[56] Uduman, N., Qi, Y., Danquah, M. K., Forde, G. M., & Hoadley, A. (2010). Dewatering of microalgal cultures: a major bottleneck to algae-based fuels. Journal of renewable and sustainable energy, 2(1), 012701.
[57] Chen, C. Y., Yeh, K. L., Aisyah, R., Lee, D. J., & Chang, J. S. (2011). Cultivation,

photobioreactor design and harvesting of microalgae for biodiesel production: a critical review. Bioresource technology, 102(1), 71-81.
[58] Lee, A. K., Lewis, D. M., & Ashman, P. J. (2013). Harvesting of marine microalgae by electroflocculation: the energetics, plant design, and economics. Applied Energy, 108, 45-53.
[59] Dassey, A. J., & Theegala, C. S. (2014). Reducing electrocoagulation harvesting costs for practical microalgal biodiesel production. Environmental technology, 35(6), 691-697.
[60] Chen, C. L., Chang, J. S., & Lee, D. J. (2015). Dewatering and drying methods for microalgae. Drying technology, 33(4), 443-454.
[61] Vandamme, D., Pontes, S. C. V., Goiris, K., Foubert, I., Pinoy, L. J. J., & Muylaert, K. (2011). Evaluation of electro-coagulation–flocculation for harvesting marine and freshwater microalgae. Biotechnology and bioengineering, 108(10), 2320-2329.
[62] Pahl, S. L., Lee, A. K., Kalaitzidis, T., Ashman, P. J., Sathe, S., & Lewis, D. M. (2013). Harvesting, thickening and dewatering microalgae biomass. In Algae for biofuels and energy (pp. 165-185). Springer, Dordrecht.
[63] Singh, A., Nigam, P. S., & Murphy, J. D. (2011). Mechanism and challenges in commercialisation of algal biofuels. Bioresource technology, 102(1), 26-34.
[64] Phoochinda, W., & White, D. A. (2003). Removal of algae using froth flotation. Environmental technology, 24(1), 87-96.
[65] Hanotu, J., Bandulasena, H. H., & Zimmerman, W. B. (2012). Microflotation performance for algal separation. Biotechnology and bioengineering, 109(7), 1663-1673.
[66] Park, J. B. K., Craggs, R. J., & Shilton, A. N. (2011). Wastewater treatment high rate algal ponds for biofuel production. Bioresource technology, 102(1), 35-42.
[67] Henderson, R. K., Parsons, S. A., & Jefferson, B. (2009). The potential for using bubble modification chemicals in dissolved air flotation for algae removal. Separation Science and Technology, 44(9), 1923-1940.
[68] Nguyen, T. L., Lee, D. J., Chang, J. S., & Liu, J. C. (2013). Effects of ozone and peroxone on algal separation via dispersed air flotation. Colloids and Surfaces B: Biointerfaces, 105, 246-250.
[69] Coward, T., Lee, J. G., & Caldwell, G. S. (2013). Development of a foam flotation system for harvesting microalgae biomass. Algal Research, 2(2), 135-144.
[70] Cheng, Y. L., Juang, Y. C., Liao, G. Y., Ho, S. H., Yeh, K. L., Chen, C. Y., ... & Lee, D. J. (2010). Dispersed ozone flotation of Chlorella vulgaris. Bioresource Technology, 101(23), 9092-9096.
[71] de Souza, M. P., Hoeltz, M., Brittes Benitez, L., Machado, Ê. L., & de Souza Schneider, R. D. C. (2019). Microalgae and Clean Technologies: A Review. CLEAN–Soil, Air, Water, 47(11), 1800380.
[72] Bennamoun, L., Afzal, M. T., & Léonard, A. (2015). Drying of alga as a source of bioenergy feedstock and food supplement–A review. Renewable and Sustainable Energy Reviews, 50, 1203-1212.

[73] Baker, C. G. J., & McKenzie, K. A. (2005). Energy consumption of industrial spray dryers. Drying Technology, 23(1-2), 365-386.
[74] Dong, T., Knoshaug, E. P., Davis, R., Laurens, L. M., Van Wychen, S., Pienkos, P. T., & Nagle, N. (2016). Combined algal processing: A novel integrated biorefinery process to produce algal biofuels and bioproducts. Algal Research, 19, 316-323.
[75] Xu, L. (2011). Brilman, DWF, Withag, JAM, Brem, G. & Kersten, S. Assessment of a dry and a wet route for the production of biofuels from microalgae: Energy balance analysis. Bioresource Technology, 102, 5113-5122.
[76] Bensalem, S., Lopes, F., Bodénès, P., Pareau, D., Français, O., & Le Pioufle, B. (2018). Understanding the mechanisms of lipid extraction from microalga Chlamydomonas reinhardtii after electrical field solicitations and mechanical stress within a microfluidic device. Bioresource technology, 257, 129-136.
[77] Salinas-Salazar, C., Garcia-Perez, J. S., Chandra, R., Castillo-Zacarias, C., Iqbal, H. M., & Parra-Saldívar, R. (2019). Methods for Extraction of Valuable Products from Microalgae Biomass. In Microalgae Biotechnology for Development of Biofuel and Wastewater Treatment (pp. 245-263). Springer, Singapore.
[78] Vickers, N. J. (2017). Animal Communication: When I'm Calling You, Will You Answer Too?. Current Biology, 27(14), R713-R715.
[79] Bligh, E. G., & Dyer, W. J. (1959). A rapid method of total lipid extraction and purification. Canadian journal of biochemistry and physiology, 37(8), 911-917.
[80] Aarthy, A., Kumari, S. M. I. T. A., Turkar, P. R. A. C. H. I., & Subramanian, S. A. N. G. E. E. T. H. A. (2018). An insight on algal cell disruption for biodiesel production. Asian J Pharm Clin Res, 11(2), 21-26.
[81] Sierra, L. S., Dixon, C. K., & Wilken, L. R. (2017). Enzymatic cell disruption of the microalgae Chlamydomonas reinhardtii for lipid and protein extraction. Algal research, 25, 149-159.
[82] Heo, Y. M., Lee, H., Lee, C., Kang, J., Ahn, J. W., Lee, Y. M., ... & Kim, J. J. (2017). An integrative process for obtaining lipids and glucose from Chlorella vulgaris biomass with a single treatment of cell disruption. Algal research, 27, 286-294.
[83] Esquivel-Hernández, D. A., López, V. H., Rodríguez-Rodríguez, J., Alemán-Nava, G. S., Cuéllar-Bermúdez, S. P., Rostro-Alanis, M., & Parra-Saldívar, R. (2016). Supercritical carbon dioxide and microwave-assisted extraction of functional lipophilic compounds from Arthrospira platensis. International journal of molecular sciences, 17(5), 658.
[84] Hernández, D., Solana, M., Riaño, B., García-González, M. C., & Bertucco, A. (2014). Biofuels from microalgae: lipid extraction and methane production from the residual biomass in a biorefinery approach. Bioresource technology, 170, 370-378.
[85] Ghasemi Naghdi, F., González González, L. M., Chan, W., & Schenk, P. M. (2016). Progress on lipid extraction from wet algal biomass for biodiesel production. Microb Biotechnol 9: 718–726.
[86] Paré, J. J., Matni, G., Bélanger, J. M., Li, K., Rule, C., Thibert, B., ... & Jacquault,

P. (1997). Use of the microwave-assisted process in extraction of fat from meat, dairy, and egg products under atmospheric pressure conditions. Journal of AOAC International, 80(4), 928-933.
[87] Peterson, A. A., Vogel, F., Lachance, R. P., Fröling, M., Antal Jr, M. J., & Tester, J. W. (2008). Thermochemical biofuel production in hydrothermal media: a review of sub-and supercritical water technologies. Energy & Environmental Science, 1(1), 32-65.
[88] Biller, P., Ross, A. B., Skill, S. C., Lea-Langton, A., Balasundaram, B., Hall, et al, (2012). Nutrient recycling of aqueous phase for microalgae cultivation from the hydrothermal liquefaction process. Algal Research, 1(1), 70-76.
[89] Fajardo, A. R., Cerdan, L. E., Medina, A. R., Fernández, F. G. A., Moreno, P. A. G., & Grima, E. M. (2007). Lipid extraction from the microalga Phaeodactylum tricornutum. European Journal of Lipid Science and Technology, 109(2), 120-126.
[90] Guderjan, M., Elez-Martínez, P., & Knorr, D. (2007). Application of pulsed electric fields at oil yield and content of functional food ingredients at the production of rapeseed oil. Innovative Food Science & Emerging Technologies, 8(1), 55-62.
[91] Sialve, B., Bernet, N., & Bernard, O. (2009). Anaerobic digestion of microalgae as a necessary step to make microalgal biodiesel sustainable.
[92] Zhu, L. (2014). The combined production of ethanol and biogas from microalgal residuals to sustain microalgal biodiesel: A theoretical evaluation. Biofuels, Bioproducts and Biorefining, 8(1), 7-15.
[93] Ehimen, E. A., Sun, Z. F., Carrington, C. G., Birch, E. J., & Eaton-Rye, J. J. (2011). Anaerobic digestion of microalgae residues resulting from the biodiesel production process. Applied Energy, 88(10), 3454-3463.
[94] Podkuiko, L., Ritslaid, K., Olt, J., & Kikas, T. (2014). Review of promising strategies for zero-waste production of the third generation biofuels. Agronomy Research, 12(2), 373-390.
[95] Wang, Q., Oshita, K., Nitta, T., & Takaoka, M. (2020). Evaluation of a sludge-treatment process comprising lipid extraction and drying using liquefied dimethyl ether. Environmental Technology, 1-10.
[96] Oshita, K., Toda, S., Takaoka, M., Kanda, H., Fujimori, T., Matsukawa, K., & Fujiwara, T. (2015). Solid fuel production from cattle manure by dewatering using liquefied dimethyl ether. Fuel, 159, 7-14.
[97] Kanda, H., Hoshino, R., Murakami, K., Zheng, Q., & Goto, M. (2020). Lipid extraction from microalgae covered with biomineralized cell walls using liquefied dimethyl ether. Fuel, 262, 116590.

Chapter 2 Flocculation properties of eight microalgae by aluminium chloride, chitosan, ACPAM and alkaline flocculation: LCA for screening of species and harvesting methods

2.1 Introduction

Various microalgae show promise for the production of biodiesel [1,2] and high value-added chemicals in pharmaceuticals [3], nutraceuticals [4], food [5], and cosmetics [6] due to their high growth and metabolic rates [7]. Fossil-fuel combustion releases huge amounts of greenhouse gases into the atmosphere [8,9], which are considered the main cause of climate change [10]. Biodiesel extracted from microalgae is particularly recognized as a renewable carbon-neutral fuel to alleviate this problem [11–13]. Microalgae can be cultivated in nonarable land [14] and can even be integrated with wastewater treatment plants for the removal of nitrates and phosphates [12]. Carbon dioxide emitted from plants (e.g., flue gas from a thermal power plant) is also suitable as a carbon source for microalgae cultivation [15]. Microalgae cultivation does not compete with food production, and the utilization of wastewater saves freshwater resources by reducing the N/P content of the effluent. In addition, absorption and sequestration of CO_2 by microalgae from waste flue gas can reduce greenhouse gas emissions, which further enhances the environmental sustainability of energy production from microalgae.

Before lipids or high-value products are extracted from microalgae, an appropriate harvesting method is needed to concentrate the biomass. Effectively harvesting microalgae is a crucial step and a challenge for commercialization due to its low biomass concentration (0.5–5 g/L), small cell size (5–50 μm), and relative stability in culture medium [16,17]. Several techniques have been applied to successfully harvest microalgae. For example, centrifugation can harvest microalgae in a short time, although it consumes large amounts of energy. Electrophoresis, which is appropriate for certain species, neutralizes microalgae surface charge and then aggregates them with high energy efficiency. Flotation by air bubbles can be applied to small, unicellular microalgae and filtration intercepts microalgae but allows water to pass through a membrane. The addition of various types of flocculants causes microalgae flocculation, which facilitates sedimentation. Finally, gravity sedimentation has very low energy and chemical demands but requires long times and land area [18,19]. Among these methods, flocculation has low material and energy costs and is suitable for a wide variety of microalga species [18,20], and thus is considered a promising approach for the large-scale harvesting of microalgae [21].

A wide variety of flocculants, such as high-valency cations (Al^{3+}, Fe^{3+}, Ti^{4+}), cationic

polyacrylamide, and chitosan, can induce flocculation [22]. However, flocculation performance varies by microalga species and flocculant type due to different cell sizes, cell surface features, cell densities, zeta potentials, and cell stabilities. For example, in one study, the addition of 0.1 g/L aluminum sulfate harvested 90% of *Chromochloris zofingiensis* [23], whereas in another study, a maximum flocculation efficiency (FE) of 82.6% for *Phaeodactylum tricornutum* was obtained by adding 0.03 g/L aluminum sulfate, and 0.02 g/L achieved 91.8% FE for the same species [24]. The choice of cultivation medium and growth stage affects the performance of a flocculant for a given microalga species. For example, in one study, 0.08 g/L chitosan harvested ~90% of *Scenedesmus sp*. [23], but in another study, 0.06 g/L chitosan was sufficient to harvest ~100% of the same species [21]. Therefore, a flocculant that successfully harvests one species may not work on other species, and the optimal dosage of flocculant may vary even if it works. Considering that different studies have typically used different cultivation and growth conditions, which affect flocculation, a comparison of these data are challenging. Hence, evaluation of various species in a single study is necessary for precise evaluation and assessment of possible harvesting processes.

Life-cycle assessment (LCA) is an important methodology for evaluating and assessing the environmental sustainability of biodiesel production from microalgae [25,26]. This methodology can assess a technology in its initial development phases by combining an existing database and experimental data. In an LCA, the goal and scope are first defined, an inventory referring to inputs and outputs (materials and energy within the system boundary) is subsequently established, and then the environmental impacts are calculated using standard evaluation methods [28]. For biodiesel production, global warming potential (GWP), eutrophication potential (EP), fossil fuel depletion potential (FFDP), and acidification potential (AP) are impact factors commonly used to draw conclusions [12,22,29].

In the first part of this study, four freshwater microalgae (*Chlamydomonas reinhardtii*, *Chlorella sorokiniana*, *Coccomyxa sp*. *KJ*., and *Tetradesmus obliquus*) and four marine water microalgae (*Chlorella vulgaris*, *Fistulifera solaris*, *Mayamaea sp*., and *Nannochloropsis oculata*) were flocculated by four types of flocculants (aluminium chloride, chitosan, and amphoteric polyacrylamide, and pH adjustment using HCl and NaOH). Based on the results, the second part of this study used LCA to compare the different microalga species according to different harvesting methods, i.e., flocculation combined with centrifugation or filter pressing, direct centrifugation, and crossflow filtration without flocculation. The LCA mainly examined energy consumption, greenhouse gas emissions, and eutrophication emissions.

2.2 Materials and methods

2.2.1 Microalgae species and cultivation

To study the flocculation performance on different microalgae species, 8 species including 4 marine microalgae with 4 fresh water microalgae were selected. The 8 species were selected, because all of them were reported to have high lipid content and a potential to be used for biodiesel production [45-49]. The strains of freshwater

microalgae, *Coccomyxa sp*. *KJ* (*Coccomyxa K.J.*) and *Chlorella sorokiniana*, were supplied by the laboratory of Professor Miyashita at Kyoto University (Kyoto, Japan). Marine microalgae strains of *Nannochloropsis oculata* and *Chlorella vulgaris* and freshwater microalgae strains of *Chlamydomonas reinhardtii* and *Tetradesmus obliquus* were obtained from the Microbial Culture Collection at the National Institute for Environmental Studies (Tsukuba, Japan). The media for cultivating the freshwater and marine microalgae were AF-6 and ESM, respectively (Table S1). These microalgae were cultivated in 20 L bucket photobioreactors (12 h/12 h light/dark cycles; Photograph S1) at 20–25°C. During cultivation, the culture media were continuously aerated with filtered air and biomass concentrations were monitored until the microalgae entered the stationary phase. After 10–20 days of cultivation, the stationary-phase microalgae were used in the flocculation tests. Two other well-cultivated marine microalgae, *Fistulifera solaris* and *Mayamaea sp*., were directly obtained from a microalgae cultivation plant at a yield of 1,000 kg dry algae/year (Wakamatsu Department of J-Power Company, Kitakyushu, Fukuoka, Japan).

The dry cell weights of the microalgae were measured in their stationary phase. Several milliliters of microalgae (10–30 mL, depending on the species) were filtered through preweighed glass microfiber filter papers (GF/C; 1.2 µm, 4.7 cm; Whatman plc, UK) by vacuum filtration, and the papers were rinsed with deionized water. After the papers were dried in an oven at 105°C for 2 h to a constant weight, their dry weights were measured. The dry weights combined with cell shape, size, cell volume, surface area, zeta-potential, and lipid content obtained from the literature are shown in Table S2.

2.2.2 Experimental process of flocculation

Flocculation experiments were performed in 100 mL beakers [50]. After adding flocculant ($AlCl_3$ ranged from 0~1 g/L, chitosan of 0~0.5 g/L, ACPAM of 0~ 0.8 g/L, NaOH of 0~1 g/L), the microalgae suspensions were intensively mixed (350 rpm) for 2 min, followed by a gentle mixing (50 rpm) for 10 min by magnetic stirring (MG120; Yamato Scientific Co., Ltd., Tokyo, Japan). The suspensions were subsequently allowed to settle for 15 min. The supernatant was sampled from the middle of the clarified zone and the optical absorbance (OD) was measured at 680 nm by spectrophotometry (UV-1200; Shimadzu, Kyoto, Japan). The FE was determined in terms of the absorbance according to Equation (2.1) as follows:

$$\text{Flocculation efficiency (\%)} = \left(1\text{-}\frac{\text{ODfinal}}{\text{ODinitial}}\right) \times 100 \quad (2.1)$$

where $OD_{initial}$ is the optical absorbance before flocculation and OD_{final} is the optical absorbance after flocculation was completed.

Three types of flocculants were used in the flocculation experiment: $AlCl_3$ (inorganic salt; 30 g/L; FUJIFILM Wako Pure Chemical Corporation, Tokyo, Japan), chitosan (organic polymer; 5 g/L dissolved in 0.2% acetic acid; FUJIFILM), and amphoteric flocculant ACPAM (KA305BH; Mitsubishi Chemical Corp., Tokyo, Japan); pH-induced (37.5% HCl, 10 mol/L NaOH) flocculation was also investigated. All experiments were repeated three times.

2.2.3 Settling tests and Capillary Suction Time (CST) measurement

The optimal flocculant dosages (identified using the procedure detailed in section 2.2.2) were added to 100 mL each of the microalgae samples. Then the samples were intensively mixed for 2 min followed by 10 min of gentle mixing. Then each mixture was gently transferred to a 100 mL graduated cylinder, and the change in the solid/liquid interface height (mudline) was recorded for 30–40 min. The mudline height (h) was plotted as a function of settling time (t) to determine the final settling time and concentration factors (CFs). The supernatants were withdrawn, and the microalgae residues were collected for CST measurement by a CST meter (Type 304M; Triton Electronics Ltd., UK).

2.2.4 Life cycle assessment

An overview of the system boundary is shown in Figure 2.1. A functional unit of 1 kg dry weight microalgae was considered the basis. The system boundary included microalgae harvesting (condensing biomass concentration from 0.26–1.22 g/L to 200–240 g/L) and treatment of its produced waste. In Table S3, 10 scenarios ($AlCl_3$ + filter press, chitosan + filter press, ACPAM + filter press, pH adjustment + filter press, $AlCl_3$ + centrifugation, chitosan + centrifugation, ACPAM + centrifugation, pH adjustment + centrifugation, cross-flow filtration, and two-step centrifugation) for each of the eight microalga species are compared. The cultivation and lipid extraction process for a given species were assumed to be equivalent for all of the scenarios [22]. The produced wastewater containing unharvested microalgae was assumed to be recycled and reused for microalgae cultivation [22], but wastewater from the pH-adjustment experiments was first neutralized. Produced solid waste (i.e., used polyethylene filters) was assumed to be landfilled.

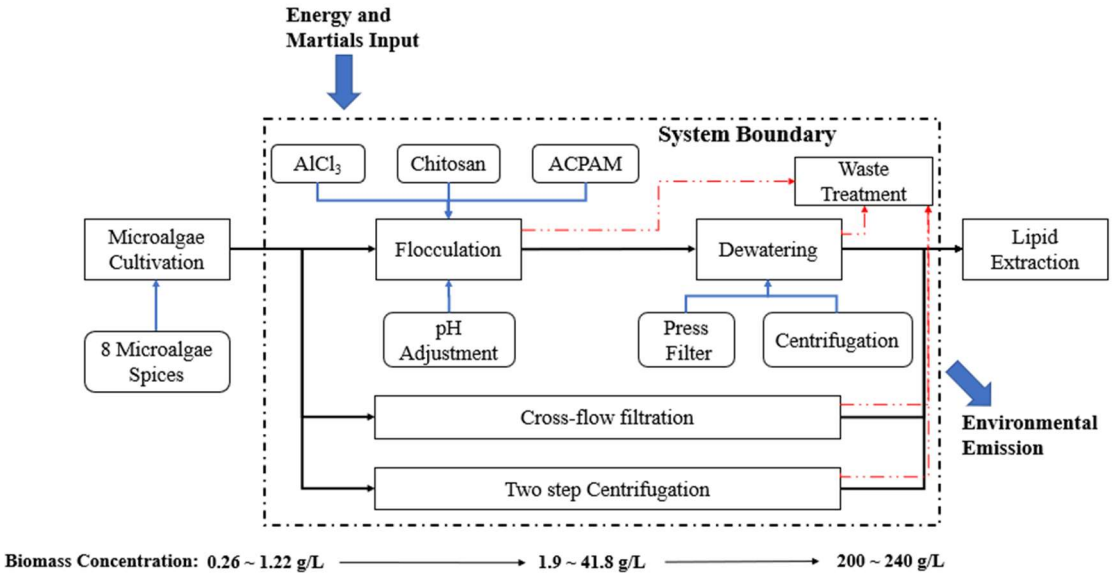

Figure 2.1 Overview of the system boundary.

Dewatering. Two methods (filter press and centrifugation) were considered to dewater a flocculated microalgae slurry (Table 1). A small amount of microalgae biomass was lost due to the recovery rates of the filter press (98% assumed) and centrifugation (95% assumed). The respective dewatered biomass concentrations were 200 and 220 g/L. The electrical requirement for operating the filter press and centrifugation to treat 1 L flocculation-condensed sample was 0.5 and 8 Wh, respectively. The volume of the flocculation-condensed sample for each scenario was calculated according to the CFs of the experimental data. The material inputs for the filter press process included polyethylene (filter cloth replacement, 42 g per m^3 treated microalgae [22]) and polyacrylamide (PAM), the consumption of which was related to the CST of the microalgae slurry (obtained from experiments described in section 2.2.3). Because a high CST impedes filtration, a certain amount of PAM was needed to adjust the CST value; the detailed dosage calculation is described in section 2.3.2. No material inputs were involved in the centrifugation process.

Flocculation. The added amounts (Table 2.1) of $AlCl_3$, chitosan, ACPAM, and NaOH were determined by their optimal dosages determined from the experiments described in section 2.2.2. Because the initial biomass concentration varied with microalga species, the volume for harvesting 1 kg dry microalgae differed. The volume for each species was calculated according to the initial dry weight of the microalgae, FE, and the recovery rate in the dewatering step. The electrical consumption was derived from agitation during flocculation, and was assumed to be 33.3 Wh/m^3 microalgae. The database entries concerning chitosan refer to the process described in a previous study [30] in which chitosan was produced from chitin derived from shrimp waste. The shrimp waste was decalcified by treatment with HCl, then deproteinated and deacetylated by NaOH treatment to obtain chitin. The byproduct from the process was protein sludge, which can be used as fertilizer. The production was assumed to be in India, with energy inputs representative of the Indian electricity grid and fuel quality.

Two-step centrifugation. The two-step centrifugation process described in a previous study [31] was compared to the flocculation + dewatering procedure. In the method, microalgae were first preconcentrated (first centrifugation) to a biomass concentration of 20 g/L, and then further concentrated to 220 g/L by a second centrifugation. The recovery rate for both steps was 95%. The electrical requirements for the two steps were 0.9 Wh/L (initial microalgae) and 8 Wh/L (preconcentrated microalgae). Details for each species are presented in Table 1. This process was selected for comparison, because it is a common method to harvest microalgae and suitable for any type of species.

Cross-flow filtration. This method, which was reported by Pacific Northwest National Laboratory [32], has the merits of high harvesting efficiency (~100%) and low energy requirement. Even though it was seldom studied, it was also selected for comparison due to its prospect on harvesting microalgae. During filtration, the microalgae liquid flows through a metallic membrane at an angle parallel to it, and the water in the microalgae passes through the porous membrane while the microalgae cells are retained. Microalgae biomass concentration gradually increases (to ultimately 240 g/L) as the liquid flows through the membrane. Because the membrane is made of nickel metal

with a special structure (tough, flexible, corrosion resistant, and evenly distributed pores), its cost is relatively high. However, the membrane consumption is very low (1.048×10^{-8} m^3 Ni to harvest 1 kg dry microalgae), and so its material inputs can be ignored [26]. The electrical consumption was estimated to be 173 kWh/m^3 of initial microalgae. Details for each species are presented in Table 2.1.

The LCA was conducted using SimaPro 9 software (PRé Sustainability, The Netherlands). Once the life-cycle inventory analysis (LCI, Table 1) results were entered into the software, the impacts on the environment, ecosystem, and human health by the 10 scenarios of the eight species were determined using the TRACI 2.1 impact assessment model [27,44]. Figure 2.2 (*Chlorella vulgaris*) and Figure S1 (other species) shows the process value chain for lipid production from the eight microalgae.

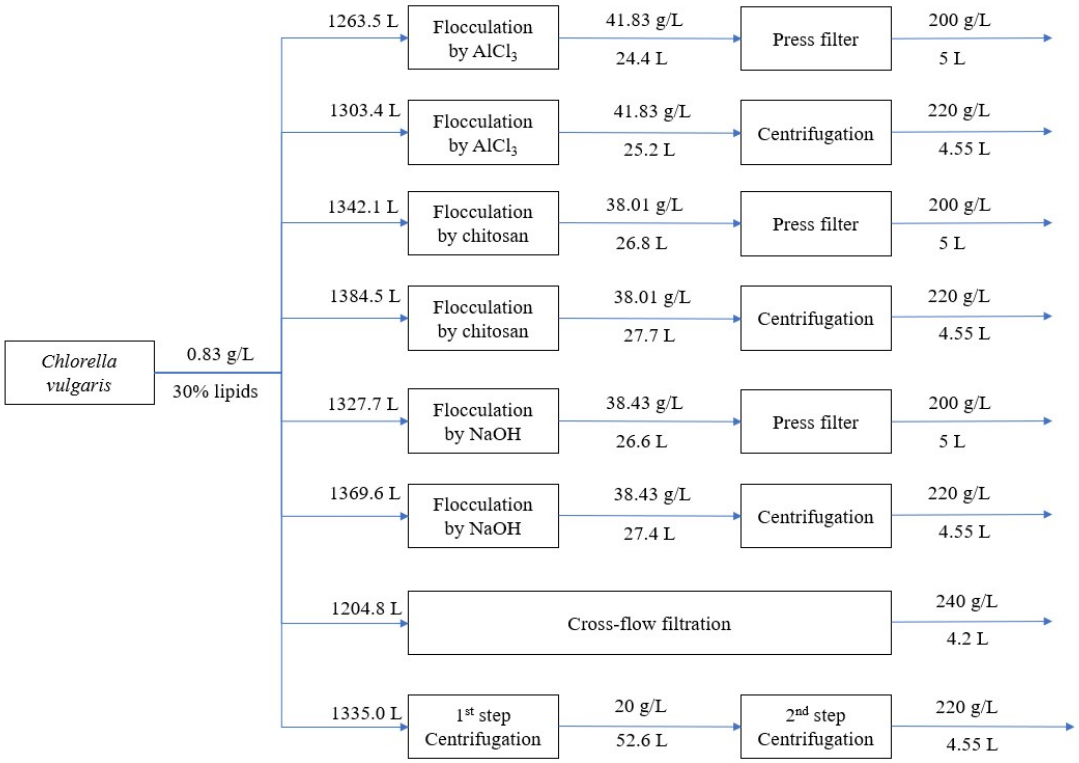

Figure 2.2 The process value chain for lipid production from *Chlorella vulgaris*.

Table 2.1 Summary of LCI for harvesting 1 kg dry microalgae.

Scenario	APF	CPF	KPF	SPF	AC	CC	KC	SC	CF	TC
Chlorella sorokiniana	N/A	Chitosan 63.2 g; PAM 3.7g; Polyethylene 3.2 g; Electricity[a] 28.1 Wh; Electricity[b] 37.9 Wh; Waste landfill 3.2 g	N/A	N/A	N/A	Chitosan 65.2 g; Electricity[a] 29.0 Wh; Electricity[c] 626.2 Wh	N/A	N/A	Electricity[d] 141.8 Wh	Electricity[e] 817.4 Wh; Electricity[f] 421.1 Wh
Mayamaea sp.	$AlCl_3$ 699.6 g; PAM 9.0 g; Polyethylene 6.8 g; Electricity[a] 77.7 Wh; Electricity[b] 81.5 Wh; Waste landfill 6.8 g	N/A	N/A	NaOH 1.04 kg; PAM 22.7 g; Polyethylene 22.9 g; Electricity[a] 69.5 Wh; Electricity[b] 274.5 Wh; Waste landfill 22.9 g; HCl 1.15 kg	$AlCl_3$ 721.7 g; Electricity[a] 80.2 Wh; Electricity[c] 1345.8 Wh	N/A	N/A	NaOH 1.08 kg; Electricity[a] 71.7 Wh; Electricity[c] 4531 Wh; HCl 1.18 kg	Electricity[d] 339.2Wh	Electricity[e] 1955.4 Wh; Electricity[f] 421.1 Wh
Coccomyxa sp. KJ	$AlCl_3$ 62.2 g; PAM 0.1 g; Polyethylene 3.1 g; Electricity[a] 51.8 Wh; Electricity[b] 37.4 Wh; Waste landfill 3.1 g	Chitosan 11.9 g; Polyethylene 2.4 g; Electricity[a] 53 Wh; Electricity[b] 29.3 Wh; Waste landfill 2.4 g	ACPAM 162.5 g; PAM 18.6 g; Polyethylene 2.6 g; Electricity[a] 51.6 Wh; Electricity[b] 31.0 Wh; Waste landfill 2.6 g	N/A	$AlCl_3$ 64.1 g; Electricity[a] 53.4 Wh; Electricity[c] 616.5 Wh	Chitosan 167.6 g; Electricity[a] 53.2 Wh; Electricity[c] 510.9 Wh	ACPAM 167.6 g; Electricity[a] 53.2 Wh; Electricity[c] 510.9 Wh	N/A	Electricity[d] 262.1 Wh	Electricity[e] 1511.0 Wh; Electricity[f] 421.1 Wh
Chlamydomonas reinhardtii	$AlCl_3$ 104.3 g; PAM 10 g; Polyethylene 5.8 g; Electricity[a] 30.2 Wh; Electricity[b] 69.7 Wh; Waste landfill 5.8 g	Chitosan 73 g; PAM 24.5 g; Polyethylene 3 g; Electricity[a] 30.4 Wh; Electricity[b] 36.5 Wh; Waste landfill 3 g	ACPAM 454.3 g; Polyethylene 1.6 g; Electricity[a] 31.6 Wh; Electricity[b] 18.9 Wh; Waste landfill 1.6 g	N/A	$AlCl_3$ 107.6 g; Electricity[a] 31.2 Wh; Electricity[c] 1151.1 Wh	Chitosan 75.4 g; Electricity[a] 31.4 Wh; Electricity[c] 602.8 Wh	ACPAM 468.7 g; Electricity[a] 32.5 Wh; Electricity[c] 312.5 Wh	N/A	Electricity[d] 153.1 Wh	Electricity[e] 882.5 Wh; Electricity[f] 421.1 Wh
Chlorella vulgaris	$AlCl_3$ 37.9 g; Polyethylene 1 g; Electricity[a] 42.1 Wh; Electricity[b] 12.2 Wh; Waste landfill 1 g	Chitosan 33.6 g; Polyethylene 1.1 g; Electricity[a] 44.7 Wh; Electricity[b] 13.4 Wh; Waste landfill 1.1 g	N/A	NaOH 345.2 g; Polyethylene 1.1 g; Electricity[a] 44.3 Wh; Electricity[b] 13.3 Wh; Waste landfill 1.1 g; HCl 379.7 g	$AlCl_3$ 39.1 g; Electricity[a] 43.4 Wh; Electricity[c] 201.3 Wh	Chitosan 34.6 g; Electricity[a] 46.2 Wh; Electricity[c] 221.5 Wh	N/A	NaOH 356.1 g; Electricity[a] 45.7 Wh; Electricity[c] 219.1 Wh; HCl 391.7 g	Electricity[d] 208.4 Wh	Electricity[e] 1201.5 Wh; Electricity[f] 421.1 Wh
Nannochloropsis oculate	$AlCl_3$ 131.6 g; Polyethylene 3.1 g;	N/A	N/A	NaOH 1.3 kg; PAM 9.0 g;	$AlCl_3$ 135.8 g; Electricity[a] 56.6 Wh;	N/A	N/A	NaOH 1.3 kg; Electricity[a] 56.1 Wh;	Electricity[d] 270.3 Wh	Electricity[e] 1558.2 Wh; Electricity[f] 421.1 Wh

	Electricity[a] 54.8 Wh; Electricity[b] 37.1 Wh; Waste landfill 3.1 g			Polyethylene 12.1 g; Electricity[a] 54.3 Wh; Electricity[b] 145.6 Wh; Waste landfill 12.1 g; HCl 1.4 kg	Electricity[c] 611.7 Wh			Electricity[c] 2402.5 Wh; HCl 1.5 kg		
Tetradesmus obliquus	$AlCl_3$ 78.9 g; Polyethylene 2.7 g; Electricity[a] 37.6 Wh; Electricity[b] 32.2 Wh; Waste landfill 2.7 g	Chitosan 56.3 g; Polyethylene 2.3 g; Electricity[a] 37.5 Wh; Electricity[b] 28.2 Wh; Waste landfill 2.3 g	ACPAM 58.8 g; PAM 24.5 g; Polyethylene 1.2 g; Electricity[a] 37.3 Wh; Electricity[b] 14.9 Wh; Waste landfill 1.2 g	N/A	$AlCl_3$ 81.4 g; Electricity[a] 38.8 Wh; Electricity[c] 531.6 Wh	Chitosan 58.1 g; Electricity[a] 38.7 Wh; Electricity[c] 464.6 Wh	ACPAM 60.7 g; Electricity[a] 38.5 Wh; Electricity[c] 246.6 Wh	N/A	Electricity[d] 188.0 Wh	Electricity[e] 1083.9 Wh; Electricity[f] 421.1 Wh
Fistulifera solaris	$AlCl_3$ 1031.0 g; PAM 4.4 g; Polyethylene 6.7 g; Electricity[a] 229.1 Wh; Electricity[b] 79.9 Wh; Waste landfill 6.7 g	N/A	N/A	NaOH 2.5 kg; PAM 15.9 g; Polyethylene 21.5 g; Electricity[a] 234 Wh; Electricity[b] 258.1 Wh; Waste landfill 21.5 g; HCl 2.8 kg	$AlCl_3$ 1063.6 g; Electricity[a] 236.3 Wh; Electricity[c] 1319.1 Wh	N/A	N/A	NaOH 2.6 kg; Electricity[a] 241.4 Wh; Electricity[c] 4260.3 Wh; HCl 2.9 kg	Electricity[d] 665.4 Wh	Electricity[e] 3835.5 Wh; Electricity[f] 421.1 Wh

a Electricity input for flocculation [12][33].
b Electricity input for press filter [31].
c Electricity input for centrifugation [12] [31].
d Electricity input for cross-flow filter [26] [52].
e Electricity input for preconcentration of the two-step centrifugation [31].
f Electricity input for 2nd centrifugation [31].

2.3 Results and discussion

2.3.1 Flocculation performance of 4 flocculants for microalgae species

The performance of flocculants for the eight microalga species is presented in Figures 2.3 and S2. The performance is represented by the region of maximum FE, i.e., the region for which the flocculant dosage gave acceptable FE. The FE was sharply lower below the dosage range. Above the dosage range, the FE remained stable. Thus, underdosage and overdosage could be avoided during flocculation by referring to the figure.

Seven of the eight microalga species were successfully flocculated by $AlCl_3$; no flocculation was observed for *Chlorella sorokiniana* even at a very high dosage of 1,000 mg/L. Among the seven species, five were within the dosage range of 30–115 mg/L and had FEs exceeding 90%. Specifically, 30 mg/L $AlCl_3$ induced flocculation of both *Coccomyxa sp*. *KJ*. and *Chlorella vulgaris* with FEs of ~97%, while 100 mg/L $AlCl_3$ was needed to achieve the same FE for *Chlamydomonas reinhardtii*. The dosage for flocculating *Mayamaea sp*. ranged from 300 to 600 mg/L, which was much higher than the others, and the maximum FE of ~85% was slightly lower. The lowest maximum FE of 45–55% was observed for *Fistulifera solaris* at dosages ranging from 100 to 200 mg/L $AlCl_3$.

Chitosan had a lower dosage requirement than $AlCl_3$. Among the five species successfully flocculated by chitosan, the dosage ranged from 7.5 to 150 mg/L with FEs of 85–99%. The FE of *Coccomyxa sp*. *KJ*. reached ~97% after adding 7.5 mg/L chitosan. An FE of ~92% was obtained using 25 mg/L chitosan with *Chlorella vulgaris*. For the remaining three species, higher FEs of ~99% were achieved by adding 45, 75, and 80 mg/L chitosan, respectively. However, the optimal dosage range of chitosan was narrower than that of $AlCl_3$. For example, the range for *Coccomyxa sp*. *KJ*. was 7.5–15 mg/L and that for *Tetradesmus obliquus* was 50–52.5 mg/L. These findings indicate that accurate dosing control is necessary to prevent underdosage and overdosage.

We also found that pH adjustment (NaOH) successfully flocculated four types of microalgae. Although there were no significant differences in maximum FE between flocculation by NaOH and by $AlCl_3$ and chitosan, the dosage requirement was much higher. To obtain an FE of 92.5% for *Chlorella vulgaris*, 275 mg/L NaOH was necessary, while 30 mg/L $AlCl_3$ achieved an FE of 97% and 25 mg/L chitosan achieved an FE of 92%. For *Nannochloropsis oculata*, 800 mg/L NaOH provided an FE of ~97% while the same FE was obtained with just 80 mg/L $AlCl_3$. In addition, flocculation by pH adjustment with NaOH occurred when the pH exceeded ~10.0.

Only three microalgae, *Tetradesmus obliquus*, *Coccomyxa sp*. *KJ*., and *Chlamydomonas reinhardtii*, could be flocculated by ACPAM. In each case, the FE exceeded 95%, which was almost the same as flocculation by $AlCl_3$ and chitosan. The optimal dosages of ACPAM (100 and 520 mg/L) were higher than that of $AlCl_3$ (40 and 115 mg/L) and chitosan (7.5 and 80 mg/L) for *Coccomyxa sp*. *KJ*. and *Chlamydomonas reinhardtii*, respectively. But for *Tetradesmus obliquus*, 60 mg/L ACPAM dosage resembled dosages of 70 mg/L $AlCl_3$ and 50 mg/L chitosan. These findings imply that

although ACPAM displayed poorer flocculation performance than $AlCl_3$ and chitosan, it should still be considered an alternative flocculant for microalgae flocculation.

The different flocculation performances of the four methods is attributed to mechanistic differences. The main mechanism for $AlCl_3$ flocculation in pH ~8.0 medium is double-adsorption strength [35,36]. Thus, $AlCl_3$ successfully flocculated all four marine species. Unlike $AlCl_3$, chitosan failed to flocculate marine microalgae (no flocculation for three species and low FE for the remaining one) but flocculated all four freshwater microalgae with lower dosage than $AlCl_3$. This is because chitosan uses adsorption/bridging to flocculate microalgae, and chitosan coils in high ionic strength medium to mask its functional groups and lose its configuration [37,38]. Therefore, chitosan is suitable for freshwater microalgae, while $AlCl_3$ can be used for both freshwater and marine algae. Like chitosan, ACPAM is an organic flocculant and is inhibited by salt. In this study, ACPAM failed to flocculate all four marine microalgae. The freshwater microalgae *Chlorella sorokiniana* was the most difficult to flocculate; neither $AlCl_3$ nor ACPAM were effective, and only chitosan worked but with the highest dosage among the species. Due to the sweeping mechanism [39,40], addition of NaOH flocculated the four types of marine microalgae. There was no flocculation observed with addition of NaOH until the pH increased to the critical point of precipitate formation. This demonstrated that hydroxide precipitate sweeping of microalgae cells led to the flocculation. The very low ion concentration in the freshwater microalgae medium prevented NaOH from flocculating the microalgae. This mechanism has potential for harvesting difficult-to-flocculate species. Notably, the freshwater microalgae *Chlorella sorokiniana* was flocculated by $AlCl_3$ after the pH was adjusted to ~4.7 (Figure S3). At this pH, aluminum hydroxide precipitated and captured the microalgae cells.

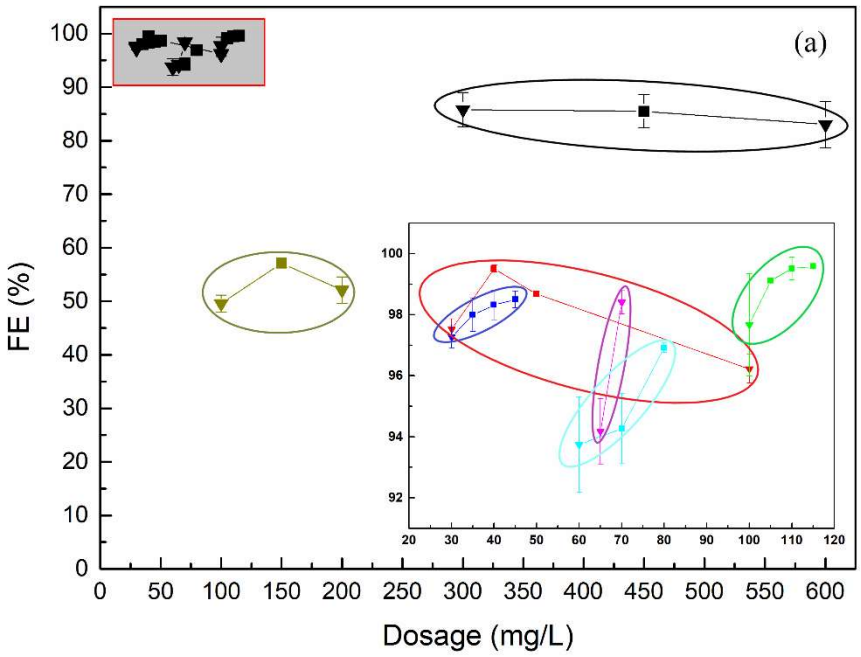

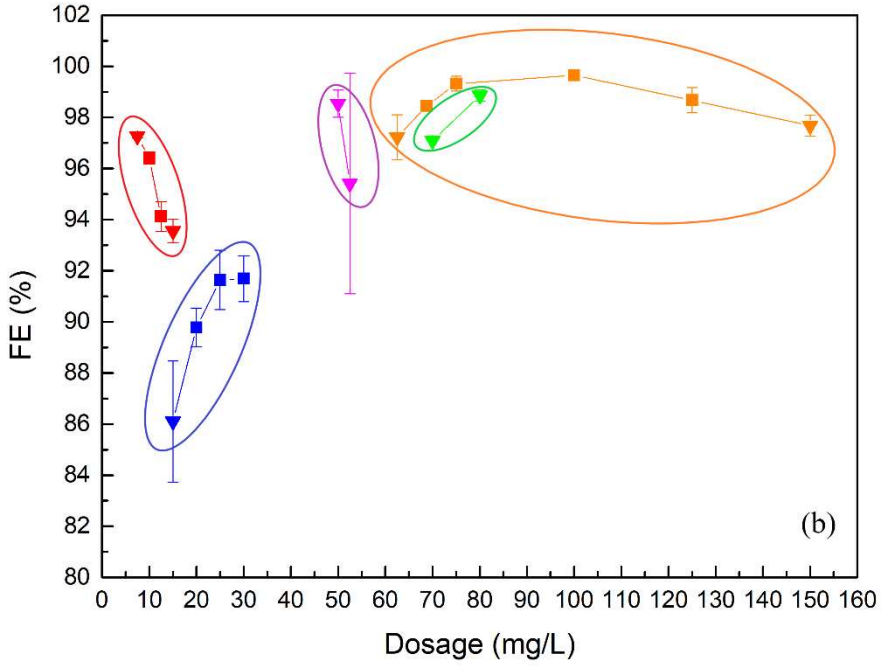
FE (%)
Dosage (mg/L)
(b)

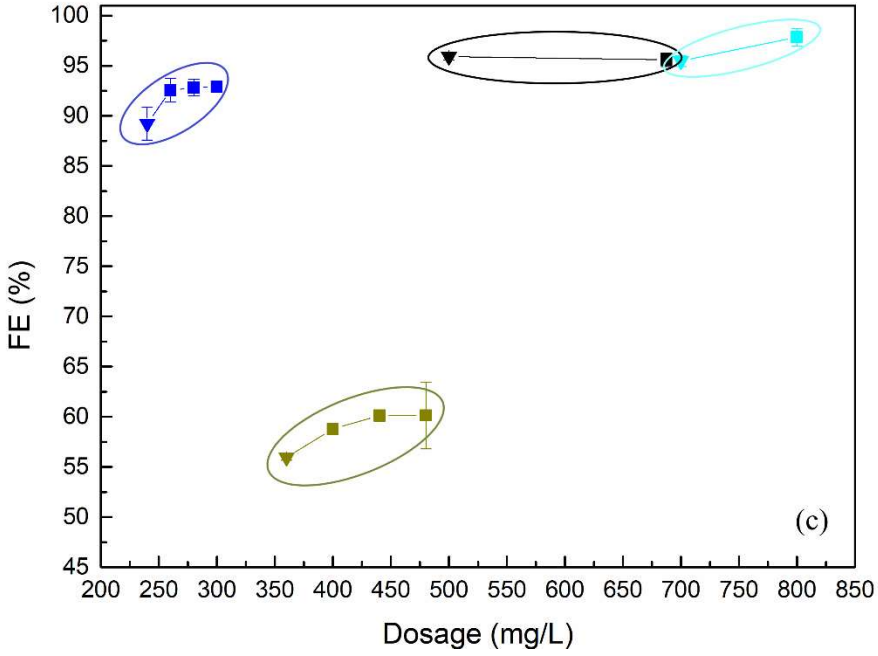
FE (%)
Dosage (mg/L)
(c)

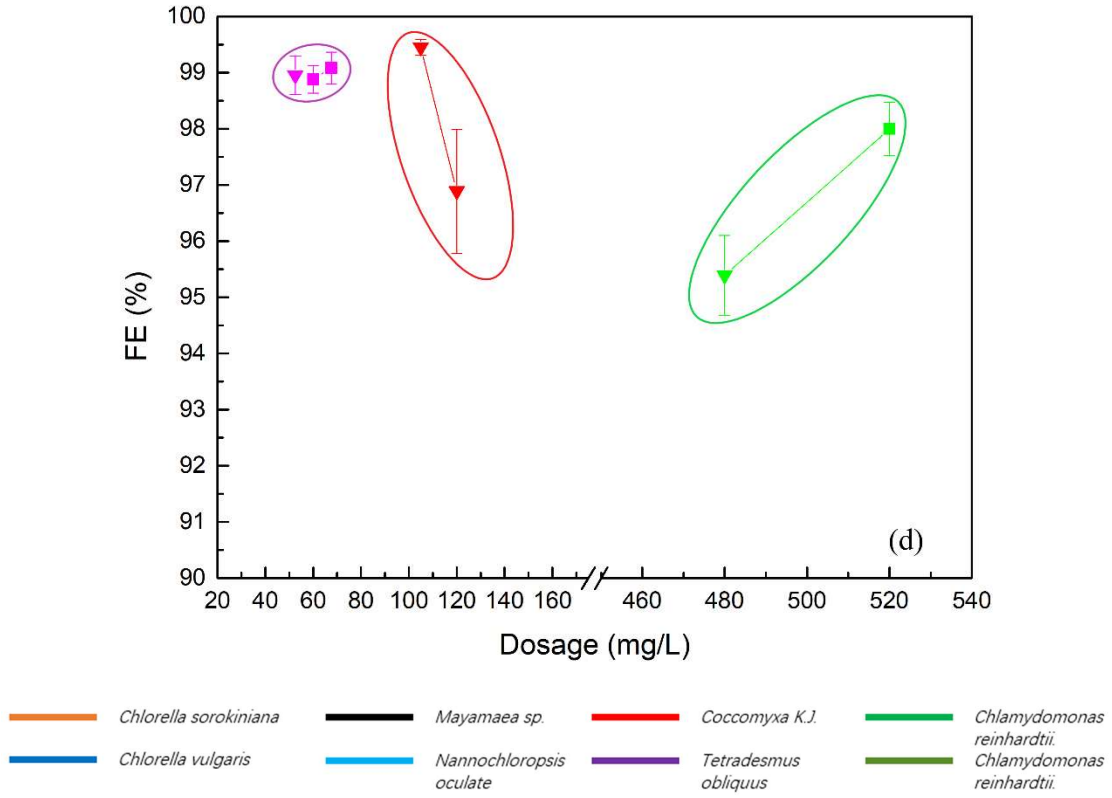

Figure 2.3 Maximum flocculation efficiency area with the corresponding flocculant dosage, a) by $AlCl_3$, b) by chitosan, c) by NaOH, a) by ACPAM

2.3.2 Settling tests and estimation of PAM demand by CST

In addition to the FE and optimal dosage, the settling time, CF, and CST are important when evaluating the total harvesting process. A shorter settling time indicates higher settling velocity. Because CF reflects the floc volume with changing biomass concentration, a higher CF means a lower floc volume with higher biomass concentration of the floc. On the one hand, settling time and CF determine the required area of the settling tank; a shorter settling time with higher CF indicates that less area is needed. On the other hand, the CF determines the volume of flocculated microalgae entering the dewatering process, which directly affects the cost of the process. In addition, the CST reflects the dewaterability of the floc, and the CST should be reduced to 20 s by adding a conditioner (such as PAM) before dewatering in filters [41]. In this study, it was found that ACPAM gave the shortest settling times (0.5–0.6 min) while flocculation by NaOH had the longest settling times (13–40 min). Species type affected the CF; *Chlorella vulgaris* had the highest CF (~50) by all three methods ($AlCl_3$, chitosan, and NaOH). The CST ranged from 7.1 to 410.3 s, and those for *Chlorella vulgaris* (9.3–10.7s) were relatively lower than the others. This indicated that conditioner addition was necessary. Because the water content of a floc greatly affects the CST (increasing water content decreases the CST), the standardized CST, defined as the CST divided by the microalgae concentration [42], was used for the comparisons. Figure 2.4 shows the standardized CST as a function of PAM addition taken from 30 literature references. The edge points were fitted by two equations ($f_1(x)$ and $f_2(x)$), and

all data were distributed between the curves of the two equations. Thus, the PAM requirement in this study was estimated by the following Equation (2.2):

$$F(x) = \frac{F_0 - f_1(0)}{f_2(0) - f_1(0)} \times (f_2(x) - f_1(x)) + f_1(x) \quad (2.2)$$

where x is the PAM dosage, F_0 is the initial standardized CST, and F is the standardized CST after adding PAM.

The solids concentration of thickened sludge is ~2% and reducing the CST to 20 s is recommended for thickened sludge dewatering [43]. The target standardized CST was 1.0 sL/g. The PAM requirements in this study were calculated by substituting equation $F(x) = 1$ into Equation (2.2). The results show that flocs were created as follows: by chitosan for *Coccomyxa sp. KJ.*, by ACPAM for *Chlamydomonas reinhardtii*, by three methods ($AlCl_3$, chitosan, and NaOH) for *Chlorella vulgaris*, by $AlCl_3$ for *Nannochloropsis oculata*, and by two methods ($AlCl_3$ and chitosan) for *Tetradesmus obliquus*. *Tetradesmus obliquus* did not require PAM addition, but all others required PAM addition ranging from 0.1 to 24 mg/g of dry algae.

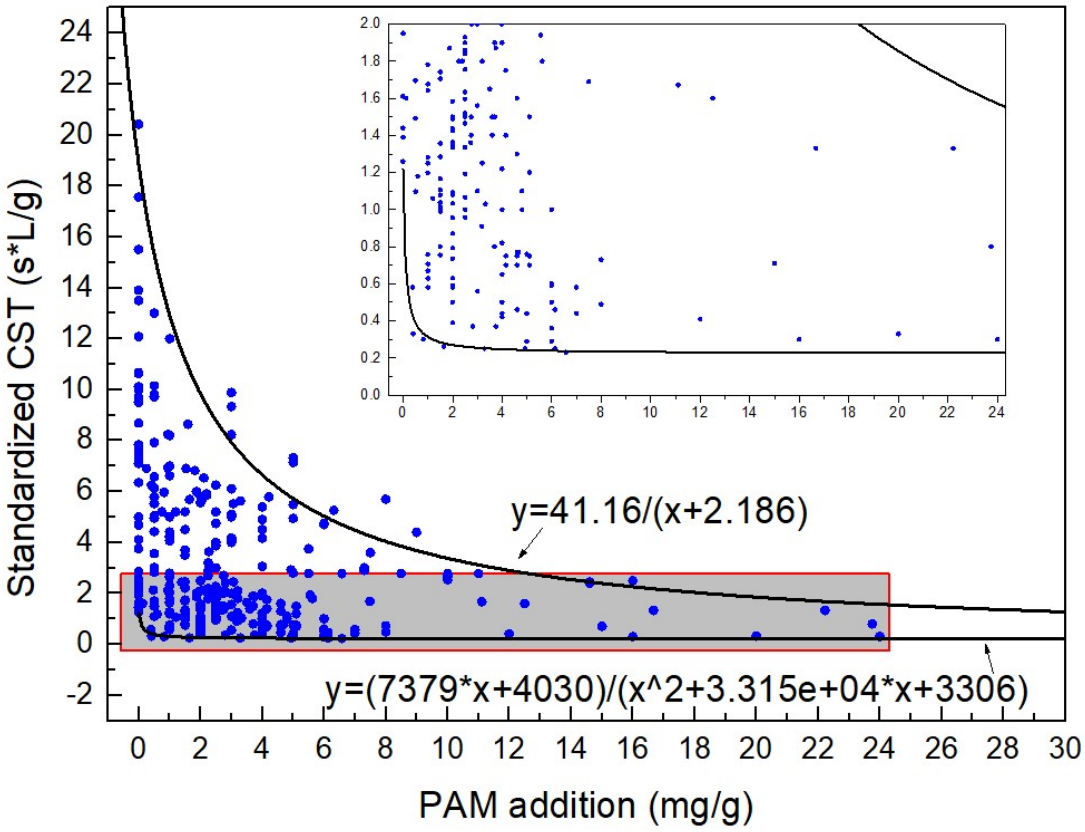

Figure 2.4 Summary of data of CST changing with PAM addition from references [S29-58].

Table 2.2 Summary of settle time, CF and CST by the 4 flocculation methods.

	Settle time (min)				CF				CST (s)			
	$AlCl_3$	Chitosan	ACPAM	NaOH	$AlCl_3$	Chitosan	ACPAM	NaOH	$AlCl_3$	Chitosan	ACPAM	NaOH
Chlorella sorokiniana	-	15	-	-	-	11.1	-	-	-	42.0±3.5	-	-
Mayamaea sp.	10	-	-	35	14.3	-	-	3.8	31.7±2.4	-	-	19.7±1.0
Coccomyxa sp. KJ	9.5	8.5	0.6	-	20.8	27.1	25	-	21.3±1.8	15.9±0.8	143.3±15.3	-
Chlamydomonas reinhardtii	20	1.4	0.5	-	6.5	12.5	25	-	40.0±5.1	234.4±20.7	7.1±1.7	-
Chlorella vulgaris	13.0	12.0	-	29	51.8	50	-	50	9.3±0.3	10.7±0.4	-	9.8±0.4
Nannochloropsis oculate	10	-	-	40	22.2	-	-	5.6	11.5±0.9	-	-	18.0±1.0
Tetradesmus obliquus	15	5	0.5	-	17.5	20	37.5	-	14.8±0.6	12.1±0.6	410.3±107.8	-
Fistulifera solaris	25	-	-	13	43	-	-	13.6	22.0±4.2	-	-	15.3±2.3

2.3.3 Life cycle assessment

The life-cycle impacts were obtained by the TRACI 2.1 method for six commonly reported impact categories: ozone depletion potential (ODP; kg CFC-11 eq), GWP (kg CO_2 eq), AP (kg SO_2 eq), EP (kg N eq), respiratory effects potential (REP; kg PM2.5 eq), and FFDP (MJ surplus) [44]. The results are shown in Figure 3. Scenario CF (cross-flow filtration) had the best profile because it had the lowest values for all six categories for eight species except for GWP, EP, and FFDP, which were were slightly higher than those of Scenario CPF (chitosan + filter press) for two species (*Coccomyxa sp*. *KJ*. and *Chlorella vulgaris*). However, the novel method of cross-flow filtration [32] has not been previously investigated; it was included in this study as a potential technique rather than for direct comparison with other approaches. Concerning the dewatering process after the four types of flocculation, filter pressing was better than centrifugation. Its advantages were much more obvious when the LCA of *Coccomyxa sp*. *KJ*. was examined. The ODP, GWP, AP, EP, REP, and FFDP of CC (chitosan + centrifugation) were 100%, 45%, 100%, 65%, 100%, and 20% (relative values), respectively, which were much higher than the corresponding 7%, 5%, 7%, 6%, 7%, and 3% of CPF (chitosan + filter press). Thus, for either type of flocculation, the filter press should be chosen as the dewatering process. The four types of flocculation could not be used for all eight species (as explained in section 2.3.1). The four marine species, which could be flocculated by NaOH, did not have good LCAs (see Figure 2.5). This was attributed to the large amount of NaOH used and corresponding HCl consumption for neutralizing. In addition, the lower CF caused by the NaOH (Table 2.2) resulted in more microalgae slurry volume to be dewatered. For the five species successfully flocculated by chitosan, the LCA of using chitosan to harvest had the best profile, despite the relatively higher AP that resulted from the use of chitosan during production. Of the remaining three species, two of them, Mayamaea sp. and Fistulifera Solaris, were difficult to flocculate by $AlCl_3$ or NaOH (high flocculant consumption), and TC (two-step centrifugation) showed better results. The remaining species (*Nannochloropsis oculata*), which was flocculated by much less $AlCl_3$, had the overall best LCA (Figure 2.5 (f)) with ODP, GWP, AP, EP, REP, and FFDP of CPF of 16%, 12%, 7%, 2%, 3%, and 18%, respectively. In summary, the best harvesting methods for each species was selected by the LCA and illustrated in Figure 4.

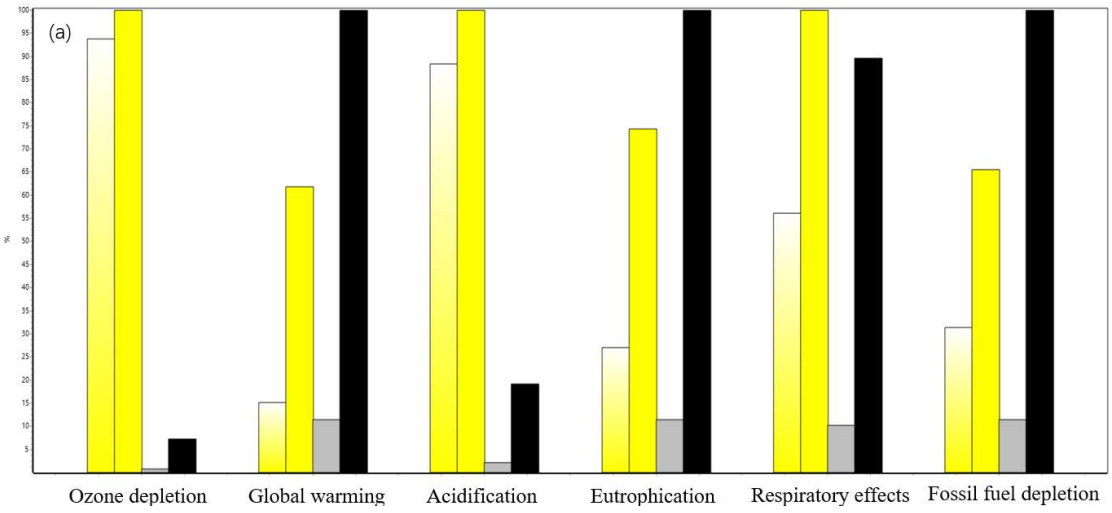
(a)
%
Ozone depletion
Global warming
Acidification
Eutrophication
Respiratory effects
Fossil fuel depletion

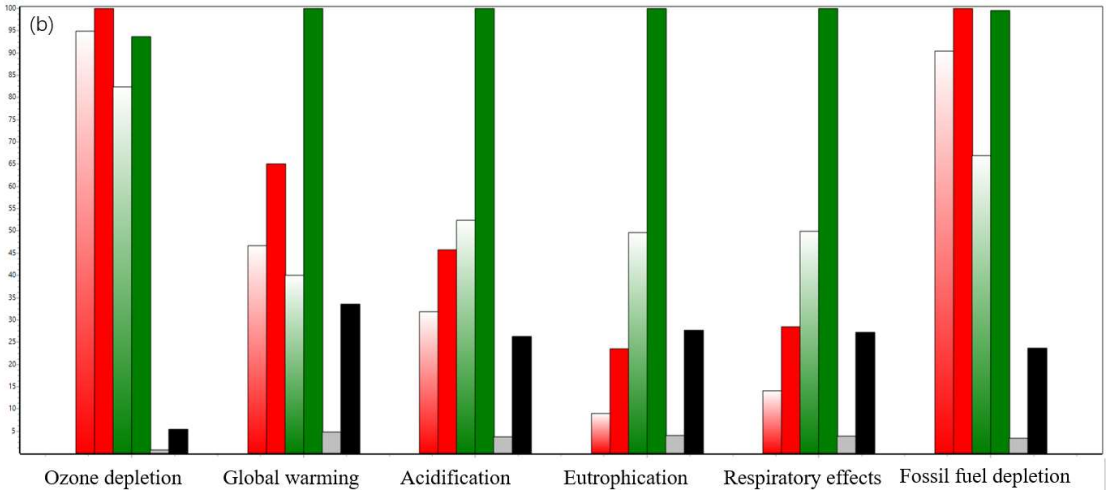
(b)
Ozone depletion
Global warming
Acidification
Eutrophication
Respiratory effects
Fossil fuel depletion

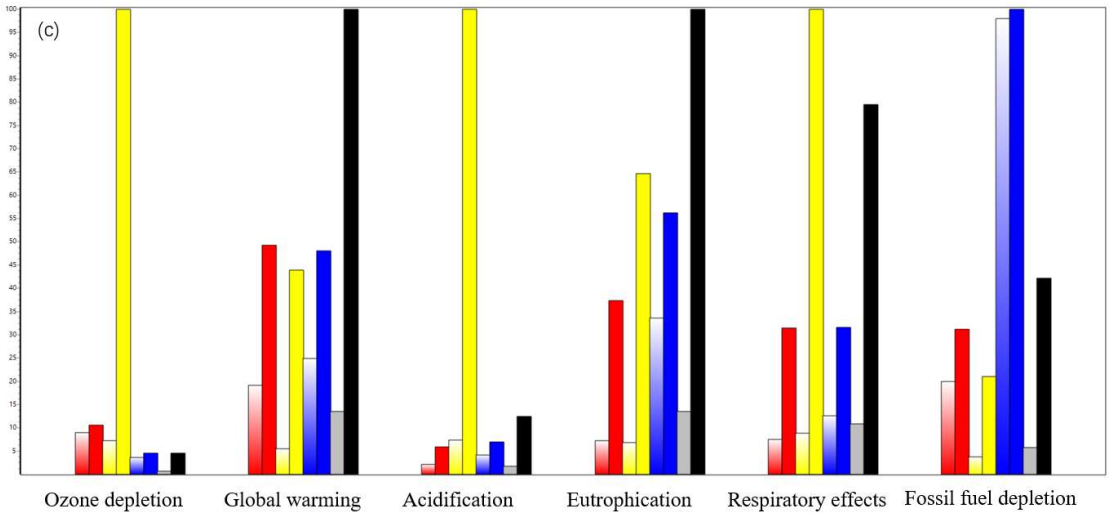
(c)
Ozone depletion
Global warming
Acidification
Eutrophication
Respiratory effects
Fossil fuel depletion

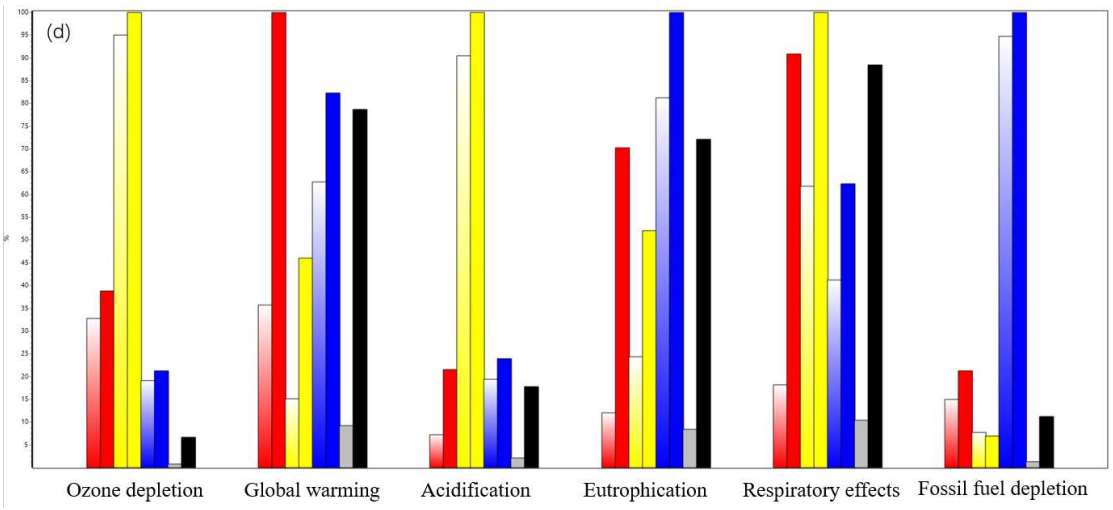
(d)
%
Ozone depletion
Global warming
Acidification
Eutrophication
Respiratory effects
Fossil fuel depletion

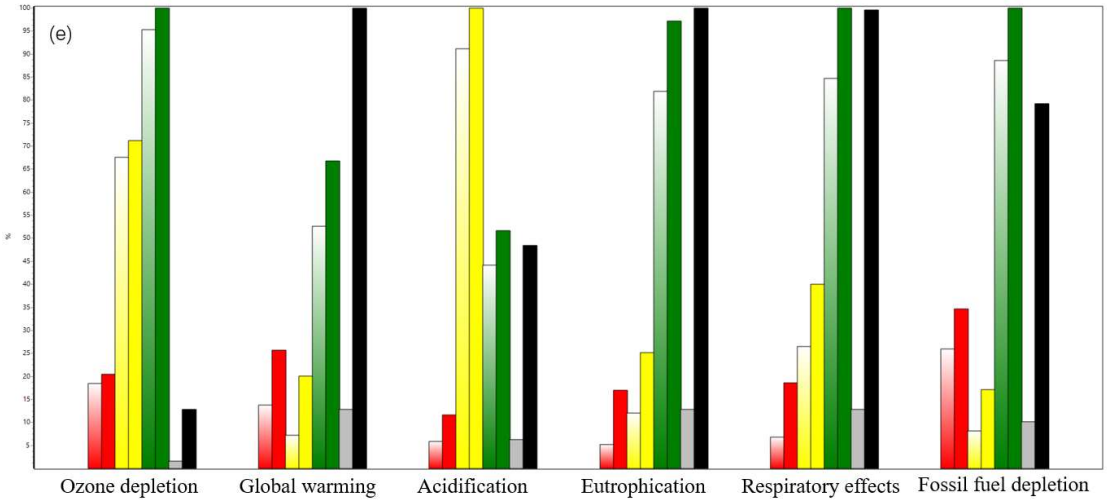
(e)
%
Ozone depletion
Global warming
Acidification
Eutrophication
Respiratory effects
Fossil fuel depletion

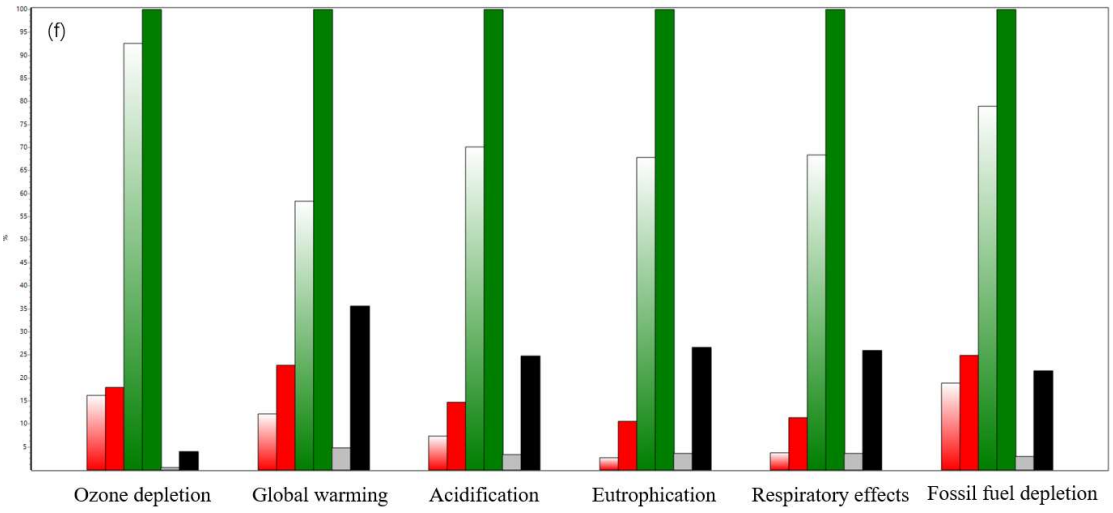
(f)
%
Ozone depletion
Global warming
Acidification
Eutrophication
Respiratory effects
Fossil fuel depletion

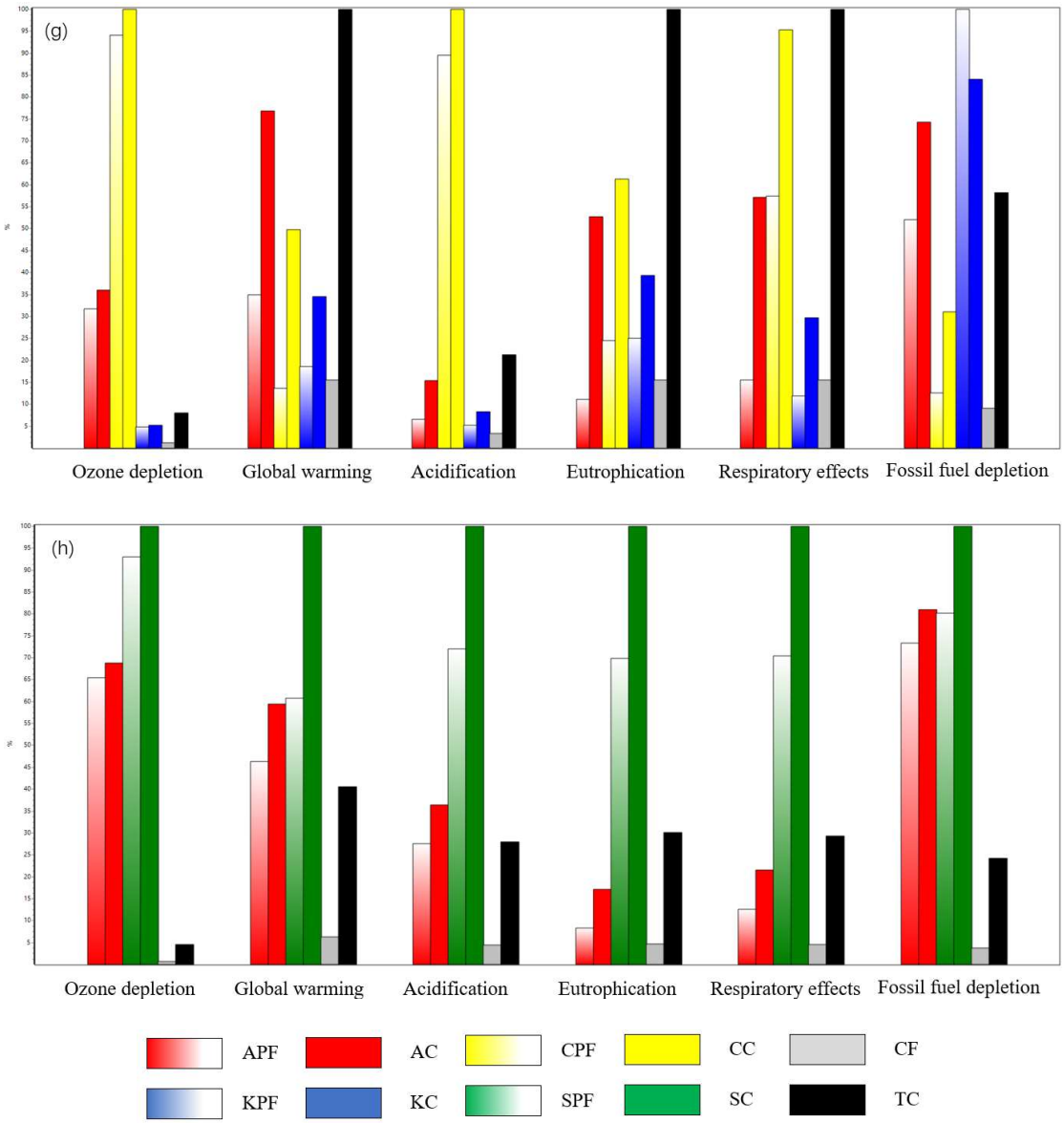

Figure 2.5 Cumulative life cycle impacts (relative value) of the 10 scenarios involved in harvesting of the 8 microalgae, a) *Chlorella sorokiniana*, b) *Mayamaea sp.*, c) *Coccomyxa sp. KJ.*, d) *Chlamydomonas reinhardtii*, e) *Chlorella vulgaris*, f) *Nannochloropsis oculate*, g) *Tetradesmus obliquus*, h) *Fistulifera solaris*.

The LCA of each species was compare, and the results for the three most important impact categories [22] (GWP, EP, and FFDP) are presented in Figure 2.6. Each category was divided into five contributing sections, i.e., "from material consumption during precondensation," "from energy consumption during precondensation," "from material consumption during dewatering," "from energy consumption during dewatering," and "from waste treatment." TC was selected to harvest *Mayamaea sp*. and *Fistulifera Solaris*, and the two species had a more notable environmental impact than the others. Because there was no material consumed by TC, the environmental impact mainly derived from the huge electricity demand, of which the precondensation step contributed 83–90% to the total environmental impact. This analysis demonstrates that using centrifugation to condense the low cell density of microalgae was an energy-

extensive process. The APF approach was the only one selected for harvesting *Nannochloropsis oculata*, and its environmental impacts derived primarily from material consumption in the flocculation step. The calculated GWP was 0.68 kg CO_2 eq, EP was 7.47×10^{-4} kg N eq, and FFDP was 0.62 MJ surplus. Although APF cannot compete with CPF, it remains an acceptable choice for marine species because chitosan and other organic flocculants are typically ineffective in salt water. Similar to APF and TC, the precondensation step also dominated the environmental impacts of CPF for the five species. In this study, *Chlamydomonas reinhardtii* was the only marine species that could be flocculated by chitosan. Its LCA was satisfactory, but its CPF was higher than that of the four freshwater microalgae. The combination with the least environmental impact was *Coccomyxa sp*. *KJ*. with CPF whose total GWP, EP, and FFDP were 0.12 kg CO_2 eq, 9.1×10^{-4} kg N eq, and 0.07 MJ surplus. All of the assessments were made on the basis of harvesting 1 kg dry weight of microalgae, but the lipids content varied with species (Figure 4). For biodiesel production from microalgae, a higher ratio of lipids content to environmental impacts is better. Based on this view, *Coccomyxa sp*. *KJ*., *Chlorella vulgaris*, and *Tetradesmus obliquus* treated by CPF have the advantage.

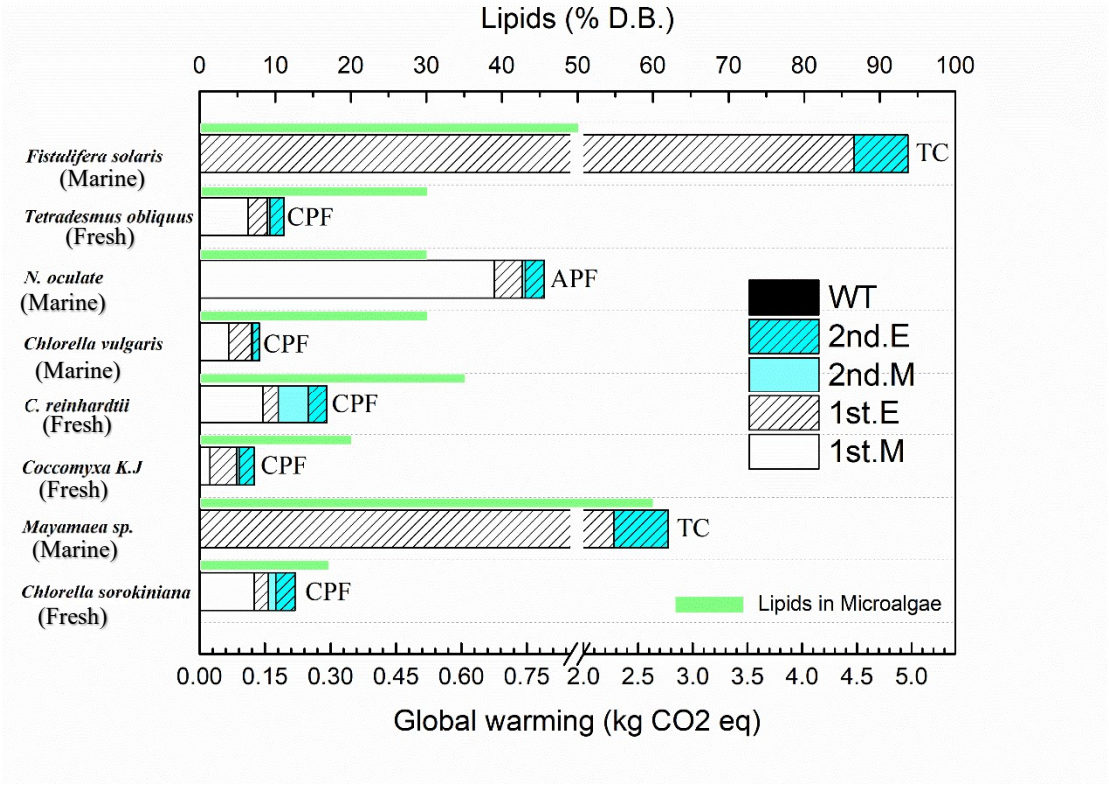

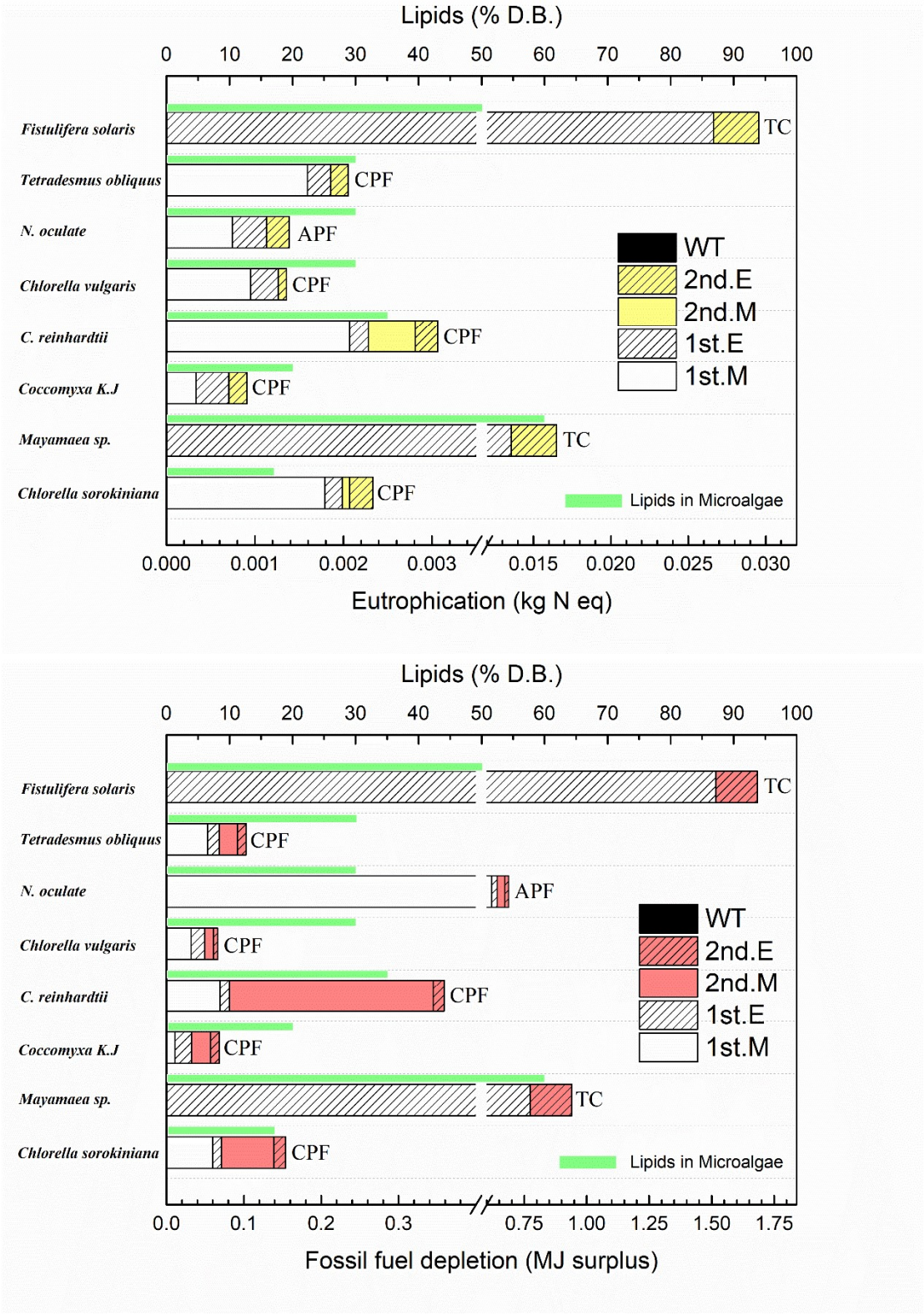

Figure 2.6 Comparison of environmental impacts of selected scenarios and contribution of various sections.

2.4 Conclusion

Flocculation experiments demonstrated that $AlCl_3$ successfully flocculated seven of the eight microalga species at a dosage ranging from 30 to 115 mg/L and provided FEs that

exceeded 90%. Chitosan had a lower dosage requirement than $AlCl_3$ but was ineffective at flocculating marine species. Among the five species (four freshwater + one marine microalgae), the dosage ranged from 7.5 to 150 mg/L with FEs of 85–99%. Only marine species could be successfully flocculated by pH adjustment (NaOH), and this occurred when the pH exceeded ~10.0. Although there were no significant differences in maximum FE observed with the NaOH, $AlCl_3$, and chitosan treatments, the dosage requirement of NaOH was much higher. Three microalgae were flocculated by ACPAM with FEs exceeding 95%; this flocculant is thus an alternative for microalgae flocculation. In addition to the FE and optimal dosage, the settling time, CF, and CST are important for evaluating the total harvesting process. The settling times with ACPAM were the shortest (0.5–0.6 min) while flocculation by NaOH gave the longest settling times (13–40 min). Flocculation of *Chlorella vulgaris* provided the highest CF of ~50. Because the CST varied with species and flocculants and spanned a wide range (7.1–410.3 s), its relationship with PAM addition to improve dewaterability was established by summarizing data from the literature. Finally, LCA analyses revealed that the CPF harvesting method was best suited to five species, TC to two others, and APF more appropriate for one species. The two LCAs for the TC scenario indicated that the electrical demand of the precondensation step contributed the vast majority (83–90%) of the total environmental impact, and using centrifugation to condense the microalgae was an energy-extensive process. APF cannot compete with CPF, but it can be used for marine species, for which chitosan is ineffective. Comparing the findings for these eight species, harvesting *Coccomyxa sp. KJ.*, *Chlorella vulgaris* and *Tetradesmus obliquus* by CPF is advantageous for biodiesel production when considering the species-dependent lipid content.

Reference

[1] Enamala, M. K., Enamala, S., Chavali, M., Donepudi, J., Yadavalli, R., Kolapalli, B., ... & Kuppam, C. (2018). Production of biofuels from microalgae-A review on cultivation, harvesting, lipid extraction, and numerous applications of microalgae. Renewable and Sustainable Energy Reviews, 94, 49-68.

[2] Sati, H., Mitra, M., Mishra, S., & Baredar, P. (2019). Microalgal lipid extraction strategies for biodiesel production: A review. Algal research, 38, 101413.

[3] Yan, N., Fan, C., Chen, Y., & Hu, Z. (2016). The potential for microalgae as bioreactors to produce pharmaceuticals. International journal of molecular sciences, 17(6), 962.

[4] Sathasivam, R., Radhakrishnan, R., Hashem, A., & Abd_Allah, E. F. (2019). Microalgae metabolites: A rich source for food and medicine. Saudi journal of biological sciences, 26(4), 709-722.

[5] Begum, H., Yusoff, F. M., Banerjee, S., Khatoon, H., & Shariff, M. (2016). Availability and utilization of pigments from microalgae. Critical reviews in food science and nutrition, 56(13), 2209-2222.

[6] Couteau, C., & Coiffard, L. (2018). Microalgal application in cosmetics. In Microalgae in health and disease prevention (pp. 317-323). Academic Press.

[7] Daneshvar, E., Zarrinmehr, M. J., Hashtjin, A. M., Farhadian, O., & Bhatnagar, A. (2018). Versatile applications of freshwater and marine water microalgae in dairy wastewater treatment, lipid extraction and tetracycline biosorption. Bioresource technology, 268, 523-530.

[8] Umar, T., & Egbu, C. (2018, July). Global commitment towards sustainable energy. In Proceedings of the Institution of Civil Engineers-Engineering Sustainability (Vol. 172, No. 6, pp. 315-323). Thomas Telford Ltd.T.

[9] Brennan, L., & Owende, P. (2010). Biofuels from microalgae—a review of technologies for production, processing, and extractions of biofuels and co-products. Renewable and sustainable energy reviews, 14(2), 557-577.

[10] Togarcheti, S. C., kumar Mediboyina, M., Chauhan, V. S., Mukherji, S., Ravi, S., & Mudliar, S. N. (2017). Life cycle assessment of microalgae based biodiesel production to evaluate the impact of biomass productivity and energy source. Resources, Conservation and Recycling, 122, 286-294.

[11] Jankowska, E., Sahu, A. K., & Oleskowicz-Popiel, P. (2017). Biogas from microalgae: Review on microalgae's cultivation, harvesting and pretreatment for anaerobic digestion. Renewable and Sustainable Energy Reviews, 75, 692-709.

[12] Adesanya, V. O., Cadena, E., Scott, S. A., & Smith, A. G. (2014). Life cycle assessment on microalgal biodiesel production using a hybrid cultivation system. Bioresource technology, 163, 343-355.

[13] Singh, K., Kaloni, D., Gaur, S., Kushwaha, S., & Mathur, G. (2020). Current research and perspectives on microalgae-derived biodiesel. Biofuels, 11(1), 1-18.

[14] Goh, B. H. H., Ong, H. C., Cheah, M. Y., Chen, W. H., Yu, K. L., & Mahlia, T. M. I. (2019). Sustainability of direct biodiesel synthesis from microalgae biomass: A critical review. Renewable and Sustainable Energy Reviews, 107, 59-74.

[15] Collotta, M., Champagne, P., Mabee, W., Tomasoni, G., Leite, G. B., Busi, L., &

Alberti, M. (2017). Comparative LCA of flocculation for the harvesting of microalgae for biofuels production. Procedia CIRP, 61, 756-760.
[16] Garzon-Sanabria, A. J., Davis, R. T., & Nikolov, Z. L. (2012). Harvesting Nannochloris oculata by inorganic electrolyte flocculation: effect of initial cell density, ionic strength, coagulant dosage, and media pH. Bioresource technology, 118, 418-424.
[17] Lam, M. K., & Lee, K. T. (2012). Microalgae biofuels: a critical review of issues, problems and the way forward. Biotechnology advances, 30(3), 673-690.
[18] Mubarak, M., Shaija, A., & Suchithra, T. V. (2019). Flocculation: An effective way to harvest microalgae for biodiesel production. Journal of Environmental Chemical Engineering, 103221.
[19] Pragya, N., Pandey, K. K., & Sahoo, P. K. (2013). A review on harvesting, oil extraction and biofuels production technologies from microalgae. Renewable and Sustainable Energy Reviews, 24, 159-171.
[20] Jankowska, E., Sahu, A. K., & Oleskowicz-Popiel, P. (2017). Biogas from microalgae: Review on microalgae's cultivation, harvesting and pretreatment for anaerobic digestion. Renewable and Sustainable Energy Reviews, 75, 692-709.
[21] Lama, S., Muylaert, K., Karki, T. B., Foubert, I., Henderson, R. K., & Vandamme, D. (2016). Flocculation properties of several microalgae and a cyanobacterium species during ferric chloride, chitosan and alkaline flocculation. Bioresource technology, 220, 464-470.
[22] Beach, E. S., Eckelman, M. J., Cui, Z., Brentner, L., & Zimmerman, J. B. (2012). Preferential technological and life cycle environmental performance of chitosan flocculation for harvesting of the green algae Neochloris oleoabundans. Bioresource technology, 121, 445-449.
[23] Chen, L., Wang, C., Wang, W., & Wei, J. (2013). Optimal conditions of different flocculation methods for harvesting Scenedesmus sp. cultivated in an open-pond system. Bioresource technology, 133, 9-15.
[24] Şirin, S., Trobajo, R., Ibanez, C., & Salvadó, J. (2012). Harvesting the microalgae Phaeodactylum tricornutum with polyaluminum chloride, aluminium sulphate, chitosan and alkalinity-induced flocculation. Journal of applied phycology, 24(5), 1067-1080.
[25] Collotta, M., Busi, L., Champagne, P., Mabee, W., Tomasoni, G., & Alberti, M. (2016). Evaluating microalgae-to-energy-systems: different approaches to life cycle assessment (LCA) studies. Biofuels, Bioproducts and Biorefining, 10(6), 883-895.
[26] Shi, R., Handler, R. M., & Shonnard, D. R. (2019). Life cycle assessment of novel technologies for algae harvesting and oil extraction in the renewable diesel pathway. Algal research, 37, 248-259.
[27] Solano–Olivares, K., Romero, R. J., Santoyo, E., Herrera, I., Galindo–Luna, Y. R., Rodríguez–Martínez, A., ... & Cerezo, J. (2019). Life cycle assessment of a solar absorption air-conditioning system. Journal of Cleaner Production, 240, 118206.

[28] DeRose, K., DeMill, C., Davis, R. W., & Quinn, J. C. (2019). Integrated techno economic and life cycle assessment of the conversion of high productivity, low lipid algae to renewable fuels. Algal research, 38, 101412.
[29] Grierson, S., Strezov, V., & Bengtsson, J. (2013). Life cycle assessment of a microalgae biomass cultivation, bio-oil extraction and pyrolysis processing regime. Algal Research, 2(3), 299-311.
[30] Muñoz, I., Rodríguez, C., Gillet, D., & Moerschbacher, B. M. (2018). Life cycle assessment of chitosan production in India and Europe. The International Journal of Life Cycle Assessment, 23(5), 1151-1160.
[31] Grima, E. M., Belarbi, E. H., Fernández, F. A., Medina, A. R., & Chisti, Y. (2003). Recovery of microalgal biomass and metabolites: process options and economics. Biotechnology advances, 20(7-8), 491-515.
[32] Liu, W., & Canfield, N. (2012). Development of thin porous metal sheet as micro-filtration membrane and inorganic membrane support. Journal of membrane science, 409, 113-126.
[33] Stephenson, A. L., Kazamia, E., Dennis, J. S., Howe, C. J., Scott, S. A., & Smith, A. G. (2010). Life-cycle assessment of potential algal biodiesel production in the United Kingdom: a comparison of raceways and air-lift tubular bioreactors. Energy & Fuels, 24(7), 4062-4077.
[34] Wu, Z., Zhang, X., Zhou, C., Pang, J. L., & Zhang, P. (2017). Adsorption neutralization model and floc growth kinetics properties of aluminum coagulants based on sips and Boltzmann equations. ACS applied materials & interfaces, 9(7), 5992-5999.
[35] Cui, Y., Yuan, W., & Cheng, J. (2014). Understanding pH and ionic strength effects on aluminum sulfate-induced microalgae flocculation. Applied biochemistry and biotechnology, 173(7), 1692-1702.
[36] Rattanakawin, C., & Hogg, R. (2001). Aggregate size distributions in flocculation. Colloids and Surfaces A: Physicochemical and engineering aspects, 177(2-3), 87-98.
[37] Roselet, F., Burkert, J., & Abreu, P. C. (2016). Flocculation of Nannochloropsis oculata using a tannin-based polymer: bench scale optimization and pilot scale reproducibility. Biomass and Bioenergy, 87, 55-60.
[38] Grima, E. M., Belarbi, E. H., Fernández, F. A., Medina, A. R., & Chisti, Y. (2003). Recovery of microalgal biomass and metabolites: process options and economics. Biotechnology advances, 20(7-8), 491-515.
[39] Feng, L., Zhao, S., Sun, S., Wang, W., Gao, B., & Yue, Q. (2015). Effect of pH with different purified aluminum species on coagulation performance and membrane fouling in coagulation/ultrafiltration process. Journal of hazardous materials, 300, 67-74.
[40] Shi, B., Li, G., Wang, D., Feng, C., & Tang, H. (2007). Removal of direct dyes by coagulation: The performance of preformed polymeric aluminum species. Journal of hazardous materials, 143(1-2), 567-574.
[41] To, V. H. P., Nguyen, T. V., Vigneswaran, S., & Ngo, H. H. (2016). A review on sludge dewatering indices. Water Science and Technology, 74(1), 1-16.

[42] Chen, Y. P., Guo, J. S., Wang, J., Yan, P., Ji, F. Y., Fang, F., & Dong, Y. (2016). A grit separation module for inorganic matter removal from activated sludge: investigation on characteristics of split sludge from the module. Environmental technology, 37(24), 3168-3176.
[43] Stefanakis, A., Akratos, C. S., & Tsihrintzis, V. A. (2014). Vertical flow constructed wetlands: eco-engineering systems for wastewater and sludge treatment. Newnes.
[44] Hasik, V., Ororbia, M., Warn, G. P., & Bilec, M. M. (2019). Whole building life cycle environmental impacts and costs: A sensitivity study of design and service decisions. Building and Environment, 163, 106316.
[45] Roy, M., & Mohanty, K. (2020). Valorization of waste eggshell-derived bioflocculant for harvesting T. obliquus: Process optimization, kinetic studies and recyclability of the spent medium for circular bioeconomy. Bioresource Technology, 123205.
[46] Shen, Y., Cui, Y., & Yuan, W. (2013). Flocculation optimization of microalga Nannochloropsis oculata. Applied biochemistry and biotechnology, 169(7), 2049-2063.
[47] Matsumoto, M., Sugiyama, H., Maeda, Y., Sato, R., Tanaka, T., & Matsunaga, T. (2010). Marine diatom, Navicula sp. strain JPCC DA0580 and marine green alga, Chlorella sp. strain NKG400014 as potential sources for biodiesel production. Applied biochemistry and biotechnology, 161(1-8), 483-490.
[48] Maltsev, Y., Maltseva, I., Maltseva, S., Kociolek, J. P., & Kulikovskiy, M. (2019). Fatty acid content and profile of the novel strain of Coccomyxa elongata (Trebouxiophyceae, Chlorophyta) cultivated at reduced nitrogen and phosphorus concentrations. Journal of phycology, 55(5), 1154-1165.
[49] Enamala, M. K., Enamala, S., Chavali, M., Donepudi, J., Yadavalli, R., Kolapalli, B.,et al. (2018). Production of biofuels from microalgae-A review on cultivation, harvesting, lipid extraction, and numerous applications of microalgae. Renewable and Sustainable Energy Reviews, 94, 49-68.
[50] Lama, S., Muylaert, K., Karki, T. B., Foubert, I., Henderson, R. K., & Vandamme, D. (2016). Flocculation properties of several microalgae and a cyanobacterium species during ferric chloride, chitosan and alkaline flocculation. Bioresource technology, 220, 464-470.

Chapter 3 Harvesting of *Nannochloropsis oculata* by chitosan and $AlCl_3$ induced flocculation: effects of cell density, salinity, and pH

3.1 Introduction

Fossil fuel contributes to nearly 80% of global energy consumption, and its use results in the release of huge amounts of greenhouse gases into the atmosphere [1][2]. To meet the growing energy demand with less CO_2 discharge, various types of renewable energy have been explored, and biofuel, including biodiesel and bio-solid fuel produced from microalgae, has attracted a great deal of attention over the last few decades because of its rapid growth rate and high per-acre yield [3]. Marine microalgae may have potential for development because cultivation does not use arable land and fresh water. After cultivation of microalgae, enormous amounts of water must be removed from aqueous suspensions for recovery of biomass. However, the low biomass concentration (0.5–5 g/L), small cell size (5–50 μm), and relative stability of microalgae in culture medium make separation a challenge [16][17]. Considering efficiency and costs, harvesting represents the bottleneck for commercial biofuel production from microalgae.

Several methods for harvesting of microalgae, including chemical flocculation, electrical processes, centrifugation, and filtration, show potential [6]. Although centrifugation and filtration can achieve high concentrations of microalgae, these processes require much more energy than flocculation processes [7]. In addition, even though electrical processes do not require addition of chemical reagents, they have high energy and equipment costs [3]. Therefore, to achieve a high concentration of microalgae at low cost, it is common to combine two or more of these methods, as reported by Schlesinger [8], to significantly reduce harvesting costs. Therefore, the harvesting process can be divided into two sequential steps: initial condensing and further dewatering. The first step increases the solid content of condensed microalgae to 1–2% through flocculation induced by addition of inorganic salt or polymer organic compounds (e.g., chitosan, polyacrylamide, starch, etc.) with gravitational sedimentation [9][10]. The volume-reduced microalgal preparation is then further dewatered to a solid content of 10–30% by filtration or centrifugation with less energy consumption during the second step [11].

The mechanism of flocculation can be summarized as follows (Fig 3.1): (a) double layer compression—addition of flocculant with the opposite charge to the microalgal cell surface increases the concentration of counter ions in the diffuse layer, and so a smaller volume of diffuse layer is needed to maintain electrostatic balance, and aggregation due to the attractive force between particles becomes dominant; (b) charge neutralization—some flocculants with a charge opposite that of the cell surface can be adsorbed at the

surface, which reduces the surface potential and destabilizes these microalgal suspensions; (c) sweep flocculation—a metal salt is added to water and precipitation of metal hydroxides is induced under optimal pH conditions, and then microalgae can be captured by the precipitates; and (d) adsorption and bridging—organic polymers attach onto the cell surface and form bridges between the microalgal cells [3,9,12].

This process is influenced by several factors, including cell density, microalgal species, growth phase, pH, and ionic strength affected by salinity. Harvesting of microalgae at the stationary growth phase has been reported to be advantageous due to the increased lipid accumulation, reduced cell mobility, and ease of flocculation at this stage [13][14]. pH also can affect flocculation by acting on the surface charge of microalgal cells, metal precipitation, and ionization of the organic polymer [15]. Salinity has a significant inhibitory effect on flocculation efficiency (FE), especially for marine species, and studies of the effects of salinity on cationic polymeric flocculant have indicated that reduction of cationic charge, rather than polymeric coiling, is the main reason for decreases in FE [16][17]. However, there have been few studies of the effects of cell density on flocculation, and the results have been inconsistent. For example, it was reported that low-cell-density cultures required five times greater $AlCl_3$ levels to achieve the same FE [16], while another study concluded that higher cell density led to a lower FE due to excessive negative charge, thus requiring more flocculant for neutralization [18]. In addition, interaction effects among these three factors in the flocculation process have not been investigated in detail.

$AlCl_3$ and Chitosan respectively are typical inorganic and organic flocculant. The investigation of these two commonly used flocculants is representative. Thus, this study was performed to evaluate the effects of three key factors, pH, cell density, and salinity, on the FE of two flocculants, $AlCl_3$ and chitosan, for marine microalgae. The independent influences of each variable were investigated using single-factor experiments, and response surface methodology (RSM) was then applied to explore their interactions. Finally, the flocculation performance of a combination of chitosan and $AlCl_3$ under different conditions was investigated. This study helps to clarify the mechanism of microalgal flocculation.

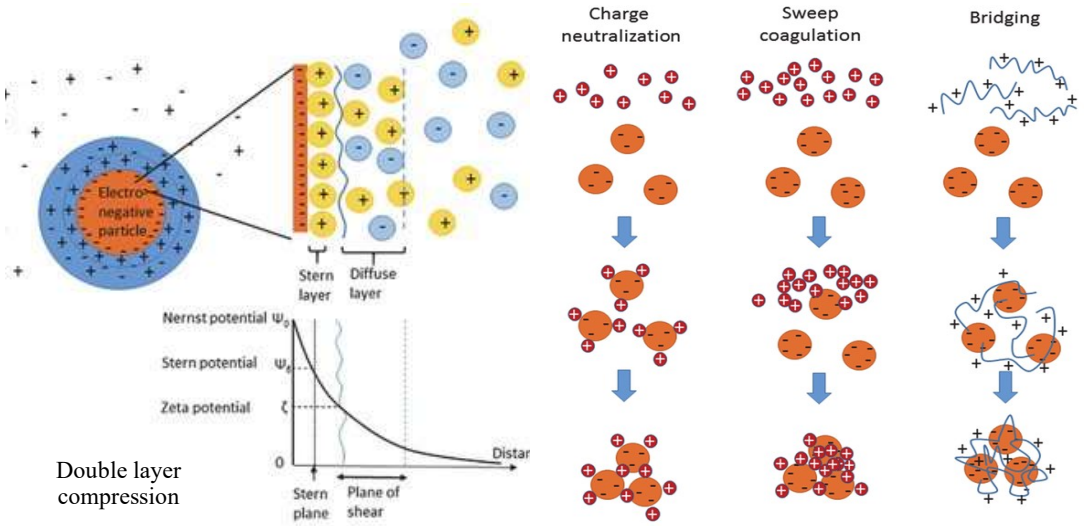

Figure 3.1 Mechanism of flocculation [51].

3.2 Material and methods

3.2.1 Strain and culture conditions

The marine microalga, *Nannochloropsis oculata*, was obtained from the Microbial Culture Collection at the National Institute for Environmental Studies (Tsukuba, Japan). This strain is a unicellular, oval-shaped, nonmobile marine microalga with a diameter of 3–8 μm. This strain was cultivated in Erdschreiber's modified (ESM) medium [19] containing $NaNO_3$ (0.12 g/L), K_2HPO_4 (5 mg/L), vitamin B_{12} (1 μg/L), biotin (1 μg/L), thiamine HCl (0.1 mg/L), Fe-EDTA (0.26 mg/L), Mn-EDTA (0.33 mg/L), Tris(hydroxymethyl)aminomethane (1 g/L) (FUJIFILM Wako Pure Chemical Corporation, Tokyo, Japan), and artificial seawater (33.4 g/L; Osaka Yakken Co., Ltd., Mino, Osaka, Japan). The microalgae were cultivated in this medium adjusted to pH 8.0 at a temperature of 20°C ± 2°C for 2 weeks to stationary phase in a 20-L bucket photobioreactor (12 h/12 h light/dark cycle).

3.2.2 Measurement of biomass concentration

Dry cell weight (DCW) in stationary phase was measured as the biomass concentration of microalgae. Using a vacuum filter, samples of 25 mL of microalgae were filtered through preweighed and deionized water-cleaned glass microfiber filter paper (GF/C, 1.2 mm, 4.7 cm; Whatman, Boston, MA, USA). Subsequently, the filters were dried in an oven at a temperature of 105°C for 24 h to a constant weight, and then cooled to room temperature for weight measurement. This process was repeated in triplicate and the results indicated a DCW of 0.64 ± 0.01 g/L of *N. oculata*.

3.2.3 Sample preparation and flocculation experimental method

To facilitate adjustment of the microalgal samples to a specific state (pH, cell density, and salinity), cultivated microalgal suspensions were centrifuged at 5000 rpm for 15 min to recover biomass. These 100× concentrated microalgae were stored at 4°C. Before the flocculation experiment, specific pH, cell density, and salinity of microalgae were obtained by mixing the concentrates and ion-exchanged water with fresh ESM medium and then adjusting the pH (37.5% HCl, 10 mol/L NaOH). Indicators of the prepared microalgae were checked using a spectrophotometer (Uvmini-1240; Shimadzu, Kyoto, Japan), pH meter (D-71S; Horiba, Kyoto, Japan), and salinometer (HI-96822; Hanna Instruments, Woonsocket, RI, USA).

Two flocculants were examined: $AlCl_3$ (inorganic salt, 30 g/L) and chitosan (organic polymer, 5 g/L dissolved in 0.2% acetic acid) (FUJIFILM Wako Pure Chemical Corporation). Flocculation experiments were performed in 100-mL beakers. After addition of flocculant, the microalgal suspensions were mixed vigorously (350 rpm) using a magnetic stirrer (MG120; Yamato Scientific Co., Ltd., Tokyo, Japan) for 2 min, followed by gentle mixing (50 rpm) for 10 min. The suspensions were subsequently allowed to settle for 15 min. The supernatant was sampled in the middle of the clarified zone and optical density (OD) was measured at 680 nm using a spectrophotometer. FE was determined in terms of absorbance using Eq. (3.1):

$$\text{Flocculation efficiency (\%)} = \left(1-\frac{\text{ODfinal}}{\text{ODinitial}}\right) \times 100 \quad (3.1)$$

where $OD_{initial}$ and OD_{final} are the OD before and after flocculation, respectively.

3.2.4 Experimental design

3.2.4.1 Single-factor experiments

Single-factor experiments were designed to investigate the individual influences of pH, cell density, and salinity on flocculation by chitosan or $AlCl_3$. The pH was adjusted using HCl or NaOH to 4.0, 5.0, 7.0, 9.0, and 10.0 with salinity fixed at 0.4 g/L and cell density fixed at 0.556 g/L. To investigate the effects of salinity, a centrifuged microalgae-to-diluent ratio of 1:99 was used with mixing of ion-exchange water with fresh ESM medium in different proportions to control final salinity at 0.4, 2.4, 4.4, 8.4, and 16.4 g/L to obtain a constant cell density of 0.556 g/L with pH set to 7.0. To investigate the effects of cell density, the microalgal concentrate-to-diluent ratio was varied to achieve cell densities of 0.278, 0.417, 0.556, 0.834, and 1.112 g/L with pH and salinity maintained at 7.0 and 0.4 g/L, respectively. During the experiments, different amounts of chitosan or $AlCl_3$ were added to the above microalgal suspensions, and FE was monitored to reflect flocculation performance. These experiments were performed in triplicate.

3.2.4.2 Evaluation of interaction effects

RSM was used to explore the influence of interactions among the three investigated variables, and a Box–Behnken design (BBD) was established for RSM. For each of the flocculants, a total of 45 experimental runs (including triplicate replicates) were conducted, and the results were processed to fit the quadratic polynomial equation described in Eq. (3.2):

$$y = \beta_0 + \sum_{i=1}^{k} \beta_i X_i + \sum_{i=1}^{k} \beta_{ii} X_i^2 + \sum_{1 \le i \le j}^{k} \beta_{ij} X_i X_j + \varepsilon \quad (3.2)$$

where β_0 is a constant, β_i and β_{ii} are linear and quadratic coefficients, respectively, β_{ij} is an interaction coefficient, X_i and X_j represent different variables, ε represents the experimental residual, and y is the response variable (FE).

In the BBD, pH ranged from 5.0 to 9.0, cell density ranged from 0.417 to 0.695 g/L, and salinity ranged from 0.2 to 8.2 g/L. Chitosan and $AlCl_3$ were added at concentrations of 1.5 and 30 mg/L, respectively. The experimental design is shown in Tables S4 and S5 in the Supporting Information.

3.2.5 Combination of chitosan and $AlCl_3$

To investigate the flocculation performance of a combination of chitosan and $AlCl_3$, three sets of experiments with a two-level central composite design (CCD) consisting of cube points, axial points, and center points were conducted under the following conditions to fit Eq. (2): low, pH 5.0, salinity 0.4 g/L, cell density 0.417 g/L; medium, pH 7.0, salinity 4.4 g/L, cell density 0.556 g/L; and high, pH 9.0, salinity 8.4 g/L, cell density, 0.695 g/L. To assess the synergistic effects of the two flocculants, the center point was set as the sum of 50% of the dosage of each flocculant individually used to

obtain a FE of ~90%. Because the order of addition of the two flocculants significantly affects floc formation and FE [10], $AlCl_3$ was added first based on preliminary experiments.

3.2.6 Statistical analysis

All data were calculated for each replicate and the results are presented as the means ± standard deviation. Differences were compared between groups by one-way analysis of variance (ANOVA) followed by Fisher's least significant difference test with Minitab 18 (Minitab, State College, PA, USA). In all analyses, $P < 0.05$ was taken to indicate statistical significance.

3.3 Results and discussion

3.3.1 Single-factor experiments

3.3.1.1 Influence of pH on flocculation efficiency using $AlCl_3$ and chitosan

To determine the influence of pH on the effects of the two flocculants, $AlCl_3$ and chitosan, the salinity and cell density of microalgae were held constant in each flask and different amounts of $AlCl_3$ or chitosan were added to the cultures. Because no obvious flocculation was observed at pH 4.0–10.0 without flocculants, we ignored the effects of autoflocculation induced by pH in these experiments [16][20].

The effects of pH on $AlCl_3$ are shown in Fig. 3.2(a). $AlCl_3$ showed high flocculation performance within the pH range of 7.0–10.0, and FE > 90% was achieved after addition of nearly 50 mg $AlCl_3$/g biomass in this range. However, at pH 5.0, an approximately 5× higher dosage was needed to obtain the same FE of ~90%, and at pH 4, FE reached a maximum of just 70.4% ± 8.0% at 432.0 mg/g biomass. Therefore, $AlCl_3$ showed better flocculation performance under alkaline conditions, with both a decrease in maximum FE and an increase in optimal dosage under acidic conditions. In contrast, chitosan showed better performance under acidic conditions (Fig. 3.2(b)). A level of 2.5 mg chitosan/g biomass was sufficient to achieve FE of ~95% when pH was adjusted within the range of 4.0–7.0. However, 2.5 mg chitosan/g biomass was not sufficient to induce flocculation at pH 9.0 or 10.0. Unlike the effect of pH on flocculation performance of $AlCl_3$ with regard to both maximum FE and optimal dosage, only a change in optimal dosage of chitosan was observed after increasing pH to 9.0 and 10.0. Specifically, 8.1 mg chitosan/g biomass was required to reach a maximum FE of 95% at pH of 9.0, and such a high FE could not be obtained unless the dosage reached 27.0 mg/g biomass at pH 10.0. In addition, when the dosage exceeded the optimal value, a sharp decline in FE was observed at all pH values due to charge reversal of the microalgal cell surface [21] or competition between cell surface adsorption and cell–flocculant–cell bridge formation caused by an excessive dosage of chitosan [22].

The effects of pH on the performance of both flocculants can be explained by their mechanism of action. As aluminum (Al) salt is added to water, hydrolysis and polymerization form a series of Al species, including monomeric Al species (Al_a) (e.g.,

Al^{3+}, $Al(OH)^{2+}$, $Al(OH)_2^{+}$, $Al(OH)_3$, and $Al(OH)_4^{-}$, dimeric $Al_2(OH)_2^{4+}$, trimeric $Al_3(OH)_4^{5+}$, some small polymers, and rapid reactive surface species also classified into this category); medium polymeric species (Al_b) with molecular weights ranging from 500 to 3000 Da; and large polymeric or colloidal species (Al_c) with molecular weights > 3000 Da [23]. $AlCl_3$ forms primarily Al_a species, which are sensitive to pH value, as well as small amounts of Al_b and no Al_c, both of which are rarely affected by pH [24]. At pH < 3.0, Al is mainly present in solution in the form of Al^{3+}, and the main flocculation mechanism involves double-layer compression and charge neutralization in this pH range. With increasing pH, Al^{3+} is hydrolyzed into $Al(OH)^{2+}$ and $Al(OH)_2^{+}$, and some polymerization occurs; thus, adsorption/bridging becomes the main flocculation mechanism. With further increases to alkaline pH, Al species transform into $Al(OH)_3$ precipitate, and sweep flocculation becomes the main mechanism of flocculation [25]. Therefore, the low flocculation performance of $AlCl_3$ at pH 4.0 in this study could be ascribed to the restriction of Al^{3+} hydrolysis, and high dosages were required if flocculation only occurred via the double-layer compression with charge neutralization mechanism. With increases to pH 5.0 and 7.0, adsorption/bridging became more dominant, with lower dosage requirements and higher FE. With a further increase to pH 10.0, the appearance of sweep flocculation prevented a decrease in flocculation performance. These findings are in agreement with previously reports [26,27].

The influence of pH on the flocculation effect of chitosan is related to changes in the charge density and solubility of chitosan. Under acidic conditions, chitosan is positively charged with a high charge density, and these charged functional groups keep the molecular structure of chitosan as a linear chain [28][29], which is beneficial for charge neutralization and adsorption/bridging. The positive charge is slowly reduced with increasing pH to alkaline conditions. However, the solubility of chitosan decreases with increasing pH and even becomes insoluble above pH 7.0 [30]. In the present study, increasing the dosage of flocculant achieved the same maximum FE as under acidic conditions even at pH 10.0. This indicated that additional chitosan could compensate for the effects of high pH, mainly because the function of chitosan was not completely inhibited by basic pH, and chitosan still possessed some positive charges.

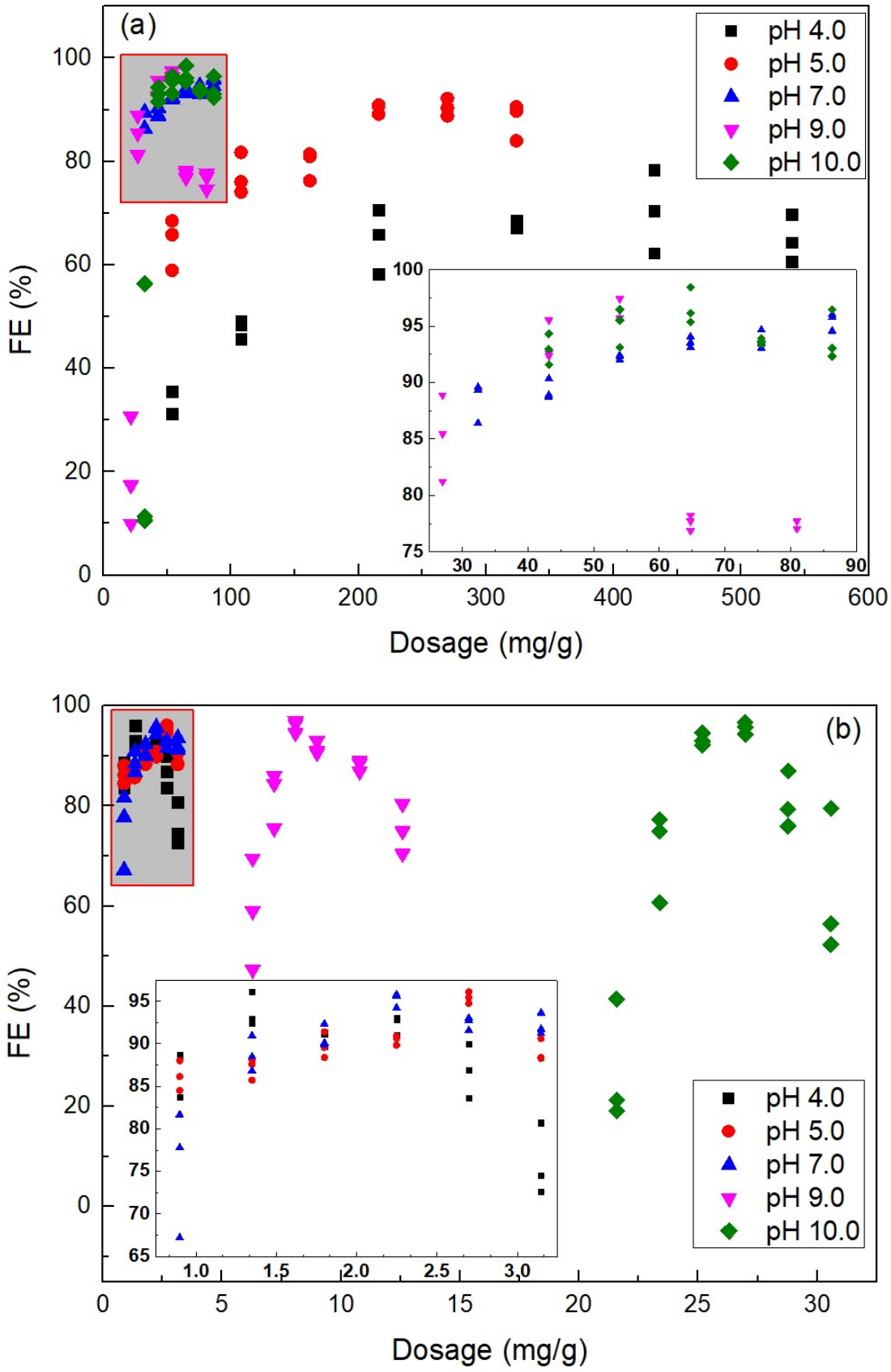

Fig. 3.2. Effects of pH on the flocculation efficiency (FE) of (a) $AlCl_3$ and (b) chitosan with salinity fixed at 0.4 g/L and cell density fixed at 0.556 g/L.

3.3.1.2 Influence of salinity on flocculation efficiency using $AlCl_3$ and chitosan

The pH and microalgal cell density were held constant to investigate the influence of salinity on the FE of $AlCl_3$ and chitosan. Figure 3.3(a) shows the FE of microalgal suspensions in the presence of $AlCl_3$ at different dosages under salinity conditions of 0.4–16.4 g/L. Flocculation was observed under salinity of 16.4 g/L with a critical dosage (i.e., the lowest dosage that induced flocculation) of 16.2 mg/g biomass, whereas this dosage did not induce flocculation at other salinity levels. Three groups (salinity of 2.4, 4.4, and 8.4 g/L) started to show flocculation when the $AlCl_3$ dosage was increased to 21.6 mg/g biomass, while no flocculation was observed until the dosage was increased to 32.4 mg/g biomass for salinity of 0.4 mg/L. These observations indicated that a lower dosage of $AlCl_3$ was required to induce flocculation under conditions of higher salinity. However, aside from the effect on the critical dosage of $AlCl_3$, the positive effect of salinity on $AlCl_3$ was otherwise limited. Only slight differences were observed among salinity values of 0.4–4.4 g/L above the critical dosage, for instance, the average FE under salinity of 4.4 g/L was just ~3% higher than under salinity of 0.4 and 2.4 g/L (both almost equivalent at each point) over the $AlCl_3$ concentration range of 32.4–75.6 mg/L. Increasing salinity to 8.4 g/L resulted in a decrease of ~8.6% in the average FE compared to 4.4 g/L, indicating an inhibitory effect on $AlCl_3$. Notably, a sharp decline in FE caused by a high $AlCl_3$ dosage (> 32.4 mg/g biomass) was observed at salinity of 16.4 g/L, suggesting that the inhibition became significant under high-salinity conditions.

Unlike $AlCl_3$, the flocculation performance of chitosan decreased monotonously with increasing salinity (Fig. 3.3(b)). After addition of 2.25 mg chitosan/g biomass, FE reached a maximum of 95.2% ± 0.85% under salinity of 0.4 g/L. The maximum FE decreased slightly to 93.5% ± 0.7% and 86.8% ± 2.1% under salinity conditions of 2.4 and 4.4 g/L, respectively. Progressively greater degrees of reduction in FE were seen with further increases in salinity, and the maximum FE was ~20% at salinity of 16.4 g/L. The above findings indicate that chitosan can tolerate salinity up to 4.4 g/L, while higher salinity strongly attenuates, and even blocks, the flocculation performance of chitosan.

Several studies have focused on the mechanism underlying the influence of salinity, with regard to ionic strength or concentration, on the flocculation performance of Al^{3+}. However, the conclusions have been inconsistent. Zeta potential was measured with FE under different salinity conditions and the results indicated that the thickness of the diffuse double layer decreased with increasing ionic strength (i.e., increasing salinity), and improved microalgal flocculation performance of Al^{3+} [31]. Similarly, compressing the double layer (i.e., reduction of zeta potential) by adding NaCl promoted coagulation by overcoming the repulsive energy barrier between particles when using Al salts as flocculants [32,33,34]. Zhao [35] reported that the same mechanism was also applicable to the flocculant $TiCl_4$. However, some conflicting reports by other authors suggested that compression of the double layer was impeded and adsorption/bridging was the main mechanism active when salinity exceeded a certain value. A previous report suggested that the FE of $AlCl_3$ decreased with increasing ionic strength (i.e., increasing salinity) because the hydrolysis of Al species decreased with increasing ionic strength

[36]. This mechanism was suggested to be responsible for the slight decrease of FE in high-salinity medium [4][37]. Furthermore, competitive surface adsorption of Na^+ on the Al^{3+} flocculant was proposed as another explanation for the decline of FE under conditions of high salinity [38]. In this study, salinity not only improved the flocculation performance of $AlCl_3$, as indicated by the lower critical dosage for higher salinity, but salinity exceeding 8.4 g/L also showed an inhibitory effect with a decrease in maximum FE. Therefore, we speculated that both mechanisms were active in this system, with masking and screening of the polymer functional groups, and inhibition becoming predominant at salinity > 8.4 g/L.

The mechanism for chitosan is relatively clear. The chitosan molecule, which is highly hydrated and has an extended linear structure in low-ionic-strength medium becomes coiled with masking of functional groups and loss of its configuration in high-ionic-strength medium, preventing chitosan from bridging among particles [39,40,41]. Giraldo [42] reported that the more fundamental reason for the observed effects was that high salinity lowered the cationic charge. The poor flocculation performance of chitosan under conditions of high salinity (8.4 and 16.4 g/L) in this study could be explained by this mechanism.

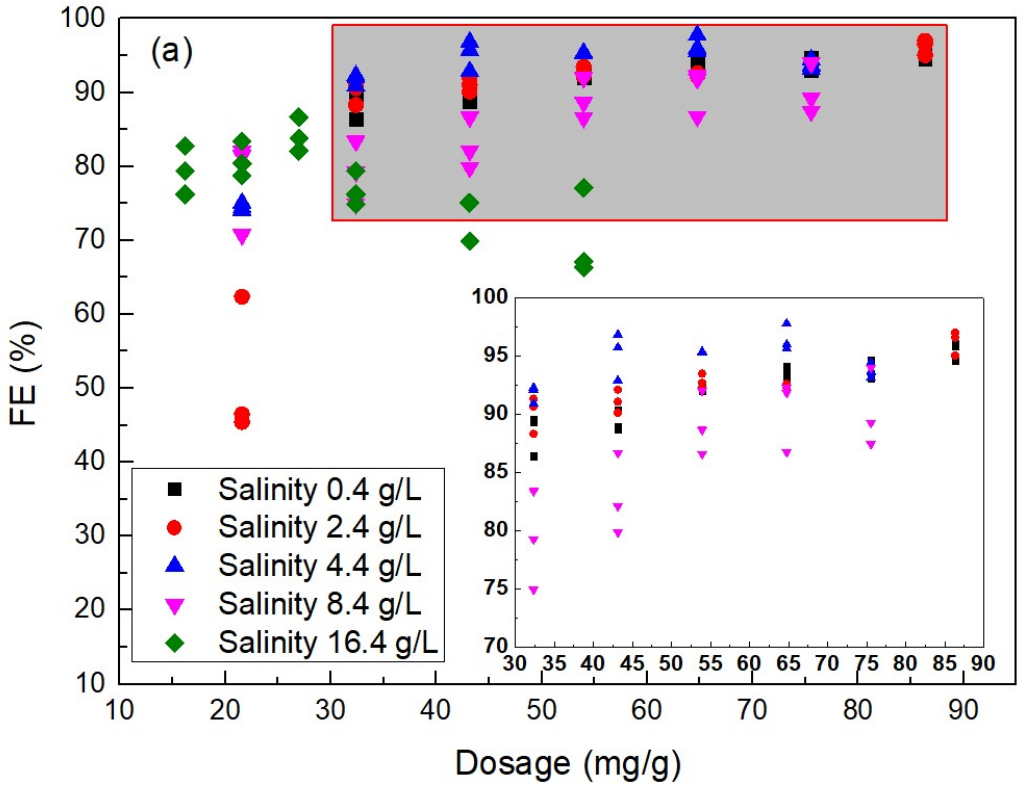

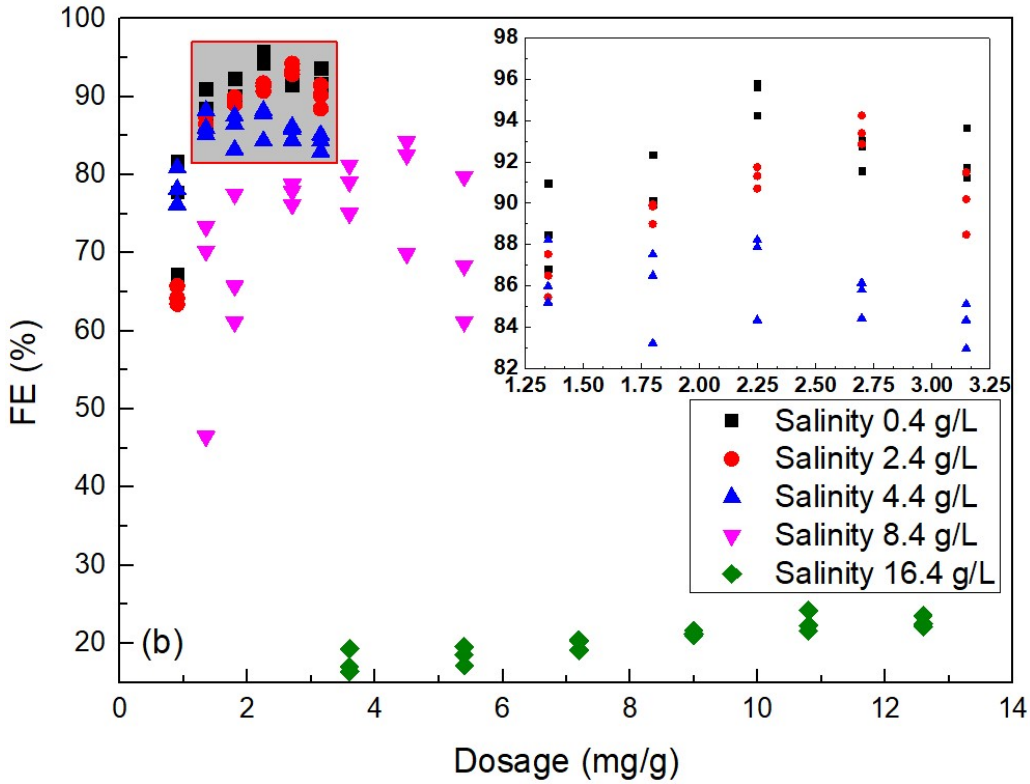

Fig. 3.3. Effects of salinity on the flocculation efficiency (FE) of (a) $AlCl_3$ and (b) chitosan with pH fixed at 7.0 and cell density fixed at 0.556 g/L.

3.3.1.3 Influence of cell density on flocculation efficiency using $AlCl_3$ and chitosan

The effects of cell density are shown in Fig. 3.4 (relative values) and Fig. 3.5 (absolute values). Generally, both $AlCl_3$ and chitosan induced considerable flocculation under all cell density conditions examined in these experiments, and higher FE with the same dosage of flocculant (mg/g biomass) was observed with higher cell density (Fig. 3.4). The maximum FE of $AlCl_3$ slowly increased from ~93% to 99% with increasing cell density, whereas chitosan showed a more obvious increase from ~84% to 99% (Fig. 3.5). Fig. 3.5 also presents the relationship between cell density and optimal dosage (absolute value). The results showed that the optimal dosage of $AlCl_3$ increased by 3.7 times when cell density was increased from 0.278 to 0.556 g/L, but remained constant at ~26 g/L above a cell density of 0.556 g/L, which was similar to previous findings [43]. Chitosan showed a linear relationship between optimal dosage and cell density within the range examined. As cell density increased 4 times from the lowest to highest tested concentration, the optimal chitosan dosage only increased 2 times (Fig. 3.5). This linear relationship was consistent with a previous study of two types of cationic polymer flocculant [44].

These findings illustrate that it is easier to harvest microalgae at high cell densities due to the higher chance of cells colliding and aggregating. In addition, at a high cell density, cells coagulated by flocculant could further capture the remaining cells, thereby improving FE via the sweep mechanism [44]. In this study, at cell densities above 0.556 g/L, the absolute optimal dosage of $AlCl_3$ was independent of cell density, indicating that the thickness of the diffuse double layer is mainly dependent on the dosage of Al^{3+}

rather than cell density; therefore, there is no need to supply additional flocculant at higher cell density. Finally, the experiments also indicated that chitosan interacted efficiently with microalgae and had a probability of attracting more cells at higher cell density, which was in agreement with previous research [45].

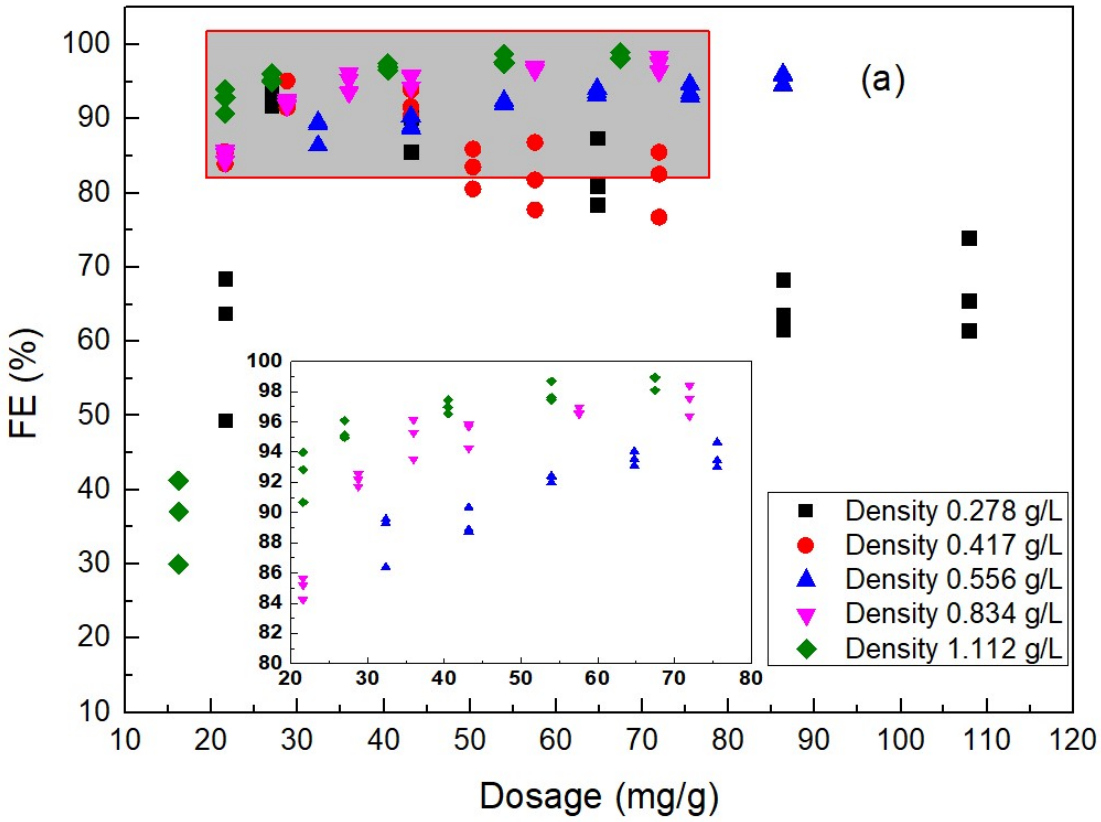

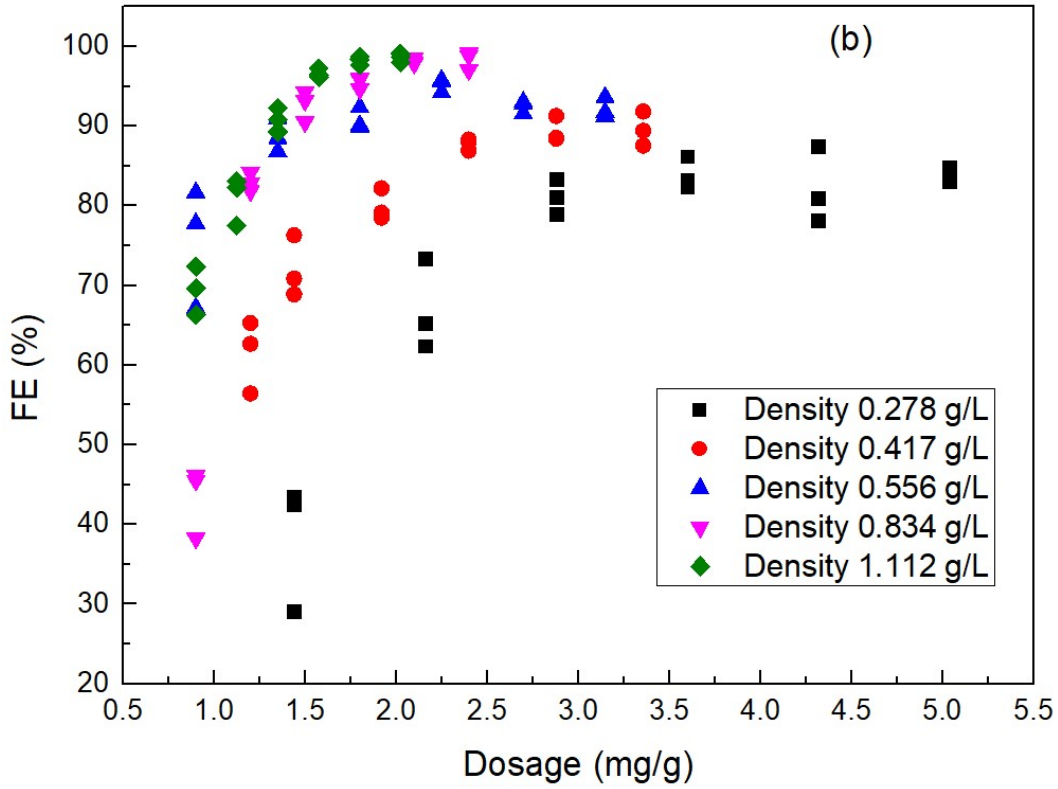

Fig. 3.4. Effects of cell density on the flocculation efficiency (FE) of (a) $AlCl_3$ and (b) chitosan with pH fixed at 7.0 and salinity fixed at 0.4 g/L.

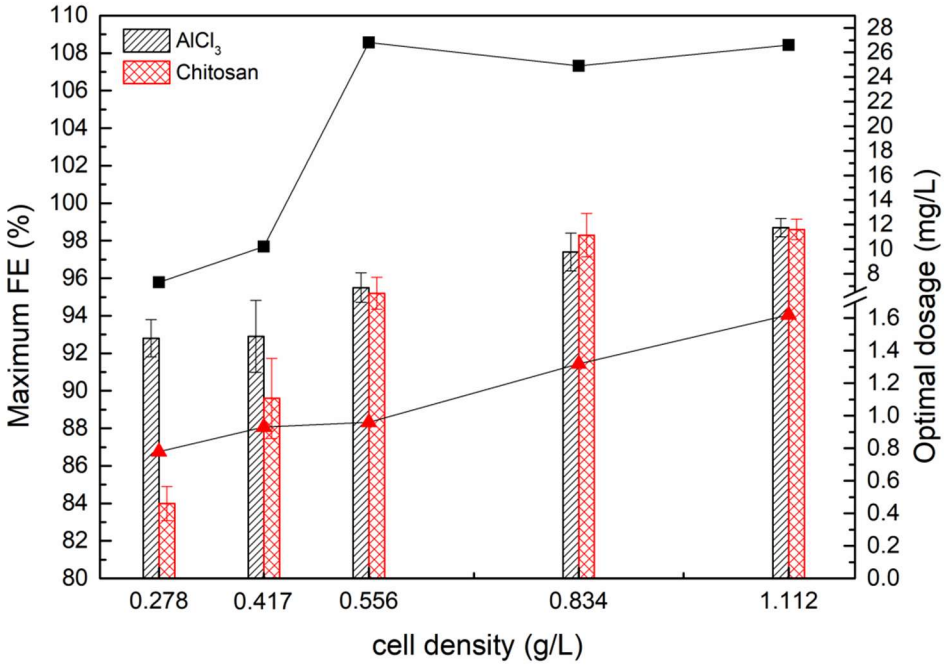

Fig. 3.5. Relationship between cell density and maximum flocculation efficiency (FE) and the optimal dosage.

3.3.2 Interaction effects

3.3.2.1 Interaction effects on $AlCl_3$ flocculation efficiency

Based on the experimental results presented in Section 3.3.1, a BBD with three levels (−1, 0, +1) of three factors (pH, salinity, cell density) was designed with pH 7.0, salinity of 4.4 g/L, and cell density of 0.834 g/L as the respective central points (Table S4). The fitted quadratic polynomial equation for FE with $AlCl_3$ at a concentration of 30 mg/L is shown below as Eq. (3.3):

$$\text{FE}\ (\%) = -754.7 + 187.67[\text{pH}] + 6.65[\text{salinity}] + 331.7[\text{cell density}] - 10.908[\text{pH}]^2 - 0.0669[\text{salinity}]^2 - 108.4[\text{cell density}]^2 - 0.100[\text{pH}][\text{salinity}] - 21.41[\text{pH}][\text{cell density}] - 8.65[\text{salinity}][\text{cell density}] \quad (3.3)$$

Table 3.1. Analysis of variance for the response surface quadratic model referring to $AlCl_3$

Source	DF	Adj SS	Adj MS	T-value	F-value	*P*-value
Model	9	54779.5	6086.6		287.66	< 0.0001
Linear	3	30135.7	10045.2		474.75	< 0.0001
pH	1	26583.8	26583.8	35.45	1256.37	< 0.0001
Salinity	1	1248.7	1248.7	−7.68	59.01	< 0.0001
Cell density	1	2303.3	2303.3	−10.43	108.85	< 0.0001
Square	3	21449.0	7149.7		337.90	< 0.0001
pH × pH	1	21089.5	21089.5	−31.57	996.71	< 0.0001
Salinity × salinity	1	12.7	12.7	−0.77	0.60	0.4438
Cell density × cell density	1	777.8	777.8	−6.06	36.76	< 0.0001
Two-way interaction	3	2817.3	939.1		44.38	< 0.0001
pH × salinity	1	7.7	7.7	−0.60	0.36	0.5507
pH × cell density	1	1700.0	1700.0	−8.96	80.34	< 0.0001
Salinity × cell density	1	1109.6	1109.6	−7.24	52.44	< 0.0001

Table S4 also shows a comparison between the means of observed values and predicted values according to Eq. (3). The coefficient of determination (R^2) was 0.987, indicating a close correlation between observed versus predicted results, and a good model fit. ANOVA for the BBD is shown in Table 3.1. The linear terms [pH], [salinity], and [cell density], square terms $[\text{pH}]^2$ and $[\text{cell density}]^2$, and two-way interaction terms [pH][cell density] and [salinity][cell density] were highly significant ($P < 0.0001$), while $[\text{salinity}]^2$ and [pH][salinity] were not significant ($P \geq 0.05$).

Considering the T-values of the linear and square terms, where positive (negative) T-values indicate positive (negative) correlations of factors with FE, respectively, the independent influences of these three factors on FE are shown in Fig. 3.6; these results were consistent with the results presented in Section 3.3.1. For example, the positive T-value of [pH] and negative T-value of $[\text{pH}]^2$ indicated that the effects of pH on FE may be not monotonous, and Fig. 3.6(a) and Fig. 3.6(c) show that FE increased markedly with increasing pH over the pH range 5.0–8.0, and then became stable or decreased

slightly at pH 8.0–9.0, similar to the conclusions presented in Section 3.3.1.1.

It should be noted that the two-way interaction analysis reflected two interaction effects: [salinity][cell density] and [pH][cell density]. These two terms had negative effects on FE. As shown in Fig. 3.6(b), both over the studied cell density range (0.556–1.112 g/L) with low salinity or over the studied salinity range (0.4–8.4 g/L) with low cell density, FE > 90% could be obtained after addition of a given dosage of $AlCl_3$. However, increases in both salinity and cell density resulted in a significant decrease in FE to ~60%. Thus, $AlCl_3$ showed good flocculation performance under conditions of either high cell density or high salinity but poor performance with both high cell density and high salinity together. This could be explained by the different key mechanisms of flocculation under conditions of high cell density or high salinity as described in Section 3.3.1. The key to obtaining a FE of 90% at high salinity was the presence of polymerized high-charge Al species (e.g., $Al_2(OH)_2^{4+}$ and $Al_3(OH)_4^{5+}$) attached to the cell surface; therefore, a certain ratio of these Al species to cells is required [4][37]. The FE was maintained above 90% at a cell density of 0.556–1.112 g/L because double layer compression was the key mechanism and it induced flocculation as long as 30 mg/L $AlCl_3$ was added independently of cell density [43]. In summary, under conditions of high cell density with high salinity, flocculation should depend on the adsorption mechanism of these polymerized high-charge Al species, sensitive to the ratio of Al to cells; therefore, simultaneously increasing cell density and salinity decreases FE.

Fig. 3.6(c) shows the relatively weak interaction effect of [pH][cell density]. This interaction effect can be divided into two stages: (1) at pH 5.0–6.5, FE was mainly affected by pH and was not related to cell density (i.e., nearly the same FE was obtained at the same pH but various cell densities); (2) at pH 6.5–9.0, the influence of cell density became increasingly significant, and FE tended to decrease with increasing cell density from 0.556 to 1.112 g/L (FE decreased from > 95% to ~60% at pH 9.0). This could be ascribed to changes in the distribution of Al species under different pH conditions, as described in Section 3.1.1. The different Al species distributions indicate that double layer compression, which is independent of cell density, was the main flocculation mechanism at low pH of 5.0, whereas the mechanism shifted to charge neutralization or adsorption/bridging with increasing pH, related to the ratio of $AlCl_3$ to cells [24].

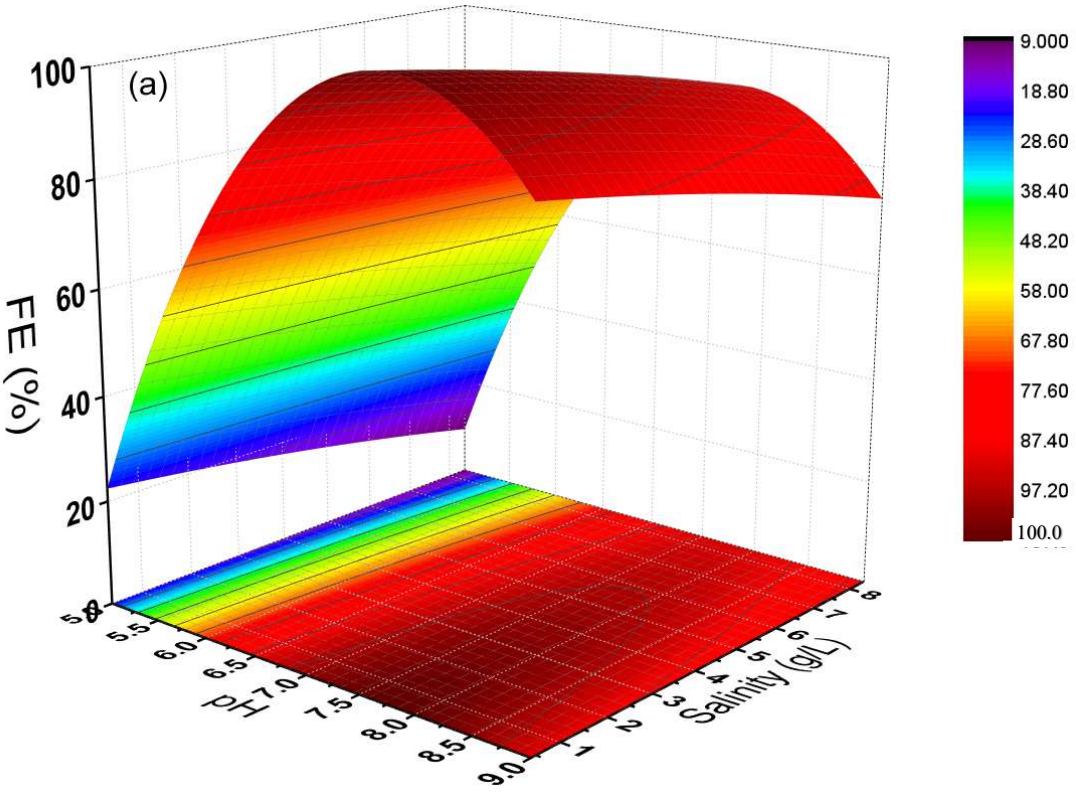
(a)
FE (%)
100
80
60
40
20
pH
5.5
6.0
6.5
7.0
7.5
8.0
8.5
9.0
Salinity (g/L)
1
2
3
4
5
6
7
8
9.000
18.80
28.60
38.40
48.20
58.00
67.80
77.60
87.40
97.20
100.0

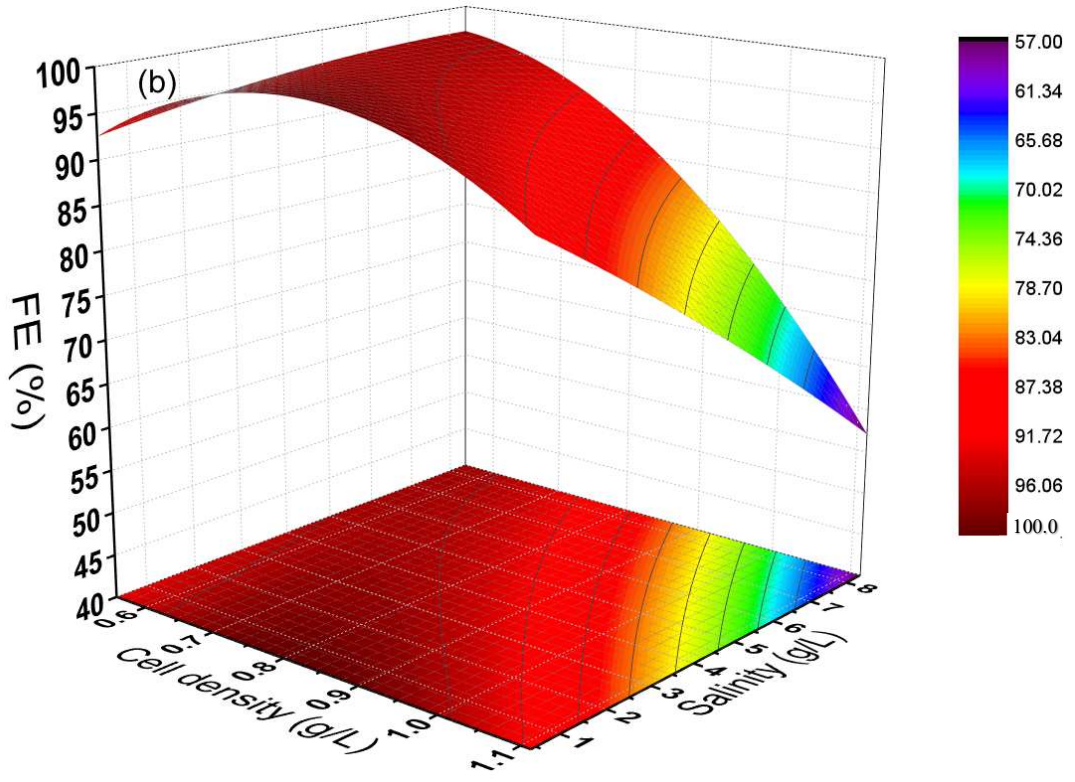
(b)
FE (%)
100
95
90
85
80
75
70
65
60
55
50
45
40
Cell density (g/L)
0.6
0.7
0.8
0.9
1.0
1.1
Salinity (g/L)
1
2
3
4
5
6
7
8
57.00
61.34
65.68
70.02
74.36
78.70
83.04
87.38
91.72
96.06
100.0

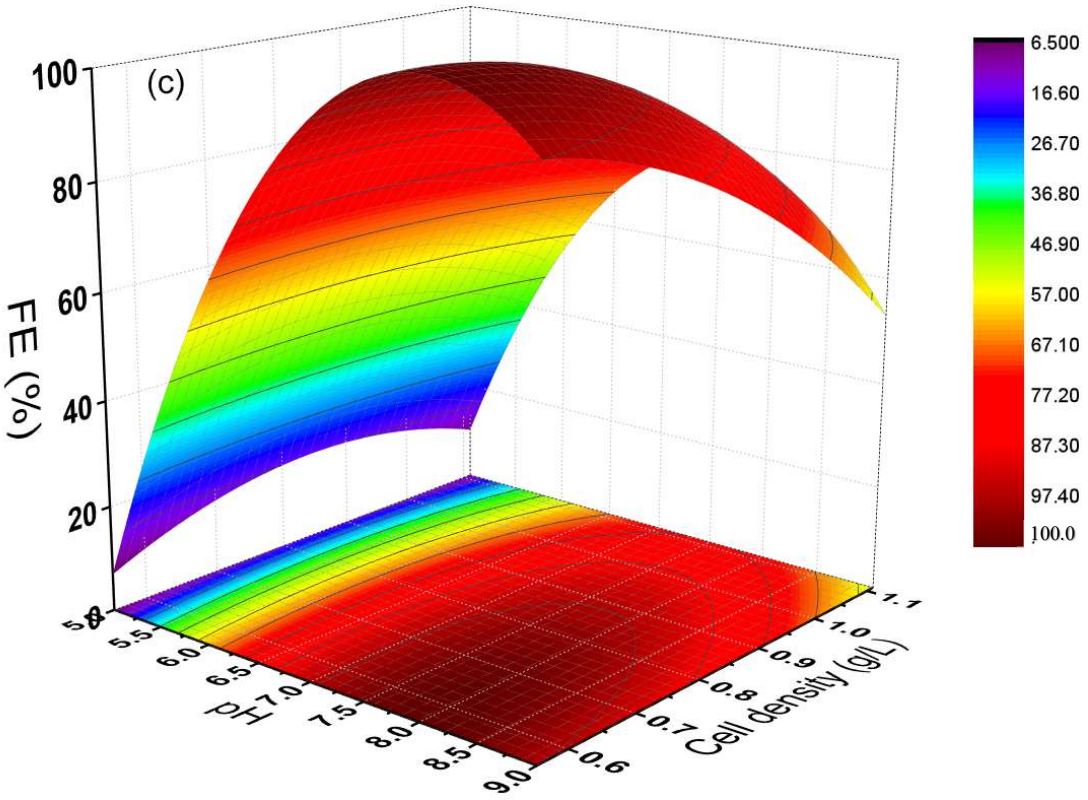

Fig. 3.6. Effects of pH, salinity, and cell density on the flocculation efficiency (FE) of 30 mg/L $AlCl_3$ when these parameters were fixed at: (a) cell density 0.834 g/L, (b) pH 7.0, and (c) salinity 4.4 g/L.

3.3.2.2 Interaction effects on chitosan flocculation efficiency

According to the BBD described in Table S5, the quadratic polynomial model Eq. (4) was used to fit FE after adding 1.5 mg/L chitosan under various pH, salinity, and cell density conditions:

$$FE\ (\%) = -273.2 + 116.05[pH] - 1.06[salinity] + 104.2[cell\ \ density] - 9.893[pH]^2 - 0.2546[salinity]^2 - 62.3[cell\ \ density]^2 + 0.128[pH][salinity] - 1.04[pH][cell\ \ density] + 2.026[salinity][cell\ density] \quad (3.4)$$

Table 3.2. Analysis of variance for the response surface quadratic model referring to chitosan.

Source	DF	Adj SS	Adj MS	T-value	F-value	*P*-value
Model	9	67464.6	7496.1		660.89	< 0.0001
Linear	3	49996.5	16665.5		1469.31	< 0.0001
pH	1	49847.2	49847.2	−66.29	4394.75	< 0.0001
Salinity	1	145.6	145.6	−3.58	12.84	0.0010
Cell density	1	3.7	3.7	0.57	0.33	0.5693
Square	3	17390.5	5796.8		511.07	< 0.0001
pH × pH	1	17346.3	17346.3	−39.11	1529.33	< 0.0001
Salinity × salinity	1	183.9	183.9	−4.03	16.21	0.0003
Cell density × cell density	1	257.2	257.2	−4.76	22.67	< 0.0001
Two-way interaction	3	77.5	25.8		2.28	0.0966
pH × salinity	1	12.6	12.6	1.05	1.11	0.2990
pH × cell density	1	4.0	4.0	−0.60	0.36	0.5541
Salinity × cell density	1	60.9	60.9	2.32	5.37	0.0265

Comparing the observed and predicted values in Table S5, the R^2 value was 0.994, which confirmed that Eq. (3.4) showed a good fit to the observations. Based on the T-values and *P*-values shown in Table 3.2, [pH], $[pH]^2$, and $[\text{cell density}]^2$ were highly significant ($P < 0.0001$) variables affecting FE, $[\text{salinity}]^2$ was a very significant ($P < 0.001$) variable, [salinity] was a rather significant ($P < 0.01$) variable, [salinity][cell density] was a significant ($P < 0.05$) variable, and the others were not significant ($P \geq 0.05$). Therefore, [pH] showed the most obvious influence. As shown in Figs. 3.7(a) and (c), FE decreased sharply with increasing pH above 7.0 but remained constant at pH < 7.0. ANOVA revealed negative correlations of salinity and cell density with FE, and the effect of salinity was more significant than that of cell density over this range. Therefore, the independent influences of the three factors represented by this RSM were consistent with the conclusions obtained from the experiments described in Section 3.3.1.

Only [salinity][cell density] had a significant interaction effect on chitosan FE (Table 2). Considering the negative correlations between FE and these two factors independently, the positive T-value suggested that one of the factors may slightly alleviate the negative effect of the other. As shown in Fig. 3.7(b), when salinity > 4.0 g/L, FE showed less of a decrease with increasing cell density. In addition, the decrease in FE with increasing salinity from 0.4 to 8.4 g/L at lower cell density (0.556–0.834 g/L) was greater than that at higher cell density (0.834–1.112 g/L). This unexpected discrepancy suggested that the reduction of zeta potential by appropriate salinity may facilitate flocculation of algae at a lower chitosan-to-cell ratio and that increasing cell density can reduce the distance between cells and thus compensate to some extent for the influence of the coiling of chitosan by salinity [31][40]

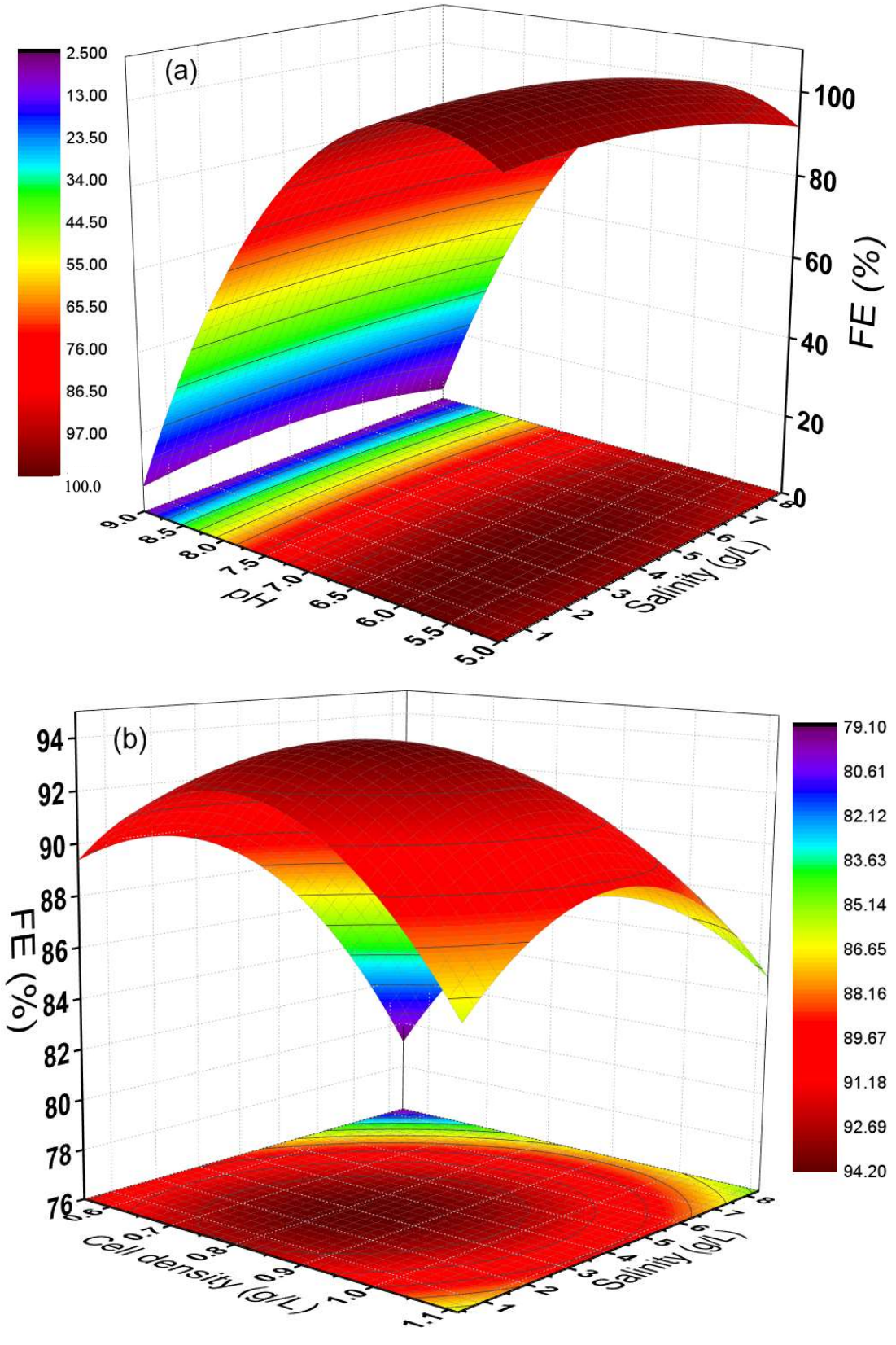
(a)
2.500
13.00
23.50
34.00
44.50
55.00
65.50
76.00
86.50
97.00
100.0
100
80
60
40
20
0
FE (%)
9.0
8.5
8.0
7.5
7.0
6.5
6.0
5.5
5.0
pH
1
2
3
4
5
6
7
8
Salinity (g/L)
(b)
94
92
90
88
86
84
82
80
78
76
FE (%)
79.10
80.61
82.12
83.63
85.14
86.65
88.16
89.67
91.18
92.69
94.20
0.6
0.7
0.8
0.9
1.0
1.1
Cell density (g/L)
1
2
3
4
5
6
7
8
Salinity (g/L)

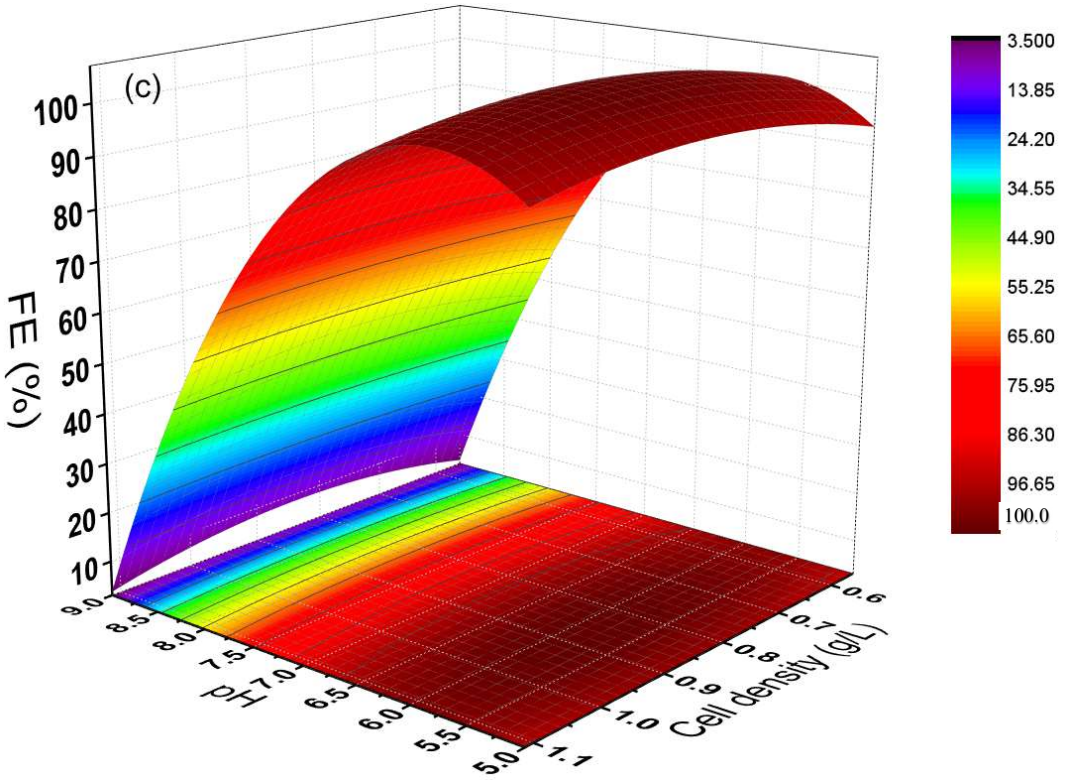

Fig. 3.7. Effects of pH, salinity, and cell density on flocculation induced by 1.5 mg/L chitosan when these parameters were fixed at: (a) cell density 0.834 g/L, (b) pH 7.0, and (c) salinity 4.4 g/L.

3.3.3 Dual flocculation performance of $AlCl_3$ + chitosan

Next, we investigated the flocculation performance of a combination of $AlCl_3$ with chitosan. Tables S6, S7, and S8 show the CCD arrangement and results under three conditions. In addition, Table S9 presents the results of ANOVA of these three RSM analyses obtained from the CCD; all fits were highly significant ($P < 0.0001$). The results showed an obvious improvement in FE by using a dual flocculant consisting of $AlCl_3$ + chitosan. Under low-level conditions (pH 5.0, salinity 0.2 g/L, cell density 0.417 g/L) (Fig. 3.8(a)), adding 0.35 mg/L chitosan after 8 mg/L $AlCl_3$ achieved FE > 90%. However, a 2.9 times higher dosage of chitosan or 11.3 times higher dosage of $AlCl_3$ were needed to obtain the same FE with the use of either flocculant alone (Table 3.3). It was possible to reach a FE of 75% at very low dosages with a combination of both flocculants (3 mg/L $AlCl_3$ + 0.1 mg/L chitosan). Similarly, under medium-level conditions (pH 7.0, salinity 8.4 g/L, cell density 0.556 g/L) (Fig. 3.8(b)), 5.5 mg/L $AlCl_3$ + 0.55 mg/L chitosan achieved the same FE (~90%) as using a 3.3 times higher dosage of $AlCl_3$ or 2.7 times higher dosage of chitosan alone (Table S10). In the high-level condition (pH 9.0, salinity 8.4 g/L, cell density 0.695 g/L) (Fig. 3.8(c)), FE showed little change with various chitosan dosages, as its flocculation performance was impeded by the high pH, salinity, and cell density. For example, adding 1.0 mg/L chitosan after 14.4 mg/L $AlCl_3$ achieved a FE of ~90% in comparison to 14 mg/L $AlCl_3$ alone to obtain the same FE (Table S10). When 9 mg/L $AlCl_3$ + 0.5 mg/L chitosan were

added, the FE reached > 70%, which was almost same with the FE obtained by individually using 9 mg/L $AlCl_3$.

The results demonstrated synergistic activities between the two flocculants, and the combination of $AlCl_3$ and chitosan could reduce the required dosage in the low-level and medium-level conditions, but this synergism was not observed in the high-level condition because of the strong inhibitory effect on chitosan. Similarly, it was reported that a combination of *Enteromorpha* polysaccharides with Al salts could improve dye color removal [46]. It was also reported that Al sulfate bioflocculant (with Al salt added first) could achieve large floc size and good recovery of kaolin–humic acid [47]. In addition, turbid water was successfully treated using lower concentrations of Al salt with chitosan than either Al salt or chitosan alone [48]. This study indicated that these synergistic effects could also be applied to harvesting of microalgae. This improved flocculation performance can be explained by the Al salt helping to neutralize negatively charged microalgal cells and compressing the double layer, which are beneficial for adsorption of chitosan onto the cells, allowing the charge-neutralized cells to aggregate more easily to form larger flocs [49][50].

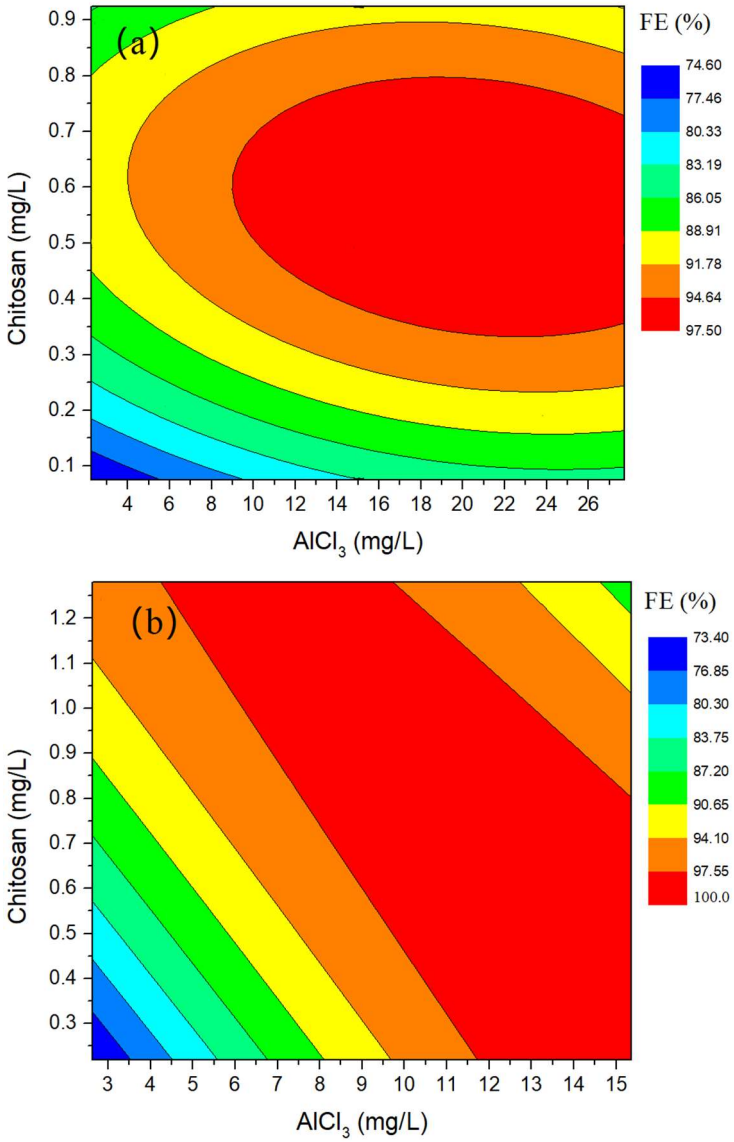

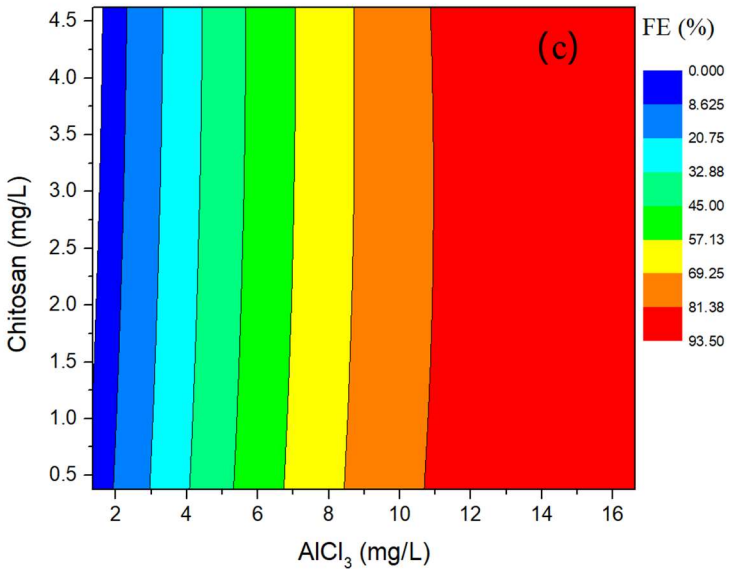

Figure 3.8. Dual flocculation efficiency (FE) of $AlCl_3$ + chitosan under various conditions: (a) low level: pH 5.0, salinity of 0.2 g/L, cell density of 0.417 g/L; (b) medium level: pH 7.0, salinity of 8.4 g/L, cell density of 0.556 g/L; (c) high level: pH 9.0, salinity of 8.4 g/L, cell density of 0.695 g/L.

Table.3.3 Comparison of $AlCl_3$ and chitosan used as individual flocculants.

	Low-level		Medium-level		High-level	
$AlCl_3$	Dosage (mg/L)	FE (%)	Dosage (mg/L)	FE (%)	Dosage (mg/L)	FE (%)
	90	89.7	18.0	92.4	14	92.3
Chitosan	Dosage (mg/L)	FE (%)	Dosage (mg/L)	FE (%)	Dosage (mg/L)	FE (%)
	1.0	88.9	1.5	91.8	N/A	N/A

3.4 Conclusion

This study demonstrated the flocculation performance of $AlCl_3$ and chitosan under various conditions of pH, salinity, and cell density. $AlCl_3$ showed better performance under alkaline conditions (pH 7.0–10.0), whereas chitosan showed better performance under acidic conditions (pH 4.0–7.0). FE decreased significantly when salinity exceeded 8.4 g/L, whereas salinity had a very limited influence on the FE of $AlCl_3$. The optimal dosage of $AlCl_3$ increased by 3.7 times with increasing cell density from 0.278 to 0.556 g/L, and then remained constant at ~26 g/L with further increases in cell density. There was a positive linear relationship between the optimal dosage of chitosan and cell density in the studied range. Based on the BBD, [salinity][cell density] and [pH][cell density] had significant interaction effects on the FE of $AlCl_3$. That is, $AlCl_3$ tolerated either high cell density or high salinity with FE > 90%, but FE became poor at ~60% under conditions where both cell density and salinity were high. In addition, the interaction of [pH][cell density] was more obvious within the range of pH 6.5–9.0 than

pH < 6.5. Meanwhile, [salinity][cell density] had a significant interaction effect on the FE of chitosan. Despite the negative correlations of FE with cell density and salinity, interaction analysis indicated that one of the factors slightly alleviated the negative effect of the other. Finally, CCD revealed enhanced flocculation performance by a combination of $AlCl_3$ and chitosan, and a higher FE could be obtained with lower dosages compared to use of either flocculant alone.

References

[1] Umar, T., & Egbu, C. (2018, July). Global commitment towards sustainable energy. In Proceedings of the Institution of Civil Engineers-Engineering Sustainability (Vol. 172, No. 6, pp. 315-323). Thomas Telford Ltd.T.

[2] Brennan, L., & Owende, P. (2010). Biofuels from microalgae—a review of technologies for production, processing, and extractions of biofuels and co-products. Renewable and sustainable energy reviews, 14(2), 557-577.

[3] Barros, A. I., Gonçalves, A. L., Simões, M., & Pires, J. C. (2015). Harvesting techniques applied to microalgae: a review. Renewable and Sustainable Energy Reviews, 41, 1489-1500.

[4] Garzon-Sanabria, A. J., Davis, R. T., & Nikolov, Z. L. (2012). Harvesting Nannochloris oculata by inorganic electrolyte flocculation: effect of initial cell density, ionic strength, coagulant dosage, and media pH. Bioresource technology, 118, 418-424.

[5] Lam, M. K., & Lee, K. T. (2012). Microalgae biofuels: a critical review of issues, problems and the way forward. Biotechnology advances, 30(3), 673-690.

[6] Liu, J., Zhu, Y., Tao, Y., Zhang, Y., Li, A., Li, T., ... & Zhang, C. (2013). Freshwater microalgae harvested via flocculation induced by pH decrease. Biotechnology for biofuels, 6(1), 98.

[7] Sander, K., & Murthy, G. S. (2010). Life cycle analysis of algae biodiesel. The International Journal of Life Cycle Assessment, 15(7), 704-714.

[8] Schlesinger, A., Eisenstadt, D., Bar-Gil, A., Carmely, H., Einbinder, S., & Gressel, J. (2012). Inexpensive non-toxic flocculation of microalgae contradicts theories; overcoming a major hurdle to bulk algal production. Biotechnology advances, 30(5), 1023-1030.

[9] Klein, B. C., Bonomi, A., & Maciel Filho, R. (2018). Integration of microalgae production with industrial biofuel facilities: A critical review. Renewable and Sustainable Energy Reviews, 82, 1376-1392.

[10] M.A. Alam, D. Vandamme, W. Chun, X. Zhao, I. Foubert, Z. Wang, K. Muylaert, Z. YuanBioflocculation as an innovative harvesting strategy for microalgae Rev Environ Sci Bio/Technol, 15 (2016), pp. 573-583.

[11] Das, P., Thaher, M. I., Hakim, M. A. Q. M. A., Al-Jabri, H. M. S., & Alghasal, G. S. H. (2016). Microalgae harvesting by pH adjusted coagulation-flocculation, recycling of the coagulant and the growth media. Bioresource technology, 216, 824-829.

[12] Suopajärvi, T. (2015). Functionalized nanocelluloses in wastewater treatment applications. Acta Universitatis Ouluensis C, 526.

[13] Matter, I. A., Darwesh, O. M., & Eida, M. F. (2018). Harvesting of Scenedesmus obliquus by Bioflocculation: Appropriate Chitosan Concentrations with Various pH Values at Different Growth Stages. Jordan Journal of Biological Sciences, 11(5).

[14] Vu, C. H. T., Chun, S. J., Seo, S. H., Cui, Y., Ahn, C. Y., & Oh, H. M. (2019). Bacterial community enhances flocculation efficiency of Ettlia sp. by altering extracellular polymeric substances profile. Bioresource technology, 281, 56-65.

[15] Roselet, F., Vandamme, D., Roselet, M., Muylaert, K., & Abreu, P. C. (2017).

Effects of pH, salinity, biomass concentration, and algal organic matter on flocculant efficiency of synthetic versus natural polymers for harvesting microalgae biomass. BioEnergy Research, 10(2), 427-437.
[16] Pérez, L., Salgueiro, J. L., Maceiras, R., Cancela, Á., & Sánchez, Á. (2017). An effective method for harvesting of marine microalgae: pH induced flocculation. Biomass and bioenergy, 97, 20-26.
[17] Giraldo, J. B., Vermuë, M. H., Olivieri, G., Eppink, M. H. M., & Wijffels, R. H. (2016). Understanding the salinity effect on cationic polymers in inducing flocculation of the microalga Neochloris oleoabundans. Journal of biotechnology, 225, 10-17.
[18] Lunprom, S., Phanduang, O., Salakkam, A., Liao, Q., & Reungsang, A. (2019). A sequential process of anaerobic solid-state fermentation followed by dark fermentation for bio-hydrogen production from Chlorella sp. International Journal of Hydrogen Energy, 44(6), 3306-3316.
[19] Tsuzuki, M., Okada, K., Isoda, H., Hirano, M., Odaka, T., Saijo, H., ... & Fujiwara, S. (2019). Physiological Properties of Photoautotrophic Microalgae and Cyanobacteria Relevant to Industrial Biomass Production. Marine Biotechnology, 21(3), 406-415.
[20] Castrillo, M., Lucas-Salas, L. M., Rodríguez-Gil, C., & Martínez, D. (2013). High pH-induced flocculation–sedimentation and effect of supernatant reuse on growth rate and lipid productivity of Scenedesmus obliquus and Chlorella vulgaris. Bioresource technology, 128, 324-329.
[21] Kaith, B. S., Jindal, R., & Sharma, R. (2016). Study of ionic charge dependent salt resistant swelling behavior and removal of colloidal particles using reduced gum rosin-poly (acrylamide)-based green flocculant. Iranian Polymer Journal, 25(4), 349-362.
[22] Grima, E. M., Belarbi, E. H., Fernández, F. A., Medina, A. R., & Chisti, Y. (2003). Recovery of microalgal biomass and metabolites: process options and economics. Biotechnology advances, 20(7-8), 491-515.
[23] Yan, M., Wang, D., Qu, J., He, W., & Chow, C. W. (2007). Relative importance of hydrolyzed Al (III) species (Ala, Alb, and Alc) during coagulation with polyaluminum chloride: a case study with the typical micro-polluted source waters. Journal of Colloid and Interface Science, 316(2), 482-489.
[24] Wu, Z., Zhang, X., Zhou, C., Pang, J. L., & Zhang, P. (2017). Adsorption neutralization model and floc growth kinetics properties of aluminum coagulants based on sips and Boltzmann equations. ACS applied materials & interfaces, 9(7), 5992-5999.
[25] Wang, W., Yue, Q., Gao, B., & Li, R. (2016). Floc proprieties and ultrafiltration characteristics by chitosan compound aluminum species coagulant under different pH conditions. Journal of the Taiwan Institute of Chemical Engineers, 68, 224-231.
[26] Feng, L., Zhao, S., Sun, S., Wang, W., Gao, B., & Yue, Q. (2015). Effect of pH with different purified aluminum species on coagulation performance and membrane fouling in coagulation/ultrafiltration process. Journal of hazardous

materials, 300, 67-74.
[27] Shi, B., Li, G., Wang, D., Feng, C., & Tang, H. (2007). Removal of direct dyes by coagulation: The performance of preformed polymeric aluminum species. Journal of hazardous materials, 143(1-2), 567-574.
[28] Augustine, A., Kumaran, J., Puthumana, J., Sabu, S., Singh, I. B., & Joseph, V. (2017). Multifactorial interactions and optimization in biomass harvesting of marine picoalga Picochlorum maculatum MACC3 with different flocculants. Aquaculture, 474, 18-25.
[29] Augustine, A., Tanwar, A., Tremblay, R., & Kumar, S. (2019). Flocculation processes optimization for reuse of culture medium without pH neutralization. Algal Research, 39, 101437.
[30] Yadav, A., Mukherji, S., & Garg, A. (2013). Removal of chemical oxygen demand and color from simulated textile wastewater using a combination of chemical/physicochemical processes. Industrial & Engineering Chemistry Research, 52(30), 10063-10071.
[31] Cui, Y., Yuan, W., & Cheng, J. (2014). Understanding pH and ionic strength effects on aluminum sulfate-induced microalgae flocculation. Applied biochemistry and biotechnology, 173(7), 1692-1702.
[32] Rattanakawin, C., & Hogg, R. (2001). Aggregate size distributions in flocculation. Colloids and Surfaces A: Physicochemical and engineering aspects, 177(2-3), 87-98.
[33] Zhao, Y., Zhang, L. Y., Ni, F., Xi, B., Xia, X., Peng, X., & Luan, Z. (2011). Evaluation of a novel composite inorganic coagulant prepared by red mud for phosphate removal. Desalination, 273(2-3), 414-420.
[34] Shen, Y., Cui, Y., & Yuan, W. (2013). Flocculation optimization of microalga Nannochloropsis oculata. Applied biochemistry and biotechnology, 169(7), 2049-2063.
[35] Zhao, Y. X., Shon, H. K., Phuntsho, S., & Gao, B. Y. (2014). Removal of natural organic matter by titanium tetrachloride: The effect of total hardness and ionic strength. Journal of environmental management, 134, 20-29.
[36] Wang, Y., Gao, B. Y., Xu, X. M., & Xu, W. Y. (2010). The effect of total hardness and ionic strength on the coagulation performance and kinetics of aluminum salts to remove humic acid. Chemical Engineering Journal, 160(1), 150-156.
[37] Wang, C., Shang, C., Chen, G., & Zhu, X. (2013). Mechanisms of nC60 removal by the alum coagulation–flocculation–sedimentation process. Journal of colloid and interface science, 411, 213-219.
[38] Paton-Morales, P., & Talens-Alesson, F. I. (2001). Effect of ionic strength and competitive adsorption of Na+ on the flocculation of lauryl sulfate micelles with Al3+. Langmuir, 17(20), 6059-6064.
[39] Sukenik, A., Bilanovic, D., & Shelef, G. (1988). Flocculation of microalgae in brackish and sea waters. Biomass, 15(3), 187-199.
[40] Roselet, F., Burkert, J., & Abreu, P. C. (2016). Flocculation of Nannochloropsis oculata using a tannin-based polymer: bench scale optimization and pilot scale reproducibility. Biomass and Bioenergy, 87, 55-60.

[41] Grima, E. M., Belarbi, E. H., Fernández, F. A., Medina, A. R., & Chisti, Y. (2003). Recovery of microalgal biomass and metabolites: process options and economics. Biotechnology advances, 20(7-8), 491-515.
[42] Giraldo, J. B., Vermuë, M. H., Olivieri, G., Eppink, M. H. M., & Wijffels, R. H. (2016). Understanding the salinity effect on cationic polymers in inducing flocculation of the microalga Neochloris oleoabundans. Journal of biotechnology, 225, 10-17.
[43] Farid, M. S., Shariati, A., Badakhshan, A., & Anvaripour, B. (2013). Using nano-chitosan for harvesting microalga Nannochloropsis sp. Bioresource technology, 131, 555-559.
[44] Roselet, F., Vandamme, D., Roselet, M., Muylaert, K., & Abreu, P. C. (2017). Effects of pH, salinity, biomass concentration, and algal organic matter on flocculant efficiency of synthetic versus natural polymers for harvesting microalgae biomass. BioEnergy Research, 10(2), 427-437.
[45] Gerde, J. A., Yao, L., Lio, J., Wen, Z., & Wang, T. (2014). Microalgae flocculation: impact of flocculant type, algae species and cell concentration. Algal research, 3, 30-35.
[46] Zhao, S., Gao, B., Yue, Q., & Wang, Y. (2014). Effect of Enteromorpha polysaccharides on coagulation performance and kinetics for dye removal. Colloids and Surfaces A: Physicochemical and Engineering Aspects, 456, 253-260.
[47] Bo, X., Gao, B., Peng, N., Wang, Y., Yue, Q., & Zhao, Y. (2012). Effect of dosing sequence and solution pH on floc properties of the compound bioflocculant–aluminum sulfate dual-coagulant in kaolin–humic acid solution treatment. Bioresource technology, 113, 9-96.
[48] Hu, C. Y., Lo, S. L., Chang, C. L., Chen, F. L., Wu, Y. D., & Ma, J. L. (2013). Treatment of highly turbid water using chitosan and aluminum salts. Separation and Purification Technology, 104, 322-326.
[49] Ma, C., Pei, H., Hu, W., Wang, Y., Xu, H., & Jin, Y. (2017). The enhanced reduction of C-and N-DBP formation in treatment of source water containing Microcystis aeruginosa using a novel CTSAC composite coagulant. Science of the Total Environment, 579, 1170-1178.
[50] Ma, C., Hu, W., Pei, H., Xu, H., & Pei, R. (2016). Enhancing integrated removal of Microcystis aeruginosa and adsorption of microcystins using chitosan-aluminum chloride combined coagulants: effect of chemical dosing orders and coagulation mechanisms. Colloids and Surfaces A: Physicochemical and Engineering Aspects, 490, 258-267.
[51] Suopajärvi, T. (2015). Functionalized nanocelluloses in wastewater treatment applications. Acta Universitatis Ouluensis C, 526.

Chapter 4 Evaluation of flocculation performance of amphoteric flocculant when harvesting microalgae *Coccomyxa sp. KJ* by response surface methodology

4.1 Introduction

In recent years, microalgal applications in energy, pharmaceuticals, nutraceuticals, food, and cosmetics have been gained increasing research attention. Biodiesel production from microalgae is considered a promising solution for the energy crisis [1,2], particularly as a renewable carbon-neutral fuel [3]. The use of microalgal bioreactors combined with genetic engineering can be an attractive method for producing pharmaceuticals, such as vaccines, enzymes, immune regulators, hormones, and anticancer agents [4]. Various byproducts of microalgae can be used as food additives or even as a high-protein supplement for human nutrition; these include carotenoids, polyunsaturated fatty acids, and food pigments [5,6]. In addition, the potential use of microalgae in hydrating, anti-aging, sunscreen, and whitening cosmetics has been investigated [7]. All of these potential uses are possible due to advantageous features of microalgae, including high growth and production rates and potential for cultivation over a wide area [8]. However, an appropriate harvesting method is needed before a target product can be extracted, because of the small cell size of microalgae and their low density in media. Sedimentation, filtration, and centrifugation are three commonly used methods to separate microalgae from water, and sedimentation is considered the most economical one among these [3]. Typically, sedimentation is induced by a flocculant, because the low surface charge of cells prevents their aggregation and their similar density to water hinders spontaneous gravity-induced sedimentation [9]. Flocculants can be separated into cationic, anionic, non-ionic, and amphoteric types according to the charges carried on their respective functional groups. Considering the negative surface charge of microalgal cells in natural conditions, studies have focused on cationic flocculants (metal salts, chitosan, cationic starch, and so forth) and demonstrated that they successfully flocculate diverse microalgae species [10,11]. By contrast, anionic or non-ionic flocculants cannot effectively induce sedimentation of microalgae [12]. Although anionic polymers can bind to these cells' surfaces via the chemical force of hydrogen bonding (rather than the electrostatic force involved with cationic polymers), they are unable to form bridges and therefore flocs [13,14]. As for amphoteric flocculants, which contain both anionic and cationic functional groups, they have been successfully used for the treatment of industrial water, municipal water, and oilfields [15,16]. However, very few studies have evaluated their performance in harvesting microalgae.

Therefore, in this study, the amphoteric flocculant acrylamide-methacrylic acid ester-acrylic acid copolymer (ACPAM) was chosen to harvest the freshwater microalgae *Coccomyxa sp. KJ*. Considering the species can rapidly growth in minimal mineral media and accumulate huge amount of lipid (30% ~ 60%), hence as a potential species for biodiesel production [17][18]. In experiments, flocculant dosage, pH and stirring speed of intensive mixing step were firstly screened from 7 potential factors. Those three parameters were modelled and optimized by Response Surface Methodology (RSM). Then, as a type of organic flocculant, its thermal stability should be evaluated [20]. Thus, influence of heating treatment on the flocculant was investigated by TG, FTIR and XRD. Finally, the ACPAM was compared with two common flocculants ($AlCl_3$ and Chitosan) for other two microalgae species to confirm its applicability. The objectives were to study applicability of the amphoteric flocculant on harvesting microalgae, its thermal stability and how to optimize flocculation condition.

4.2 Materials and Methods

4.2.1 Microalgal cultivation and biomass concentration

The strain of freshwater microalgae, *Coccomyxa sp. KJ*, was supplied by the laboratory of Professor Miyashita at Kyoto University (Kyoto, Japan). The medium used for cultivation was AF-6, whose components are shown in Table S10. With temperature controlled at 20–25°C, the microalgae were cultivated in a 20 L bucket photobioreactor (12/12 light/dark cycles). After sterilization in an oven at a temperature of 105°C for 24 h, the culture medium was continuously aerated with filtered air during cultivation. After 15 days, the microalgae entered the stationary phase, and the cultivation process was complete.

The dry cell weight in the stationary phase was measured as the biomass concentration of the microalgae. Using a vacuum filter, 25 mL microalgae were filtered through glass microfiber filter paper (GF/C, 1.2 μm, 4.7 cm; Whatman plc, United Kingdom) that had been preweighed and then cleaned with deionized water. Then the filter was dried in an oven at a temperature of 105°C for 24 h, until it reached a constant weight, and cooled to room temperature for weight measurement. This process was repeated in triplicate; the dry cell weight obtained was 0.72 ± 0.01 g/L.

4.2.2 Experimental process of flocculation

The amphoteric flocculant ACPAM was supplied by Mitsubishi Chemical Corporation (KA305BH, Tokyo, Japan). The flocculant was dissolved in deionized water at a concentration of 5 g/L. Before the flocculation tests, the microalgae were putted into a refrigerator for several minutes until to their temperature below 10 ℃, and their pH was adjusted using hydrochloric acid or sodium hydroxide (both guaranteed reagent grade, Wako Co., Ltd, Japan). Then the flocculation tests were performed in beakers with a volume of 100 mL. After adding the flocculant, the microalgae suspensions were intensively mixed by magnetic stirrer to ensure the flocculant's complete dispersal,

followed by gentle mixing to facilitate the formation of flocs [18]. The suspensions were subsequently allowed to settle for 15 min. The supernatant was sampled in the middle of the clarified zone and its optical density (OD) was measured at 680 nm using a spectrophotometer (UV-1200, Shimadzu, Kyoto, Japan). All of the flocculation tests were repeated in triplicate. The flocculation efficiency (FE) was determined in terms of OD using the following equation:

$$FE\ (\%) = \left(1 - \frac{OD_{final}}{OD_{initial}}\right) \times 100\% \quad (4.1)$$

4.2.3 Screening via Plackett–Burman experiments

As shown in Table 4.1, seven influencing factors with a potential to affect flocculation, the speed and time of the intensive and gentle mixing steps (ω_1, t_1, ω_2, and t_2, respectively), pH of the microalgae, temperature of the microalgae (T), and dosage of flocculant, with four virtual factors (V_1, V_2, V_3, and V_4) had appropriate values selected to conduct experiments using a Plackett–Burman (PB) design [19,20]. After screening, experiments were conducted to establish the path of steepest ascent (Table S12). This region represented the optimal conditions, which were further explored by response surface methodology (RSM) using a Box–Behnken design (BBD) [21].

4.2.4 Box–Behnken design for RSM

RSM was conducted with a BBD [18,22] using statistical software (Minitab 18.1). The BBD with three independent variables ($X_1 = \omega_1$, X_2 = pH, X_3 = dosage of flocculant) at three levels (-1, 0, +1) were used in a set of 17 experiments as shown in Table S13. The response variable (Y) that represented the FE was fitted to a second-order model in the form of a quadratic polynomial equation [23]:

$$Y = \beta_0 + \sum_{i=0}^{n} \beta_i X_i + \sum_{i=0}^{n} \beta_{ii} X_i^2 + \sum_{\substack{1 \le i \le n \\ i<j \le n}} \beta_{ij} X_i X_j \quad (4.2)$$

where n is the number of independent variables and β_0, β_i, β_{ii}, and β_{ij} represent the regression coefficients for the constant, linear, quadratic, and interaction between X_i and X_j terms, respectively.

4.2.5 Effect of thermal treatment on the flocculant

4.2.5.1 Pretreatment of flocculant sample

ACPAM was treated by heating it in an oven (KLO-45M, Koyo Thermo System Co., Ltd., Nara, Japan) at different temperatures (40°C, 60°C, 80°C, 100°C, and 120°C) for 2 h, with some stored at room temperature (20°C) as a control. Then a sample mill (T1–100, Shimadzu) was used to grind the flocculant into a powder. The powders were collected into plastic bags, sealed, and stored in a desiccator at room temperature, before FTIR and XRD analyses.

Table 4.1 Results of the Plackett-Burman design

Run	t_1 (min)	t_2 (min)	ω_1 (rpm)	ω_2 (rpm)	T (℃)	pH	dosage (mg/L)	V.1	V.2	V.3	V.4	FE (%)
1	1(-1)	5 (-1)	200(-1)	50(-1)	10(-1)	6.1(-1)	15(-1)	-1	-1	-1	-1	21.2
2	2(+1)	10(+1)	350(+1)	100(+1)	10(11)	6.1(-1)	20(+1)	1	-1	1	1	98.0
3	1(-1)	10(+1)	350(+1)	100(+1)	20(+1)	6.1(-1)	15(-1)	1	1	-1	1	66.2
4	2(+1)	10(+1)	200(-1)	50(-1)	20(+1)	10.7(+1)	15(-1)	1	1	-1	-1	42.0
5	2(+1)	5(-1)	200(-1)	50(-1)	10(-1)	10.7(+1)	15(-1)	1	-1	1	1	56.0
6	1(-1)	10(+1)	200(-1)	100(+1)	10(-1)	10.7(+1)	20(+1)	1	1	-1	-1	84.5
7	2(+1)	10(+1)	200(-1)	100(+1)	20(+1)	6.1(-1)	15(-1)	-1	-1	1	-1	31.8
8	1(-1)	10(+1)	350(+1)	50(-1)	20(+1)	10.7(+1)	15(-1)	-1	-1	-1	1	73.6
9	2(+1)	5(-1)	350(+1)	50(-1)	20(+1)	10.7(+1)	20(+1)	1	-1	-1	1	94.5
10	2(+1)	5(-1)	200(-1)	100(+1)	20(+1)	6.1(-1)	20(+1)	1	-1	-1	-1	40.2
11	2(+1)	5(-1)	350(+1)	100(+1)	10(-1)	6.1(-1)	15(-1)	-1	1	-1	1	87.6
12	1(-1)	5(-1)	350(+1)	50(-1)	20(+1)	6.1(-1)	20(+1)	1	1	1	-1	91.6
13	2(+1)	10(+1)	350(+1)	50(-1)	10(-1)	10.7(+1)	20(+1)	-1	1	1	-1	97.0
14	2(+1)	10(+1)	200(11)	50(-1)	10(-1)	6.1(-1)	20(+1)	-1	1	-1	1	41.9
15	1(-1)	5(-1)	200(-1)	50(-1)	20(+1)	6.1(-1)	20(+1)	-1	1	1	1	33.9
16	1(-1)	10(+1)	200(-1)	100(+1)	20(+1)	10.7(+1)	20(+1)	-1	-1	1	1	65.0
17	2(+1)	5(-1)	350(+1)	100(+1)	20(+1)	10.7(+1)	15(-1)	-1	1	1	-1	74.5
18	1(-1)	5(-1)	350(+1)	100(+1)	10(-1)	10.7(+1)	20(+1)	-1	-1	-1	-1	96.7
19	1(-1)	10(+1)	350(+1)	50(-1)	10(-1)	6.1(-1)	15(-1)	1	-1	1	-1	82.1
20	1(-1)	5(-1)	200(-1)	100(+1)	10(-1)	10.7(+1)	15(-1)	1	1	1	1	44.1

4.2.5.2 Structure and morphology analyses

After mixing with KBr powder, the thermally treated flocculant was measured in the range 400–4000 cm^{-1} via an FTIR spectrometer (FTIR-8400, Shimadzu) combined with a diffuse reflectance spectroscope (DRS-8000A).

The flocculants were also analyzed by XRD (RINT-UltimaPC, Rigaku Ltd., Tokyo, Japan) equipped with a Cu-*Kα* radiation source (k = 0.15418) with settings of 40 kV and 30 mA, and a diffraction angle scan speed of 8° per min within a 2θ range of 5–90°.

TG and differential thermal analyses (DTAs) were performed on the non-thermally-treated, control flocculant (ThermoPlus TG8120, Rigaku Ltd.) under an air atmosphere with a heating rate of 10°C/min from 20°C to 1000°C.

4.2.5.3 Flocculation performance after the thermal treatment

Under the optimal conditions obtained from the process described in 4.2.4, the flocculation performances of the various thermally treated ACPAM samples were compared to the untreated control using the method described in 4.2.2.

4.2.6 Applicability of ACPAM

Next, to investigate if the flocculation performance of ACPAM is comparable to the common flocculants and can be used for other species. We compared the flocculant efficiency of ACPAM with two other flocculants commonly used to harvest microalgae, $AlCl_3$ and chitosan. These were compared not only in terms of harvesting *Coccomyxa sp. KJ* but also two other microalgal species, *Chlamydomonas reinhardtii* (initial pH of 8.80) and *Tetradesmus obliquus* (initial pH of 8.90). Both of the species were cultivated in same system and medium as *Coccomyxa sp. KJ* to their stationary phase (dry weight of 1.13 and 0.92g/L, respectively). All these flocculation experiments were conducted under the condition (ω_1 of 350rpm, t_1 of 2 min, ω_2 of 100 rpm, and t_2 of 10 min, their respectively initial pH and room temperature). The optimized flocculant doses with maximum flocculation efficiency by the 3 flocculants were compared.

4.3. Results and Discussion

4.3.1. Results of PB experiments

Regression analyses of the seven factors identified in PB experiments were performed (Table 4.2). The p-values of all four virtual factors were much greater than 0.05, which means that the effect of any experimental error was nonsignificant, and the experimental results were credible. Thus, the significant factors (p-value < 0.05) influencing the flocculation process were identified as ω_1, pH, and flocculant dosage.

Table 4.2 Regression coefficients and analysis of variance of factors identified via Plackett–Burman experiments.

Source	[1]Coef	[2]Adj SS	[3]Adj MS	F-Value	p-value
Model		11317.7	1028.89	9.17	0.0021
Linear	66.12	11317.7	1028.89	9.17	0.0021
t_1	0.23	1.0	1.04	0.01	0.9255
t_2	2.1	88.0	87.96	0.78	0.4018
ω_1	20.07	8058.9	8058.86	71.83	<0.001
ω_2	2.74	150.3	150.34	1.34	0.2804
T	-4.78	457.3	457.30	4.08	0.0782
pH	6.67	888.9	888.89	7.92	0.0227
Dosage	8.21	1349.1	1349.06	12.02	0.0085
V_1	3.81	290.4	290.43	2.59	0.1463
V_2	0.2	0.8	0.80	0.01	0.9348
V_3	1.29	33.0	33.03	0.29	0.6022
V_4	-0.04	0.0	0.04	0.00	0.9854
Error		897.6	112.19		
Total		12215.3			

[1]Regression coefficient, [2]adjusted sum of squares, [3]adjusted mean squares

When considering the regression coefficients, all of the factors had positive effects on the flocculation process except for T. This means that the FE would be improved by increasing the dosage of flocculant, pH, and ω_1, but decreasing T. The reason for investigating temperature was to evaluate whether the activity of ACPAM would be inhibited in a low-temperature environment, such as during winter [24]. Yet, as discussed above, the flocculation performance of ACPAM was less affected by temperature than by other factors and even improved at lower temperatures. Therefore, the subsequent flocculation experiments for the steepest ascent and BBD were conducted with only ω_1, pH, and dosage as the primary variables.

In analysis of variance (ANOVA), the p-value of the model overall (0.0021) was less than 0.01, indicating that the model fitted well across all of the data. The overall coefficient of determination (R^2) was 0.880, indicating that the model was adequate and could explain 88.0% of the variation in the data [25]. The adjusted R^2 (adj-R^2) was 0.849, indicating that the model could explain 84.9% of the change in the response value [20]; this confirmed that the model was significant. The predicted R^2 (pred-R^2) was 0.7873, indicating that the model was predicted to explain 78.73% of the change in the response value for new observations. The difference between pred-R^2 and adj-R^2 was less than 0.2, indicating a good agreement between the experimental and predicted values [26].

The multiple regression equation is given below:

$$FE\ (\%) = 66.12 + 20.07\omega_1 - 4.78T + 6.67pH + 8.21dosage \quad (4.3)$$

4.3.2. Results of steepest ascent experiments

In the steepest ascent experiments, t_1, t_2, ω_2, and T were fixed at 2 min, 10 min, 100 rpm, and 20°C, respectively. All three variables that had passed screening by PB, ω_1, pH, and dosage, increased during the six runs. The steepest ascent design and its results are shown in Table S12. FE was 15.2% under the initial condition and increased to a maximum of 95.6% under ω_1 = 350 rpm, pH = 10.0, and dosage = 25 mg/L. It decreased when the variables increased beyond those values, reaching a value of 69.4% when they reached the top of their ranges. Thus, these parameters were used in subsequent RSM experiments using a BBD.

4.3.3 Results of RSM experiments using a Box–Behnken design

A three-factor, three-level BBD experiment was conducted, as shown in Table S13. These three independent variables were varied to three levels (coded -1, 0 and +1). The central point condition had pH, dosage, and ω_1 with values of 10.0, 25 mg/L and 350 rpm, respectively. And pH, dosage, and ω_1 values at 9.0, 15 mg/L, and 250 rpm, respectively, as the -1 level, at 11.0, 35 mg/L, and 450 rpm, respectively as the +1 level. Based on the results, a quadratic model for the relationship between FE and the three variables was obtained, as follows:

$$FE(\%) = 95.06 + 1.31X_1 + 3.87X_2 + 12.31X_3 - 4.04X_1^2 - 11.57X_2^2 - 14.59X_3^2 + 4.50X_1X_2 + 0.13X_1X_3 - 7.70X_2X_3 \quad (4.4)$$

where X_1, X_2, and X_3 were the pH, ω_1 (rpm), and dosage of ACPAM (mg/L), respectively.

ANOVA was conducted on the results (Table 4.3). Among the linear terms, ω_1 and dosage were significant ($p < 0.05$). Among the square terms, ω_1^2 and dosage^2 (with p-values of 0.0004 and 0.0001, respectively) were significant. As for two-way interaction terms, only $\omega_1 \cdot$ dosage was identified as a significant factor. In general, all of the terms containing pH were nonsignificant, and FE was mainly affected by ω_1 and dosage.

The sign of a coefficient in the BBD model usually indicates the direction of that term's effect [20], such that factors with positive signs in Eq. (4) would increase the dependent variable with increasing the factors, and those with negative signs would decrease it. The absolute value of a coefficient in the BBD model indicates the magnitude of that term's effect, so terms in Eq. (4) with a high absolute value tend to have more impact than those with low absolute values. In this BBD model, the coefficients of ω_1 and ω_1^2 (3.87 and -11.57, respectively) indicate that the effect of ω_1 on FE was not constant: FE initially increased with ω_1, then decreased, within the studied range. The same tendency was found for the other significant factor, dosage. As for the interaction term, the coefficient of $\omega_1 \cdot$ dosage was -7.70; that this was negative indicates that there was an antagonistic effect between ω_1 and dosage [27].

Table 4.3 Analysis of variance for the results of BBD experiments

Source	[1]DF	[2]Seq SS	Contribution	[3]Adj SS	[4]Adj MS	F-Value	p-value
Model	9	3356.69	97.38%	3356.69	372.97	28.94	0.0001
Linear	3	1421.18	41.23%	1349.25	449.75	34.89	0.0001
pH	1	6.23	0.18%	9.69	9.69	0.75	0.4147
[5]ω_1	1	202.17	5.87%	100.63	100.63	7.81	0.0267
Dosage	1	1212.78	35.18%	1212.78	1212.78	94.09	< 0.001
Square	3	1654.38	48.00%	1665.63	555.21	43.08	0.0001
pH^2	1	92.32	2.68%	54.34	54.34	4.22	0.0791
ω_1^2	1	600.52	17.42%	520.72	520.72	40.4	0.0004
$Dosage^2$	1	961.54	27.90%	802.88	802.88	62.29	0.0001
Two-way interaction	3	281.12	8.16%	281.12	93.71	7.27	0.0148
$pH \cdot \omega_1$	1	43.9	1.27%	43.9	43.9	3.41	0.1075
pH · dosage	1	0.06	0.00%	0.06	0.06	0	0.9464
ω_1 · dosage	1	237.16	6.88%	237.16	237.16	18.4	0.0036
Error	7	90.22	2.62%	90.22	12.89		
Lack-of-fit	3	68.41	1.98%	68.41	22.8	4.18	0.1003
Pure error	4	21.81	0.63%	21.81	5.45		
Total	16	3446.91	100.00%				

[1]Degrees of freedom, [2]sequential sums of squares, [3]adjusted sum of squares, [4]adjusted mean squares, [5]mixing speed during intensive mixing

To evaluate the adequacy of this model, several statistical parameters were examined. The p-value (0.0001) of this model was less than 0.05, even below 0.01, which indicates that the model fit very well across all of the data. The p-value for a lack of fit (0.1003) was more than 0.05, indicating that it was nonsignificant, thus supporting that the model was adequate [20,21]. However, the difference between adj-R^2 (0.940) and pred-R^2 (0.595) was more than 0.2, indicating that overfitting had occurred [26,27], despite an excellent value for R^2 (0.974). Therefore, that this model explained 97.4% of the data variation could be ascribed to its overfitting, suggesting a very poor model. This was because of highly nonsignificant terms, such as pH and pH · dosage, were contained in the model. Thus, we removed those terms or conducted a Box–Cox transformation on the data [28–30].

Table 4.4 Comparison of models' reliability and adequacy after removing nonsignificant terms or a Box–Cox transformation on the data.

	P-value of model	p-value of lack of fit	R^2	adj-R^2	pred-R^2
Initial model	0.1×10^{-3}	0.1003	0.974	0.940	0.595
Nonsignificant factors removed model	0.1×10^{-5}	0.110	0.952	0.931	0.773
Box–Cox transformed model	0.3×10^{-7}	0.8669	0.9975	0.9943	0.9878

The simplified model showed much better results (Table 4.4), indicating higher reliability and adequacy. The new regression equation was:

$$FE(\%) = 93.87 + 5.10X_2 + 12.31X_3 - 10.49X_2^2 - 15.97X_3^2 - 7.70X_2X_3 \quad (4.5)$$

Next, Box–Cox transformation was conducted on this model, again improving its accuracy (Table 4.4).

This new regression equation was:

$$-FE(\%)^{-1} = -0.010543 + 0.000022X_1 + 0.001056X_2 + 0.002491X_3 - 0.000134X_1^2 - 0.001767X_2^2 - 0.002853X_3^2 + 0.000396X_1X_2 + 0.000029X_1X_3 - 0.001 \quad (4.6)$$

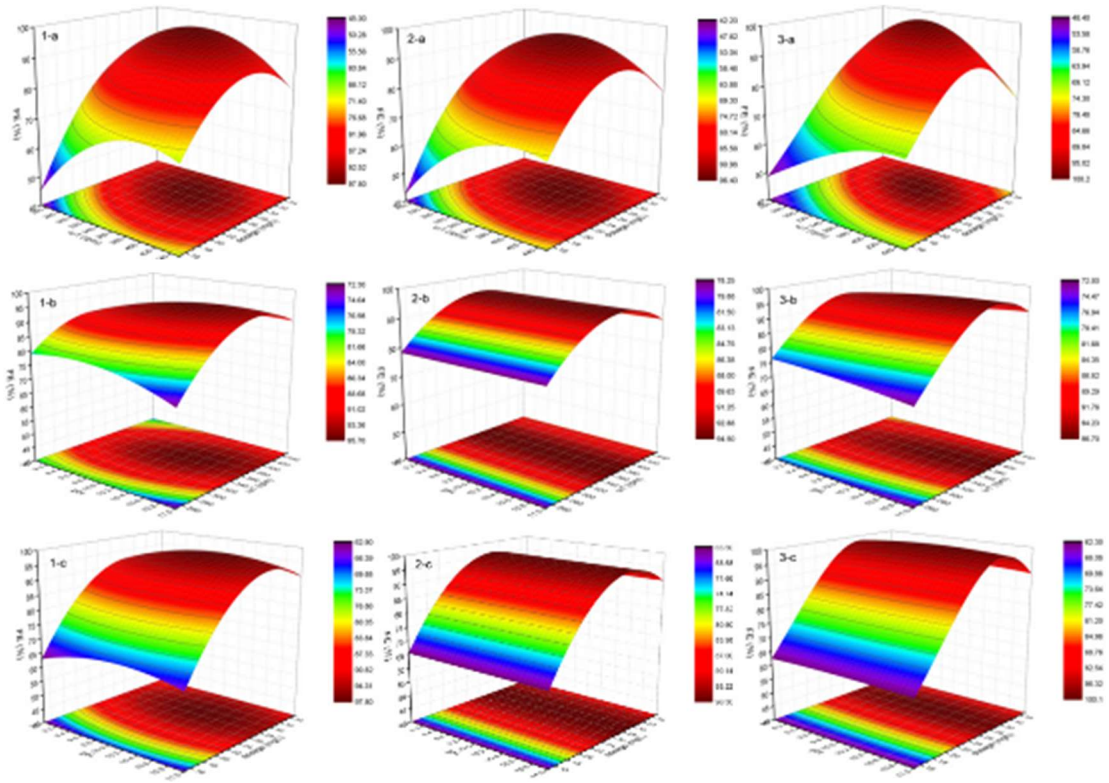

Figure 4.1. Plots of flocculation efficiency (FE) from three response surface methodology models: initial (1), nonsignificant factors removed (2), and Box–Cox transformed (3), in which the values of the independent variables were set in turn to pH = 10 (a), dosage = 25 mg/L (b), and mixing speed during intensive mixing,

ω_1 = 350 rpm (c).

Three-dimensional surface plots from the three models, displaying the effects of the independent variables on the FE, are shown in Figure 4.1.

Generally, the overall trend of the three was the same but with different details. With a constant pH of 10.0, increasing ω_1 from 250 to 360 rpm and increasing dosage from 15 to 28 mg/L increased the value of FE to a maximum; however, further increases in ω_1 or dosage reduced FE. The effects of ω_1 can be explained by changes in hydraulic conditions: a low stirring speed prevented the effective dispersion of the flocculant in the liquid, whereas a high speed destroyed flocs [31,32]. For the dosage of flocculant, zeta potential was not sufficiently reduced to induce flocculation until enough flocculant was added, however, an excess caused a charge reversal of the microalgal cell surface or triggered competition between cell surface adsorption and cell–flocculant–cell bridge formation [33,34]. An antagonistic effect of ω_1 and dosage on the FE was found, because high-speed stirring improved the dispersion of flocculant and hence strengthened the excess effect.

An important difference among the three models was that the FE reached a higher value with a steeper slope in the Box–Cox transformed model compared to the others. FE was changed more by ω_1 than by pH and reached a maximum value with $\omega_1 \approx 360$ rpm. The two models incorporating pH as a factor (initial and Box–Cox transformed) predicted that a maximum could be achieved at a pH below 10; it was possible to obtain an acceptable value of FE by appropriately lowering the pH while varying ω_1. When ω_1 was fixed at 350 rpm, a maximum of FE was reached at dosage ≈ 28 mg/L regardless of the value of the pH, indicating that ACPAM can be utilized in a certain pH range (9–11) without being significantly inhibited.

Both the model with nonsignificant factors removed and that with Box–Cox transformation were suitable for prediction of optimal conditions. The former is simpler but the latter is more adequate. Thus, statistical software was used to calculate the optimal experimental conditions according to both. The former predicted an optimized FE value of 96.4% at pH, ω_1, and dosage of 9.0, 361 rpm, and 28.5 mg/L, respectively, while the latter predicted values of 98.03%, 9.0, 347.0 rpm, and 30.6 mg/L, respectively. Considering the costs of the flocculation process, it is desirable if an acceptable FE can be reached with a lower stirring speed and less flocculant. Based on this consideration, the maximum FE was inspected for narrowing ranges of ω_1 and dosage until the achieved FE was less than 98%. For example, FE was initially inspected for ω_1 and dosage values in the ranges 250–345 rpm and 15–30.4 mg/L, respectively; however, the maximum value of FE obtained was higher than 98%, so the ranges were narrowed to 250–343 rpm and 15–30.2 mg/L, respectively, to evaluate the new maximum FE, and so on. Ultimately, a set of conditions (pH = 9.0, ω_1 = 339.3 rpm, and dosage = 28.54 mg/L) was identified that resulted in a maximum value of FE of 98.00% for the Box–Cox transformed model. This condition was experimentally validated in triplicate, and the obtained value of FE = 98.06 ± 0.36% was found to agree sufficiently

with the value predicted by that model.

4.3.4 Flocculant after thermal treatment

4.3.4.1 Thermogravimetric analyses of ACPAM

As shown in Figure 4.2, four stages of weight loss were observed during the TG analyses of the ACPAM. In the first stage, a weight loss of 8% occurred as the temperature increased from 30°C to 175°C, with a differential TG (DTG) peak at 74.2°C. Based on an endothermic peak at 77.7°C, this weight loss could be due to the removal of adsorbed water from the surface of the flocculant [35]. The second stage of weight loss was observed between 175°C and 325°C (DTG peak at 275.9°C) with a value of 40% and an endothermic DTA peak at 295.7°C, which indicated the decomposition of some functional groups (ester and peptidyl groups) [20]. The weight loss (22%) at the third stage (325–450°C) showed one large DTG peak (394.1°C), which was assigned to the rupture of the main carbon chain [36]. The final stage was from 450°C to 680°C (DTG peak at 583.0°C), with a weight loss of 29.1% and an exothermic DTA peak, which was on account of the ACPAM combusting. The residual weight percentage of the ACPAM after heating to 1000°C was measured to be 0.8%.

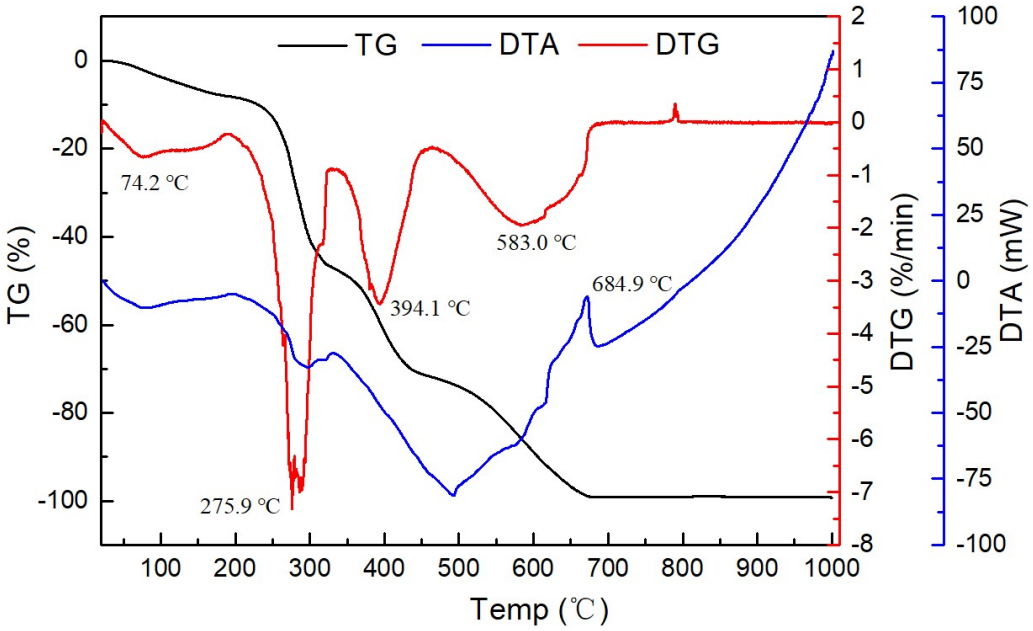

Figure 4.2. Thermal gravimetry (TG), differential TG (DTG), and differential thermal (DTA) analyses of ACPAM amphoteric flocculant.

4.3.4.2 FTIR of ACPAM

The FTIR spectra of the ACPAM after thermal treatment are shown in Figure 4.3. The peaks at 2,922 and 2,851 cm^{-1} correspond to C-H stretching in CH_2 due to asymmetrical and symmetrical vibrations, respectively [37,38]. The five peaks at 1,738, 1,730, 1,717, 1,695, and 1,680 cm^{-1} were related to C=O stretching vibration in different groups (ester, carboxyl, acetyl, and amino groups) [39,40]. The series of peaks from 1,487 to

1,416 cm^{-1} corresponded to C-H bending vibrations in CH, CH_2, and CH_3 [39]. The peak at 1,416 cm^{-1} also corresponded to a symmetrical stretching vibration of O-C-C with an O-H bending vibration. Another overlapping peak, due to an O-C-C asymmetrical stretching vibration with an O-H bending vibration, was located at 1,290 cm^{-1}; its "fingerprint peaks" at 1,240, 1,190, and 1,130 cm^{-1} confirmed the presence of this group. C-O stretching and C-C stretching vibrations coupled to cause the peak at 1059 cm^{-1}. The peak at 953 cm^{-1} corresponded to an O-H swing vibration. All of the peaks were found in the spectra of every ACPAM sample, from the untreated control sample (20°C) up to that treated at 120°C. The main spectral difference observed was that samples treated at higher temperatures had greater peak intensities. This was because the more moisture in ACPAM that was evaporated by higher temperatures, the greater the abundance of pure ACPAM in the sample.

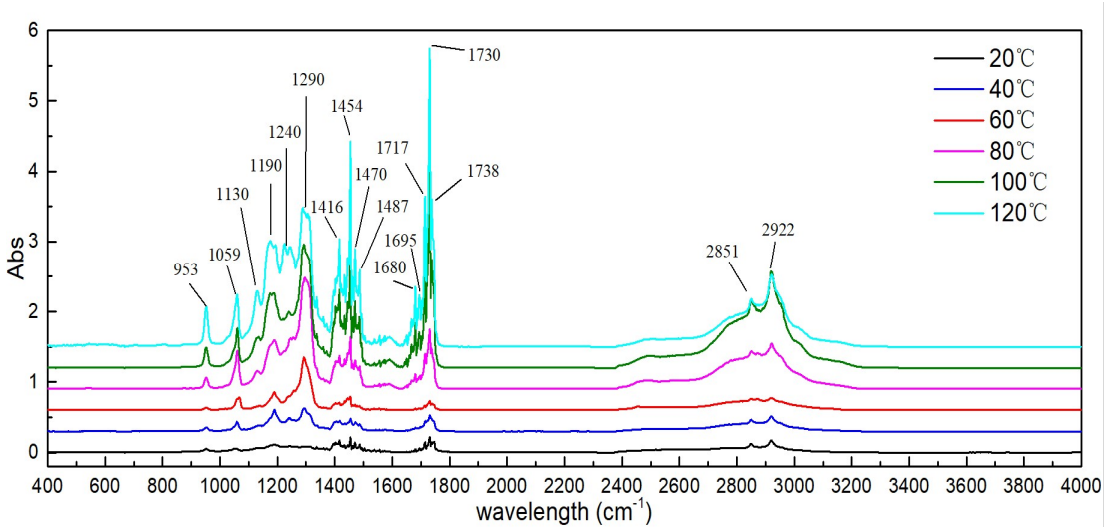

Figure 4.3. Fourier transform infrared spectra of ACPAM amphoteric flocculant after thermal treatment at different temperatures and of an untreated control sample. Kramers–Kroing transformation was applied.

4.3.4.3 XRD of ACPAM

The XRD spectrum of the ACPAM control sample without thermal treatment is shown in Figure 4.4. It exhibits a broad peak in the range $10 < 2\theta < 60°$ with a maximum at 22°, which indicates that it was an almost completely amorphous substance with disarranged molecules causing this scattered shape [41]. After the ACPAM was thermally treated at 40°C, some sharp peaks appeared on the broad peak, which indicated that a crystal structure had formed in the amorphous substance [42]. These sharp peaks at 18.2°, 22.2°, 24.0°, 24.5°, 26.4°, 31.3°, 32.7°, 33.0°, and 36.9° became stronger at 60°C, and corresponded to sulfamic acid [43]. For the ACPAM treated at 80°C, 100°C, and 120°C, the intensity of these peaks decreased with higher temperature; thus, the crystal substance started to degrade from 80°C. Considering that all six samples exhibited the same broad peak, we can conclude that the ACPAM, as the main component in the flocculant, was relatively stable within the studied temperature range.

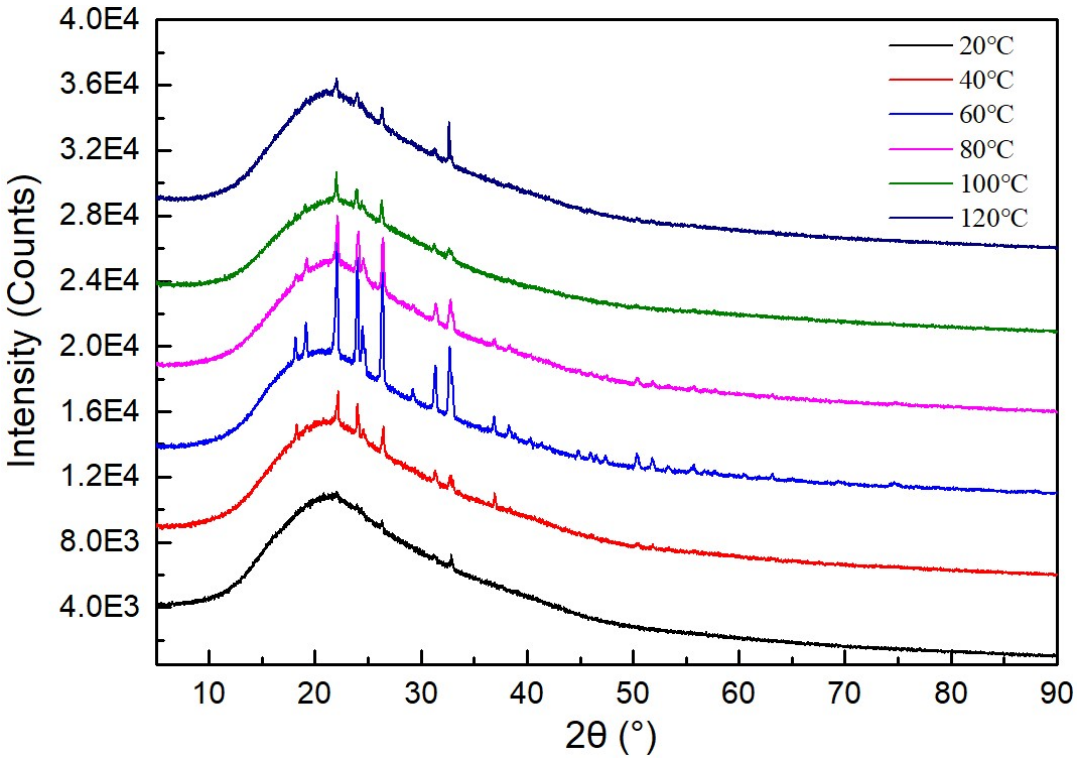

Figure 4.4. X-ray diffraction spectra of ACPAM amphoteric flocculant after thermal treatment at different temperatures and of an untreated control sample.

4.3.4.4 Flocculation performance of ACPAM after thermal treatment

As shown in Figure 4.5, flocculant that had not undergone thermal treatment obtained an FE of 98.06% under the final conditions described in Section 3.3. Thermal treatment at 40°C for 2 h increased FE slightly to 99.76%. Thermal treatment at 60°C, 80°C, and 100°C achieved similar FEs (99.77%, 99.56%, and 99.44%, respectively), which verified the thermal stability of the flocculant.

However, the FE value significantly decreased to 89.91% after treatment at 120°C, which indicated a structural change in the ACPAM. This was due to the ACPAM molecule containing amino and carboxyl groups; heating above 100°C causes imidization between the amino groups and condensation between the amino and carboxyl groups, which would cause crosslinking among the molecules (Figure S5) [44,45]. Both the crosslinked structure and the reduction in the number of functional groups (amino and carboxyl) weakens the ability of the flocculant to stretch in water and attach to the surface of microalgae, resulting in worse performance.

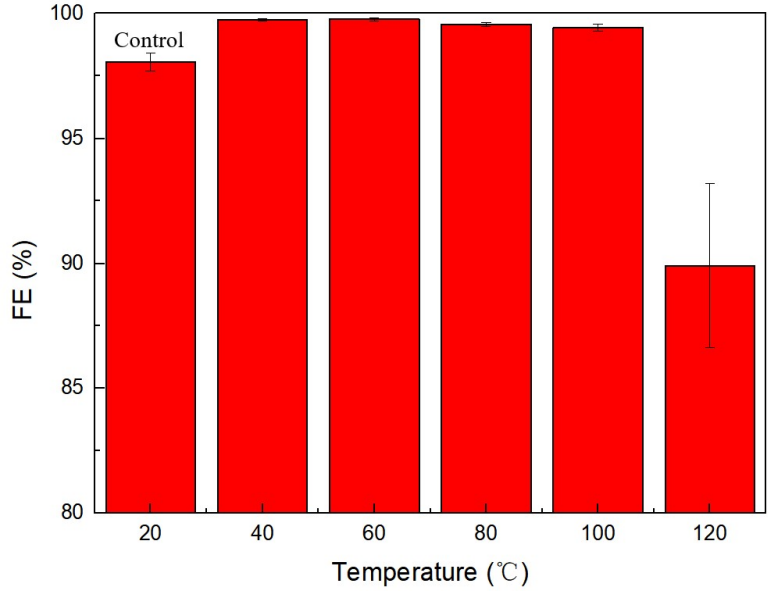

Figure 4.5. Flocculation efficiencies of ACPAM amphoteric flocculant after thermal treatment at different temperatures and of an untreated control sample.

4.3.5 Applicability of ACPAM

Next, ACPAM was compared to two other common flocculants ($AlCl_3$ and chitosan). Using 20 mg/L $AlCl_3$ obtained an FE of 63.3 ± 3.1%, which increased to 97.5 ± 0.35% for 30 mg/L $AlCl_3$, and achieved a maximum above 99.5% for 40 mg/L. Less chitosan (7.5 mg/L) was needed to achieve its maximum FE of 97.2%, but only half of the biomass was harvested when the dosage was decreased to 5.0 mg/L. Thus, the flocculation performance of ACPAM was similar to $AlCl_3$, but less effective than chitosan, for harvesting *Coccomyxa sp. KJ*.

In addition, two other species (*C. reinhardtii* and *T. obliquus*) were investigated with these three flocculants, as shown in Figure 4.6. When harvesting *C. reinhardtii*, the maximum values of FE were 99.6% 99.0%, and 98.5% for the $AlCl_3$, chitosan, and ACPAM, respectively. Although there were no significant differences in these values, the optimal dosages to achieve such efficiency differed greatly: 115 mg/L $AlCl_3$ vs. 80 mg/L chitosan vs. 520 mg/L ACPAM. This indicates that the ACPAM was less effective than the other two flocculants for harvesting *C. reinhardtii*.

However, for *T. obliquus*, the results were significantly different. Using 22.5 mg/L ACPAM induced flocculation (FE = 53.9%) while no flocculation was observed at the same dosage of $AlCl_3$ or chitosan. The optimal dosage for $AlCl_3$ was 70 mg/L for a maximum FE of 98.4%, whereas 50 mg/L chitosan harvested 98.5% of microalgal biomass. The performance of ACPAM was similar, with 52.5 mg/L achieving an FE of 99.0%. Totally, we tested 8 species for the ACPAM (chapter 2.1), and results showed it worked for 3 fresh water species among them as shown above. Thus, ACPAM was possible to utilize the ACPAM, a type of amphoteric flocculant, to harvest various fresh water microalgae species, and amphoteric flocculants, as well as cationic ones, should

be considered for microalgal flocculation.

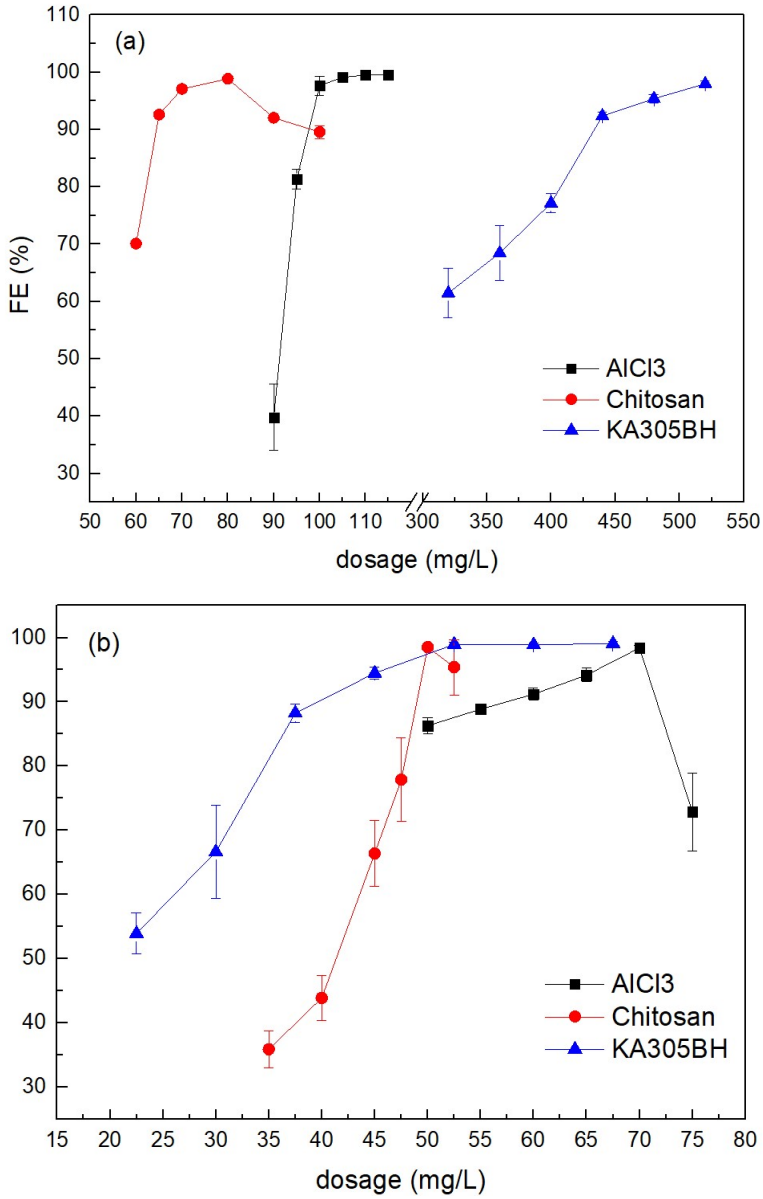

Figure 4.6. Flocculation efficiencies of three flocculants when harvesting two microalgal species: a) *Chlamydomonas reinhardtii* and b) *Tetradesmus obliquus*. KA305BH: ACPAM amphoteric flocculant.

4.4 Conclusions

We used RSM to investigate the flocculation performance of ACPAM for harvesting microalgae. We identified the most important factors affecting performance, and then optimized them to ultimately achieve an FE of ~98%. Thermal stability analyses indicated that the ACPAM was generally stable below 100°C, but at higher temperatures underwent a slight weight loss caused by the evaporation of absorbed moisture. Crosslinking of its molecules by imidization and condensation occurred at

120°C, which explained a decline of flocculation performance at that temperature. Finally, ACPAM was compared to other two flocculants ($AlCl_3$ and chitosan) for the harvest of three microalgal species; the results indicated that ACPAM can be applied to a range of microalgal species.

References

[1] Enamala, M. K., Enamala, S., Chavali, M., Donepudi, J., Yadavalli, R., Kolapalli, B., ... & Kuppam, C. (2018). Production of biofuels from microalgae-A review on cultivation, harvesting, lipid extraction, and numerous applications of microalgae. Renewable and Sustainable Energy Reviews, 94, 49-68.

[2] Sati, H., Mitra, M., Mishra, S., & Baredar, P. (2019). Microalgal lipid extraction strategies for biodiesel production: A review. Algal research, 38, 101413.

[3] Jankowska, E., Sahu, A. K., & Oleskowicz-Popiel, P. (2017). Biogas from microalgae: Review on microalgae's cultivation, harvesting and pretreatment for anaerobic digestion. Renewable and Sustainable Energy Reviews, 75, 692-709.

[4] Yan, N., Fan, C., Chen, Y., & Hu, Z. (2016). The potential for microalgae as bioreactors to produce pharmaceuticals. International journal of molecular sciences, 17(6), 962.

[5] Sathasivam, R., Radhakrishnan, R., Hashem, A., & Abd_Allah, E. F. (2019). Microalgae metabolites: A rich source for food and medicine. Saudi journal of biological sciences, 26(4), 709-722.

[6] Begum, H., Yusoff, F. M., Banerjee, S., Khatoon, H., & Shariff, M. (2016). Availability and utilization of pigments from microalgae. Critical reviews in food science and nutrition, 56(13), 2209-2222.

[7] Couteau, C., & Coiffard, L. (2018). Microalgal application in cosmetics. In Microalgae in health and disease prevention (pp. 317-323). Academic Press.

[8] Daneshvar, E., Zarrinmehr, M. J., Hashtjin, A. M., Farhadian, O., & Bhatnagar, A. (2018). Versatile applications of freshwater and marine water microalgae in dairy wastewater treatment, lipid extraction and tetracycline biosorption. Bioresource technology, 268, 523-530.

[9] Menegazzo, M. L., & Fonseca, G. G. (2019). Biomass recovery and lipid extraction processes for microalgae biofuels production: a review. Renewable and Sustainable Energy Reviews, 107, 87-107.

[10] Gerchman, Y., Vasker, B., Tavasi, M., Mishael, Y., Kinel-Tahan, Y., & Yehoshua, Y. (2017). Effective harvesting of microalgae: Comparison of different polymeric flocculants. Bioresource technology, 228, 141-146.

[11] Vu, H. P., Nguyen, L. N., Lesage, G., & Nghiem, L. D. (2020). Synergistic effect of dual flocculation between inorganic salts and chitosan on harvesting microalgae Chlorella vulgaris. Environmental Technology & Innovation, 100622.

[12] Mathimani, T., & Mallick, N. (2018). A comprehensive review on harvesting of microalgae for biodiesel–Key challenges and future directions. Renewable and Sustainable Energy Reviews, 91, 1103-1120.

[13] Van Haver, L., & Nayar, S. (2017). Polyelectrolyte flocculants in harvesting microalgal biomass for food and feed applications. Algal Research, 24, 167-180.

[14] Tenney, M. W., Echelberger, W. F., Schuessler, R. G., & Pavoni, J. L. (1969). Algal flocculation with synthetic organic polyelectrolytes. Appl. Environ. Microbiol., 18(6), 965-971.

[15] He, K., Lou, T., Wang, X., & Zhao, W. (2015). Preparation of lignosulfonate–acrylamide–chitosan ternary graft copolymer and its flocculation performance. International journal of biological macromolecules, 81, 1053-1058.
[16] Cui, G., Wang, X., Xun, J., & Lou, T. (2017). Microwave assisted synthesis and characterization of a ternary flocculant from chitosan, acrylamide and lignin. International Biodeterioration & Biodegradation, 123, 269-275.
[17] Li, X., Zheng, H., Gao, B., Zhao, C., & Sun, Y. (2017). UV-initiated polymerization of acid-and alkali-resistant cationic flocculant P (AM-MAPTAC): synthesis, characterization, and application in sludge dewatering. Separation and Purification Technology, 187, 244-254.
[18] Pérez, L., Salgueiro, J. L., Maceiras, R., Cancela, Á., & Sánchez, Á. (2016). Study of influence of pH and salinity on combined flocculation of Chaetoceros gracilis microalgae. Chemical Engineering Journal, 286, 106-113.
[19] Pandey, A., Shah, R., Yadav, P., Verma, R., & Srivastava, S. (2020). Harvesting of freshwater microalgae Scenedesmus sp. by electro–coagulation–flocculation for biofuel production: effects on spent medium recycling and lipid extraction. Environmental Science and Pollution Research, 27(3), 3497-3507.
[20] Zhao, C., Shao, S., Zhou, Y., Yang, Y., Shao, Y., Zhang, L., ... & Luo, L. (2018). Optimization of flocculation conditions for soluble cadmium removal using the composite flocculant of green anion polyacrylamide and PAC by response surface methodology. Science of The Total Environment, 645, 267-276.
[21] Joyce, A. P., & Leung, S. S. (2013). Use of response surface methods and path of steepest ascent to optimize ligand-binding assay sensitivity. Journal of immunological methods, 392(1-2), 12-23.
[22] Li, Y., Xu, Y., Liu, L., Jiang, X., Zhang, K., Zheng, T., & Wang, H. (2016). First evidence of bioflocculant from Shinella albus with flocculation activity on harvesting of Chlorella vulgaris biomass. Bioresource technology, 218, 807-815.
[23] Bezerra, M. A., Santelli, R. E., Oliveira, E. P., Villar, L. S., & Escaleira, L. A. (2008). Response surface methodology (RSM) as a tool for optimization in analytical chemistry. Talanta, 76(5), 965-977.
[24] Fitzpatrick, C. S. B., Fradin, E., & Gregory, J. (2004). Temperature effects on flocculation, using different coagulants. Water Science and Technology, 50(12), 171-175.
[25] Le Man, H., Behera, S. K., & Park, H. S. (2010). Optimization of operational parameters for ethanol production from Korean food waste leachate. International Journal of Environmental Science & Technology, 7(1), 157-164.
[26] Rai, A., Mohanty, B., & Bhargava, R. (2016). Supercritical extraction of sunflower oil: A central composite design for extraction variables. Food chemistry, 192, 647-659.
[27] Owolabi, R. U., Usman, M. A., & Kehinde, A. J. (2018). Modelling and optimization of process variables for the solution polymerization of styrene using response surface methodology. Journal of King Saud University-Engineering

Sciences, 30(1), 22-30.
[28] Ghafari, E., Costa, H., & Júlio, E. (2014). RSM-based model to predict the performance of self-compacting UHPC reinforced with hybrid steel micro-fibers. Construction and Building Materials, 66, 375-383.
[29] Bhardwaj, B., Kumar, R., & Singh, P. K. (2014). An improved surface roughness prediction model using Box-Cox transformation with RSM in end milling of EN 353. Journal of Mechanical Science and Technology, 28(12), 5149-5157.
[30] Çırak, M. (2018). Improvement of RSM Prediction and Optimization by Using Box-Cox Transformation: Separation of Colloidal Contaminants From Mineral Processing Effluents via Electrocoagulation. In Handbook of Research on Predictive Modeling and Optimization Methods in Science and Engineering (pp. 156-191). IGI Global.
[31] Zeng, D. F., Hu, D., & Cheng, J. (2012). Experimental study on chitosan composite flocculant for treating papermaking wastewater. Journal of Water Chemistry and Technology, 34(1), 35-41.
[32] Sun, Y., Chen, A., Pan, S. Y., Sun, W., Zhu, C., Shah, K. J., & Zheng, H. (2019). Novel chitosan-based flocculants for chromium and nickle removal in wastewater via integrated chelation and flocculation. Journal of environmental management, 248, 109241.
[33] Kaith, B. S., Jindal, R., & Sharma, R. (2016). Study of ionic charge dependent salt resistant swelling behavior and removal of colloidal particles using reduced gum rosin-poly (acrylamide)-based green flocculant. Iranian Polymer Journal, 25(4), 349-362.
[34] Grima, E. M., Belarbi, E. H., Fernández, F. A., Medina, A. R., & Chisti, Y. (2003). Recovery of microalgal biomass and metabolites: process options and economics. Biotechnology advances, 20(7-8), 491-515.
[35] Kundu, S. K., & Bhaumik, A. (2015). A triazine-based porous organic polymer: a novel heterogeneous basic organocatalyst for facile one-pot synthesis of 2-amino-4 H-chromenes. RSC Advances, 5(41), 32730-32739.
[36] Ma, J., Fu, K., Fu, X., Guan, Q., Ding, L., Shi, J., ... & Jiang, L. (2017). Flocculation properties and kinetic investigation of polyacrylamide with different cationic monomer content for high turbid water purification. Separation and Purification Technology, 182, 134-143.
[37] Samanta, A., Ojha, K., & Mandal, A. (2011). Interactions between acidic crude oil and alkali and their effects on enhanced oil recovery. Energy & Fuels, 25(4), 1642-1649.
[38] Li-Chan, E., Chalmers, J. M., & Griffiths, P. R. (Eds.). (2010). Applications of vibrational spectroscopy in food science; p325. John Wiley & Sons.
[39] Popescu, C. M., Popescu, M. C., & Vasile, C. (2011). Structural analysis of photodegraded lime wood by means of FT-IR and 2D IR correlation spectroscopy. International journal of biological macromolecules, 48(4), 667-675.
[40] Badri, K. B. H., Sien, W. C., Shahrom, M. S. B. R., Hao, L. C., Baderuliksan, N.

Y., & Norzali, N. R. (2010). FTIR spectroscopy analysis of the prepolymerization of palm-based polyurethane. Solid State Sci. Technol, 18(2), 1-8.
[41] Freitas, T. K. F. S., Oliveira, V. M., De Souza, M. T. F., Geraldino, H. C. L., Almeida, V. C., Fávaro, S. L., & Garcia, J. C. (2015). Optimization of coagulation-flocculation process for treatment of industrial textile wastewater using okra (A. esculentus) mucilage as natural coagulant. Industrial Crops and Products, 76, 538-544.
[42] Lin, Q., Peng, H., Zhong, S., & Xiang, J. (2015). Synthesis, characterization, and secondary sludge dewatering performance of a novel combined silicon–aluminum–iron–starch flocculant. Journal of hazardous materials, 285, 199-206.
[43] Bardhan, K., Mukhopadhyay, S., & Chatterjee, S. R. (1977). Grafting of acrylamide onto methyl cellulose by persulfate ion. Journal of Polymer Science: Polymer Chemistry Edition, 15(1), 141-148.
[44] Caulfield, M. J., Qiao, G. G., & Solomon, D. H. (2002). Some aspects of the properties and degradation of polyacrylamides. Chemical reviews, 102(9), 3067-3084.
[45] Zhorin, V. A., Kiselev, M. R., & Roldugin, V. I. (2016). The effect of plastic deformation under high pressure on the thermal effects in polyacrylamide. International Polymer Science and Technology, 43(9), 19-24.

Chapter 5 Evaluation of a Sludge Treatment Process Comprising Lipid Extraction and Drying using Liquefied Dimethyl Ether

5.1 Introduction

The environmental problems caused by fossil fuels and the uncertainties of future petroleum supplies have increased interest in biodiesel [1,2]. However, the price of biodiesel cannot compete with fossil fuel, because it is mostly extracted from edible vegetable oilseeds, which represent 85% of overall biodiesel cost [3, 4, 5]. Furthermore, large-scale cultivation of oilseeds for biodiesel may promote famine [6]. Due to the worldwide increase of sludge that contains high amounts of lipids being generated, municipal sludge is a cost-effective alternative for biodiesel production. For example, 27% lipid and 19% biodiesel yields (on a dry sludge basis) have been achieved from primary sludge [7]. The lipid yield accounted for one-third of dried scum sludge [8]. By Soxhlet extraction, 2.5–10.3% lipids were extracted from dried sewage sludge [9]. The biodiesel yield of activated sludge was increased from 2.10 to 7.78% by sub-critical water treatment [10]; and the highest yield of fatty acid methyl esters (FAMEs; 18 wt%) and the lowest energy input (17 MJ/kg-FAME) were achieved by hexane extraction followed by methanolysis of extracted lipids [11].

The increasing quantity of sewage sludge generated as a by-product of sewage treatment of municipal or industrial wastewater requires the development of novel disposal methods [12]. As of the end of 2016, more than 2.2 million tons of sludge (dry basis) are annually generated in Japan [13]. The annual production of sewage sludge in China was reported to be 6 million tons (dry basis) and to be increasing [14]. Wastewater treatment plants in South Korea produce over 1.9 million tons of sludge (dry basis) [15]. Over 6.2 million tons of dried sewage sludge are generated in the United States (US) annually [16]. In Europe, around 10 million tons of sludge (dry basis) are produced annually [17]. Compared with landfill, anaerobic digestion, and composting, incineration of sludge reduces land use and the thermal energy recovered represents a sustainable carbon-neutral resource [18, 19, 20]. Thus, incineration of sludge could be an attractive disposal method for countries or districts with limited space, such as Japan. However, for incineration [18, 21], large amounts of water must be removed from the sludge or supplemental fuel must be co-combusted with the sludge, hence involving highly energy-intensive processes.

The requirement for renewable energy and sustainable sewage-sludge treatment has prompted exploration of innovative methods for sludge treatment [22, 23]. The solid-liquid liquefying dimethyl ether (DME) technique [19] enables simultaneous lipid

extraction and drying of sludge with relatively low energy consumption [24, 25, 26]. Raw lipids and moisture are removed from sludge, and the dewatered sludge is suitable for incineration directly as a solid fuel, while the raw lipids extracted can be refined to biodiesel. DME is widely available and relatively inexpensive, and is produced in China at low cost [27, 28]. In Europe, DME produced via black liquor gasification has been used as a fuel in Volvo trucks [29]. In addition, the physical characteristics of DME facilitate the extraction of lipids and moisture from sludge. DME is a gas at room temperature and ambient pressure. It has a boiling point of $-25℃$ and readily liquefies at 0.51–0.59 MPa at room temperature (20–25℃). DME is partially miscible in water (7–8 wt.% at room temperature) and has high affinity for organic compounds [30]. After extraction, liquid DME can be evaporated by depressurization, and the extracted water separated. Because of its low boiling point, the recycling of DME (evaporation and liquefaction) permits use of unharnessed low-level heat sources, so the drying energy is almost half that required by conventional thermal drying techniques [31].

In a previous study [32], DME was used to remove water from wet sawdust and wet wood chips, resulting in a water content of 8–15%. Therefore, DME-mediated drying of solid biomass feedstock is energy efficient. DME has been used for extraction of water and lipids from four common vegetable biomasses; it removed ~ 81.3–88.7% of water and yielded 5.8–16.8% lipids (dry weight) [33]. DME-mediated extraction of lipids from seven microalga species resulted in raw lipid yields of 9.9–40.1% by dry weight [34]. In our previous study [25], we evaluated the ability of the DME method to remove water from sewage sludge, and so its performance in terms of raw lipid yields needs to be investigated. Moreover, the effect of extraction time, DME to sludge ratio, sludge ball size, and properties of the sewage sludge on the DME performance need to be further studied. Also, the DME method requires optimization and analysis of its economic performance before commercialization.

Even though our main study is lipid extraction from microalgae by DME, we'd like to start from lipid extraction from sludge. It's because the DME method for sludge has been well investigated in our lab and rest of unfinished part should be completed. Based on this chapter, the obtained results can support and compare with research on lipid extraction from microalgae. In this study, a fixed-bed extraction apparatus was used to determine the optimal sludge ball size, extraction time, and DME to sludge ratio. We evaluated the DME and Bligh and Dyer (B&D) methods [35] in terms of the raw lipid yield and water content of five types of sewage sludge. We also assessed the effect of reuse of DME on the raw lipid yield and water content. Furthermore, energy consumption analysis is getting more and more attention, such as ~50% of overall gross energy saving has been achieved by recycling solvent hexane in vegetable oil extraction process [36,37]. Thus, based on the findings, we also evaluated the production cost and output of value-added products per kilogram sludge to support commercialization of the DME method.

5.2 Materials and Methods

5.2.1 Sludge collection and preparation

Three types of dewatered sludge from undigested sludges (A, B, and C) and two types of dewatered sludge from anaerobically digested sludges (D and E) were collected from wastewater treatment plants in Aichi, Tokyo, Kanagawa, Kumamoto, and Osaka prefecture, Japan. The initial water contents of the dewatered sludges were 76.5, 73.2, 78.5, 78.2, and 82.7 %, respectively.

5.2.2 The B&D method

The lipids and other organics in the dewatered sludges were extracted by a modified B&D method. Samples (10.0 g) were placed in an oven for 12 h at 105℃, and 10.0 mL of methanol, 5.0 mL of chloroform (Guaranteed Reagent, Wako Co., Ltd, Japan) and 4.0 mL of pure water were added per 1 g of sample. The samples were crushed using a homogenizer (T25, IKA Co., Ltd, Germany) at 10,000 rpm for 5 min and vortex-mixed using a Vortex Genie (SI-0236, SI Co., Ltd.) for 5 min. Next, 5.0 mL of chloroform and 5.0 mL of pure water were added and the samples were vortex-mixed for 2 min. Phases were separated by centrifugation at 3,000 rpm (2410, Kubota Co., Ltd, Japan) for 5 min, and the samples were divided into three layers from top to bottom: the water-methanol, sludge, and chloroform layers. After recovering the lipid-rich chloroform layer, it was passed through a 0.45-μm membrane (DISMIC-13HP, Advantec Co., Ltd., Japan) to remove particles. Most of the solvent in the lipid-rich filtrate was removed using a rotary evaporator at 40℃ under a vacuum. The remaining solvent was removed in a nitrogen gas flow solvent evaporator (Nitrogen Termovap Sample Concentrator, Ishii Tatami Shop Co., Ltd., Japan), and the extract was weighed and stored at < 0℃ until analysis by gas chromatography-mass spectrometry (GC-MS).

5.2.3 The DME method

Figure 5.1 shows a schematic diagram of the liquefied DME flow experimental apparatus. It consists of six main parts: a vessel for storing liquefied DME (vessel 1, TVS-1-100, 500 cm^3, Taiatsu Techno Corp., Saitama, Japan), a vessel for measuring the volume of DME (vessel 2, 100 cm^3, HPG-96-3, 26.5 mm φ × 238 mm, Taiatsu Techno Corp.), a vessel for sludge drying (vessel 3, 100 cm^3, HPG-96-3, 26.5 mm φ × 238 mm, Taiatsu Techno Corp.), a vessel for storing the separated liquid (vessel 4, 100 cm^3, HPG-96-3, 100 cm^3, Taiatsu Techno Corp.), a moisture-trap column (HPG-10-5, 11.6 mm φ × 190 mm, Taiatsu Techno Corp.) containing $CaCl_2$, and a condensation vessel for storing gaseous DME (vessel 6, SUS-316, 100 cm^3, Taiatsu Techno Corp., Saitama, Japan). The experimental apparatus without vessel 6 was used for drying. The complete apparatus was employed for the recovery and reuse of DME.

The drying experiment was conducted using liquefied DME with five types of dewatered sludge. After cooling gaseous DME (420 D, Tamiya Co., Ltd., Shizuoka, Japan) with ethanol (Guaranteed Reagent, Wako Co., Ltd., Japan) and ice, liquefied DME was stored in vessel 1. Next, DME was pushed from vessel 1 to 2 by N_2 gas pressure (ZERO-A, Sumitomo Seika Chemicals Co., Ltd., Japan). Sludge (1.0 g) was packed into vessel 3 with DME from vessel 2. After extraction, the liquid portion containing extracted raw lipids, extracted water, and DME was transferred to vessel 4, and the solid portion was removed from vessel 3 for analysis. In vessel 4, DME was separated from the lipids by reducing the pressure to ambient pressure, which evaporated DME. Gaseous DME containing moisture was passed through a column containing 10.0 g of $CaCl_2$ (Guaranteed Reagent, Wako Co., Ltd., Japan) for 1 h to trap moisture, re-liquefied in vessel 5, and cooled using ice and ethanol for reuse. The raw lipid in vessel 4 was re-dissolved in 5.0 mL of chloroform and passed through a 0.45-μm membrane filter. Chloroform was removed by nitrogen flow, and the extract was weighed and stored at < 0°C.

Figure 5.1 Schematic of the DME flow-type experimental apparatus.

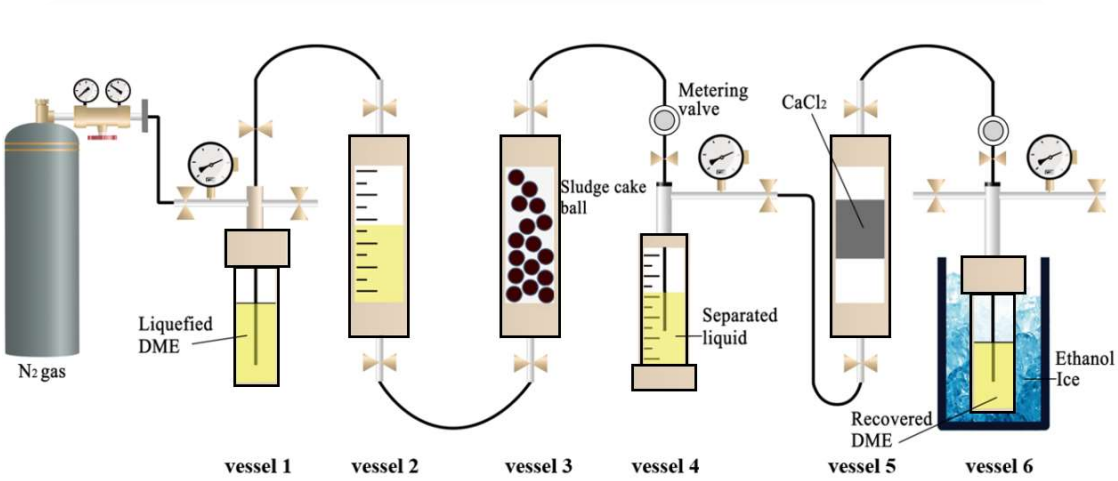

5.2.4 Experimental design

5.2.4.1 Optimization of the DME method

Single-factor experiments were conducted to investigate the effect of three factors on the DME method using dewatered sludge A (Table 5.1). To control the contact area between liquefied DME and dewatered sludge, balls 11.7, 9.5, 7.6, 5.8, 4.6, and 3.7 mm in diameter were made from the dewatered sludge samples. In this study, the dewatered sludge was rubbed into several little spherical balls by hands. To control the diameter of the sludge balls, a certain weight of sludge cake was taken and weighted by Balance for each diameter condition before this sludge-ball-making process. Then diameter of the made sludge balls were checked by Vernier scale. At a DME–sludge ratio of 50

mL/g and an extraction time of 20 min, the sludge balls were treated with liquefied DME. To evaluate the effect of extraction time, sludge balls (5.8 mm) were immersed in DME for 5, 10, 15, 20, 25, or 30 min at a DME-sludge ratio of 50 mL/g. To investigate the effect of the DME-sludge ratio, 5.8-mm sludge balls at DME-sludge ratios of 10, 20, 30, 50, 80, and 100 mL/g were treated with DME for 20 min. The experiments described above were repeated twice.

Table 5.1 Experimental conditions.

	DME method optimization	Comparison of two methods	Reuse of DME
Amount of sewage sludge	0.5-1.0 g	1.0 g	0.75 g
Liquefied DME:Sludge ratio	10-100 mL/g	50 mL/g	60 mL/g
extraction time	5-30 min	20 min	20 min
Diameter of sewage sludge ball size	3.7-11.7 mm	5.8 mm	5.8 mm

5.2.4.2 Comparison of the DME and B&D methods

Under the conditions listed in Table 5.1, the five sludges were treated by the DME and B&D methods. The mass balance (total solid content, separated water, residual water, and extracted raw lipids) before and after treatment was analyzed. GC-MS was used to quantify fatty acid methyl esters (FAMEs) to evaluate post-processing of biodiesel. The lower heating value (LHV) of treated sludge was calculated from the higher heating value (HHV). The water content and carbon, hydrogen, and nitrogen (CHN) percentages of the sludge were determined to evaluate its potential for electricity generation after incineration.

5.2.4.3 Recovery and reuse of liquefied DME

Using a sludge ball size of 5.8 mm, an extraction time of 20 min and a DME-sludge ratio of 60 mL/g, the reusability of DME was evaluated using sludge C. Gaseous DME was liquefied by a mixture of ice and ethanol and used for extraction five times. Changes in the raw lipid yield and drying ratio were analyzed.

5.2.5 Economic analysis

The cost and output of value-added product (biodiesel) of treating 1 ton of undigested sludge were analyzed using the DME conventional solvent extraction, and conventional heat-drying methods. For the conventional solvent extraction method, cost was estimated as the sum of the costs of mechanical dewatering, sludge drying, lipid extraction, and biodiesel purification, which were obtained from prior studies [38, 39, 40]. For the DME method, while mechanical dewatering and biodiesel purification costs per gram of raw lipids were assumed to be equivalent to those of the conventional solvent extraction method, the lipid extraction cost was calculated by multiplying the

energy consumed by the price of electricity (TEPCO Energy Partner Co., Ltd.; Appendix Data 5.1.1). When the water content of sludge had decreased sufficiently to allow direct incineration, the dried sludge produced was assumed to be incinerated with municipal solid waste (MSW) for energy recovery with a net electricity-generation efficiency of 10% of its LHV [41], and the recovered energy was subtracted from the total cost. Next, lipid production was evaluated based on experimental data. For the conventional heat-drying method, which involves mechanical dewatering and a rotary dryer, while the cost of the mechanical dewatering step was calculated as above, that of the drying step was calculated based on energy consumption (Appendix Data 1.3). Finally, energy from incinerating dried sludge was also considered. It should be noticed that the economic analysis is mainly based on experiments-scale, and are hence tentative only.

5.2.6 Instruments and analysis

The obtained raw lipids from the two methods were re-dissolved in 5 ml dichloromethane (Guaranteed Reagent, Wako Co., Ltd., Japan), then subjected to methanolysis using 2 mL of 14% BF_3-methanol solution (First Grade, Wako Co., Ltd., Japan). The mixture was vortex-mixed and reacted at 65℃ for 40 min. Next, the mixture was cooled to room temperature and 4 mL of saturated aqueous NaCl (Guaranteed Reagent, Wako Co., Ltd., Japan) solution was added. The CH_2Cl_2 layer containing FAMEs was recovered by pipetting. To the recovered FAMEs solution, 100 ppm 2,6-di-t-butyl-4-methylphenol (Special Grade, Wako Co., Ltd., Japan) was added as an antioxidant. Quantitation of the solution was conducted by GC-MS (GC/MS-QP2010 Plus, Shimadzu Corp., Kyoto, Japan) with helium gas flow (5.0 mL/min, ZERO-A, Sumitomo Seika Chemicals Co., Ltd., Japan). The GC-MS column was a SP-2560 (length 100 m; internal diameter 0.20 mm; d_f, 0.25 μm). The GC oven temperature was initially 100℃, held for 5 min, ramped to 180℃ at 4℃/min, to 240℃ at 2℃/min, which was held for 15 min. The GC-MS calibration curve was generated using a 37-component FAME standard (Sigma-Aldrich Japan, Co., Ltd., Tokyo, Japan). The higher heating value (HHV) of samples was measured by bomb calorimetry (CA-4AJ, Shimadzu Corp., Kyoto, Japan, Japan), and CHN analysis was performed using an elemental analyzer (Micro Corder JM10, J-science Labo Co., Ltd.).

5.3. Results and Discussion

5.3.1 Optimization of DME process conditions

Optimizing the DME method maximizes the raw lipid yield and minimizes the water content, and so we investigated the effect of sludge ball size, extraction time, and DME/sludge ratio in single-factor experiments. Figure 5.2(a) shows the yield of raw lipids and the water content of sludge A after extraction. The lipid yield and moisture content increased and decreased, respectively, with decreasing sludge ball size due to

an increased area of contact between the liquefied DME and the sludge ball. After DME treatment, the water content of 11.7-mm sludge decreased from 0.765 to 0.679 g/g wet-sludge, with a lipid yield of 0.0107 g raw lipids per 1 g wet-sludge extraction. The lipid yield increased almost linearly with decreasing ball size; 0.0129 (9.5 mm), 0.0153 (7.6 mm), 0.0190 (5.8 mm), 0.0214 (4.6 mm), and 0.0224 g/g (3.7 mm). The water content of 7.6-mm sludge (0.627 g/g) was 7.6% lower than that of 11.7-mm sludge, and that of 3.7-mm sludge was 38.0% lower at 0.389 g/g. Therefore, the decrease in the water content with sludge size was greater in the range 11.7–7.6 mm than in the range 7.6–3.7 mm. Thus, to obtain a high lipid yield and a low water content, the sludge ball size should be < 7.6 mm.

Figure 5.2(b) shows the raw lipid yield and water content according to extraction time using 5.8-mm sludge balls and a 50-mL/g DME/sludge ratio. The lipid yield and water content changed almost linearly with extraction time. As the extraction time increased from 5 to 30 min, the lipid yield increased from 0.0136 to 0.0227 g/g wet-sludge and the water content decreased from 0.688 to 0.504 g/g. Therefore, after extraction for 30 min DME was not saturated with lipid and moisture, and the lipid yield increased, and the water content decreased, with increasing extraction time.

Figure 5.2(c) shows the relationships among the lipid yield, water content, and DME/sludge ratio. The lipid yield and amount of water removed increased as the DME/sludge ratio increased to 50 m/g, but did not increase further at ratios of > 50 mL/g. Therefore, the lipid yield and drying ratio increased at DME/sludge ratios of < 50 mL/g. As the ratio increased from 10 to 50 mL/g, the amount of lipid extracted increased significantly from 0.0108 to 0.0190 g/g wet-sludge, and the water content decreased from 0.657 to 0.546 g/g. At a ratio of 100 mL/g, the amount of extracted lipids increased to 0.0193 g/g, and the water content decreased to 0.543 g/g. Therefore, a DME/sludge ratio of > 50 mL/g did not further enhance lipid and moisture extraction. Increasing the amount of extracted lipids and reducing the water content of sludge can be achieved by reducing sludge ball size, extending the extraction time, or increasing the DME/sludge ratio. However, increasing the DME/sludge ratio increases the material and energy costs, but reducing the sludge ball size or extending the extraction time does not. Therefore, any decline in extraction efficiency caused by a lower DME/sludge ratio can be compensated by controlling sludge ball size and extraction time, implying that the DME method is suitable for extracting lipids from sludge.

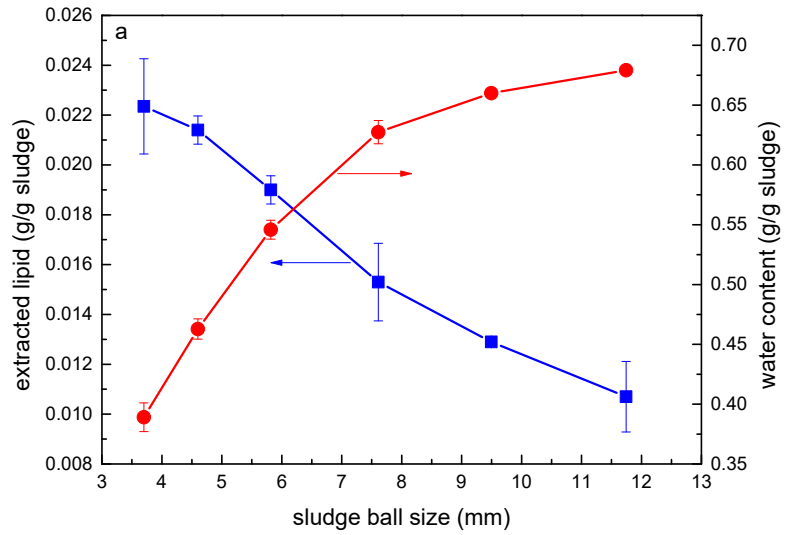
a
extracted lipid (g/g sludge)
water content (g/g sludge)
sludge ball size (mm)
0.026
0.024
0.022
0.020
0.018
0.016
0.014
0.012
0.010
0.008
0.70
0.65
0.60
0.55
0.50
0.45
0.40
0.35
3
4
5
6
7
8
9
10
11
12
13

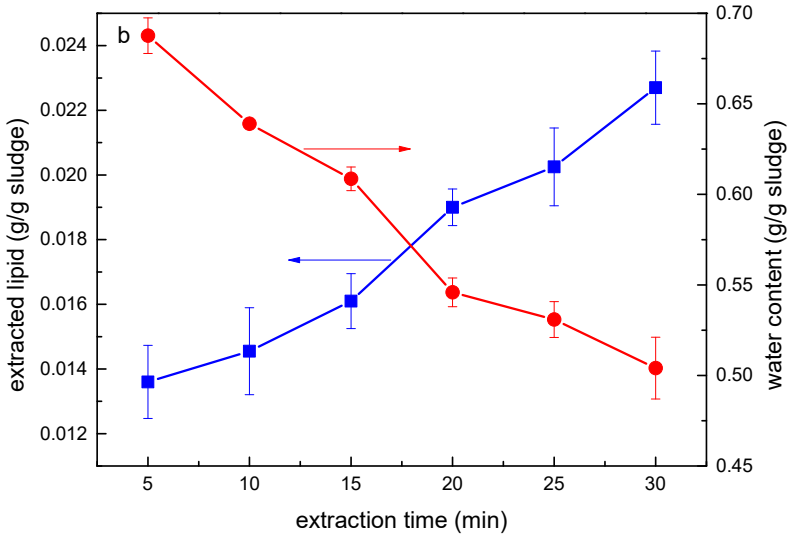
b
extracted lipid (g/g sludge)
water content (g/g sludge)
extraction time (min)
0.024
0.022
0.020
0.018
0.016
0.014
0.012
0.70
0.65
0.60
0.55
0.50
0.45
5
10
15
20
25
30

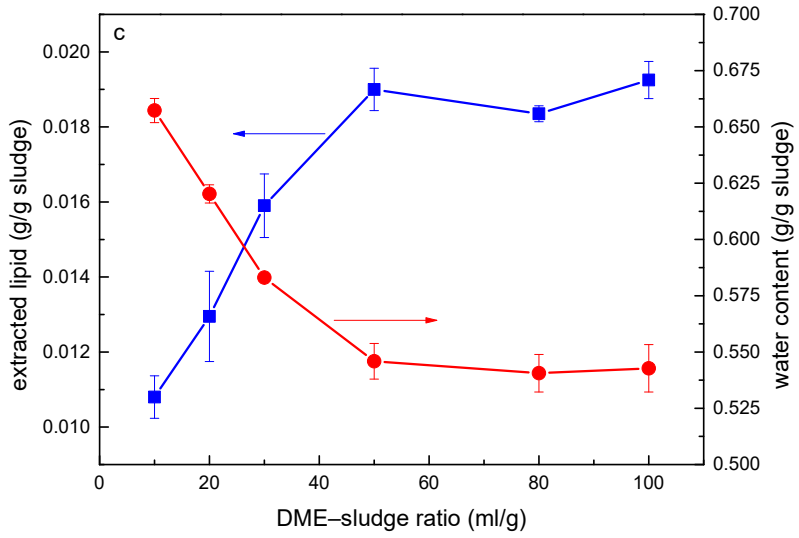

Figure 5.2. Effects on lipid extraction and drying of (a) sludge ball size with an extraction time of 20 min and DME/sludge ratio of 50; (b) extraction time with a sludge ball size of 5.8 mm and a DME/sludge ratio of 50; and (c) DME/sludge ratio with a sludge ball size of 5.8 mm and an extraction time of 20 min.

5.3.2 Comparison of the DME and B&D methods

5.3.2.1 Yields of lipid and FAMEs

We compared the FAME and lipid yields of the DME and B&D methods [35, 9]. Because extracted raw lipids contained not only triglyceride and fatty acids but also wax esters, steroids, steryl esters, hydrocarbons, terpenoids, polyhydroxyalkanoates, polycyclic aromatic hydrocarbons, and linear alkyl benzenes [42, 40, 43]. And polarity of solvents used for extraction affects proportion of the above components, which can be attributed to the "Like Dissolves Like" theory. The chloroform used in B&D method is a typical non-polar solvent, which is more beneficial to nonpolar substance, such as wax esters, steryl esters, hydrocarbons. By comparison, Sterols, phospholipids and fatty alcohols have slight polarity, are hence easier to be extracted by DME having slight polarity. Since this study assumed raw lipid extracted would be purified as biodiesel, we mainly focused on the triglyceride and fatty acids which were usually used to produce biodiesel.

Thus, we calculated the yield of FAMEs (stand for triglyceride and fatty acids). The DME method achieved a significantly greater FAMEs yield compared to the B&D method, despite a lower yield of raw lipids from three of the five sludges (Figure 5.3). For sludge A and C, the FAMEs yield of the DME method was 0.0270 and 0.0225 g/g dry-base, 94.2% and 58.5% higher than by the B&D method, respectively. The DME method yielded a greater proportion of FAMEs than did the B&D method (14.1–33.4% *vs*. 8.1–15.9%). Also, the purity of FAMEs (Percentage of FAMEs in raw lipid) was higher by the DME method (Figure 3), which may facilitate post-purification

processing by removing impurities from the extracted oil [44].

The amounts of lipid extracted varied significantly according to sludge type. For example, the raw lipid yield from primary sedimentation sludge was 12.3 wt.%, compared to 3.8 wt.% for sludge from an A^2/O tank [22]. The maximum FAME yield of 13.9 wt.% was obtained for primary sludge, compared to 2.9 wt.% for secondary sludge and 1.0 wt.% for digested sludge [45]. In this study, the average FAME yield from undigested sludge was 2.1 wt.%, compared to 0.97 wt.% from digested sludge. Therefore, undigested sludge has greater potential than digested sludge as a raw material for biodiesel production.

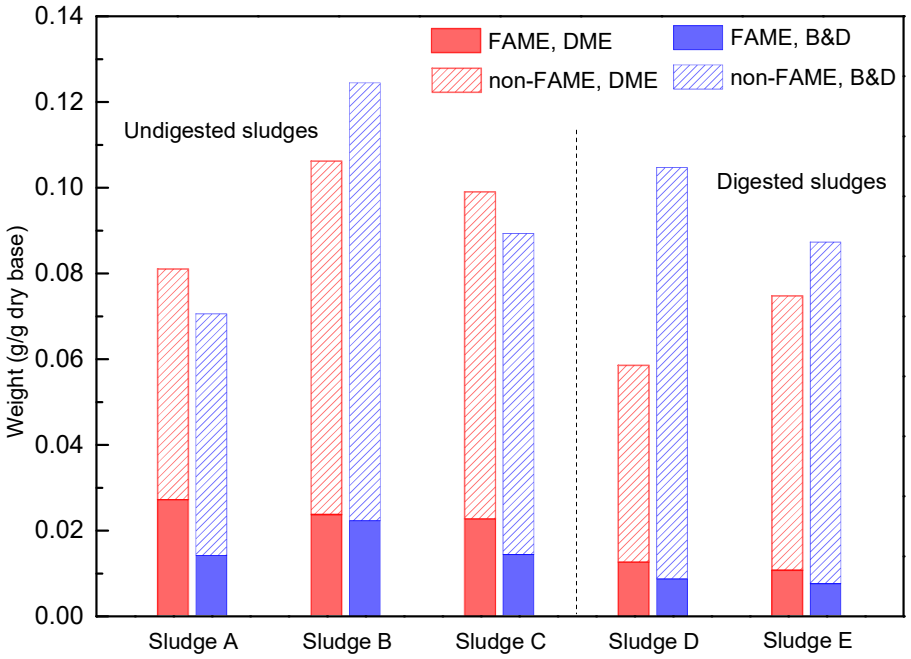

Figure 5.3. Yields of extraction of thickened and digested sludges.

5.3.2.2 FAME profile of extracted lipids

Figure 5.4 shows the FAME profiles of raw lipids extracted from the undigested and digested sludges. The FAME profiles of each type of sludge were similar, irrespective of the extraction method used. However, the FAME profiles of undigested and digested sludge differed, mainly due to the action of anaerobic bacteria [46]. Methyl palmitate (C16:0), methyl octadecanoate (C18:0), and oleic acid methyl (C18:1) were the major FAMEs extracted from the sludges (Figure 5.4), as reported previously [44]. Specifically, C18:1 accounted for ~ 32.5% in undigested sludge compared to ~ 15% in digested sludge; C16:0 accounted for ~ 28% of the total in digested sludge. In addition, the percentage of C18:2 in undigested sludge was almost threefold that in digested sludge, and the percentages of other unsaturated fatty acids were slightly higher in undigested than in digested sludge. Because the melting point of fatty acids decreases

with the degree of unsaturation and chain length [44, 47], biodiesel generated from undigested sludge likely has superior cold flow properties [45, 48, 49] because of its lower melting point. Thus, surfactants and detergent fractionation is needed for the lipid extracted from digested sludge to improve its cold flow properties [50].

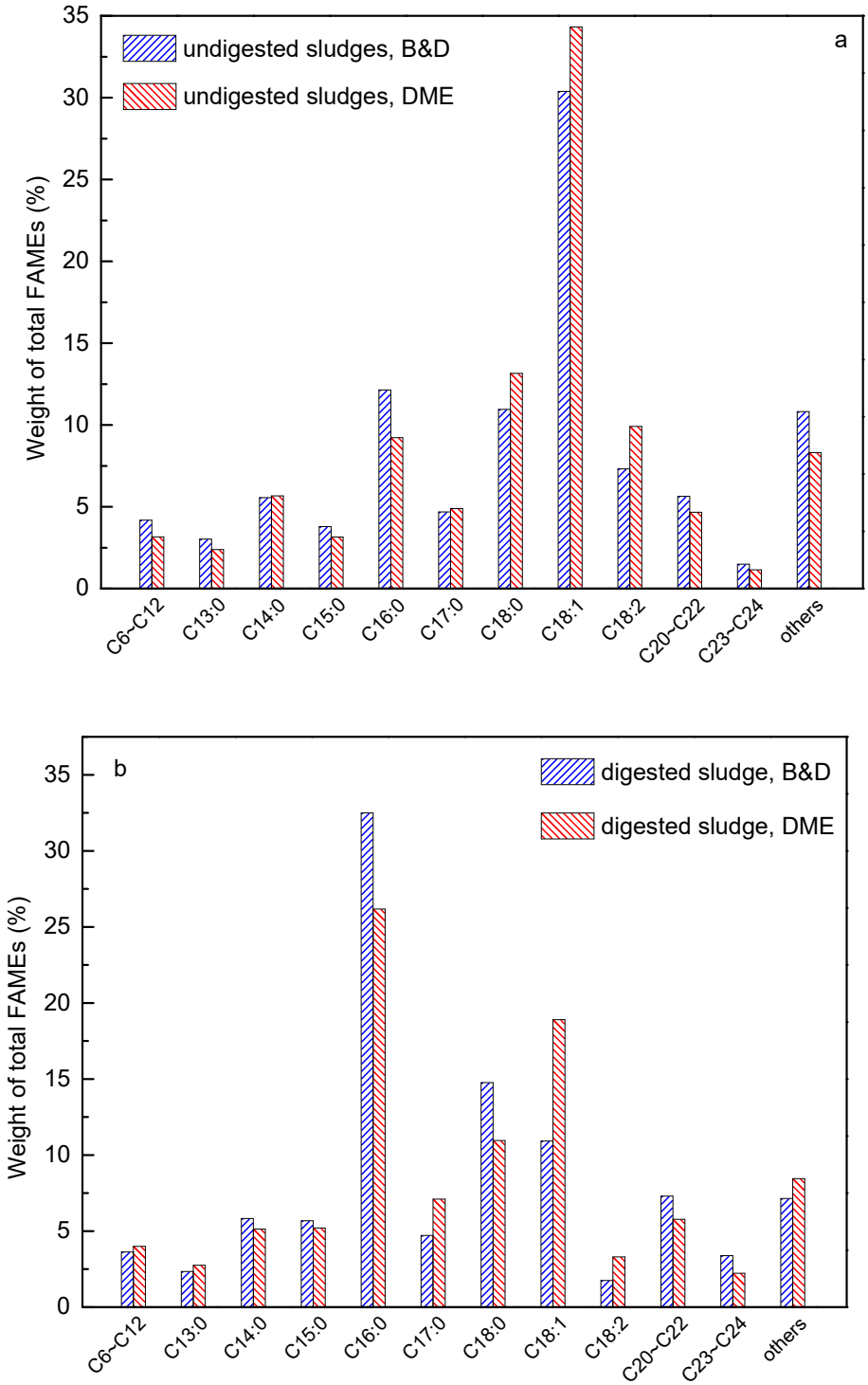

Figure 5.4. Fatty acid profiles of biodiesel from (a) thickened and (b) digested sludge using the two extraction techniques (*others, remaining unsaturated fatty acids).

5.3.2.3 Mass balance

Because the solid waste generated during solvent extraction requires proper disposal, we analysed the characteristics of treated sludges. The mass balances before and after DME or B&D treatment are shown in Figure S6 (Appendix Data 1.1); the 60% and 75% water contents of undigested and digested sludges, respectively, were reduced to ~ 53% by the DME method. However, the water content of sludge increased after B&D treatment, likely due to the addition of water. Similarly, the TS of DME-treated sludge ranged from 0.419 to 0.516 g/g (56% to 163% higher than the initial value), compared to decreases of 23% to 61% for the B&D method (Table 5.2). Thus, the solid waste generated by the B&D method needs additional treatment, such as centrifugation and heat drying, for final disposal, yet that generated by DME can be incinerated directly.

The C/H/N ratio is listed in Table 5.2. The proportions of the three elements were reduced after lipid extraction due to removal of carbohydrate and protein. Next, the H composite was used to calculate the LHV. Dried sludge can be co-combusted with municipal solid waste (LHV ~ 6.7 MJ/kg) for thermal energy production [51]. However, the co-combustion ratio is affected by the LHV of the dried sludge—the MSW/sludge ratio increases with decreasing LHV [26]. The LHV was calculated from the elemental composition and the HHV [24]. Although there was no difference in HHV between the DME and B&D methods, the sludge obtained by the DME method had a higher LHV than that produced using the B&D method (*e.g.*, for sludge D, 5.70 and 0.16 MJ/kg, respectively). Because the LHV of the fuel must be > 5.68 MJ/kg for incineration [26], the 3.74 to 5.70 MJ/kg LHV of the DME method enabled combustion either independently or at a lower MSW/sludge ratio.

Table 5.2. Characteristics of sludge before and after drying by the DME or Bligh-Dyer method.

		TS (g/g)	**H** (%-DB)	**C** (%-DB)	**N** (%-DB)	**HHV** (MJ•kg^{-1}-DB)	**LHV** (MJ•kg^{-1}-WB)
Initial value	Sludge A	0.235	8.67	50.8	5.88	18.7	2.46
	Sludge B	0.268	6.87	42.9	4.37	18.9	3.22
	Sludge C	0.215	6.36	40.0	4.31	17.8	1.85
	Sludge D	0.218	6.39	38.4	6.21	17.9	1.93
	Sludge E	0.173	5.52	32.2	4.59	15.1	0.53
After DME method	Sludge A	0.458	5.87	35.0	4.29	14.9	4.85
	Sludge B	0.459	6.41	39.2	4.57	15.6	5.14
	Sludge C	0.419	6.25	37.4	4.59	15.6	4.47
	Sludge D	0.495	5.90	35.2	5.73	15.4	5.70
	Sludge E	0.516	5.45	29.9	3.73	10.8	3.74
After B&D method	Sludge A	0.182	8.00	46.6	5.08	15.2	0.39
	Sludge B	0.105	6.81	39.6	3.88	16.1	-0.72
	Sludge C	0.115	6.12	36.0	4.27	14.7	-0.69
	Sludge D	0.164	6.34	35.5	5.92	15.2	0.16
	Sludge E	0.114	4.82	24.5	3.77	9.9	-1.21

TS, total solids; HHV, higher heating value; LHV, lower heating value; DB, dry basis; WB, wet basis

5.3.3 Reusability of DME

The effect on lipid extraction and drying performance of reuse of DME was evaluated (Figure 5.5). Using pure liquefied DME for extraction, the water content decreased from 78.5 to 59.9%. The water content of the treated sludges decreased to 56.1–59.4% following reuse. This is similar to that obtained using pure liquefied DME. In contrast, 24.4 mg/g wet-base of extracted raw lipid was achieved using pure DME, which decreased slightly with increasing number of reuses. After the third reuse, the raw lipid yield decreased 10.2% to 21.9 mg/g, and after the fourth reuse it decreased 13.5% to 21.1 mg/g. During the reuse experiments, no deterioration of liquefied DME drying performance was observed, although the lipid yield decreased slightly. Thus, DME can be reused at least five times, which could significantly reduce the cost of lipid extraction.

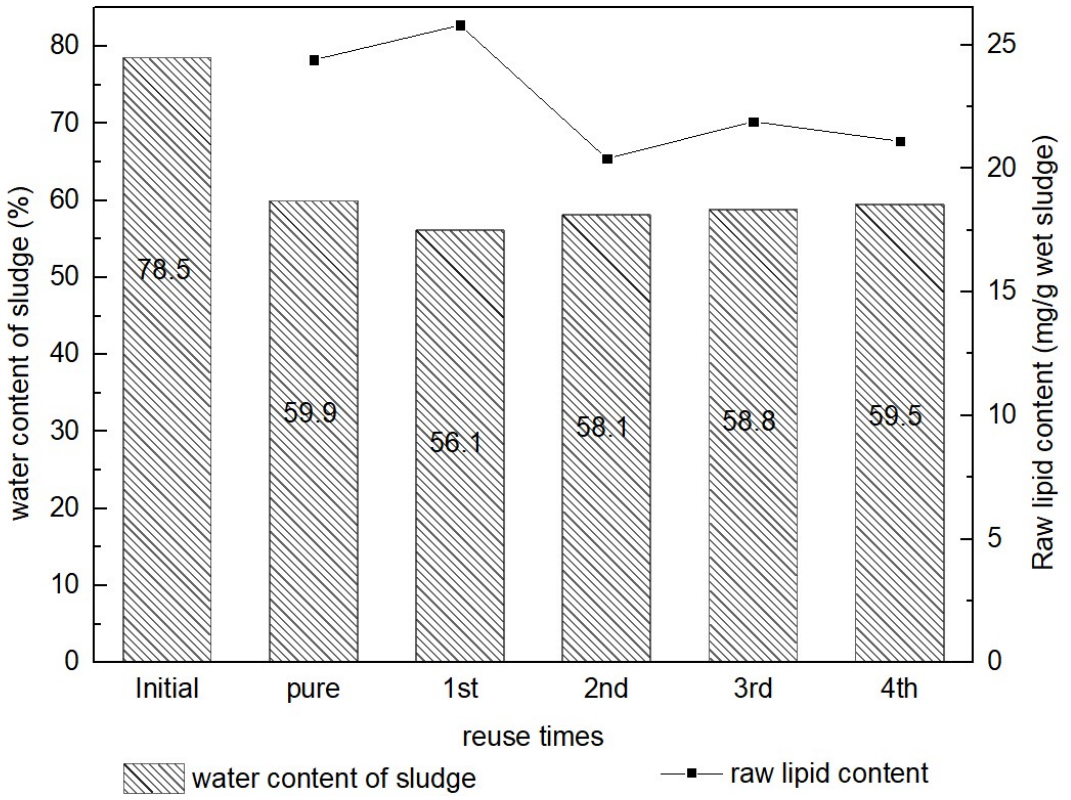

Figure 5.5. Influence of liquefied DME reuse on sludge drying and lipid extraction.

5.3.4 Economic analysis

For all three methods (Operation diagram in Fig. 5.6), the mechanical dewatering cost for 1 ton of undigested sludge (~ 97% water content) was $4.5 [39]. Assuming a raw lipid extraction ratio of 0.1 g lipid per 1 g dry-base sludge for both the DME and conventional solvent extraction methods (Figure 5.3), the biodiesel purification cost was $0.053.

Regarding lipid extraction by the DME method, a liquid DME/sludge ratio of 20.0 mL-DME/g-wet sludge (~ 80% water content), a DME density of 668.0 kg/m^3, and energy consumption to liquefy 1 kg of DME of 78.4 kJ/kg (Appendix Data 1.2), the lipid extraction cost was $5.45. Based on the average LHV of the sludges (4.82 MJ/kg, ~ 55% water content), the cost recovered by electricity generation was $1.01. The FAME proportion (~ 26% raw lipid for the DME method, 10% raw lipid extraction ratio) was used to evaluate biodiesel production; $0.86 could be recovered.

The sludge-drying and lipid-extraction costs of the conventional solvent extraction method were calculated from [38], and the biodiesel purification cost was $0.05. Also, considering the FAME percentages (~ 18% raw lipid, 10% raw lipid extraction ratio), the cost of biodiesel produced by the B&D method was $0.59.

Table 5.3 Unit cost or profit with related references of the three compared methods.

	DME method		Conventional solvent method		Conventional heat drying	
	Unit cost or profit	**References**	**Unit cost or profit**	**References**	**Unit cost or profit**	**References**
Concentration cost	$4.5/ ton sludge (97% W.C.)	[39]	$4.5/ ton sludge (97% W.C.)	[39]	$4.5/ ton sludge (97% W.C.)	[39]
Sludge drying cost	N/A	N/A	$57.2/ ton sludge (80% W.C.)	[38]	$111.3/ ton sludge (80% W.C.)	[52], [53]
Lipid extraction cost	$36.3/ ton sludge (80% W.C.)	[TEPCO Energy Partner Co., Ltd]	$23.86 / ton of dry SS	[38]	N/A	N/A
Biodiesel purification cost	0.01764$/kg raw lipids	[38]	0.01764$/kg raw lipids	[38]	N/A	N/A
Electricity generation	-$15.15/ ton sludge (55% W.C.)	[TEPCO Energy Partner Co., Ltd], [41]	N/A	N/A	-$47.2/ ton sludge (20% W.C.)	[TEPCO Energy Partner Co., Ltd], [41]
Biodiesel production	-$1.1/ kg biodiesel	[US Energy Information Administration]	-$1.1/ kg biodiesel	[US Energy Information Administration]	N/A	N/A

The cost of sludge drying using the conventional heat-drying method was calculated as shown in Appendix Data 5.1.3, assuming that the water content of the sludge cake decreased from 80% to 20% after drying, the mass flux of removed water per unit drying chamber volume S_v was 130 kg-water/($m^3 \cdot h$)), the thermal capacity coefficient H_a was 1,500 kJ/(m^3•h•°C), and the log-mean temperature Δt was 367°C [52]. The energy necessary (E_s) to dry 1 kg of sludge was 3,200 kJ/kg, for a sludge-drying cost of $16.7. The electricity generated from incineration of dried sludge was estimated from the LHV of dry base (17.0 MJ/kg) [53] and the equation $LHV_{20\%}=LHV_{dry\text{-}base}\times 0.8-r_{water}\times 0.2$ (latent heat of water vaporization [r_{water}], ~ 2.51 MJ/kg, and electricity generation reduced the cost by $1.77. Unit cost or profit of the three methods above were shown in Table 5.3.

The net costs of treating undigested sludge were 8.13, 13.28, and 19.43 $/ton by the DME, conventional solvent extraction, and heat drying methods, respectively (Table 5.4). Therefore, disposing of sludge by the DME method is economically advantageous. Almost 45% and 55% of the total cost of the DME method is accounted for by concentration and lipid extraction (Table 5.4); therefore, process improvements, such as a larger belt-press filter or a lower DME-sludge ratio, are key to reducing costs. Finally, government sludge treatment subsidies (*e.g.*, 8.7 $/ton thickened sludge in South Korea [38]), mean that the DME method can generate revenue, and the biodiesel produced will be less costly than diesel derived from fossil fuels.

Table 5.4 Cost ($) of disposing of 1 ton of undigested sludge.

	DME method	**Conventional solvent method**	**Conventional heat drying**
Concentration cost	4.5	4.5	4.5
Sludge drying cost	0	8.6	16.7[a]
Lipid extraction cost	5.45[a]	0.72	0
Biodiesel purification cost	0.053[b]	0.053[b]	0
Electricity generation	-1.01[a,c]	0	-1.77[a,c]
Biodiesel production	-0.86[d]	-0.59[d]	0
Net expenses	8.13	13.28	19.43

a Electricity price is 0.125$/kWh, TEPCO Energy Partner Co., Ltd.

b Biodiesel purification cost is 0.01764$/kg raw lipids [38].

c Electricity generation efficiency is 10% [41].

d Biodiesel price is 1.1$/kg, US Energy Information Administration.

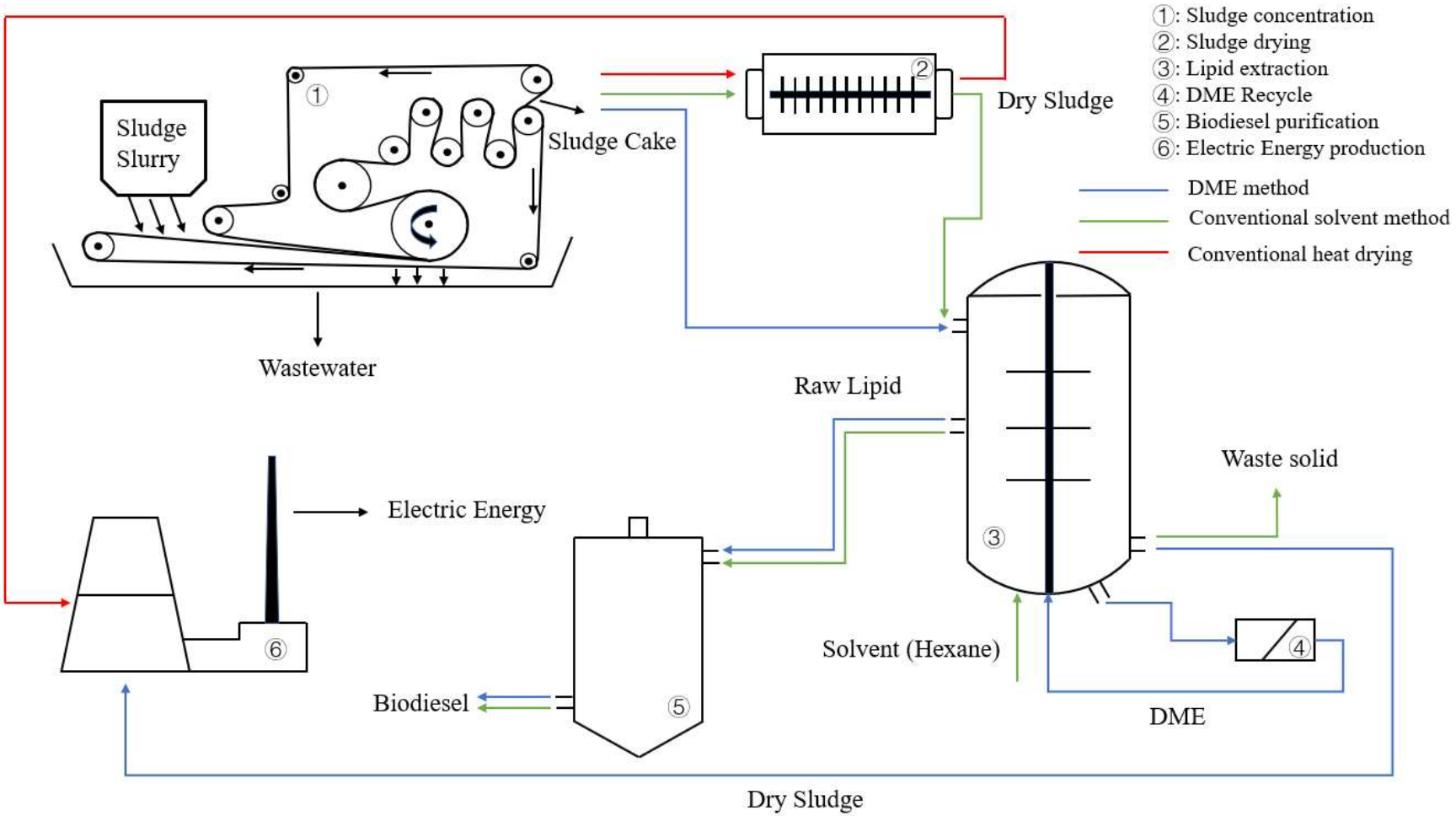

Figure 5.6 Operation diagram of (1) DME method, (2) Conventional solvent method and (3) Conventional heat drying

5.4. Conclusions

We examined the feasibility of DME as an extraction solvent for lipid production from sludge. The sludge ball size, extraction time, and DME to sludge ratio significantly affected the raw lipid yield and drying performance. The lipid yield and drying ratio increased with decreasing sludge ball size, increasing extraction time, and increasing the DME/sludge ratio. Compared with the B&D method, DME yielded FAMEs of higher purity. There was no difference between the two methods in terms of FAME composition. Because FAMEs from undigested sludge have a higher proportion of unsaturated fatty acids than those from digested sludge, the resulting lipids have superior cold flow properties. The LHV of DME-treated sludge ranged from 3.74 to 5.70 MJ/kg, implying independent combustion or at a lower MSW/sludge ratio. DME can be reused at least five times, reducing the cost of lipid extraction. Finally, the net costs of treating undigested sludge by the DME, conventional solvent extraction, and heat drying methods were 8.13, 13.28, and 19.43 $/ton, respectively. Therefore, disposing of sludge by the DME method is economically advantageous.

References

[1] Kumar, M., Ghosh, P., Khosla, K., and Thakur, I. S. (2016). Biodiesel production from municipal secondary sludge. Bioresource technology, 216, 165-171.

[2] Srivastava, N., Srivastava, M., Gupta, V. K., Manikanta, A., Mishra, K., Singh, S., ... & Mishra, P. K. (2018). Recent development on sustainable biodiesel production using sewage sludge. 3 Biotech, 8(5), 245.

[3] Sheik, A. R., Muller, E. E., and Wilmes, P. (2014). A hundred years of activated sludge: time for a rethink. Frontiers in microbiology, 5, 47.

[4] Olkiewicz, M., Torres, C. M., Jiménez, L., Font, J., and Bengoa, C. (2016). Scale-up and economic analysis of biodiesel production from municipal primary sewage sludge. Bioresource technology, 214, 122-131.

[5] Atabani, A. E., Silitonga, A. S., Badruddin, I. A., Mahlia, T. M. I., Masjuki, H. H., and Mekhilef, S. (2012). A comprehensive review on biodiesel as an alternative energy resource and its characteristics. Renewable and sustainable energy reviews, 16(4), 2070-2093.

[6] Atabani, A. E., Badruddin, I. A., Badarudin, A., Khayoon, M. S., and Triwahyono, S. (2014). Recent scenario and technologies to utilize non-edible oils for biodiesel production. Renewable and Sustainable Energy Reviews, 37, 840-851.

[7] Olkiewicz, M., Fortuny, A., Stüber, F., Fabregat, A., Font, J., and Bengoa, C. (2015). Effects of pre-treatments on the lipid extraction and biodiesel production from municipal WWTP sludge. Fuel, 141, 250-257.

[8] Wang, Y., Feng, S., Bai, X., Zhao, J., and Xia, S. (2016). Scum sludge as a potential feedstock for biodiesel production from wastewater treatment plants. Waste management, 47, 91-97.

[9] Zhu, F., Zhao, L., Jiang, H., Zhang, Z., Xiong, Y., Qi, J., and Wang, J. (2014). Comparison of the lipid content and biodiesel production from municipal sludge using three extraction methods. Energy & Fuels, 28(8), 5277-5283.

[10] Levine, R. B., Pinnarat, T., and Savage, P. E. (2010). Biodiesel production from wet algal biomass through in situ lipid hydrolysis and supercritical transesterification. Energy & Fuels, 24(9), 5235-5243.

[11] Pastore, C., Lopez, A., Lotito, V., and Mascolo, G. (2013). Biodiesel from dewatered wastewater sludge: a two-step process for a more advantageous production. Chemosphere, 92(6), 667-673.

[12] Appels, L., Baeyens, J., Degrève, J., & Dewil, R. (2008). Principles and potential of the anaerobic digestion of waste-activated sludge. Progress in energy and combustion science, 34(6), 755-781.

[13] Japan Sewage Works Association. (2011). Sewage Works in Japan 2011, Sludge Treatment and Beneficial Use of Sludge in Japan. Japan Sewage Works Association, Tokyo, 4-7.

[14] Duan, N., Dong, B., Wu, B., and Dai, X. (2012). High-solid anaerobic digestion of sewage sludge under mesophilic conditions: feasibility study. Bioresource technology, 104, 150-156.

[15] Mateo-Sagasta, J., Raschid-Sally, L., & Thebo, A. (2015). Global wastewater and sludge production, treatment and use. In Wastewater (pp. 15-38). Springer, Dordrecht.

[16] Dufreche, S., Hernandez, R., French, T., Sparks, D., Zappi, M., and Alley, E. (2007). Extraction of lipids from municipal wastewater plant microorganisms for production of biodiesel. Journal of the American Oil Chemists' Society, 84(2), 181-187.

[17] Fytili, D., and Zabaniotou, A. (2008). Utilization of sewage sludge in EU application of old and new methods—a review. Renewable and Sustainable Energy Reviews, 12(1), 116-140.

[18] Chen, H., Yan, S. H., Ye, Z. L., Meng, H. J., and Zhu, Y. G. (2012). Utilization of urban sewage sludge: Chinese perspectives. Environmental Science and Pollution Research, 19(5), 1454-1463.

[19] Kanda, H., Morita, M., Makino, H., Takegami, K., Yoshikoshi, A., Oshita, K., and Takeda, N. (2011). Deodorization and dewatering of biosolids by using dimethyl ether. Water Environment Research, 83(1), 23-25.

[20] Baeyens, J., & Van Puyvelde, F. (1994). Fluidized bed incineration of sewage sludge: a strategy for the design of the incinerator and the future for incinerator ash utilization. Journal of Hazardous Materials, 37(1), 179-190.

[21] Van Caneghem, J., Brems, A., Lievens, P., Block, C., Billen, P., Vermeulen, I., ... & Vandecasteele, C. (2012). Fluidized bed waste incinerators: Design, operational and environmental issues. Progress in Energy and Combustion Science, 38(4), 551-582.

[22] Zhu, F., Wu, X., Zhao, L., Liu, X., Qi, J., Wang, X., and Wang, J. (2017). Lipid profiling in sewage sludge. Water research, 116, 149-158.

[23] Revellame, E. D., Hernandez, R., French, W., Holmes, W. E., Benson, T. J., Pham, P. J., and Callahan II, R. (2012). Lipid storage compounds in raw activated sludge microorganisms for biofuels and oleochemicals production. RSC Advances, 2(5), 2015-2031.

[24] Oshita, K., Toda, S., Takaoka, M., Kanda, H., Fujimori, T., Matsukawa, K., and Fujiwara, T. (2015). Solid fuel production from cattle manure by dewatering using liquefied dimethyl ether. Fuel, 159, 7-14.

[25] Oshita, K., Takaoka, M., Nakajima, Y., Morisawa, S., Kanda, H., Makino, H., and Takeda, N. (2011). Sewage sludge dewatering process using liquefied dimethyl ether as solid fuel. Drying Technology, 29(6), 624-632.

[26] Lin, H., and Ma, X. (2012). Simulation of co-incineration of sewage sludge with municipal solid waste in a grate furnace incinerator. Waste management, 32(3), 561-567.

[27] Yang, C. J., and Jackson, R. B. (2012). China's growing methanol economy and its implications for energy and the environment. Energy Policy, 41, 878-884.

[28] Fleisch, T. H., Basu, A., and Sills, R. A. (2012). Introduction and advancement of a new clean global fuel: The status of DME developments in China and beyond.

Journal of Natural Gas Science and Engineering, 9, 94-107.
[29] Öhrman, O., Pettersson, E., Gullberg, M., and Westbom, U. (2011, November). Quality control of BioDME produced via black liquor gasification. In 7th Asian DME Conference, Niigata, Japan.
[30] Holldorff, H., and Knapp, H. (1988). Binary vapor-liquid-liquid equilibrium of dimethyl ether-water and mutual solubilities of methyl chloride and water: Experimental results and data reduction. Fluid Phase Equilibria, 44(2), 195-209.
[31] Kanda, H., Makino, H., and Miyahara, M. (2008). Energy-saving drying technology for porous media using liquefied DME gas. Adsorption, 14(4-5), 467-473.
[32] Öhrman, O. G., and Pettersson, E. (2013). Dewatering of biomass using liquid bio dimethyl ether. Drying technology, 31(11), 1267-1273.
[33] Li, P., Kanda, H., and Makino, H. (2014). Simultaneous production of bio-solid fuel and bio-crude from vegetal biomass using liquefied dimethyl ether. Fuel, 116, 370-376.
[34] Kanda, H., Li, P., Ikehara, T., and Yasumoto-Hirose, M. (2012). Lipids extracted from several species of natural blue–green microalgae by dimethyl ether: Extraction yield and properties. Fuel, 95, 88-92.
[35] Bligh, E. G., and Dyer, W. J. (1959). A rapid method of total lipid extraction and purification. Canadian journal of biochemistry and physiology, 37(8), 911-917.
[36] Kong, W., Baeyens, J., Qin, P., Zhang, H., & Tan, T. (2018). Towards an energy-friendly and cleaner solvent-extraction of vegetable oil. Journal of environmental management, 217, 196-206.
[37] Kong, W., Baeyens, J., De Winter, K., Urrutia, A. R., Degrève, J., & Zhang, H. (2019). An energy-friendly alternative in the large-scale production of soybean oil. Journal of environmental management, 230, 234-244.
[38] Kwon, E. E., Kim, S., Jeon, Y. J., and Yi, H. (2012). Biodiesel production from sewage sludge: new paradigm for mining energy from municipal hazardous material. Environmental science and technology, 46(18), 10222-10228.
[39] Mamais, D., Tzimas, A., Efthimiadou, A., Kiissandrakis, J., and Andreadakis, A. (2009). Evaluation of different sludge mechanical dewatering technologies.
[40] Revellame, E., Hernandez, R., French, W., Holmes, W., and Alley, E. (2010). Biodiesel from activated sludge through in situ transesterification. Journal of Chemical Technology and Biotechnology, 85(5), 614-620.
[41] Lombardi, L., Carnevale, E., and Corti, A. (2015). A review of technologies and performances of thermal treatment systems for energy recovery from waste. Waste management, 37, 26-44.
[42] Kargbo, D. M. (2010). Biodiesel production from municipal sewage sludges. Energy & Fuels, 24(5), 2791-2794.
[43] Siddiquee, M. N., and Rohani, S. (2011). Lipid extraction and biodiesel production from municipal sewage sludges: a review. Renewable and Sustainable Energy Reviews, 15(2), 1067-1072.

[44] Melero, J. A., Sánchez-Vázquez, R., Vasiliadou, I. A., Castillejo, F. M., Bautista, L. F., Iglesias, J. and Molina, R. (2015). Municipal sewage sludge to biodiesel by simultaneous extraction and conversion of lipids. Energy conversion and management, 103, 111-118.

[45] Olkiewicz, M., Fortuny, A., Stüber, F., Fabregat, A., Font, J., & Bengoa, C. (2012). Evaluation of different sludges from WWTP as a potential source for biodiesel production. Procedia Engineering, 42, 634-643.

[46] Mudge, S. M., Belanger, S. E., and Nielsen, A. M. (2008). Fatty Alcohols—Natural and Anthropogenic Sources. RSC, Cambridge.

[47] Carrero, A., and Pérez, Á. (2012). Advances in biodiesel quality control, characterisation and standards development. In Advances in Biodiesel Production (pp. 91-130). Woodhead Publishing.

[48] Olkiewicz, M., Fortuny, A., Stüber, F., Fabregat, A., Font, J., and Bengoa, C. (2012). Evaluation of different sludges from WWTP as a potential source for biodiesel production. Procedia Engineering, 42, 634-643.

[49] Huynh, L. H., Nguyen, P. L. T., Ho, Q. P., and Ju, Y. H. (2012). Catalyst-free fatty acid methyl ester production from wet activated sludge under subcritical water and methanol condition. Bioresource technology, 123, 112-116.

[50] Wang, Y., Ma, S., Zhao, M., Kuang, L., Nie, J., & Riley, W. W. (2011). Improving the cold flow properties of biodiesel from waste cooking oil by surfactants and detergent fractionation. Fuel, 90(3), 1036-1040.

[51] Bianchini, A., Bonfiglioli, L., Pellegrini, M., and Saccani, C. (2015). Sewage sludge drying process integration with a waste-to-energy power plant. Waste management, 42, 159-165.

[52] Oshita, K., Takaoka, M., Nakajima, Y., Morisawa, S., Kanda, H., Makino, H., and Takeda, N. (2012). Characteristics of Biosolids in Dimethyl Ether Dewatering Method. Water Environment Research, 84(2), 120-127.

[53] Murakami, T., Suzuki, Y., Nagasawa, H., Yamamoto, T., Koseki, T., Hirose, H., and Okamoto, S. (2009). Combustion characteristics of sewage sludge in an incineration plant for energy recovery. Fuel Processing Technology, 90(6), 778-783.

Chapter 6 A novel method to extract lipid from liquid microalgae without dewatering

6.1 Introduction

The development of renewable energy has been paid significant attention due to rapidly increased demand for fossil fuel and global warming caused by CO_2 emission from combustion of the fossil fuel[1][2][3]. Thus, biodiesel produced form microalgae is considered as a promising substitute for fossil fuels and widely studied[4][5], because they have high growth rate with high lipid content, hence have desirable carbon fixation efficiency with biodiesel productivity, and can be easily grown on non-arable land without competing with food production[6][7][8].

Biodiesel production from microalgae mainly consists of microalgae cultivation, harvesting, lipid extraction and transesterification[9]. However, to develop an energy saving and cost-effective process from microalgae to biodiesel, lipid extraction and corresponding harvesting method are the bottleneck[10][11]. Microalgae usually have small cell size (5~50μm) and low density (0.5~5g/L) in medium, which make it impossible to extract lipid directly and pretreatment of the harvesting is necessary[12][13]. The microalgae suspension can be firstly thickened (gravity sedimentation, flocculation, flotation…) to slurry with a biomass content of 3~7%, then be mechanically dewatered to cake with a biomass content of 10~25% by filtration or centrifugation, finally be thermally dried to a biomass content more than 90% [5][14][15].

Lipid extraction from the completelytotally dried microalgae is relatively easier than that from the one just being dewatered. 45% (dry base) of lipid was almost completely extracted from dried microalgae: *Shizochytrium limacinum* by using n-Hexane of Soxhlet [16]. In the study of Jie et al. [17], by using ethanol as solvent, 48% (dry base) of lipid was extracted form dried *Synechocystis PCC 6803*. In a supercritical extraction of CO_2 and ethanol, 34% (dry base) of lipid from dried *Shizochytrium limacinum* powder was achieved [16]. And 18.1% (dry base) from dried *Chlorella spp.* powder was obtained by mixed extraction solvent methanol/ethyl acetate with a volume ratio of 2:1 [18].

However, the drying is an energy intensive process, and removing 1kg water from mechanically dewatered microalgae (~20% of biomass content) by thermal drying need 3,560 kJ of energy input by a fossil fuel, which make net energy balance negative [5], meaning output energy from extracted biodiesel is less than input energy of the biodiesel production[3].

Considering energy consumption during biodiesel production from thermally dried microalgae is nearly 4,000 times higher than it from merely mechanically dewatered

ones (~20% of biomass content; wet microalgae)[19], and hence a positive net energy balance can be achieved without the thermal drying process[13][3], more and more investigations focused on the lipid extraction from the wet microalgae. For example, in the work of Lakshmikandan [20], mixed solvent of hexane with isopropanol (3:2 v/v) was used to extract lipid from centrifugation harvested microalgae *Chlorella vulgaris* (biomass content of ~8.9 %), and obtained a maximum lipid yield of 22.5% (dry base). By using ethyl acetate, lipid was extracted from wet microalgae *I. galbana* (biomass content of 5 %) with a yield of 17.6% [21]. Isopropanol/hexane (2:1 v/v) was screened from six solvent systems as a better one to extract lipids from wet *Scenedesmus obliquus* (biomass content of 20 %) giving a 7.8% lipid yield (dry base)[3]. And combining with microwave irradiation, 19.0% of lipid yield (dry base) was obtained by using chloroform/methanol/sulfuric acid (1:1:0.05 v/v) to extract lipid from centrifuged *Chlorella pyrenoidosa* (water content, 80 wt.%) [22].

Since centrifugation or filtration in dewatering process still require considerable energy comparing with the thickening process[23], directly extracting lipid from thickened microalgae can significantly improve net energy gain. Relative to other solvents, liquefied dimethyl ether (DME) is a promising one can be used to extract lipid. The liquefied DME not only has a partial miscibility with water (7~8 wt.% in DME; room temperature) but also a high affinity to organic compounds. The feature makes the DME suitable for lipid extraction from wet biomass sample and simultaneous dewatering, which is hence considered as an energy saving procedure [24][25]. In addition, DME exists as a gas under ambient condition, and can be easily liquefied at 0.51~0.59 MPa at room temperature (20~25 ℃). And DME (boiling point of -25℃) can evaporate from final product at room temperature and be recycled/reused efficiently [25][26].

Even though the DME has been successfully applied to extract lipid and further remove moisture from dewatered biomass, such as sludge [25][27], cattle manure [28], microalgae [29] and vegetables [30], its utilization on merely thickened samples has not been studied. It's because DME with low polarity is hard to miscible with liquid microalgae (high polarity of water) according to "like dissolves like" principle. Despite DME can absorb part of water as described above, exceeding the limit layers the DME and liquid microalgae, thus DME can't contact with microalgae cells and fail to extract lipid, especially for marine microalgae, this effect is very obvious due to polarity of water was enhanced by dissolved salts. One solution is using huge amount of DME, as reported in the study [31], a weight ratio of DME to microalgae (dry base) of 167:1 was needed to extract lipid from the sample with a solid content of 9%. However, the consumption of DME is not economic. Another potential solution is using solvent which is miscible with water in any ratio to adjust the polarity of DME, so that the adjusted DME can be completely mixed with water. This kind of additive agents are called entrainer, which have been proved to enhance supercritical fluid extraction [32][33].

Based on the experiments in chapter 5 of lipid extraction from sludge, experiments for microalgae were designed. Here, liquefied DME was utilized to extract lipid from

$AlCl_3$-flocculated microalgae *Nannochloropsis oculate* (solid content of 18.3g/L). The species is kind of marine microalgae. Since it is cultivated in broth with high salinity, the flocculated microalgae also contain high salinity, which results the high polarity and make it hard to mix with DME. Thus, studying a technique to extract lipid from such kind of microalgae is a challenge, yet if it works, this technique can be easier applied on fresh water species. In addition, *Nannochloropsis oculate* containing high lipid is a research hotspot of lipid extraction recently [56][57]. The entrainer for DME was screened from ethanol, dimethyl sulfoxide (DMSO), acetone and tetrahydrofuran (THF) by comparing with blank. The effect of extraction time, dosage of DME, proportion of entrainer in DME and ratio of two screened entrainer on extraction performance were investigated. The modified DME method was compared with Bligh&Dyer and Soxhlet extraction methods in terms of raw lipid yield, fatty acid yield, C/H/N composition, TG/DTA, Fourier Transform Infrared Spectrometer (FTIR) and trace elements in extracted lipid.

6.2 Materials and methods

6.2.1 Microalgae cultivation and pretreatment

Marine microalgae strain *Nannochloropsis oculata* was obtained from Microbial Culture Collection at the National Institute for Environmental Studies (Tsukuba, JAPAN). The strain is a genus of unicellular, oval-shaped and nonmobile marine microalgae with a diameter of 3~8 μm. The type of medium used to cultivate this strain was ESM [34], as showed in Table S13. The microalgae were cultivated in a 20 L bucket photo-bioreactor at a temperature of 20±2 ℃ with a light/dark cycles of 12 h/12 h. After two weeks of cultivation microalgae enter stationary phase, and was thickened by 60 mg/L $AlCl_3$ induced flocculation.

The biomass concentration of microalgae before and after flocculation was measured. Samples were filtered through vacuum filter with pre-weighted glass filter paper (GF/C, 1.2um, 4.7cm; Whatman plc, MA, USA) and were then washed several times by deionized water. Subsequently, the filter with filtrate were dried in an oven at a temperature of 105 ℃ for 24 h to a constant weight, and cooled in desiccator to room temperature for weight measurement. The process was repeated triplicate and result showed the biomass concentration of the original microalgae was 0.64 ± 0.01 g/L and increased to 18.3±0.79 g/L by flocculation.

6.2.2 DME extraction method

6.2.2.1 Device description and experimental procedure

As showed in Figure 6.1, the DME extraction system was composed of 5 parts, which contained a liquefied DME storing vessel (vessel 1, TVS-1-100, 500 cm^3, Taiatsu Techno Corp., Saitama, Japan), a vessel to measure DME (vessel 2, 100 cm^3, HPG-96-3, 26.5 mmφ×238 mm, Taiatsu Techno Corp.), a vessel for lipid extraction (vessel 3,

100 cm3, HPG-96-3, 26.5 mmφ×238 mm, Taiatsu Techno Corp.), a vessel for separating liquid from solvents (vessel 4, 100 cm3, HPG-96-3, 100 cm3, Taiatsu Techno Corp.), and a moisture trap column by $CaCl_2$ (HPG-10-5, 11.6 mmφ×190 mm, Taiatsu Techno Corp.).

In the experiments, the flocculation thickened microalgae were loaded into an extraction column with cellulose extraction thimble (glass fiber, φ25×100mm, Whatman, Maidstone, United Kingdom) inside, and the whole was putted into the vessel 3 after the entrainer added. The certain amount of liquefied DME stored in vessel 1 was firstly pushed into vessel 2 by N_2 gas (ZERO-A, Sumitomo Seika Chemicals Company, Ltd, Japan), and then the quantified DME in vessel 2 flowed to the vessel 3 owing to pressure. After several minutes of extraction, only liquid phase in the vessel 3 was transferred to vessel 4. DME in the liquid evaporated with pressure relief and raw lipid compounds deposited on the upper side of residual liquid (entrainer, water and salts) and separated from it entrainer). The separated raw lipid was dissolved by 5.0 mL of chloroform (Guaranteed Reagent, Wako Co.,Ltd, Japan) and filtered through a 0.45 μm membrane filter (DISMIC-13HP, Advantech Co., Ltd., Japan). The solvent of chloroform was then removed by nitrogen gas blow (Nitrogen Termovap Sample Concentrator, TOKYO RIKAKIKAI CO.,LTD., Japan), and recovered raw lipid concentrate was weighed and stored below 0 ℃.

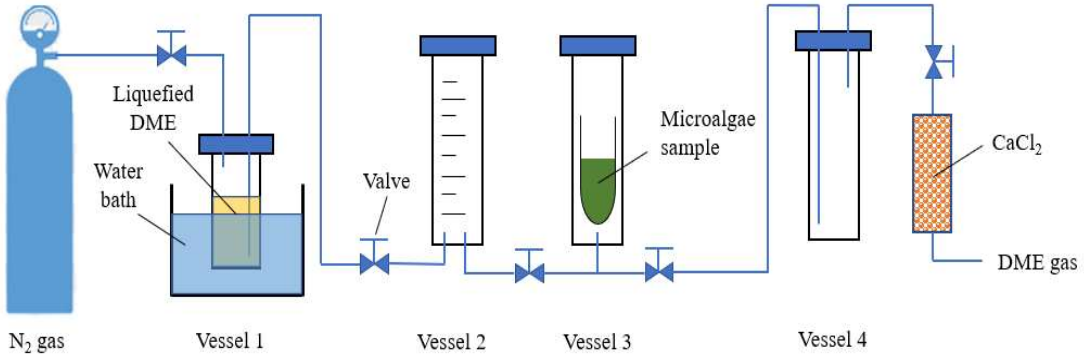

Figure 6.1 Schematic of the DME flow-type experimental apparatus.

6.2.2.2 Screening entrainer

Four potential entrainers (Table 6.1), which are miscible with water in any ratio, were tested for improving lipid extraction efficiency by DME. In the experiments, 25 mL DME was used to extract lipid from 8 mL flocculation thickened microalgae (18.3±0.79 g/L) for 30 min. The 2.5 mL of ethanol, dimethyl sulfoxide (DMSO), tetrahydrofuran (THF) or acetone (Guaranteed Reagent, Wako Co.,Ltd, Japan) was added respectively, comparing with the blank without addition of any entrainer. The entrainers were added into the microalgae in Vessel 3 and then DME was injected into it for reaction.

Table 6.1. Characteristics of solvents used in this study.

	Water	DME	Entrainers			
			Ethanol	DMSO	THF	Acetone
Formula	H_2O	C_2H_6O	C_2H_6O	C_2H_6OS	C_4H_8O	C_3H_6O
Molecular weight	18.02	46.07	46.07	78.13	72.11	58.08
Density (g/mL)	0.998	1.970	0.789	1.092	0.883	0.785
Melting point (℃)	0.0	-138.0	-114.1	18.4	-108.4	-94.7
Boiling point (℃)	100.0	-25.0	78.5	189.0	65.0	56.1
Dielectric Constant	78.54	5.02	24.60	47.00	7.52	21.01

6.2.2.3 Investigation of influence by extraction time, dosage of DM, dosage of entrainers and ratio of ethanol to acetone as entrainer.

Based on experiments in 6.2.2.2, ethanol and acetone were screened and utilized in following experiments. To study the effect by extraction time, the volume ratio of DME: microalgae: ethanol: acetone was fixed at 25:8:2:2 with extraction time varying from 10 to 45 min. To study the effect by dosage of DME, extraction time was fixed at 45 min, and dosage of DME ranged from 25 mL for 16 mL microalgae to 25 mL for 4 mL microalgae with a constant of DME: ethanol: acetone (25:2:2). To study the effect by dosage of entrainers, extraction time and ratio of DME: microalgae were fixed at 45 min and 25:8, with a range of DME: ethanol: acetone from 25:0.5:0.5 to 25:3:3. To study the effect by ratio of ethanol to acetone, 8 mL microalgae were treated by 25 mL DME for 45 min with a total amount of entrainer of 5 mL (ethanol + acetone) while changing ratio of ethanol: acetone to 1:4, 1:3, 1:2, 1:1, 2:1, 3:1 and 4:1 respectively.

6.2.3 Bligh and Dyer extraction method

The Bligh and Dyer method [35] is a classical method for lipid extraction and considered as a datum for total lipid in microalgae [29]. In this study, both the flocculation thickened microalgae and completely dried microalgae (heating at 105 °C for 24h) were applied to this method. For the dried microalgae, 5.0 mL of methanol (Guaranteed Reagent, Wako Co.,Ltd, Japan), 2.5 mL of chloroform (Guaranteed Reagent, Wako Co.,Ltd, Japan) and 2.0 mL of pure water were added and mixed with the dried sample (obtained from 10 mL flocculation thickened microalgae) in a centrifuge tube. The mixture was crushed by the homogenizer (T25, IKA Co.,Ltd, Germany) at 10,000 rpm for 5 min and mixed by the vortex genie (SI-0236, SI Co.,Ltd, USA) for 5min. Then, 2.5 mL chloroform and 2.5 mL pure water were added into the tube with 2 min of mixing. By centrifugation at 3,000 rpm (2410, KUBOTA Co.,Ltd, Japan) for 5 minutes, sample was divided into 3 layers from top to bottom: water-methanol, microalgae and lipid-chloroform layer. After the chloroform layer was recovered, this lipid-rich layer was filtered through the 0.45 μm membrane and most of the solvent was removed using a rotary evaporator at 40 ℃ under vacuum condition. The remaining solvent was removed by the nitrogen blow, and the obtained raw lipid concentration was weighed and stored below 0 ℃. As for the flocculation thickened

microalgae, a modified Bligh and Dyer method, same as the original one described except for no water adding, was applied to 5 mL sample.

6.2.4 Soxhlet extraction method

Soxhlet extraction is a common method for lipid extraction from biomass [36]. Two types of solvent, hexane and hexane-ethanol, were compared in this study. In short, for each test, 20 mL the flocculation thickened microalgae were place in cellulose extraction thimble (glass fiber, φ28×100mm, Whatman, Maidstone, United Kingdom) with adding 100 mL hexane or 100 mL mixture of hexane-ethanol (1:1 *v*:*v*), and loaded into Soxhlet extraction device. After the extraction was performed for 24 h to achieve a complete extraction, extracts were transferred to a flask and solvent were removed by the rotary evaporator under vacuum condition. Then extracts were re-dissolved in 10 ml chloroform and filtered through the 0.45μm membrane. The solvent was also removed by the nitrogen blow, and the recovered raw lipid were weighed and stored below 0 ℃.

6.2.5 Characterizations

After converting lipid fractions in raw lipid to fatty acid methyl esters (FAMEs) by transesterification, FAMEs yield was analyzed by GC-MS (GC/MS-QP2010 Plus, Shimadzu Corp., Kyoto, Japan). Specifically, recovered raw lipids were re-dissolved in 5 mL dichloromethane (Guaranteed Reagent, Wako Co., Ltd., Japan), then subjected to methylation by mixing with 2 mL of 14% BF_3-methanol solution (First Grade, Wako Co., Ltd., Japan) at 65 ℃ for 40 min and cooled to room temperature. Dichloromethane layer containing FAMEs was separated by adding 4 mL saturated aqueous NaCl solution (Guaranteed Reagent, Wako Co., Ltd., Japan) and the solvent of dichloromethane was evaporated by the nitrogen blow. The recovered FAMEs were once again dissolved in certain amount of dichloromethane for the GC-MS analysis by using a 37-component FAMEs (Sigma-Aldrich Japan, Co., Ltd., Tokyo, Japan) as standard.

The elemental analysis including Carbon(C), Hydrogen(H) and Nitrogen(N) of extracted raw lipids were performed by using an elemental analyzer (Micro Corder JM10, J-science Labo Co., Ltd.). After dropping the extracted lipids on KBr tablet (Infrared spectrophotometry grade, Wako Co.,Ltd, Japan), the samples were measured via a FTIR (Shimadzu, FTIR-8400) within the range of 400~4000 cm^{-1}. The thermal gravimetric and differential thermal analysis (TG-DTA) was performed for the extracted lipids by using TG-DTA (Rigaku, ThermoPlus TG8110) under air flow of 100 mL/min with a heating rate of 10 ℃/min from 20 to 650 ℃.

The trace elements in the extracted lipids were qualitatively analyzed by ICP-MS (XSeries 2, Thermo Fisher Scientific Co., Ltd, USA) and then quantitatively analyzed by ICP-AES (ICAP-7000, Thermo Fisher Scientific Co., Ltd, USA). The extracted lipids were firstly digested with adding 0.75 mL HNO_3 (Guaranteed Reagent, 69%,

Wako Co.,Ltd, Japan), 0.25 mL H_2O_2 (Guaranteed Reagent, 30%, Wako Co.,Ltd, Japan) and 15 mL H_2O (Ultrapure Water, Wako Co.,Ltd, Japan) for 25 mg sample in a microwave digestion system (ETHOS One, Milestone Inc., USA). The mixtures were hold for 10 minutes under 100℃ with 500W and then 10 minutes under 200℃ with 1000W. Clear liquid after digestion were collected and diluted for the analysis.

6.2.6 Statistical analysis

All data are presented as mean ± SD of the independent experiments conducted in triplicate. Data were subjected to analysis of variance (ANOVA) by Microsoft Office Excel 2010, and the differences between means were assessed by Fischer's minimum significant difference test. Statistical significance was set at $p < 0.05$.

6.3 Results and Discussion

6.3.1 Screening entrainer for improving lipid extraction by DME

Figure 6.2 showed the yields of extracted raw lipid with FAMEs by DME method (25 mL DME for 8 mL microalgae) after each of the four entrainers was added. Comparing with 14.4 mg/g (dry base) raw lipid was extracted in the blank group, 57.3, 16.4, 91.8 and 16.3 mg/g raw lipid was obtained by adding 2.5 mL ethanol, DMSO, acetone and THF respectively. It indicated that both ethanol and acetone were effective entrainers to enhance raw lipid yield 4.0 and 6.4 times than the blank respectively. However, the enhancement by DMSO and THF were not obvious and just ~ 1.1 times of raw lipid yields were achieved. The FAMEs proportions in raw lipid were also varied with different entrainers. For example, the highest FAMEs proportions of 62.0% in extracted raw lipid was occurred in blank, and experiments with THF adding had a similar value of 60.5%. The value for ethanol, DMSO and acetone added groups were 48.0%, 49.6% and 41.4% respectively, which were less than the blank. It should be noted that the amount of FAMEs obtained by adding ethanol and acetone were still much higher than blank in spite of the less FAMEs proportions. The solid content of microalgae after DME treatment with four entrainers were showed in Figure S7. In the blank group, the solid content was increased to 19.4% after DME method was applied to the flocculation thickened microalgae with over 98% of water contents. Thus, the water and lipids in the microalgae was removed simultaneously by DME and this method also could be considered as a dewatering process. However, an improvement of the dewatering by the entrainers was not observed. Solid content in the acetone or THF added group was 20.4 and 20.7%, which were no significant difference with blank group. And a slight reduction of solid content (17.2%) was found by using ethanol as entrainer. The solid content with DMSO addition was just 12.5%, which demonstrated adding DMSO was not conducive to the dewatering. In addition, FAMEs compositions were analyzed as showed in Figure S8 and no obvious difference was observed. For the all five groups

(blank+4 entrainers), FAMEs in extracted raw lipid were mainly composed of C16:0, C16:1 and C18:1n9c, which accounted for 60~70% of total FAMEs. And rest of FAMEs were distributed between C4:0 and C24:1n9. It indicated that entrainer in DME didn't affect the FAMEs composition in extracted raw lipid.

Therefore, ethanol and acetone were screened for further investigation due to their significant improvement on lipid extraction and less effect on dewatering. DME with a low polarity (dielectric constant of 5.02) should not be compatible with water of high polarity (dielectric constant of 78.54), yet the hydrogen bond formed between DME and water results in its partial miscibility with water [37], which gives DME the ability to efficiently absorb water from microalgae [29]. In this study, since water in the microalgae samples was far beyond the limit (DEM can absorb up to 7~8 wt.% of water), DME and microalgae divided into two layers. DME failed to contact with microalgae cells and extract lipid. The adding of ethanol (dielectric constant of 24.60) or acetone (dielectric constant of 21.01) adjusted the polarity of the mixture [38] so that DME-ethanol and DME-acetone could miscible with water. On the contrary, THF (dielectric constant of 7.52) of failure to improve lipid extraction was due to it salted out from the liquid of microalgae (sea water) [39], and hence lost the effect as an entrainer. Among the four entrainers, DMSO had the highest dielectric constant of 47.00, which implied its good solubility with water but poor with DME, and the less interacting with DME caused its failure to improve lipid extraction by DME. The results indicated the value of dielectric constant of an ideal entrainer should be neither too high nor too low.

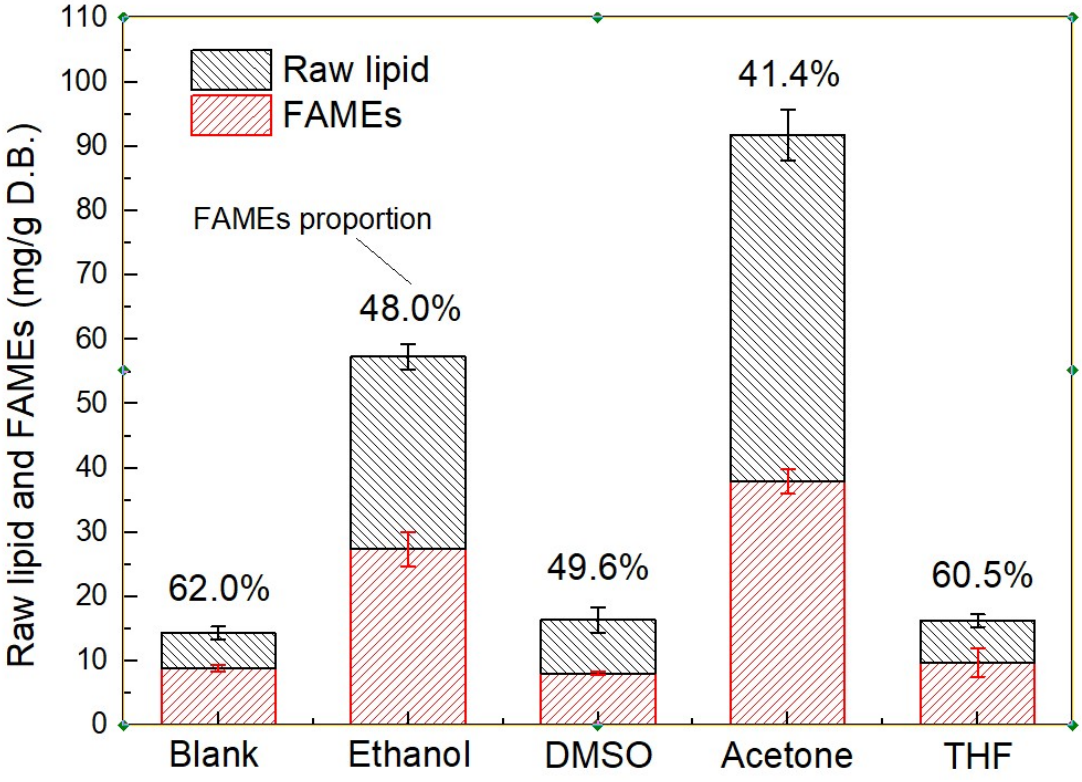

Figure 6.2 Raw lipid and FAMEs yield with 4 kinds of entrainers added.

6.3.2 DME method with entrainer of ethanol-acetone

The effect of extraction time on the DME method was showed in the Figure.6.3 (a). The raw lipid yield increased obviously with extraction time. After 10 min of extraction, raw lipid yield was reached to 0.0359 g/g dry biomass. 20 min of extraction increased the raw lipid yield to 0.0871 g/g dry biomass. At 30 min, a maximum raw lipid yield of 0.1110 g/g dry biomass was obtained, and not further increased by 45 min of extraction. The proportion of FAMEs in extracted raw lipid were ranged from 35.0 to 41.1% within the scope of the experiments. The change of FAMEs proportion by extraction time was not obvious. Similarly, the solid content of the microalgae after extraction was almost same with increasing extraction time from 10 min to 45 min. For example, the least solid content of 18.3% was observed for 10 min of extraction, and the most solid content obtained in 45 min of extraction was just 20.2%. The results indicated that 30 min of extraction was required to fully extract raw lipid, the speeds of FAMEs and non-FAMEs in microalgae transferring to DME were not much difference, and dewatering process by the DME method could be done in a short time (10 min).

The Figure.6.3 (b) showed the effect of DME dosage. The raw lipid yield was heavily increased with the dosage of DME. 0.0716 g raw lipid / g dry biomass was extracted by 1.6 ml DME/ml microalgae, comparing with 0.2333 g raw lipid / g dry biomass was extracted by DME dosage of 6.3 ml/ml. Even when dosage of DME reached to 6.3 ml/ml, the tendency of increasing raw lipid with increasing dosage of DME did not slow down. The proportion of FAMEs by DME dosage of 1.6, 2.1, 2.5 and 3.1 ml/ml were 37.1, 40.6, 41.8 and 37.9% respectively. Thus, the difference of FAMEs proportions within this DME dosage range was not obvious. However, when dosage of DME increased to 4.2 and 6.3 ml/ml, the proportion of FAMEs were reduced to 27.6% and 30.6%, which could be ascribed to a marginal effect. With more and more FAMEs were extracted, there is not much FAMEs left in microalgae; thus, FAMEs became harder to extract. In contrary, non-FAME components were still largely left, and hence the marginal effect was not obvious. This speculation was confirmed in 3.3.1. It had been observed from solid content increasing that the more water was removed from microalgae by the more dosage of DME. At DME dosage of 1.6 ml/ml, the solid content was just 14.6 % while it enhanced to 24.9 % with 6.3 ml/ml was added. The experiments by changing dosage of DME showed the increasing of DME dosage significantly improved raw lipid extraction with dewatering, yet the reduction of FAMEs proportion since the DME dosage exceeding 4.2 ml/ml implied the improvement effect of increasing DME on FAMEs extraction began to weaken.

Changing of extraction performance with entrainer dosage was illustrated in the Figure 6.3 (c), the raw lipid yield was nearly linear growth with the increasing of entrainer dosage (ethanol + acetone). 2% of entrainer (in DME) slightly increased raw lipid yield to 0.0271 g/g dry biomass compared with the blank in experiment 3.1. The enhancement by 6% of entrainer was much more notable with a value of 0.0912 g/g and after adding 12% of entrainer the raw lipid yields even reached to 0.1646 g/g. As

for the proportion of FAMEs, during the entrainer ranging from 2% to 8%, the amount of extracted FAMEs was proportional increase with the increasing of entrainer dosage with a constant FAMEs proportion of ~37.1%. However, the proportion started to reduce if the entrainer exceeded 10%, and it decreased to 27.4% with 12 % of entrainer because of the marginal effect described above. Its effect on dewatering was nonsignificant, and the observed solid content values were around 19.9%. In the study of entrainer dosage, it's found that the decrease of FAMEs proportion occurred if entrainer dosage exceeding 10%, while raw lipid yield was always grown with it. Thus, the enhancement of extracted FAMEs amount by increasing entrainer from 8% to 12% was very limited, and 8% or 10% of entrainer was suitable for the DME method if using FAMEs as a target product.

The influence from ratio of ethanol to acetone was showed in the Figure 6.3 (d). The more raw lipid yield tended to be obtained by lower ratio of ethanol to acetone. From 1:4 to 1:2, the difference of raw lipid yield was not significant and the values were around 0.1581 g/g. When the ratio increased to 1:1, the raw lipid yield started to decrease. And the values were reduced to 0.1241 and 0.1278 g/g for ratio of 3:1 and 4:1 respectively. In contrast to this, the effect of the ratio on FAMEs proportion and solid content were not obvious, and within the scope of the study, FAMEs proportions ranged from 26.5 to 32.3%, solid content ranged from19.6 to 21.1%. Therefore, to achieve higher raw lipid and FAMEs yields, the ratio of ethanol to acetone should be appropriately reduced, and the ratio of 1:3 or 1:2 was suitable for the DME method.

Generally, extracted raw lipids from microalgae contain non polar lipids (triglyceride, wax esters, steryl esters), polar lipids (phospholipid, glycolipid), free fatty acids, sterols, proteins, hydrocarbon, pigments and other algal products [1][40][41]. Since these components possess different polarity, the extraction is influenced by the polarity of solvents. Shin et al. [42] used various types of solvent to extract lipid from microalgae, and results showed the lowest lipid yield was obtained by hexane (non-polar solvent), more lipid was extracted by the medium polarity solvent of isopropanol, lipid from mixture of hexane with isopropanol was more than both of them. And the advantage of this combination of non-polar with polar solvent were also reported by other researches [3][43]. In this study, DME with low polarity acted on the neutral lipids with the help of ethanol and acetone on the polar lipids, which was the reason for the changing of raw lipid yields and FAMEs proportion. What's the important is that water in the flocculated microalgae definitely acted as a barrier between intracellular lipids in cells and DME [38][45], and the miscibility of the entrainers with water was the crucial to achieve lipid extraction from the high water contained microalgae sample with using relatively less dosage of DME. In addition, the solid content of the sample after DME treatment increased to ~20% indicated a simultaneous dewatering effect of the method.

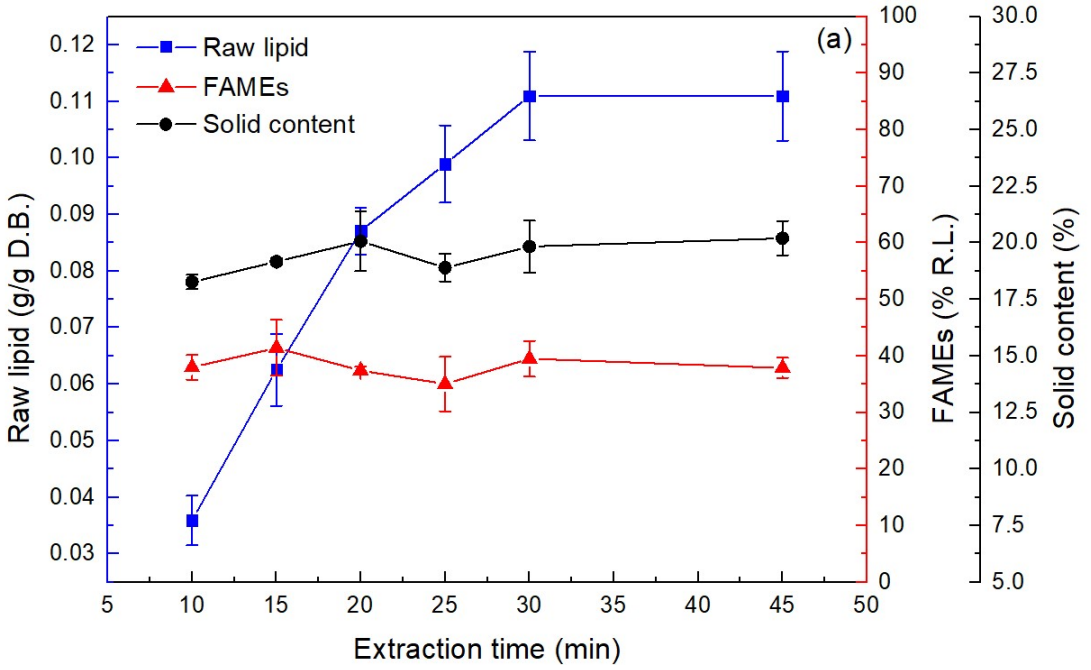
(a)
Raw lipid
FAMEs
Solid content
Raw lipid (g/g D.B.)
FAMEs (% R.L.)
Solid content (%)
Extraction time (min)

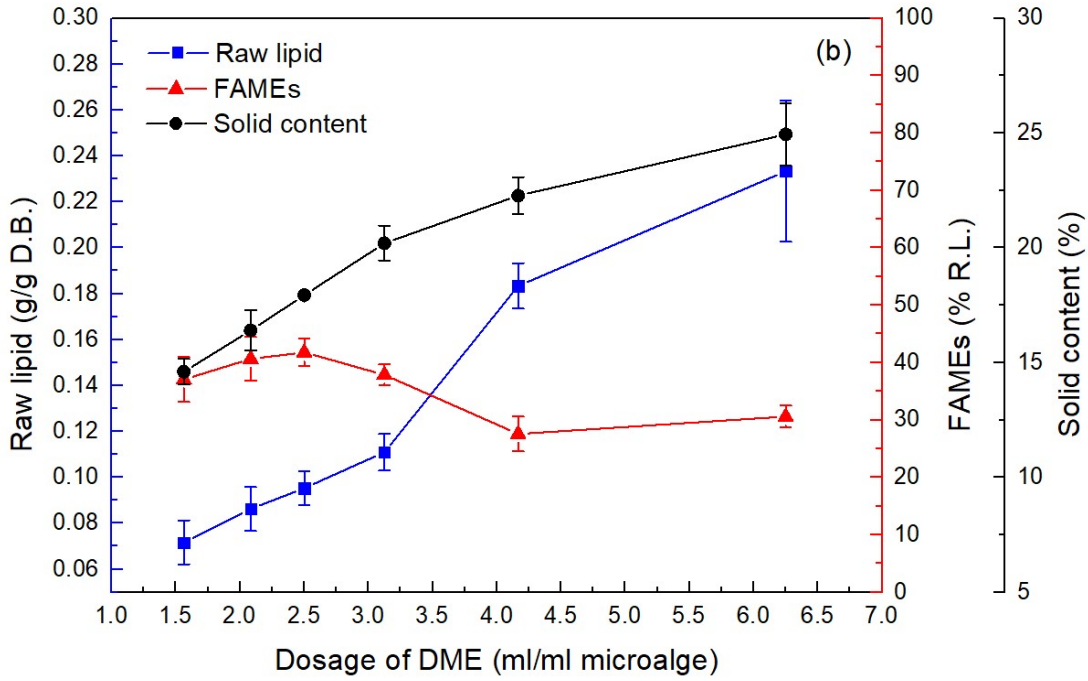
(b)
Raw lipid
FAMEs
Solid content
Raw lipid (g/g D.B.)
FAMEs (% R.L.)
Solid content (%)
Dosage of DME (ml/ml microalge)

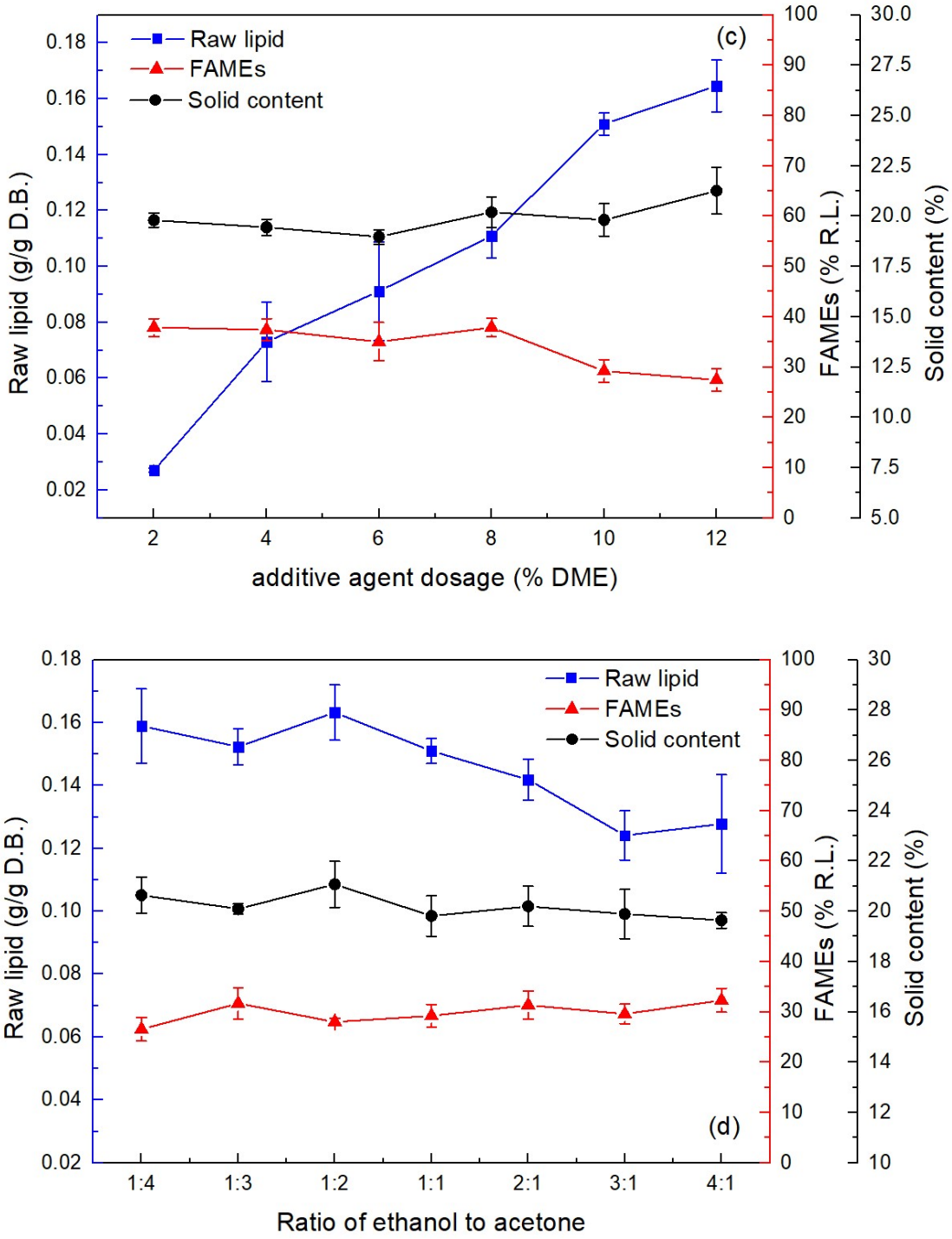

Figure 6.3 Lipid extraction and dewatering by DME method with entrainer of ethanol-acetone. Influence from a) extraction time, b) dosage of DME, c) dosage of entrainer, d) ratio of ethanol to acetone.

6.3.3 Comparison of DME method using entrainer with Soxhlet and Bligh&Dyer extraction methods

6.3.3.1 Raw lipid yields and FAMEs profile

The lipid extraction by DME method was compared with Soxhlet and Bligh&Dyer

methods as showed in the Figure 6.5 The B&D methods obtained highest raw lipid yields compared with other two methods, and dry-type of it achieved 576.6 mg/g dry biomass of raw lipid yields while wet-type had a less value of 502.2 mg/g. The DME method extracted 152.2 mg raw lipid per 1g microalgae (dry base), which was similar to Soxhlet (Hexane + ethanol) method of 144.9 mg/g. Yet the Hexane based Soxhlet method almost failed to extract the lipids. As for the FAMEs proportion, the highest one (31.7%) was obtained by DME method, followed by 15.4% of B&D (dry), 10.0% of B&D (wet) and 5.3% of Soxhlet method (hexane+ethanol, HE), which was in agreement with the research [44] In addition, significant difference in FAMEs profile among the methods were observed as showed in Figure 6.4. Even though, for all the methods, FAMEs were all mainly consisted of C14:0, C16:0, C16:1, C18:0, C18:1 and C18:2 totally accounting for 81.1~ 89.8%, the amount of each the components were different among the methods. For example, C16:0 accounted for 52.2% in FAMEs for B&D (dry) while the value by B&D (wet) was just 25.0%. Relatively higher C16:1 proportion were obtained by DME and Soxhlet (HE) methods (22.2%, 23.6%) than B&D (dry) with B&D (wet) of ~15%. And C18:1by B&D (wet) reached to 22.87%, which was much higher than others. Thus, DME method indicated an advantage for significantly increasing FAMEs extraction than Soxhlet (HE) method. The reason was the adding ethanol into hexane could not make the mixture being miscible with water, which blocked contacting between hexane with lipids. But some non-lipids substance, such as sugar and pigment, could be extracted by ethanol-water phase and transferred to ethanol-hexane phase, these composed the extracted raw lipid. Considering B&D (dry) is a benchmark for total lipid can be recovered from sample[29][46], 26.4% of total raw lipids with 54.4% of total FAMEs in the microalgae was extracted by the DME method. Even though lipids were not completely extracted by DME, the simultaneous dewatering by the process indicated a twice DME extraction step could extract rest of them from the dewatered microalgae. Since the DME could be easily recycled and reused [25], DME method was regarded to be more economic. And for the DME method, a cell disruption [1] (ultrasound, microwave, high pressure homogenization, enzymatic hydrolysis and chemical hydrolysis, et.al) was not necessarily, yet it was considered to be an indispensable pretreatment step for B&D methods.

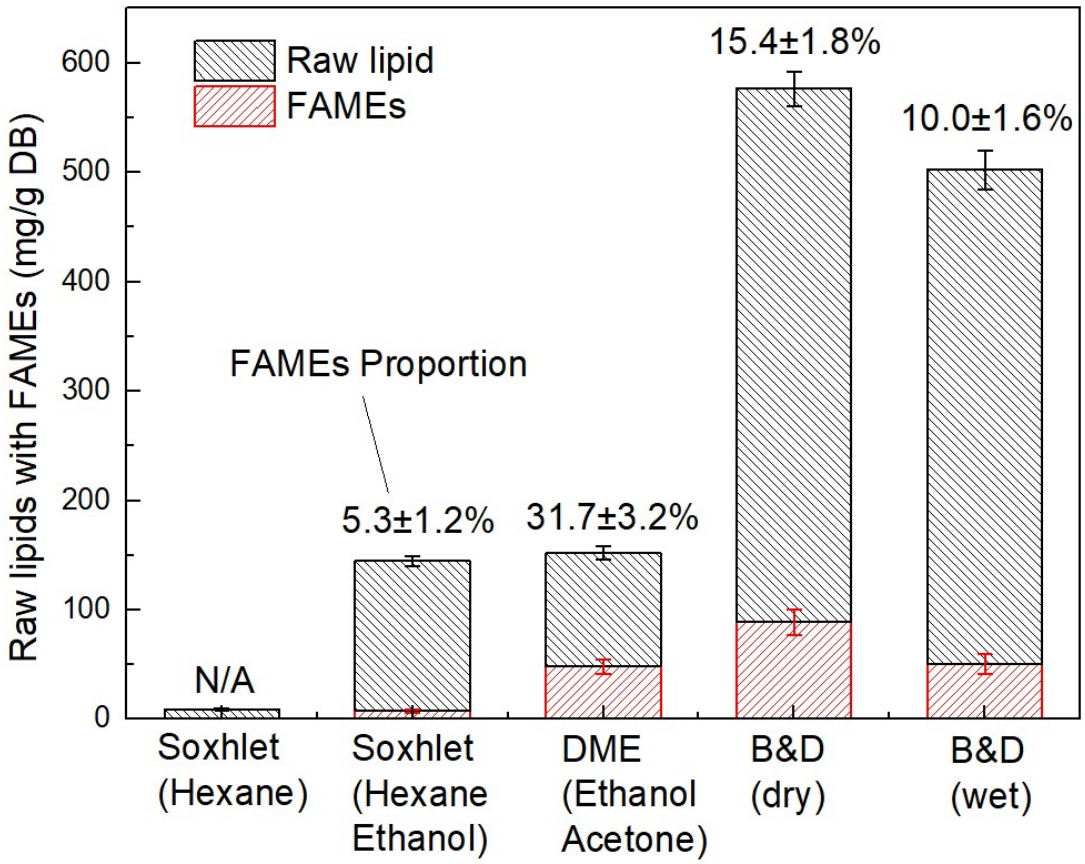

Figure 6.4 Raw lipid yields with FAMEs by different extraction methods.

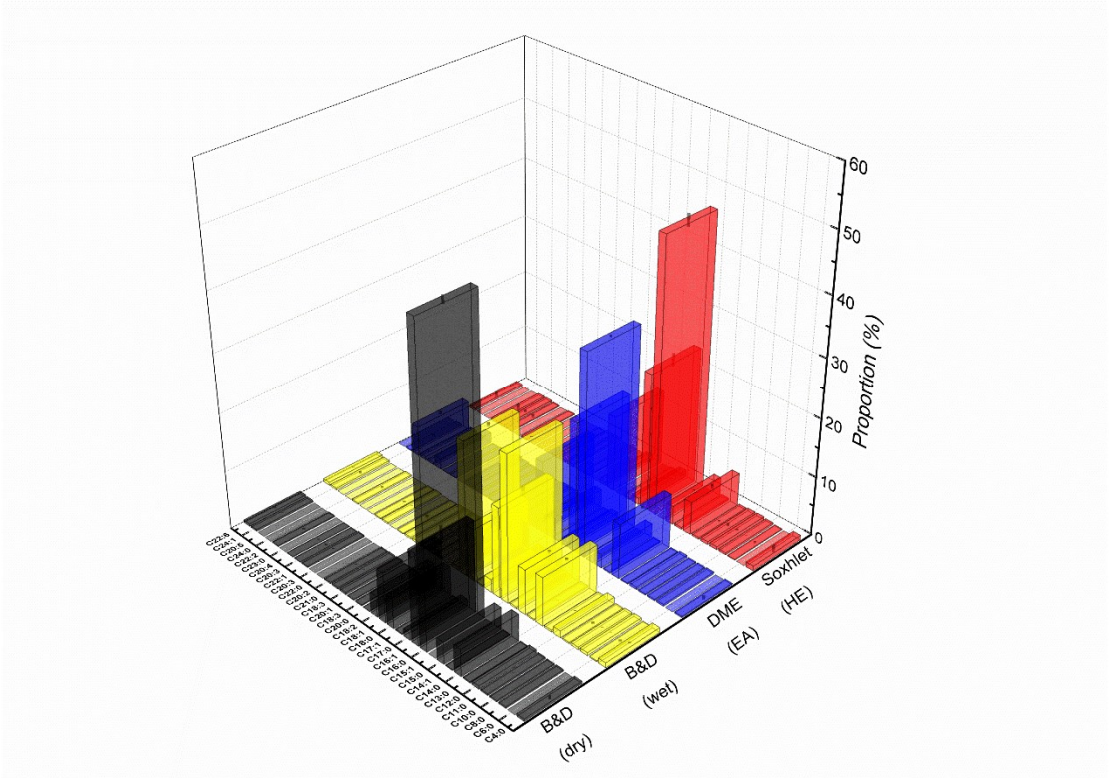

Figure 6.5 FAMEs profile by the four methods.

6.3.3.2 FTIR, TG/DTA and elemental composition

The FTIR spectra of extracted raw lipid was showed in the Figure 6.6 The peaks at 3,007 cm^{-1} were in accord with olefinic C-H stretching due to unsaturated fat [47]. The peaks at 2,953 cm^{-1} assigned to stretching vibration of C-H in $-CH_3$. The high absorptions at 2,926 and 2,855 cm^{-1} belonged to C-H stretching vibration in $-CH_2$. The double peaks at 2,359 and 2,336 cm^{-1} were related to N-H stretching vibration in amino group [48][49]. C=O stretching vibration of ester was observed at 1,745 cm^{-1}. And symmetric and asymmetric bending of methyl groups were at 1,371 and 1,466 cm^{-1} respectively. And the peaks of C-O in ester were at 1,163 cm^{-1}. Peaks at 968 cm^{-1} were stretching vibration of C-C in backbone. For the all methods, the spectra were very similar to each other, except N-H peaks (2,359, 2,336 cm^{-1}) by B&D (wet) and DME were much more significant than B&D (dry) and Soxhlet (HE), which implied the more nitrogen in extracted raw lipids by B&D (wet) and DME methods.

The results of oxidative and thermal stability of extracted raw lipids were showed in the Figure 6.7 For the 4 raw lipids, the mass loss could be roughly divided into three stages [50][51]: ~50 % of mass loss occurred during the first stage with a DTG peak and corresponding DTA exothermic peak at 350 ℃, due to alkyl radicals formed and reacted with oxygen, especially unsaturated lipids mainly decomposed in this stage; In the second stage (exothermic DTA peak), ~20% of mass loss occurred with a DTG peak at 400~415 ℃, which was attributed to degradation of carbon chains, and both rest of unsaturated lipids with saturated lipids decomposed in this stage; The last exothermic stage ranged from 450 ℃ to 550 ℃ was related to completely oxidation of the carbonaceous residues from the first two stages. Yet there was slight difference among the 4 lipids, and a small DTG peek (~3% mass loss) at 175 ℃ was observed for the raw lipids from B&D (dry). Since its exothermic peak, this could be attributed to initial degradation of esters by the action of oxygen rather than evaporation of the lipids [52]. Table S17 presented the CHN composition of extracted raw lipids. When the extracted lipids were used as biofuel, N content was an important index [53]. In this study, N contents from the 4 methods ranged from 0.09~0.23%, the low N contents were in favor of combustion. And the highest N content of 0.23% was obtained by DME method, which was consistent with the conclusion from FTIR analysis. In addition, relatively higher C content (76.21%) with lower O content (11.26%) was observed in lipids by B&D (wet), which was attributed to an isolation of a wide range of components from microalgae[29].

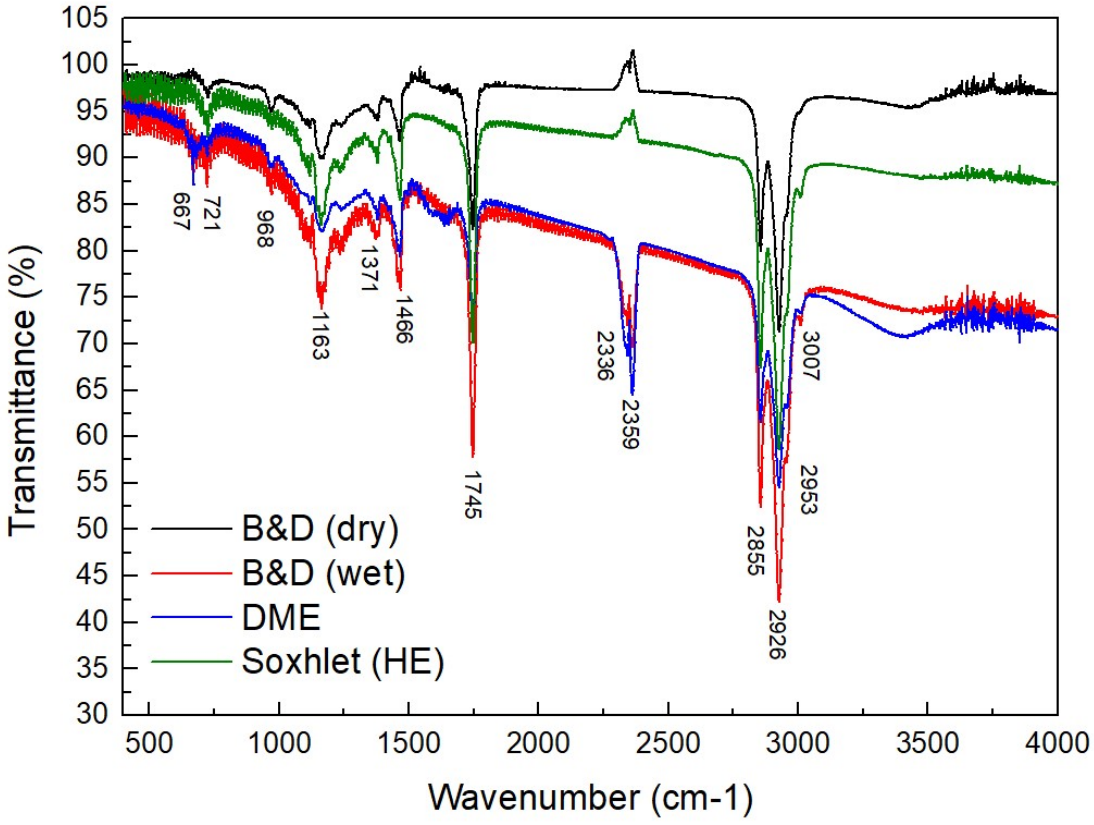

Figure 6.6 FTIR spectrum of extracted raw lipids by the 4 methods.

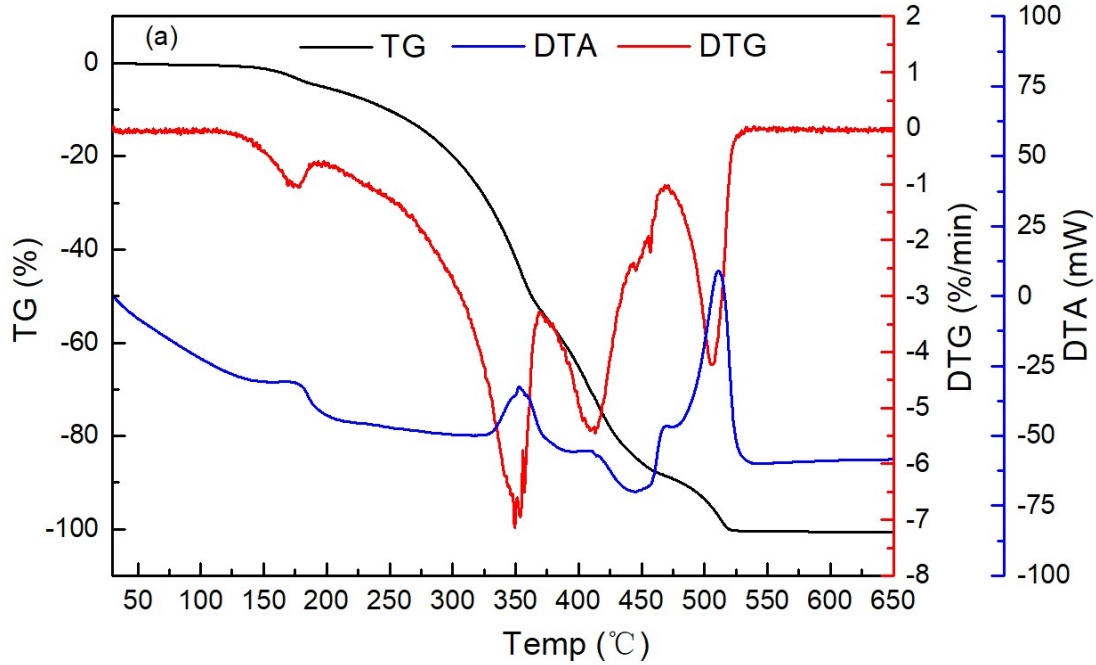

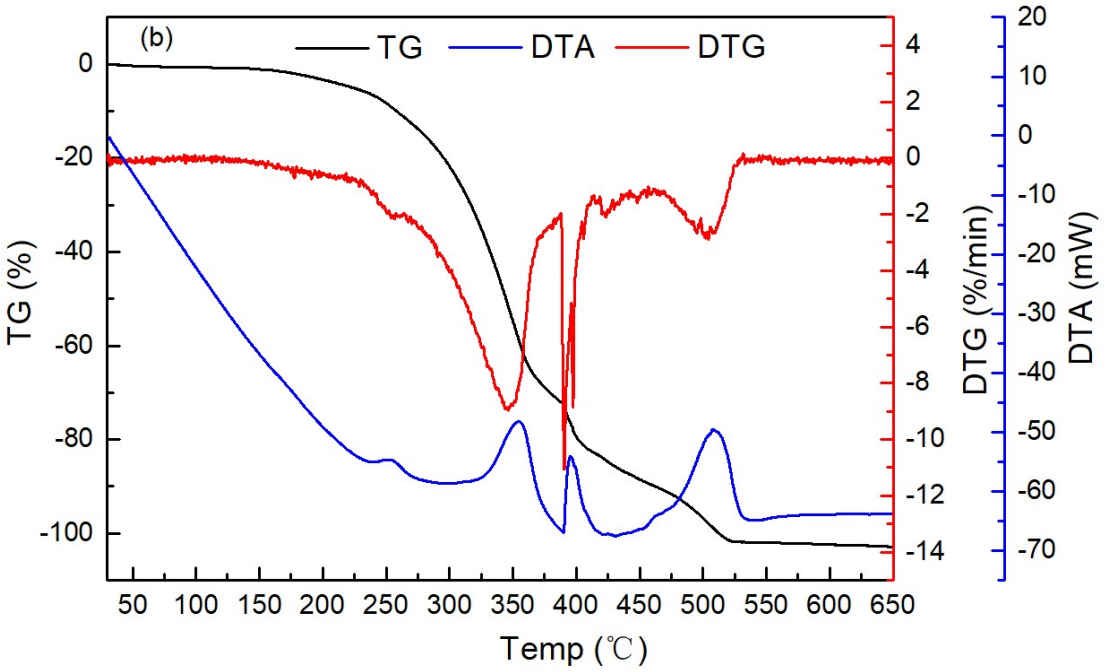
(b)
TG
DTA
DTG
TG (%)
DTG (%/min)
DTA (mW)
Temp (℃)

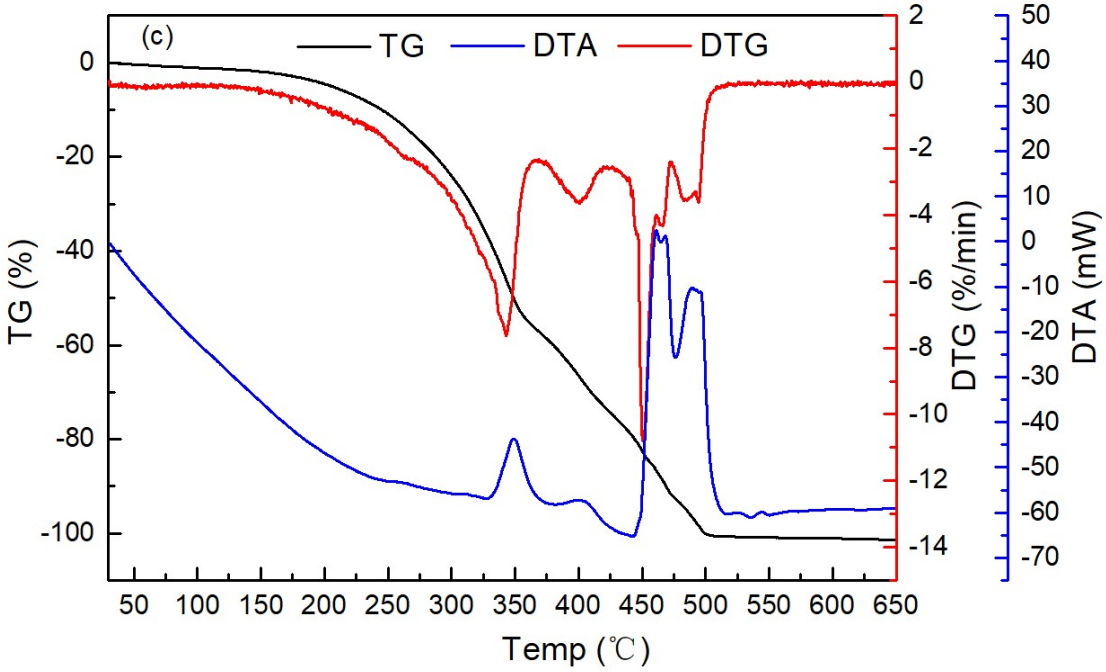
(c)
TG
DTA
DTG
TG (%)
DTG (%/min)
DTA (mW)
Temp (℃)

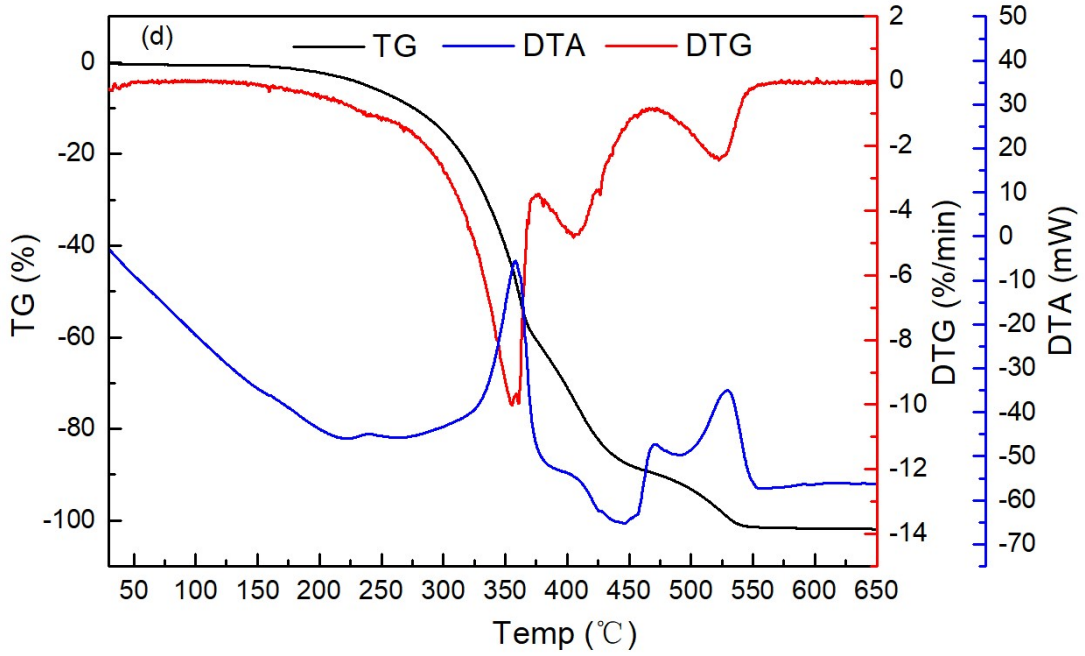

Figure 6.7 TG/DTA analysis of extracted raw lipids, a) B&D (dry); b) B&D (wet); c) DME; d) Soxhlet (HE).

6.3.3.3Trace metals analysis

The trace metals in biodiesel may cause metallic corrosion during its transport and storage, pollution emission into environment and engine deterioration [54][55]. According to Japan Standard (JIS K 2390:2008), the content of K+Na in the lipid should be less than 0.05 ‰ and Mg+Ca also should be <0.05 ‰. In this study, by comparing with blank (ultrapure water), the trace metals of Fe, Ni, Cu, Zn, Sr, Ba, Mg, K and Na had been detected in extracted raw lipids by ICP-MS. Ca and Si which were reported by Kanda, et.al (2020) [29], were not found in this study due to different microalgae species. The metals were mainly derived from the broth for cultivating microalgae and remaining might be mixed during extraction. The Table 6.2 showed the contents of these trace metals, and among them, the contents of Mg, Na, K and Fe were much higher than others, which indicated the lipid from all four method need purification for trace metal removal. Especially, Mg content in DME extracted raw lipids was 66 ‰, and the sum of Fe, Mg with Na in raw lipids from B&D (wet) method reached to 19 ‰, in order to using them as vehicle fuels proper purification should be conducted.

Table 6.2. Trace metals in the extracted raw lipids.

		Fe (‰)	Ni (‰)	Cu (‰)	Zn (‰)	Sr (‰)	Ba (‰)	Mg (‰)	K (‰)	Na (‰)
B&D (dry)	Mean.	0.416	0.029	0.049	0.041	0.326	0.200	2.067	-	4.500
	Variance	0.015	0.001	0.003	0.007	0.001	0.002	0.173	-	0.929
DME	Mean.	0.824	0.075	0.746	0.353	0.005	0.013	66.633	1.867	1.833
	Variance	0.023	0.002	0.011	0.018	0.000	0.002	0.416	0.000	0.100
Soxhlet (HE)	Mean.	0.380	0.044	0.030	0.056	0.015	0.067	3.067	-	-
	Variance	0.011	0.001	0.001	0.008	0.000	0.003	0.520	-	-
B&D (wet)	Mean.	3.334	0.388	0.082	0.173	0.042	0.043	7.933	0.533	7.867
	Variance	0.056	0.006	0.010	0.015	0.001	0.001	0.058	0.115	0.115

6.4 Conclusions

In this study, ethanol and acetone were screened to significantly improve lipids extraction from flocculation harvested microalgae by DME. After addition of ethanol or acetone in DME, the mixture can be miscible with water, and lipid yield increased 4.0 and 6.4 times than the blank respectively. According to a series of experiments, the suitable condition was determined as extraction time of 30 min, 4.2 mL DME per 1 mL microalgae, entrainer dosage of 8% and ratio (ethanol: acetone) of 1:2. Under the optimal condition, DME method (entrainer) was compared with B&D and Soxhlet methods, and results showed 26.4% of total raw lipids with 54.4% of total FAMEs in the microalgae was extracted by the DME method. FAMEs proportion was highest among all methods. Thus, the DME method was economical to extract lipid. Finally, the feature of extracted raw lipids by the methods was analyzed. FTIR implied the more N-H in extracted raw lipids by B&D (wet) and DME methods than B&D (dry) and solvent Soxhlet (HE), which was then confirmed by CHN analysis. The thermal stability by TG/DTA indicated the lipids by the 4 methods started to decompose from 150 ℃, and final decomposition temperature varied from 500 to 535 ℃. Since trace metals in biodiesel caused metallic corrosion, pollution emission into environment and engine deterioration, it was analyzed by ICP. The results showed trace metals of Fe, Ni, Cu, Zn, Sr, Ba, Mg, K and Na had been detected in extracted raw lipids by the four methods, and the high Mg content in DME extracted raw lipids indicated purification was necessary for using it as vehicle fuels.

Reference

[1] Dong, T., Knoshaug, E. P., Pienkos, P. T., & Laurens, L. M. (2016). Lipid recovery from wet oleaginous microbial biomass for biofuel production: a critical review. Applied Energy, 177, 879-895.

[2] Du, Y., Schuur, B., Kersten, S. R., & Brilman, D. W. (2018). Multistage wet lipid extraction from fresh water stressed Neochloris oleoabundans slurry–experiments and modelling. Algal research, 31, 21-30.

[3] Ansari, F. A., Gupta, S. K., Shriwastav, A., Guldhe, A., Rawat, I., & Bux, F. (2017). Evaluation of various solvent systems for lipid extraction from wet microalgal biomass and its effects on primary metabolites of lipid-extracted biomass. Environmental Science and Pollution Research, 24(18), 15299-15307.

[4] Williams, P. J. L. B., & Laurens, L. M. (2010). Microalgae as biodiesel & biomass feedstocks: review & analysis of the biochemistry, energetics & economics. Energy & Environmental Science, 3(5), 554-590.

[5] Angles, E., Jaouen, P., Pruvost, J., & Marchal, L. (2017). Wet lipid extraction from the microalga Nannochloropsis sp.: Disruption, physiological effects and solvent screening. Algal research, 21, 27-34.

[6] Ghasemi Naghdi, F., González González, L. M., Chan, W., & Schenk, P. M. (2016). Progress on lipid extraction from wet algal biomass for biodiesel production. Microbial biotechnology, 9(6), 718-726.

[7] Qiu, C., He, Y., Huang, Z., Li, S., Huang, J., Wang, M., & Chen, B. (2019). Lipid extraction from wet Nannochloropsis biomass via enzyme-assisted three phase partitioning. Bioresource technology, 284, 381-390.

[8] Sirisuk, P., Sunwoo, I., Kim, S. H., Awah, C. C., Ra, C. H., Kim, J. M., ... & Kim, S. K. (2018). Enhancement of biomass, lipids, and polyunsaturated fatty acid (PUFA) production in Nannochloropsis oceanica with a combination of single wavelength light emitting diodes (LEDs) and low temperature in a three-phase culture system. Bioresource technology, 270, 504-511.

[9] Shuba, E. S., & Kifle, D. (2018). Microalgae to biofuels: 'Promising'alternative and renewable energy, review. Renewable and Sustainable Energy Reviews, 81, 743-755.

[10] Patel, A., Arora, N., Pruthi, V., & Pruthi, P. A. (2019). A novel rapid ultrasonication-microwave treatment for total lipid extraction from wet oleaginous yeast biomass for sustainable biodiesel production. Ultrasonics sonochemistry, 51, 504-516.

[11] Seo, Y. H., Sung, M., Oh, Y. K., & Han, J. I. (2015). Lipid extraction and esterification for microalgae-based biodiesel production using pyrite (FeS_2). Bioresource technology, 191, 420-425.

[12] Garzon-Sanabria, A. J., Davis, R. T., & Nikolov, Z. L. (2012). Harvesting Nannochloris oculata by inorganic electrolyte flocculation: effect of initial cell density, ionic strength, coagulant dosage, and media pH. Bioresource technology, 118, 418-424.

[13] Lam, M. K., & Lee, K. T. (2012). Microalgae biofuels: a critical review of issues,

problems and the way forward. Biotechnology advances, 30(3), 673-690.
[14] Singh, G., & Patidar, S. K. (2018). Microalgae harvesting techniques: A review. Journal of environmental management, 217, 499-508.
[15] Barros, A. I., Gonçalves, A. L., Simões, M., & Pires, J. C. (2015). Harvesting techniques applied to microalgae: a review. Renewable and Sustainable Energy Reviews, 41, 1489-1500.
[16] Tang, S., Qin, C., Wang, H., Li, S., & Tian, S. (2011). Study on supercritical extraction of lipids and enrichment of DHA from oil-rich microalgae. The Journal of Supercritical Fluids, 57(1), 44-49.
[17] Sheng, J., Vannela, R., & Rittmann, B. E. (2011). Evaluation of methods to extract and quantify lipids from Synechocystis PCC 6803. Bioresource technology, 102(2), 1697-1703.
[18] Wu, J., Alam, M. A., Pan, Y., Huang, D., Wang, Z., & Wang, T. (2017). Enhanced extraction of lipids from microalgae with eco-friendly mixture of methanol and ethyl acetate for biodiesel production. Journal of the Taiwan Institute of Chemical Engineers, 71, 323-329.
[19] Lardon, L., Hélias, A., Sialve, B., Steyer, J. P., & Bernard, O. (2009). Life-cycle assessment of biodiesel production from microalgae.
[20] Lakshmikandan, M., Murugesan, A. G., Wang, S., Abomohra, A. E. F., Jovita, P. A., & Kiruthiga, S. (2020). Sustainable biomass production under CO_2 conditions and effective wet microalgae lipid extraction for biodiesel production. Journal of Cleaner Production, 247, 119398.
[21] Sánchez-Bayo, A., López-Chicharro, D., Morales, V., Espada, J. J., Puyol, D., Martínez, F., ... & Rodríguez, R. (2020). Biodiesel and biogas production from Isochrysis galbana using dry and wet lipid extraction: A biorefinery approach. Renewable Energy, 146, 188-195.
[22] Cheng, J., Yu, T., Li, T., Zhou, J., & Cen, K. (2013). Using wet microalgae for direct biodiesel production via microwave irradiation. Bioresource technology, 131, 531-535.
[23] Sander, K., & Murthy, G. S. (2010). Life cycle analysis of algae biodiesel. The International Journal of Life Cycle Assessment, 15(7), 704-714.
[24] Goto, M., Kanda, H., & Machmudah, S. (2015). Extraction of carotenoids and lipids from algae by supercritical CO_2 and subcritical dimethyl ether. The journal of supercritical Fluids, 96, 245-251.
[25] Wang, Q., Oshita, K., Nitta, T., & Takaoka, M. (2020). Evaluation of a sludge-treatment process comprising lipid extraction and drying using liquefied dimethyl ether. Environmental Technology, 1-10.
[26] Tallon, S., & Fenton, K. (2010). The solubility of water in mixtures of dimethyl ether and carbon dioxide. Fluid phase equilibria, 298(1), 60-66.
[27] Oshita, K., Takaoka, M., Nakajima, Y., Morisawa, S., Kanda, H., Makino, H., & Takeda, N. (2012). Characteristics of Biosolids in Dimethyl Ether Dewatering Method. Water environment research, 84(2), 120-127.

[28] Oshita, K., Toda, S., Takaoka, M., Kanda, H., Fujimori, T., Matsukawa, K., & Fujiwara, T. (2015). Solid fuel production from cattle manure by dewatering using liquefied dimethyl ether. Fuel, 159, 7-14.
[29] Kanda, H., Hoshino, R., Murakami, K., Zheng, Q., & Goto, M. (2020). Lipid extraction from microalgae covered with biomineralized cell walls using liquefied dimethyl ether. Fuel, 262, 116590.
[30] Li, P., Kanda, H., & Makino, H. (2014). Simultaneous production of bio-solid fuel and bio-crude from vegetal biomass using liquefied dimethyl ether. Fuel, 116, 370-376.
[31] Kanda, H., & Li, P. (2011). Simple extraction method of green crude from natural blue-green microalgae by dimethyl ether. Fuel, 90(3), 1264-1266.
[32] Nerome, H., Ito, M., Machmudah, S., Kanda, H., & Goto, M. (2016). Extraction of phytochemicals from saffron by supercritical carbon dioxide with water and methanol as entrainer. The Journal of Supercritical Fluids, 107, 377-383.
[33] Gadkari, P. V., Balarman, M., & Kadimi, U. S. (2015). Polyphenols from fresh frozen tea leaves (Camellia assamica L.,) by supercritical carbon dioxide extraction with ethanol entrainer-application of response surface methodology. Journal of food science and technology, 52(2), 720-730.
[34] Tsuzuki, M., Okada, K., Isoda, H., Hirano, M., Odaka, T., Saijo, H., ... & Fujiwara, S. (2019). Physiological Properties of Photoautotrophic Microalgae and Cyanobacteria Relevant to Industrial Biomass Production. Marine Biotechnology, 21(3), 406-415.
[35] Bligh, E. G., & Dyer, W. J. (1959). A rapid method of total lipid extraction and purification. Canadian journal of biochemistry and physiology, 37(8), 911-917.
[36] Nor Afifah, S., Darah, I., Shaida Fariza, S., Jain Nordin, M. M., Nurul Aili, Z., Ali-Shtayeh, M. S., ... & Andrews, J. M. (1998). Soxhlet extraction of solid matrices: An outdated technique with a promising innovative future. Journal of Applied Sciences, 10(23), 265-271.
[37] Engdahl, A., & Nelander, B. (1992). Intermolecular vibrations of the dimethyl ether–water complex. A matrix isolation study. Journal of the Chemical Society, Faraday Transactions, 88(2), 177-182.
[38] De Jesus, S. S., Ferreira, G. F., Moreira, L. S., Maciel, M. R. W., & Maciel Filho, R. (2019). Comparison of several methods for effective lipid extraction from wet microalgae using green solvents. Renewable Energy, 143, 130-141.
[39] Sada, E., Morisue, T., & Miyahara, K. (1975). Salt effects on vapor-liquid equilibrium of tetrahydrofuran-water system. Journal of Chemical and Engineering Data, 20(3), 283-287.
[40] Mitra, M., & Mishra, S. (2019). A comparative analysis of different extraction solvent systems on the extractability of eicosapentaenoic acid from the marine eustigmatophyte Nannochloropsis oceanica. Algal research, 38, 101387.
[41] Wu, C., Xiao, Y., Lin, W., Zhu, J., De la Hoz Siegler, H., Zong, M., & Rong, J. (2017). Surfactants assist in lipid extraction from wet Nannochloropsis

sp. Bioresource technology, 243, 793-799.
[42] Shin, H. Y., Ryu, J. H., Bae, S. Y., Crofcheck, C., & Crocker, M. (2014). Lipid extraction from Scenedesmus sp. microalgae for biodiesel production using hot compressed hexane. Fuel, 130, 66-69.
[43] Taher, H., Al-Zuhair, S., Al-Marzouqi, A. H., Haik, Y., & Farid, M. (2014). Effective extraction of microalgae lipids from wet biomass for biodiesel production. biomass and bioenergy, 66, 159-167.
[44] Wang, Q., Oshita, K., Nitta, T., & Takaoka, M. (2020). Evaluation of a sludge-treatment process comprising lipid extraction and drying using liquefied dimethyl ether. Environmental Technology, 1-10.
[45] Ghasemi Naghdi, F., González González, L. M., Chan, W., & Schenk, P. M. (2016). Progress on lipid extraction from wet algal biomass for biodiesel production. Microbial biotechnology, 9(6), 718-726.
[46] De Souza Silva, A. P. F., Costa, M. C., Lopes, A. C., Neto, E. F. A., Leitao, R. C., Mota, C. R., & dos Santos, A. B. (2014). Comparison of pretreatment methods for total lipids extraction from mixed microalgae. Renewable Energy, 63, 762-766.
[47] Chiplunkar, P. P., & Pratap, A. P. (2016). Utilization of sunflower acid oil for synthesis of alkyd resin. Progress in Organic Coatings, 93, 61-67.
[48] Nandiyanto, A. B. D., Oktiani, R., & Ragadhita, R. (2019). How to Read and Interpret FTIR Spectroscope of Organic Material. Indonesian Journal of Science and Technology, 4(1), 97-118.
[49] Tallis, Huw Aubrey 2009. *Novel approaches towards phosphorous containing macrocycles.* PhD Thesis, Cardiff University.
[50] Dos Santos Politi, J. R., de Matos, P. R. R., & Sales, M. J. A. (2013). Comparative study of the oxidative and thermal stability of vegetable oils to be used as lubricant bases. Journal of thermal analysis and calorimetry, 111(2), 1437-1442.
[51] Raba, D. N., Chambre, D. R., Copolovici, D. M., Moldovan, C., & Copolovici, L. O. (2018). The influence of high-temperature heating on composition and thermo-oxidative stability of the oil extracted from Arabica coffee beans. PloS one, 13(7).
[52] Eychenne, V., Mouloungui, Z., & Gaset, A. (1998). Thermal behavior of neopentylpolyol esters: Comparison between determination by TGA-DTA and flash point. Thermochimica acta, 320(1-2), 201-208.
[53] Pimentel, D., & Patzek, T. W. (2008). Biofuels, solar and wind as renewable energy systems. Benefits and risks, New York: Springer.
[54] Machmudah, S., Winardi, S., Kanda, H., & Goto, M. (2017). Sub-and Supercritical Fluids Extraction of Phytochemical Compounds from Eucheuma cottonii and Gracilaria sp. Chemical Engineering Transactions, 56, 1291-1296.
[55] Almeida, E. S., Richter, E. M., & Munoz, R. A. (2014). On-site fuel electroanalysis: Determination of lead, copper and mercury in fuel bioethanol by anodic stripping voltammetry using screen-printed gold electrodes. Analytica chimica acta, 837, 38-43.
[56] Chu, F. J., Wan, T. J., Pai, T. Y., Lin, H. W., Liu, S. H., & Huang, C. F. (2020). Use

of magnetic fields and nitrate concentration to optimize the growth and lipid yield of Nannochloropsis oculata. Journal of environmental management, 253, 109680.

[57] Sarker, P. K., Kapuscinski, A. R., Bae, A. Y., Donaldson, E., Sitek, A. J., Fitzgerald, D. S., & Edelson, O. F. (2018). Towards sustainable aquafeeds: Evaluating substitution of fishmeal with lipid-extracted microalgal co-product (Nannochloropsis oculata) in diets of juvenile Nile tilapia (Oreochromis niloticus). PLoS One, 13(7), e0201315.

Chapter 7 Influence of moisture in dewatered microalgae and cell disruption on its lipid extraction by green solvent of liquefied DME

7.1. Introduction

Limited fossil deposit and its combustion caused greenhouse gases emission resulted in increasing demand on research of alternative fuels, which is sustainable and environment-friendly [1][2]. Biodiesel production form microalgae has a potential to meet the demand, due to its high growth rate, possibility to use non-arable land, and high lipid accumulation rate [3][4][5]. In addition, microalgae can be cultivated in wastewater for further removal of N and P [6], and exhaust fumes from plants can be used as carbon source[28], which make the biodiesel from microalgae competitive and promising. The precursor of biodiesel is lipid of microalgae in the cells, which has been successfully extracted by Bligh & Dyer [8] or Soxhlet extraction methods [9]. The Bligh & Dyer method using polar solvent of methanol with nonpolar solvent of chloroform to extract both polar and nonpolar lipids in materials, is hence considered as a datum for determining total amount of lipid in sample [29]. About 53% w/w dry base of lipid was extracted from *Chlorella vulgaris* by the method as reported in [11]; the total lipid in *N. oculata* was determined as 23.8% by the method [12]; using the Bligh & Dyer method total lipid in *Nannochloropsis sp.* was measured as 47.5% [13]; and the lipid content in *B. braunii* was examined to be 49.3% by the method [14]. As for the Soxhlet extraction method, the classic solvent used was hexane, which was nonpolar and suited for capturing nonpolar lipids, such as triglyceride [14]. Other solvents for the methods were also investigated, for example, mixing hexane with isopropanol with a ratio of 3:2, lipid yield of 22.5% (dry base) was achieved from *Chlorella vulgaris* [20]; ethyl acetate could substitute hexane as solvent to extract lipid from *I. galbana* with a yield of 17.6% [21]; and 7.8% lipid yield (dry base) from *Scenedesmus obliquus* was obtained by mixed solvents (isopropanol/hexane of 2:1 v/v) [3].

Apart from the two methods, a subcritical extraction method by using liquefied dimethyl ether (DME) as solvent has received significant attention. DME gas (under ambient condition) can be easily liquefied at 0.51~0.59 MPa at room temperature (20~25 ℃). The liquefied DME has a high affinity to organic compounds and possess a medium polarity, which make the solvent suitable for extracting both polar and nonpolar lipids [18]. In addition, the liquefied DME is partially miscible with water, and can absorb 7~8 wt.% of water under room temperature. Therefore, the DME can achieve lipid extraction with dewatering simultaneously [24][25], and this feature is

especially beneficial to wet microalgae with resulting in an energy-saving. Since the boiling point of the liquefied DME is -24.8 ℃*, it can be easily* evaporated and separated from final product (extracted lipids) under room temperature, and be liquefied efficiently for recycling [25][26]. Furthermore, DEM is considered as a green solvent because it is non-toxic, environmental safe, friendly and cost effective [22][23]. The decomposition of DME in atmosphere is easy since the lack of a C-C bond, and unlike other typical ethers the DME is relatively stable without forming peroxides (toxic, flammable and explosive) [24].

Usually, cell disruption is the important step before lipid extraction from microalgae, since the lipid stores inside the cell or bound to intracellular membranes [25]. Generally, the cell wall is composed of polysaccharide, uronic acid, protein, algaenan, glycolipid, and minerals, which resulted the rigidity of microalgae cell is manifold higher than that of plant's cell wall, and since passive diffusion across cell wall is slow it significantly affect the extraction efficiency [26]. By cell disruption, solvents can directly access to intracellular lipid for improving the lipid extraction efficiency. The cell disruption can be generally categorized into mechanical (pressing, ultrasonic, microwave, electric pulse, homogenization, heating) and non-mechanical methods (acidification, nanoparticle, supercritical fluids, ionic liquid, biological enzymes), which has been proved to improve extraction performance of Bligh & Dyer and Soxhlet extraction methods [27]. As for the DME method, without a cell disruption step, lipid can be successfully extracted from some of microalgae species (*B. braunii*, *C. gracilis* and *P. carterae*) with relative thinner and weaker cell wall or by using huge dosage of DME [29][14]. However, for other species, it was found that DME failed to extract lipid from samples without cell disruption and thus the step came to be necessary for the DME method. Considering the improvement of cell disruption on DME method has not been investigated yet, it is very meaningful to clarify the mechanism of it.

In the chapter 6, a technique for lipid extraction from liquid microalgae sample was developed. Yet, it's found that for some species with thick and strong cell wall, this technique is not worked well. So the cell disruption treatment may be a solution. In the present case, effect of five cell disruption methods (acidification, ultrasonic, microwave, homogenization, and heating) on improving lipid extraction by the DME have been investigated on *Tetradesmus obliquus*. The lipid extraction with drying performance was firstly examined under various condition of moisture content in samples, extraction time and DME dosage. On the base of it, raw lipid yield, FAMEs and drying effect of the DME method from two types of microalgae samples ($AlCl_3$ flocculation + filtration, chitosan flocculation + filtration) by the five cell disruption methods were compared with blanks (flocculation + filtration and only centrifugation samples without cell disruption). In addition, the flocs before and after cell disruption were examined by microscope and particle size analyzer. The effect of cell disruption on filtrate was examined by three-dimensional excitation emission matrix (3D-EEM). Scanning Electron Microscope (SEM) was utilized to display the cell disruption on microalgae. Change of free water and bound water during the above treatment process were

measured by Differential scanning calorimetry (DSC). Besides, for the obtained dried microalgae, their feasibility to be used as biosolid fuel was evaluated by C/H/N/S elemental analyzer and Thermogravimeter-differential thermal analyzer (TG/DTA).

7.2. Materials and methods

7.2.1 Microalgae cultivation

Fresh water microalgae specie *Tetradesmus obliquus* was obtained from Microbial Culture Collection at the National Institute for Environmental Studies (Tsukuba, JAPAN). The medium of AF-6 is used to cultivate the specie, and components of the medium are shown in Table S15. The microalgae were cultivated in a 20L bucket photobioreactor with light/dark cycles of 12/12. During the cultivation, temperature was controlled at ~ 20 ℃, and filtered air was continuously aerated into the medium as carbon source for microalgae. When microalgae entered the stationary phase (about 20 days), the cultivation process was complete. The dry cell weight of microalgae in the stationary phase was measured by filtering it through pre-weighed glass microfiber filter paper (GF/C, 1.2 μm, 4.7 cm; Whatman plc, United Kingdom) and then drying the filter paper in oven (105°C for 24 h) for weight measurement. This process was repeated in triplicate; the dry cell weight obtained was 1.31±0.01 g/L.

7.2.2 Microalgae harvesting for samples preparation

To study the effect of moisture in microalgae on DME method's performance, the cultivated microalgae was firstly harvested by centrifugation (5000 rpm, 10 min), and the harvested microalgae was then totally dried in oven at 105 °C. Since the dried samples were lumps like, mortar was used to grind them to powder. This powder was mixed with pure water (Ultrapure Water, Wako Co.,Ltd, Japan) for preparing microalgae samples with certain moisture content.
While studying the cell disruption methods, microalgae was flocculated by 45 mg/L of $AlCl_3$ or 4 mg/L chitosan, and the flocs were collected and applied to the five cell disruption methods (in 7.2.5). After the cell disruption treatments, the samples were dewatered by filtration. In contrast, the samples in blank group were prepared by $AlCl_3$ + filtration, $AlCl_3$ + centrifugation, chitosan + filtration, chitosan + centrifugation and just centrifugation, respectively, without any cell disruption treatment.

7.2.3 Experimental procedure of DME method

As shown in Figure 6.1, the device used in DEM method is illustrated. During the experiments, the harvested microalgae samples were loaded into the extraction vessel 3 with cellulose thimble (glass fiber, φ25×100mm, Whatman, Maidstone, United Kingdom) inside. The certain amount of liquefied DME stored in vessel 1 was pushed into vessel 2, and then into the extraction vessel. After several minutes of extraction,

liquid containing raw lipid with water in the vessel was transferred to vessel 4. By pressure relief DME evaporated, and raw lipid separated from water.
The separated raw lipid was dissolved by 5.0 mL chloroform and filtered through a 0.45 μm membrane filter (DISMIC-13HP, Advantech Co., Ltd., Japan). The solvent of chloroform was then removed by Nitrogen blow (Nitrogen Termovap Sample Concentrator, Ishii Tatami Shop Co., Ltd., Japan), and recovered raw lipid was weighed and stored below 0 ℃ for further analysis.

7.2.4 Bligh and Dyer method

The Bligh and Dyer method in this study is considered as a datum for total lipid in the microalgae. The 0.5 g totally dried microalgae were mixed methanol/ chloroform/pure water (Guaranteed Reagent, Wako Co.,Ltd, Japan) of 5.0/2.5/2.0 mL in a centrifuge tube. The mixture was crushed by the homogenizer (T25, IKA Co.,Ltd, Germany) at 10,000 rpm for 5 min and mixed by the vortex genie (SI-0236, SI Co.,Ltd, USA) for 5min. Then, 2.5 mL chloroform and 2.5 mL pure water were added with 2 min of mixing. After centrifugation (2410, KUBOTA Co.,Ltd, Japan) at 3,000 rpm for 5 minutes, sample was divided into 3 layers from top to bottom: water-methanol, microalgae and lipid-chloroform layer. The lipid-chloroform layer was recovered and filtered through the 0.45μm membrane. With removal of most of the solvent by rotary evaporator (40 ℃, vacuum condition), the remaining solvent was removed by the nitrogen blow. The obtained raw lipid was weighed and stored below 0 ℃ for further analysis.

7.2.5 Cell disruption treatments

30 mL microalgae samples from flocculation by $AlCl_3$ or chitosan were respectively treated by the five different methods as follows: (1) microwaves, using a microwave oven (ETHOS One, Milestone Inc., USA) with the condition (20~85 °C for 1 min and then at 85 °C for 30 min; 500W, 2450 MHz), (2) heating, using water bath to heat at 85 °C for 30min, (3) acidification, adding HCl (37.5%, Wako Co.,Ltd, Japan) to adjust pH of microalgae to 1.0 for 2h, (4) homogenization (T25, IKA Co.,Ltd, Germany), using the homogenizer to treat the samples under 1000 rpm for 10 min, (5) ultrasonic treatment, using a ultrasonic disruptor (TOMY UD - 211, Japan) at a resonance of 10 kHz for 30 min with a duty cycle of 50%.

7.2.6 Analytical methodologies

7.2.6.1 Fatty acid composition analysis
The lipid fractions in the extracted raw lipid were converted to fatty acid methyl esters (FAMEs) by transesterification, FAMEs yield was analyzed by GC-MS (GC/MS-QP2010 Plus, Shimadzu Corp., Kyoto, Japan). Specifically, the raw lipids were re-dissolved in 5 mL dichloromethane (Guaranteed Reagent, Wako Co., Ltd., Japan), then subjected to methylation by mixing with 2 mL of 14% BF_3-methanol solution (First

Grade, Wako Co., Ltd., Japan) at 65℃ for 40 min and cooled to room temperature. Dichloromethane layer containing FAMEs was separated by adding 4 mL saturated aqueous NaCl solution (Guaranteed Reagent, Wako Co., Ltd., Japan) and the solvent of dichloromethane was evaporated by the nitrogen blow. The recovered FAMEs were once again dissolved in certain amount of dichloromethane for the GC-MS analysis by using a 37-component FAMEs (Sigma-Aldrich Japan, Co., Ltd., Tokyo, Japan) as standard.

7.2.6.2 Free and bound water content measurement

A differential scanning calorimetry (DSC) analyzer (Shimadzu DSC-60, Japan) was utilized to measure free and bound water [28]. The ~10 mg of samples before and after DME treatment were cooled to - 30℃ in the DSC by liquid nitrogen, assuming all free water was frozen under this condition, and then warmed up to 20 ℃ at a rate of 2 ℃/min. The endothermic curve below the base near 0℃ represent heat requirement for melting the frozen free water, and hence determine the amount of free water in samples. The bound water can be calculated by subtracting free water from total water.

7.2.6.3 scanning electron microscopy (SEM)

SEM (JED-2300M, JEOL, Tokyo, Japan) was used to observe the morphology of the disrupted microalgae cells before and after the DME treatment with an accelerating voltage of 3.0/5.0 kV. Before SEM, the freeze dryer (FDU-1100, EYELA, Tokyo, Japan) was used to dry these samples, and the Auto fine coater (JFC-1600, JELO, Tokyo, Japan) was utilized to coat carbon onto the samples.

7.2.6.4 Other analysis

The thermal gravimetric analysis was performed for the microalgae after the DME treatment by using TG-DTA (ThermoPlus TG8110, Rigaku, Japan) under an air flow of 50 mL/min with a heating rate of 10 ℃/min from 20 to 1000 ℃. The elemental analysis including Carbon (C), Hydrogen (H), Nitrogen (N) and Sulfur(S) of the DME treated samples were performed by elemental analyzer (Micro Corder JM10, J-science Labo Co., Ltd.), and the result was used to evaluate the high heating value [29]. The digital microscope (VHX-900, KEYENCE, United states) was used to examine the morphology of the microalgae flocs before and after cell disruption. And these flocs were also measured by Laser particle size analyzer (SALD-2200, Shimadzu, Japan). Property of the microalgae filtrate with or without cell disruptions was analyzed and compared by 3D-EEM (RF-5300pc, Shimadzu, Japan).

7.2.7 Statistical analysis

All data are presented as mean ± SD of the independent experiments conducted in triplicate. Data were subjected to analysis of variance (ANOVA) by Microsoft Office Excel 2010, and the differences between means were assessed by Fischer's minimum significant difference test. Statistical significance was set at $p < 0.05$.

7.3. Results and Discussion

7.3.1 Effect of moisture content in microlagae on lipids extraction and dewatering performance

The Figure 7.1 and Table S16 showed the extracted raw lipid yield by the DME method (Bligh and Dyer method as a datum; 187.4±7.0 mg/g dry microalgae) and change of solid content after DME treatment. At first, a series of experiments were conducted on samples with different initial moisture as shown in Table S19. Then by RSM, the results were used to obtain two equations (7.1 and 7.2) fitting raw lipid yield and solid content after the treatment. These two equations are displayed in the form of Figure as shown in the Fig. 7.1.

$$\text{Raw lipid yield (\%)} = 139.9 + 0.2977x - 1.673y + 0.0087z - 0.001532x\text{^}2 + 0.00929y\text{^}2 + 0.000146z\text{^}2 - 0.001038xy + 0.000652xz - 0.000148yz \quad (7.1)$$

$$\text{Solid content (\%)} = -7.4 + 0.165x + 2.52y - 0.205z - 0.00219x\text{^}2 - 0.02784y\text{^}2 + 0.000122z\text{^}2 + 0.0008xy + 0.000527xz + 0.00306yz \quad (7.2)$$

Where x is extraction time (min), y is initial water content (%) and z is DME dosage (mL/g).

For each initial moisture condition, the amount of extracted raw lipid and solid content of residuals increased with more DME dosage and longer extraction time. Especially, for samples with initial moisture content of 85%, the raw lipid yield and solid content of residual were 69.2 ± 1.3 % and 17.9 ± 1.4 % respectively, by 75 ml DME/g microalgae dry base for 20 min. And they increased to 75.8 ± 1.9 % and 21.0 ± 2.8 % when the DME dosage reached to 125 ml/g and extraction time reached to 40 min. 78.1 ± 3.3 % of raw lipid yield with 26.9 ± 1.6 % of solid content were achieved under DME dosage of 175 ml/g and extraction time of 60 min. Similarly, for the samples with initial moisture content of 75 %, the raw lipid yield with solid content increased from 71.9 ± 0.3 % with 28.6 ± 2.0 % to 77.7 ± 1.7 % with 38.1 ± 2.4 % when DME dosage with extraction time increased from 75 ml/g with 20 min to 125 ml/g with 40 min, and reached to 84.7 ± 2.9 % with 47.2 ± 1.3 % under the condition (DME dosage of 175 ml/g, extraction time of 60 min). As for the samples with initial moisture content of 65 %, the minimum values (raw lipid yield of 76.0 ± 0.3 %, residual solid content of 40.8 ± 1.6 %) were obtained by 75 ml/g of DME for 20 min, and increased to the maximum value (raw lipid yield of 90.7 ± 2.8 %, residual solid content of 51.0 ± 2.7 %) by 175 ml/g of DME for 60 min. The speed of moisture removal by DME were very fast, and with less improvement on longer time, 20 min was enough for complete most of the dewatering. In contrast, the longer extraction time was beneficial to the raw lipid extraction, and there was still significant growth on lipid yield after 50 minutes of extraction. It should be noticed that the initial moisture content of samples mainly determined ease of lipid extraction and dewatering. For example, ranges of raw lipid yield under initial moisture content of 85, 75, 65 % were 69.2 ~ 83.1 %, 71.9 ~ 84.7 % and 76.0 ~ 90.7 % respectively, while rage of the residual solid content were 17.9 ~

29.8 %, 28.6 ~ 47.2 % and 40.8 ~ 51.0 %. It demonstrated that lipid was easier to be extracted and higher residual solid content could be obtained by the DME method for microalgae with lower initial moisture content. The negative effect of moisture content on lipid extraction was agreed with reports by using other types extraction methods (ionic liquid [30], hexane solvent [31], supercritical CO_2 [32]), which can be attributed to the moisture competing with DME for act on the cell wall, and shielding the contact of lipids with DME [33]. And dewatering is affected by moisture content, mainly because of DME's absorption of water is limited (7~8 wt.%). According the results, initial moisture content below 75% was suitable for achieving an ideal raw lipid yield of >80% with a relatively high solid content of residual (> 40%), which had the potential be use as biosolid fuel combustion [34].

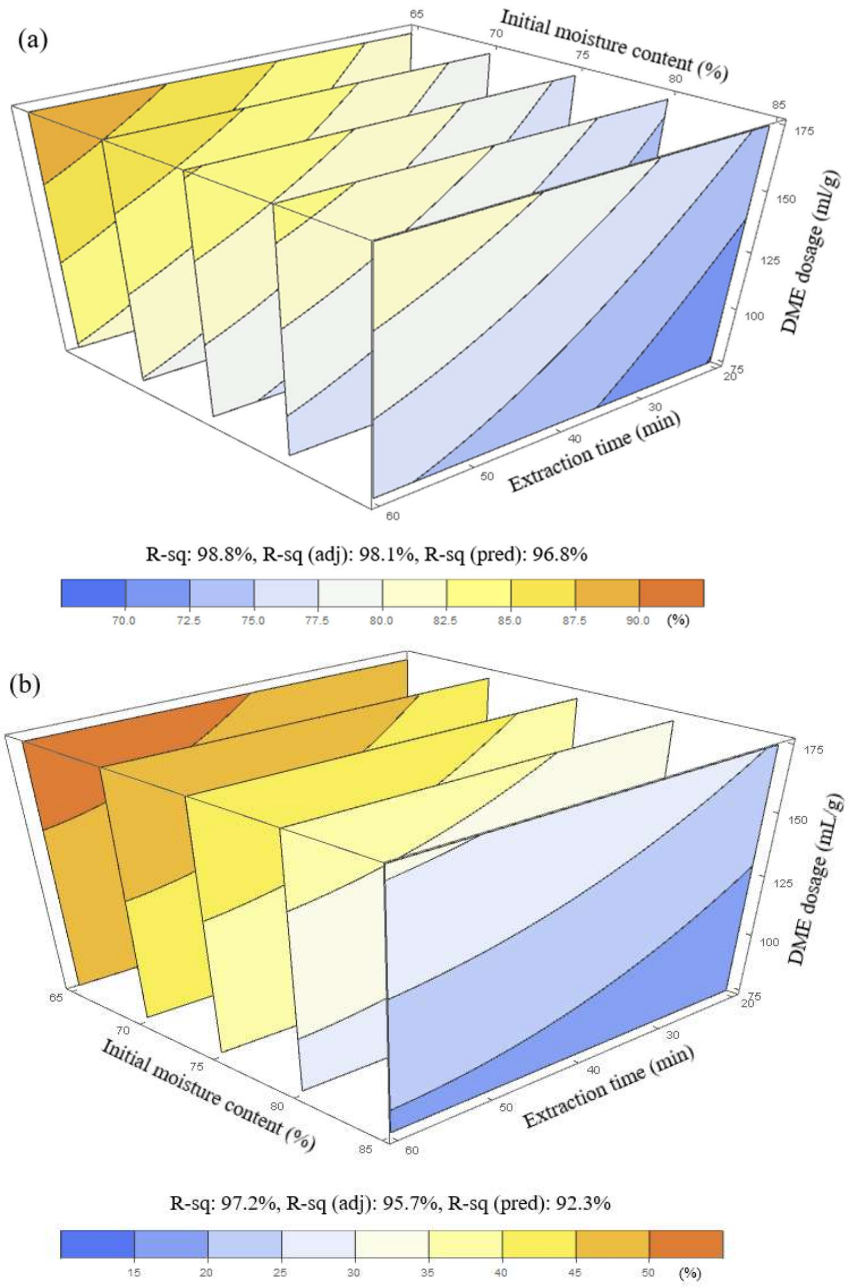

Figure 7.1 Lipids extraction with dewatering performance by DME method for microalgae with different initial moisture content, a) raw lipid yield, b) solid content after the treatment.

7.3.2 Improvement of cell disruption on the lipid extraction

To study the effect of cell disruption on lipid extraction, microalgae samples were prepared by several treatments as shown in Table 7.1 before extraction process. The results of raw lipid and FAMEs contents were shown in the Figure 7.2. By the Bligh & Dyer method (BD), 187.4 ± 7.0 mg/g raw lipid was extracted, and 40.4% of them (75.7 ± 2.6 mg/g) was FAMEs. By DME method, just 21.9 mg/g raw lipid (consist of 12.4 mg/g FAMEs) was extracted from the only centrifugation harvested microalgae (OC), which meant DME almost failed to extract lipid from the sample. In addition, the

flocculation + centrifugation harvested samples (AC, CC) obtained raw lipid contents of 26.2 and 20.5 mg/g, which was no obvious difference than the OC. Thus, the using of flocculant was no improvement in the extraction. When using flocculation + filtration to harvest microalgae (AF, CF), their raw lipid content slight increased to 40.2 mg/g and 35.5 mg/g, because the samples by filtration had less moisture content than by centrifugation. Even so, the extraction efficiency was still too low, and the cell disruption treatment was needed to improve it.

Five cell disruptions (acidification, homogenization, heating, microwave and ultrasonic) with the potential to improve the DME method were examined. The results displayed, from the samples with acidification or homogenization treatment (AAF, CAF, AGF, CGF), the raw lipid with FAMEs contents were 34.6 mg/g (17.1 mg/g), 53.8 mg/g (15.1 mg/g), 38.8 mg/g (16.2 mg/g) and 42.6 mg/g (13.7 mg/g) respectively, which were roughly equal to the samples without cell disruption (AF, CF). Therefore, acidification and homogenization were invalid for improvement of lipid extraction by the DME method. In contrast, extraction efficiency was heavily enhanced by heating, since it increased the permeability of the cell membranes with release of metabolites [35]. 223.4 mg/g raw lipid (FAMEs of 69.9 mg/g) was obtained from sample AHF, and 294.7 mg/g raw lipid (FAMEs of 72.8 mg/g) from the CHF, among which the FAMEs contents were very close to Bligh & Dyer method while the raw lipid contents were even higher than from it. Microwave or ultrasonic treatment also successfully enhanced the extraction efficiency with a slightly higher FAMEs content than the heating treatment. For example, 216.5 mg/g raw lipid including 78.7 mg/g FAMEs and 266.3 mg/g raw lipid including 83.5 mg/g FAMEs were achieved from the microwave treated samples AMF and CMF. By ultrasonic treatment, raw lipid extracted from AUF increased to 226.5 mg/g with 86.7 mg/g of FAMEs, and it from CUF reached to 293.9 mg/g with 91.0 mg/g of FAMEs. The microwave could decrease thickness and increase pore diameter of cell way with improving permeability of the cell and even damage the pectin and cellulose structures in the cell walls [36], which resulted its significant enhance on the extraction. As for the ultrasonic treatment, the high frequency acoustic waves could initiate a cavitation process inducing a shock wave formed jet streams and high shear forces to disrupt cell wall [37].

Table 7.1 Microalgae samples preparation and their abbreviation

		OC	AC	CC	AF	CF	AAF	CAF	AGF	CGF	AHF	CHF	AMF	CMF	AUF	CUF
Flocculation	$AlCl_3$		✓		✓		✓		✓		✓		✓		✓	
	Chitosan			✓		✓		✓		✓		✓		✓		✓
Cell Disruption	Acidification						✓	✓								
	Homogenization								✓	✓						
	Heating										✓	✓				
	Microwave												✓	✓		
	Ultrasonic														✓	✓
Dewatering	Centrifugation	✓	✓	✓												
	Filtration				✓	✓	✓	✓	✓	✓	✓	✓	✓	✓	✓	✓

The Figure 7.3 shown the profile of extracted FAMEs. Even though the cell disruption significantly affected the raw lipid with FAMEs extraction, its influence on profile of FAMEs was no obvious. The FAMEs by each treatment were mainly composed of C14:0, C16:0, C16:1, C18:0, C18:1, C18:2 and C18:3, which was agreement with reports [38][39]. For these lipids being well extracted groups, such as AHF, CHF, AMF, CMF, AUF, CUF, the most abundant fatty acid was C18:1, accounting for 34.7 ~ 39.5 % followed by C16:0 with 16.1~18.3%, C18:2 of 8.5~11.4%, C18:3 of 7.8 ~ 12.7%, C16:1(~6.9%), C18:0 (~6.6%) and C14:0 (~2.47%). The others detected fatty acids included C15:1, C17:1, C20:0, C20:1, C20:2 and C22:0, total of which accounted for 5.8~12.3%. FAMEs profile reflects the lipid properties (cold flow properties, cetane number and oxidative stability), which are critical for using as biodiesel [38][40]. In this case, the main component was saturated and monounsaturated fatty acids of C16~C18, which represented the good lipid properties.

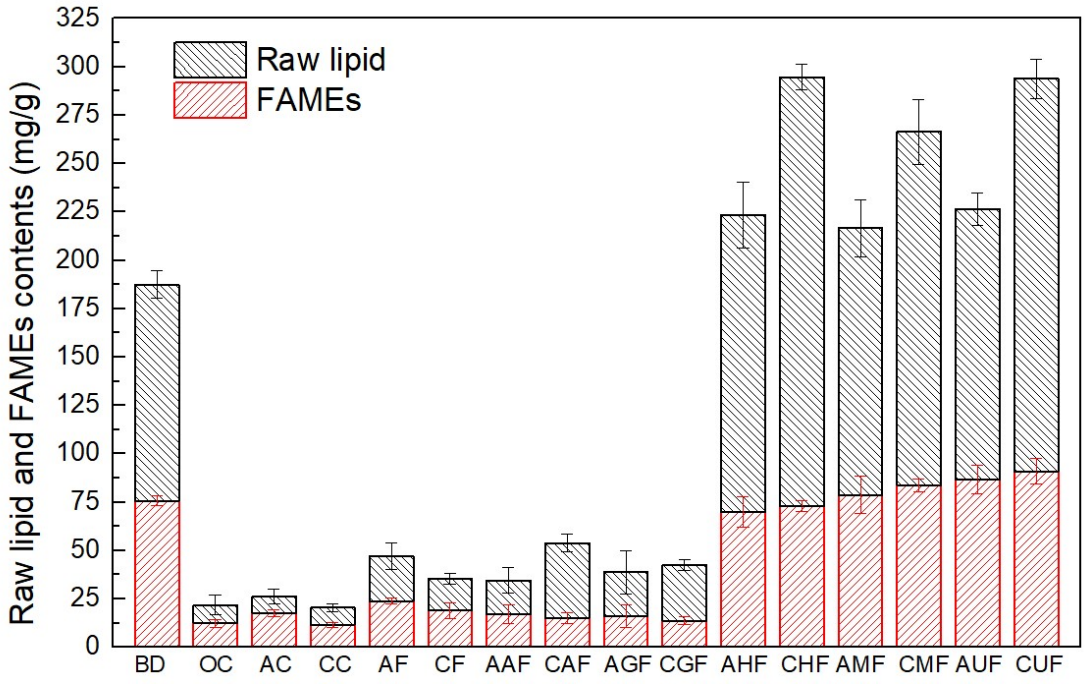

Figure 7.2 Raw lipid and FAMEs contents in extracted by B&D method (BD) or DME method with virous cell disruption.

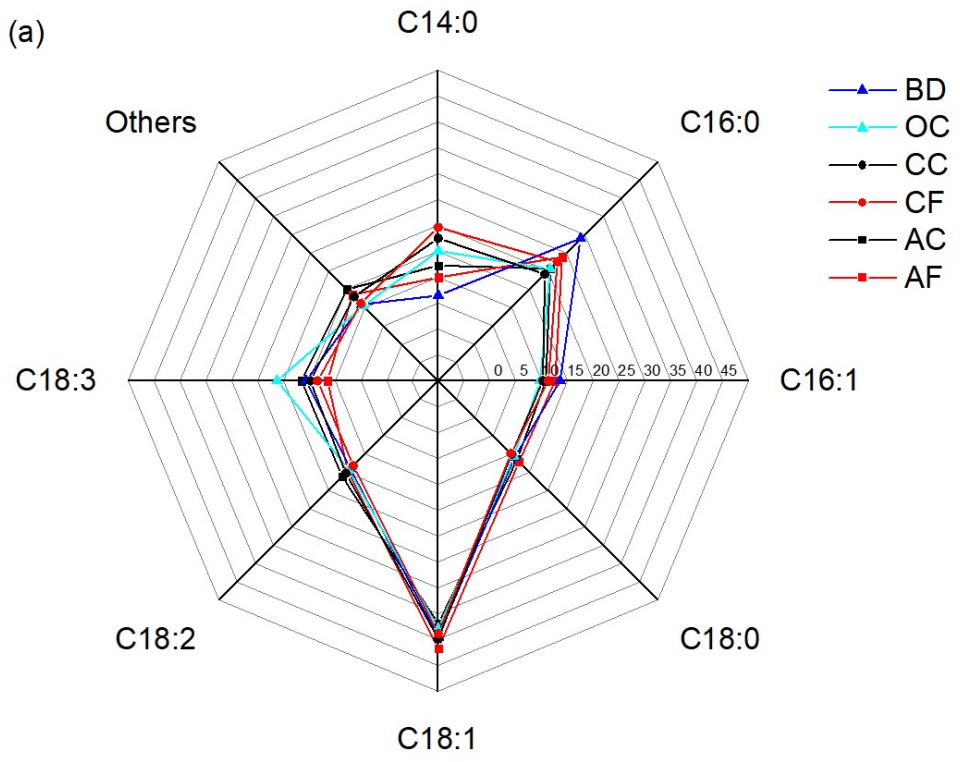
(a)
C14:0
C16:0
C16:1
C18:0
C18:1
C18:2
C18:3
Others
0 5 10 15 20 25 30 35 40 45
BD
OC
CC
CF
AC
AF

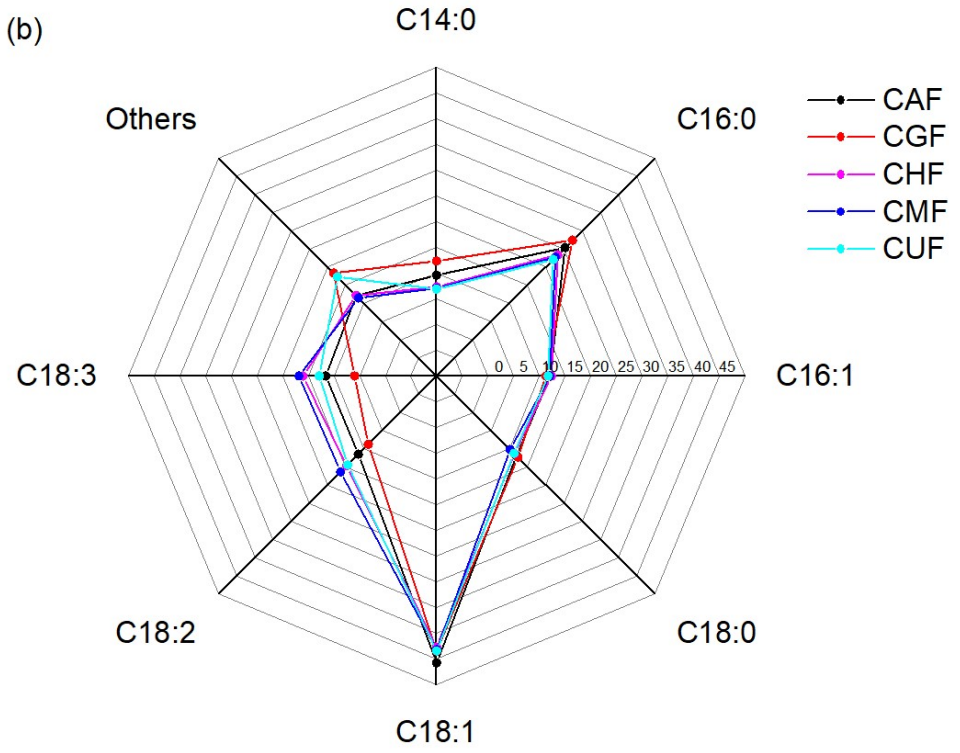
(b)
C14:0
C16:0
C16:1
C18:0
C18:1
C18:2
C18:3
Others
0 5 10 15 20 25 30 35 40 45
CAF
CGF
CHF
CMF
CUF

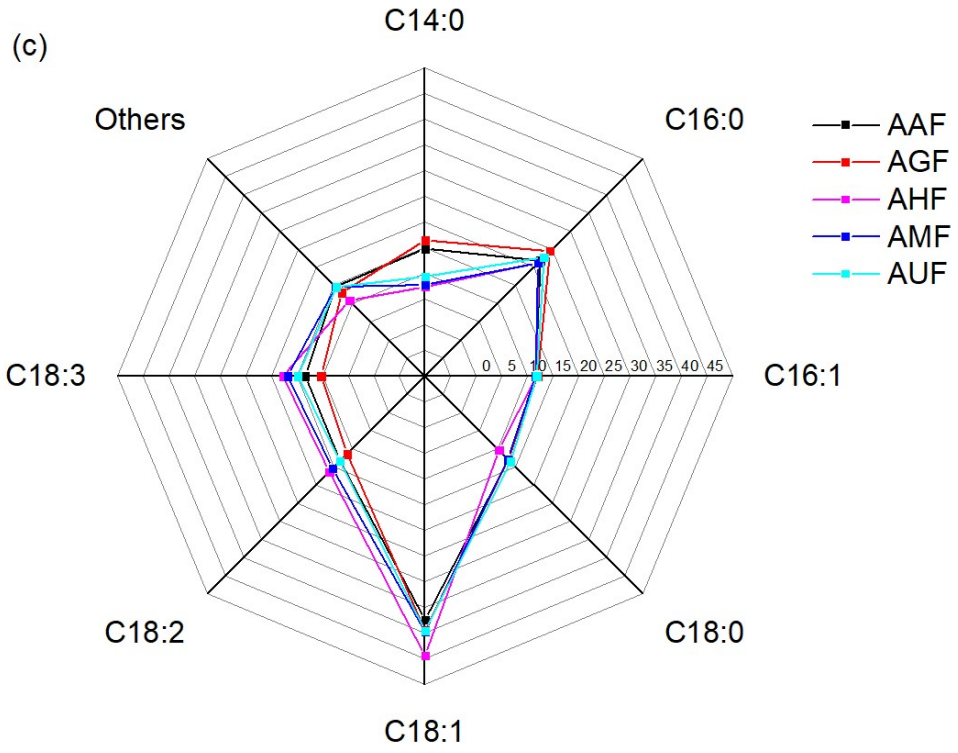

Figure 7.3 FAMEs profile (%) of biodiesel under different treatments, (a) without cell disruptions, (b) Chitosaon flocculation + cell disruptions, (c) $AlCl_3$ + cell disruptions.

7.3.3 Effect of cell disruption on microalgae samples

7.3.3.1 Cell morphology

Microalgae cell morphology (floc) before and after cell disruption treatments was examined by microscope (Picture 7.1). The Picture 1a and 1g were the formed flocs by chitosan and $AlCl_3$ respectively without cell disruption. Compared with the two pictures, it's founded that acidification (b and h) disintegrated the flocs, and dispersed cells as reported by *Chantrasakdakul*[41] and *Lorente*[42]. Especially for the floc by chitosan, it was almost separated into individual cell. Ultrasonic treatment also slightly disintegrated the floc formed by in $AlCl_3$ the Picture 1l. But for the rest, no such disintegration was observed, they had the similar morphology as the control. Totally disrupted cell can prove cell disruption action intuitively. However, in this case, microalgal cells maintained their intact unity with less difference from the controls, except few shriveled amorphous substances having low contrast appearance were observed in heating, microwave or ultrasonic treated samples, which were cell debris and intracellular materials [42][43]. The results shown the microalgae of *Tetradesmus obliquus* was highly resistant to the cell disruptions. Yet lipid extraction efficiency was heavily improved by heating, microwave and ultrasonic as described in 3.2, which could be attributed to the three treatments increasing the permeability of the cell wall due to thinner cell wall and larger pore size in it.

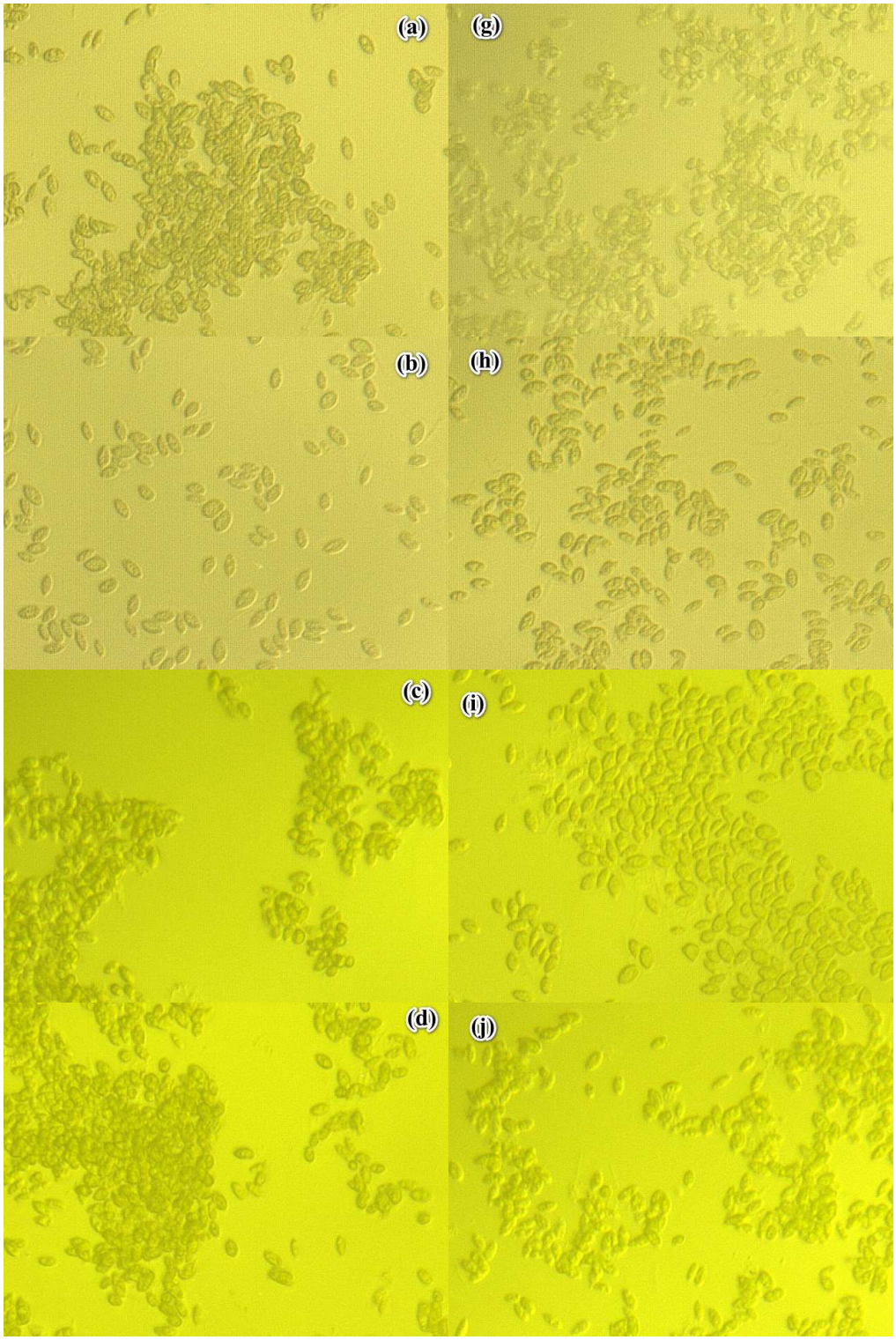
(a)
(g)
(b)
(h)
(c)
(i)
(d)
(j)

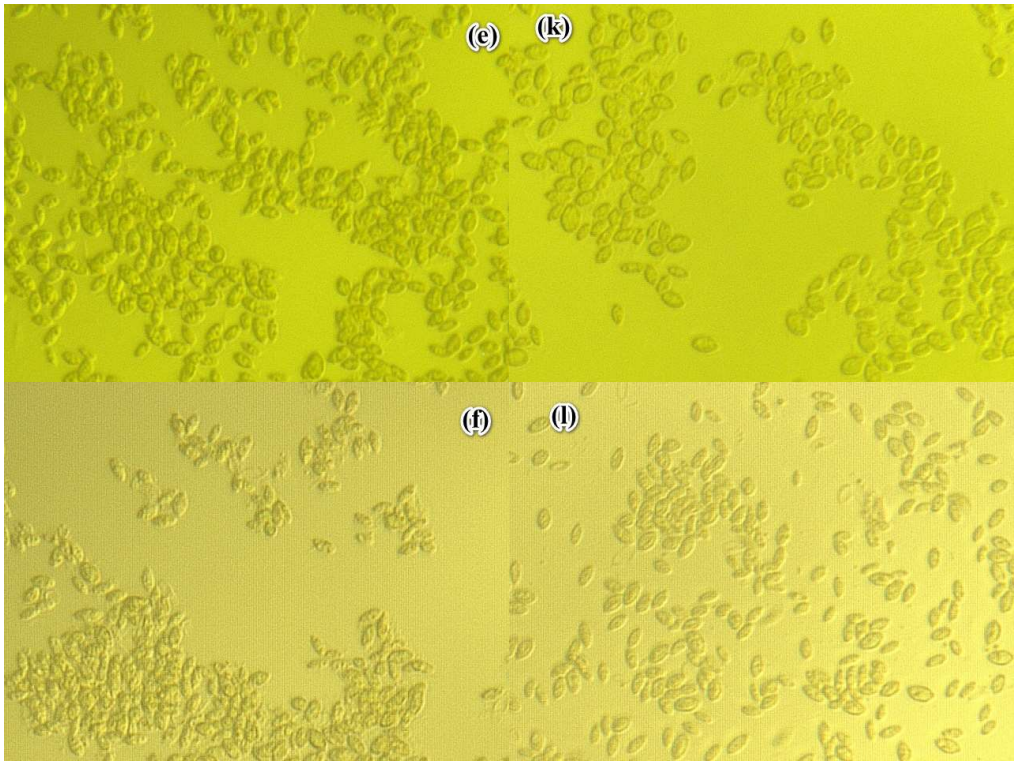

Picture 7.1 Microscope images of flocculated microalgae, (a) ~ (f): flocculated by Chitosan, (g) ~ (l): flocculated by $AlCl_3$; (a)(g) nontreatment, (b)(h) acidification, (c)(i) heating, (d)(j) homogenization, (e)(k) microwave, (f)(l) ultrasonic.

7.3.3.2 Analysis of particle size

The Figure 7.4 showed the particle size distribution (PSD) of microalgae floc before and after cell disruption. For the two untreated samples, bimodal distribution of 1 ~ 10 μm and 10 ~ 100 μm indicated individual and aggregated cells respectively. With acidification, monomodal distribution at peak of 5.5 μm for floc by chitosan, and increasing the peak of 1~10μm with decreasing the peak of 10 ~ 100 μm, indicated flocs were disintegrated, which was coincided with microscope images. After heating, microwave or ultrasonic treatments, particles distributed in larger size were observed, because some of substances (polysaccharides, proteins, salts, lipids, debris etc.) released from the disrupted cells may adsorb at surface of other cells to make the larger floc [44][45]. Compared with controls, the peak (particle size < 1 μm, ~2%) representing cell debris was not increased after cell disruption treatments, which confirmed the most microalgal cells remained structurally intact after the treatments.

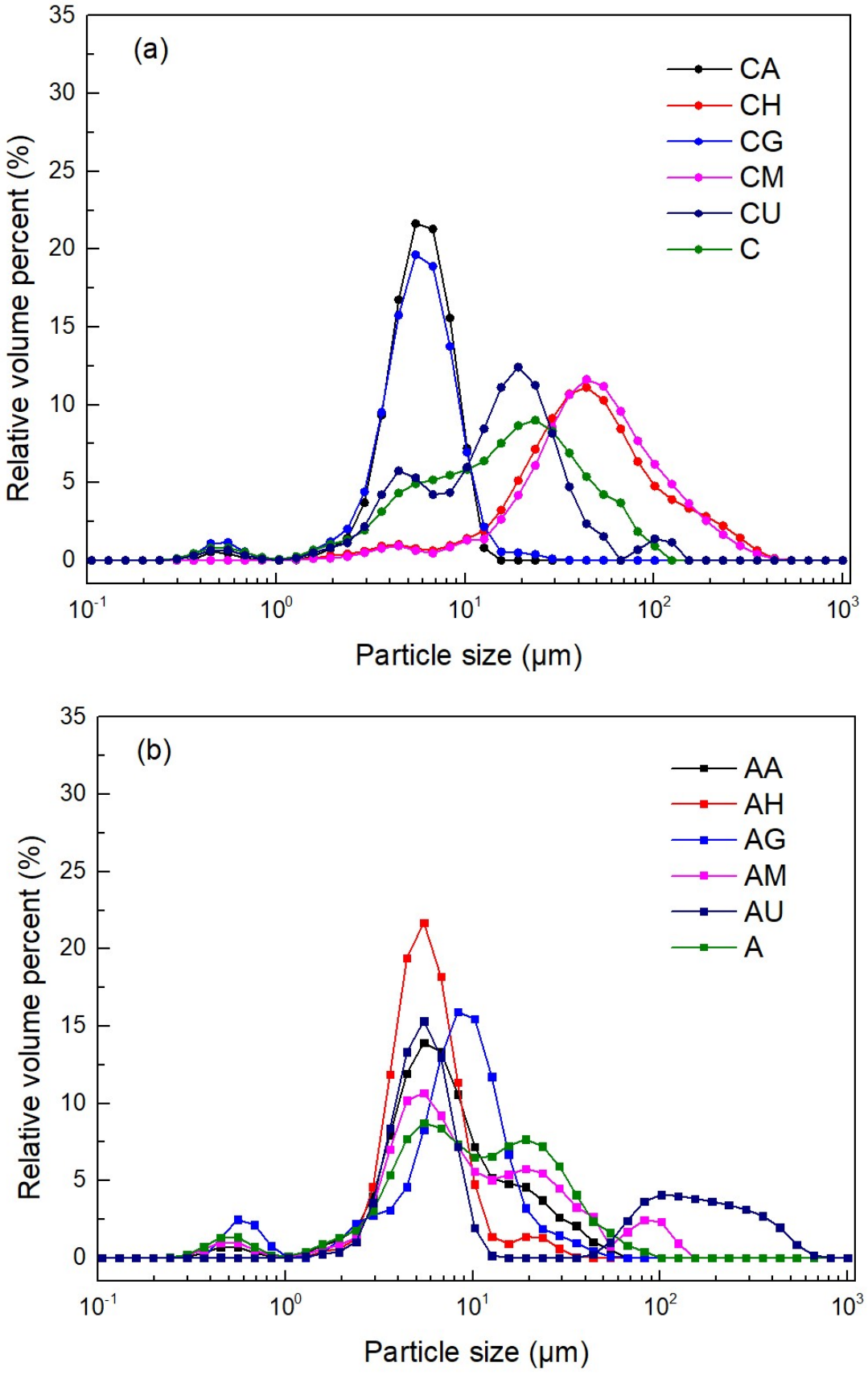

Figure 7.4 Paticle size distribution of floc by (a) Chitosan, (b) $AlCl_3$ before and after cell disruption.

7.3.3.3 Effect on component of the filtrate

Further, 3D-EEM fluorescence spectroscopy was used to probe changes of dissolved organic matter (DOM) in the filtrate of microalgae before and after cell disruption. As shown in the Figure 7.5, by comparing with controls (a, g), the two peaks were observed in the filtrates with cell disruption. The Peak A at excitation/emission (Ex/Em) of 280/350 nm was located in the soluble microbial by-product-like region, predominately the protein-derived amino acid tryptophan [46][47]. The peak B (Ex/Em of 220~225/350 nm) was located in the aromatic protein region [46]. The fluorescent intensity of the two peaks in heating, microwave and ultrasonic treated samples were very strong (peak A of 560~1011 AU, peak B of 542~997 AU), while in the samples by acidification and homogenization the intensity was relatively weak (peak A of 65~116 AU, peak B of 100~163 AU) closed to the controls (peak A of 93~100 AU, peak B of 99~ 144 AU). The results revealed the change of cell wall's permeability, and huge amount of intracellular substances entered into liquid phase by heating, microwave and ultrasonic treatment rather than other two. It was coincided with the results from morphology and PSD analysis. Besides, it should be noticed that the Peak B in chitosan flocculation + ultrasonic treated samples (l) had a 10 nm red shift in the emission wavelength, which could be relative to an increase of carbonyl, hydroxyl, alkoxyl, amino and carboxyl groups in the aromatic protein chain [48].

7.3.3.4 Change of free and bound water in the microalgae

The dewatering performance of the DME method was evaluated by changing of water content, among which the free water content was measured by DSC. Firstly, the water heat of fusion (ΔH) of pure water in this study was calculated as -339.3 J/g (Figure S9), the free and bound water in the microalgae samples could be calculated by Eq. (7.3-7.4) [49],

$$W_f = \frac{\mathrm{Q}}{\Delta H} \qquad (7.3)$$

$$W_b = W_t - W_f \qquad (7.4)$$

where Q is the heat absorbed in melting process, W_f and W_b is the free and bound water content respectively.

Similar to the results discussed in the 7.3.1, the water content of samples reduced from 63.8~70.2 % to 41.6~61.2 % after DME method extraction in the Table 7.2, and no evidence of cell disruption improving the dewatering was observed. In addition, the reduction of water could be completely attributed to a removal of free water rather than bound water. Before extraction, free water (44.6~53.6 %) accounted for a larger proportion with a free/bound ratio of 2.33~3.33. After extraction, free water in OC or chitosan used samples were reduced to 0, and for $AlCl_3$ used samples the free water content reduced to 4.5~11.6 % with the free/bound ratio of 0.09~0.32.

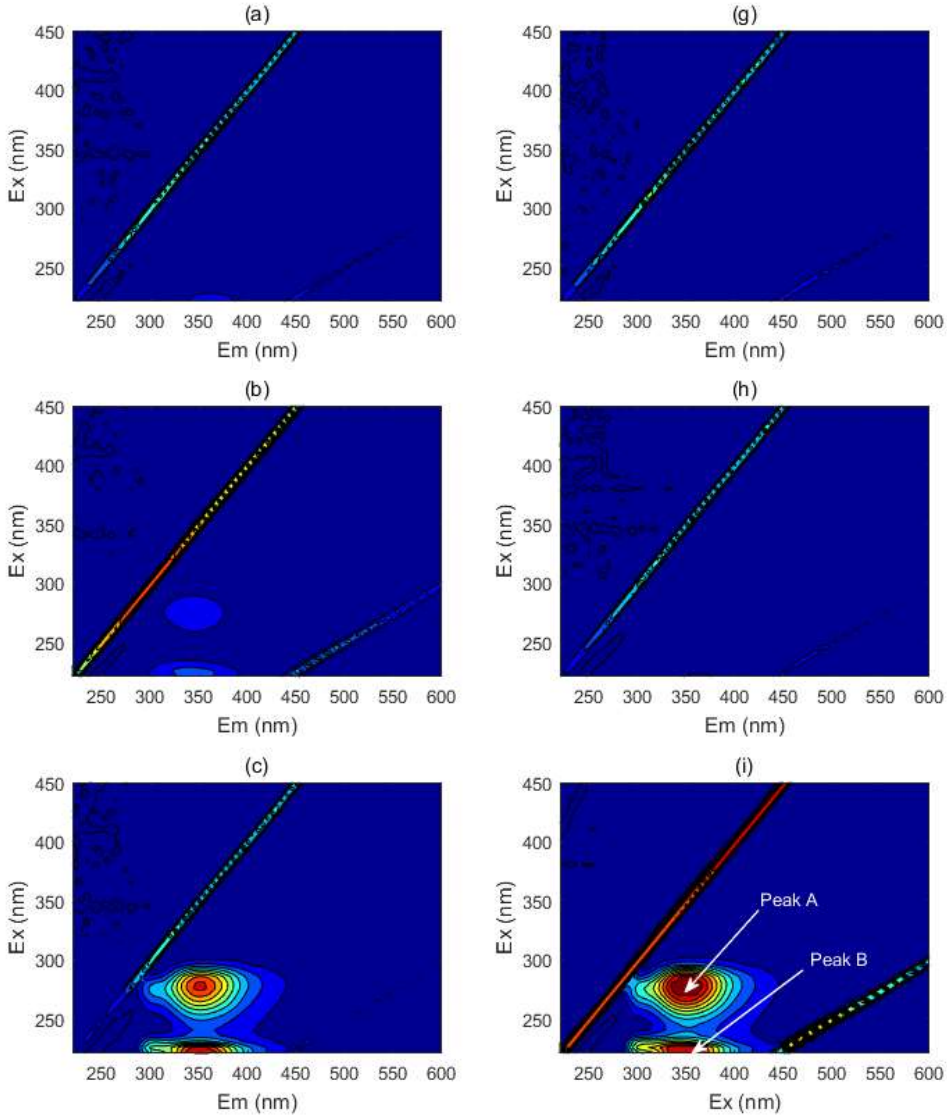
(a)
(g)
(b)
(h)
(c)
(i)
Ex (nm)
Em (nm)
250 300 350 400 450 500 550 600
Peak A
Peak B

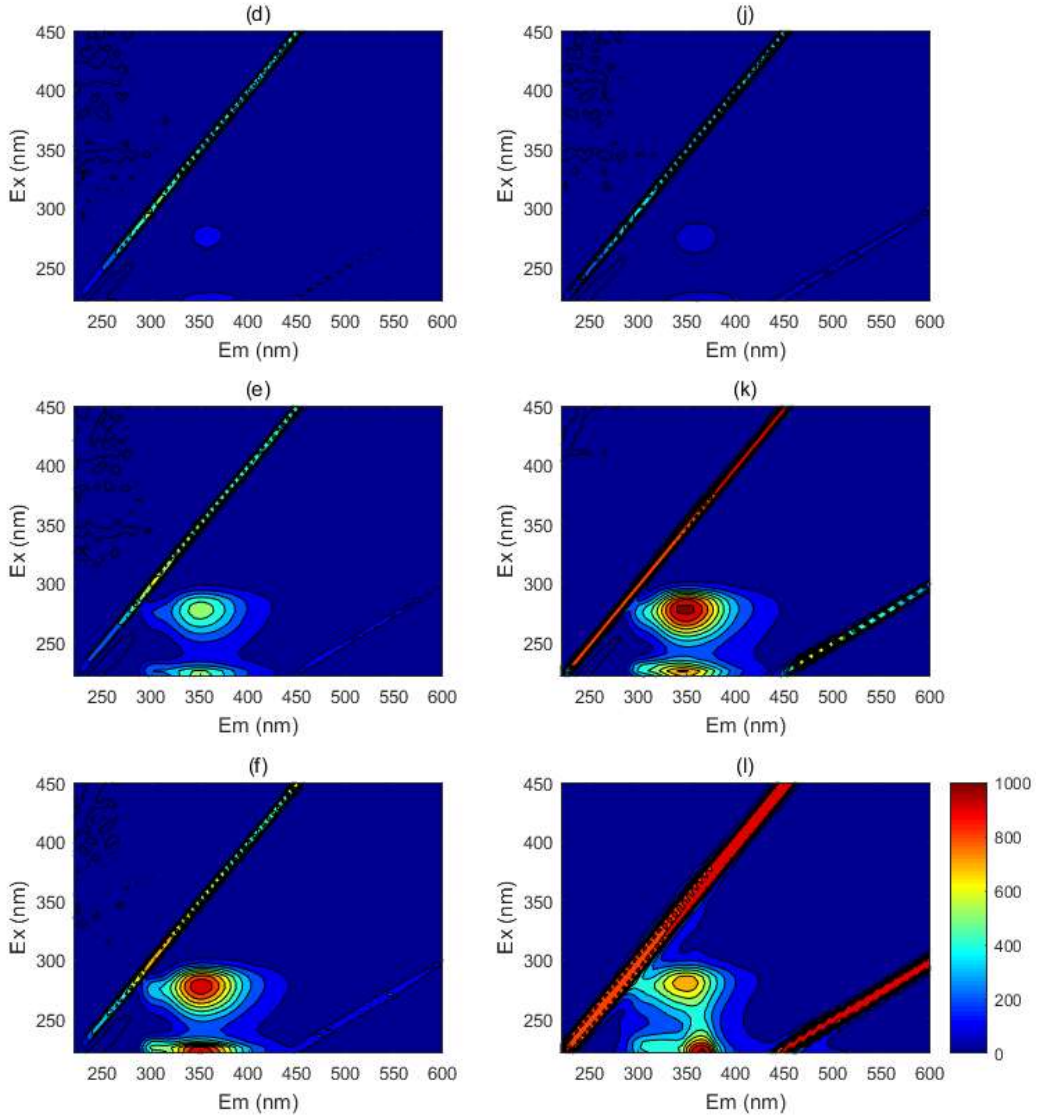

Figure 7.5 3D-EEM of microalgae filtrate, (a) ~ (f): flocculated by Chitosan, (g) ~ (l): flocculated by $AlCl_3$; (a)(g) nontreatment, (b)(h) acidification, (c)(i) heating, (d)(j) homogenization, (e)(k) microwave, (f)(l) ultrasonic.

Table 7.2 Free and bound water in microalgae before and after DME method extraction.

	Before				After			
	Total water content (%)	Free water content (%)	Bound water content (%)	Ratio of Free/Bound	Total water content (%)	Free water content (%)	Bound water content (%)	Ratio of Free/Bound
OC	70.2±0.5	52.1±0.2	18.2±0.9	2.86	54.6±2.3	0.0±0.0	54.6±2.3	0
AF	69.0±0.3	49.0±0.5	20.0±0.4	2.44	47.8±3.7	7.0±0.1	40.8±3.9	0.17
AAF	67.2±0.3	50.8±0.4	16.4±0.4	3.13	47.9±3.0	10.1±0.4	37.8±3.1	0.27
AHF	64.5±0.6	44.9±0.1	19.5±0.9	2.33	57.9±2.2	7.6±0.2	50.3±2.5	0.15
AGF	68.4±0.4	52.8±0.8	15.6±0.7	3.33	48.3±2.2	11.6±0.4	36.7±2.5	0.32
AMF	64.9±0.3	47.6±0.3	17.3±0.4	2.78	61.2±1.2	10.5±0.1	50.7±1.3	0.21
AUF	63.8±0.3	46.6±0.1	17.3±0.6	2.70	52.5±1.1	4.5±0.1	48.0±1.2	0.09
CF	70.0±0.1	53.6±0.0	16.4±0.6	3.23	48.1±0.5	0.0±0.0	48.1±0.5	0
CAF	64.7±0.7	47.8±0.5	16.9±0.4	2.86	41.6±4.1	0.0±0.0	41.6±4.1	0
CHF	67.0±1.1	46.7±0.1	20.2±1.4	2.33	53.5±2.8	0.0±0.0	53.5±2.8	0
CGF	69.1±0.7	50.9±0.4	18.1±0.4	2.78	42.7±0.8	0.0±0.0	42.7±0.8	0
CMF	67.0±0.8	47.1±0.1	19.8±0.7	2.38	48.8±1.9	0.0±0.0	48.8±1.9	0
CUF	63.9±0.4	44.6±0.4	19.3±0.9	2.33	57.9±2.3	0.0±0.0	57.9±2.3	0

7.3.3.5 Scanning electron microscope (SEM) analysis

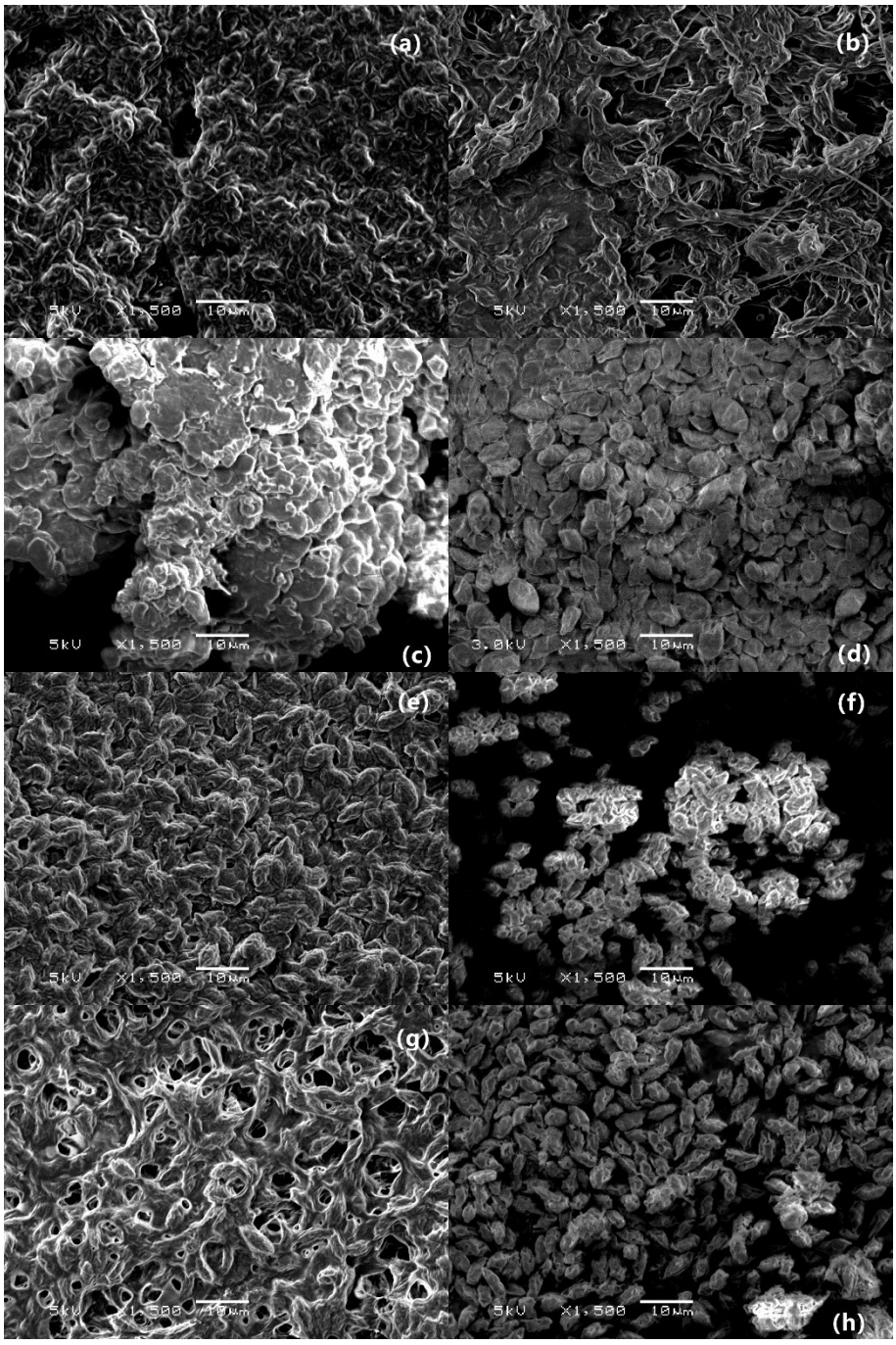

Picture 7.2 SEM images of microalgae cells before and after DME method extraction, (a) AF, (b) CF, (c) AFD, (d) CFD, (e) AHF, (f) AHFD, (g) CHF and (h) CHFD

The microalgae cells before and after DME method extraction were observed as shown in the Picture 7.2. The $AlCl_3$ flocculated microalgae without cell disruption (Picture 7.2.a) appeared to be highly clustered with ellipsoid but slightly wrinkled surface, while the surface of chitosan flocculated microalgae cells was covered and connected by numerous filaments (Picture 7.2.b). After DME method, the cells in the two samples were still to be plump, but the filaments on cell surface was disappeared, which demonstrated the DME extracted the extracellular substance rather than intracellular

substance from the samples without successful cell disruption. Picture 7.2 (e-h) showed the two examples of successful cell disruption. The (e) and (g) were heating treated samples followed by $AlCl_3$ and chitosan flocculation respectively, the AHF showed the similar appearance to the AF (a), and cells of CHF also covered by the numerous extracellular substances as CF (b). After the extraction, both of the cells became shriveled and shrink with more folds on surface, which indicated the intracellular substance had been extracted by DME. Besides, DME did not cause the cell to break into debris and they remained largely intact, which was consistent the study by *Kanda* [29].

7.3.3.6 Thermogravimetric analysis, C/H/N/S/O and heating value of the residuals

Thermogravimetric analysis (Figure 7.6) revealed the weight loss (~8%) of first stage between temperature of 30 °C~125 °C with endothermic peak at ~70 °C for the samples with various treatments, which were due to the removal of adsorbed water from the surface of the residuals [35]. And the second weight loss stage occurred during temperature of 250 °C ~ 375 °C with exothermic DTA peak at ~310 °C. For all these cells successfully disrupted samples (CUFD, AUFD, CMFD, AMFD, CHFD and AGFD), weight loss (~65%) in this stage were higher than others (~50%), which confirmed by sharper corresponding peaks in DTG. In addition, the rest of weight lost in the final stage from 375 °C to 600°C with exothermic DTA peak. Compared with the cells successfully disrupted samples, these residuals containing high lipid content showed more significant DTA peak in the third stage. The 2nd and 3rd stage related to degradation of carbon chains, lipids decomposed and completely oxidation of the carbonaceous residues [50][51]. The results indicated that after lipid was extracted, the combustion characteristic of the residuals was changed, and combustion stability reduced without lipids.

The Table 7.3 showed the elements composition of the residuals. Mainly, lower C (43.5%~47.6%) and H (7.6~8.1%) content in residuals with successfully cell disruption was observed by comparing with others (51.9~5.4% of C and 8.7~9.1% of H) due to the complete extraction of raw lipids. In addition, N with O content in the lipid well extracted samples increased. These elements composition data can be used to evaluate heating value as reported [53][54][55]. In this study, the following equations with highest R^2 was chosen from the reports to calculate the heating value.

$$LHV_{dry} = 0.2575N + 0.4188C + 0.001835H - 2.1594S - 0.05817O \text{ [55]} \quad (7.5)$$

$$NHV_{wet} = LHV_{dry} \times (100 - W)/100 - 2.44 \times \mathrm{W}/100 \quad (7.6)$$

Where LHV_{dry} is the lower heating value (MJ/kg) on dry base, C, H, N, S and O are the Carbon, hydrogen, nitrogen, sulfur and oxygen contents (wt% on dry basis), respectively. W is the water content, NHV_{wet} is the net heating value (MJ/kg) on wet base.

The results indicated the lipid in the residuals affected LHV_{dry}, the samples with lipid well extracted had less LHV_{dry}. And the net heating value ranged from 4.9~11.6 MJ/kg, which were highly determined by water content. Since the NHV_{wet} of all samples from DME method were higher than 4 MJ/kg, they were sufficient to be solid fuel for autarkic combustion [56].

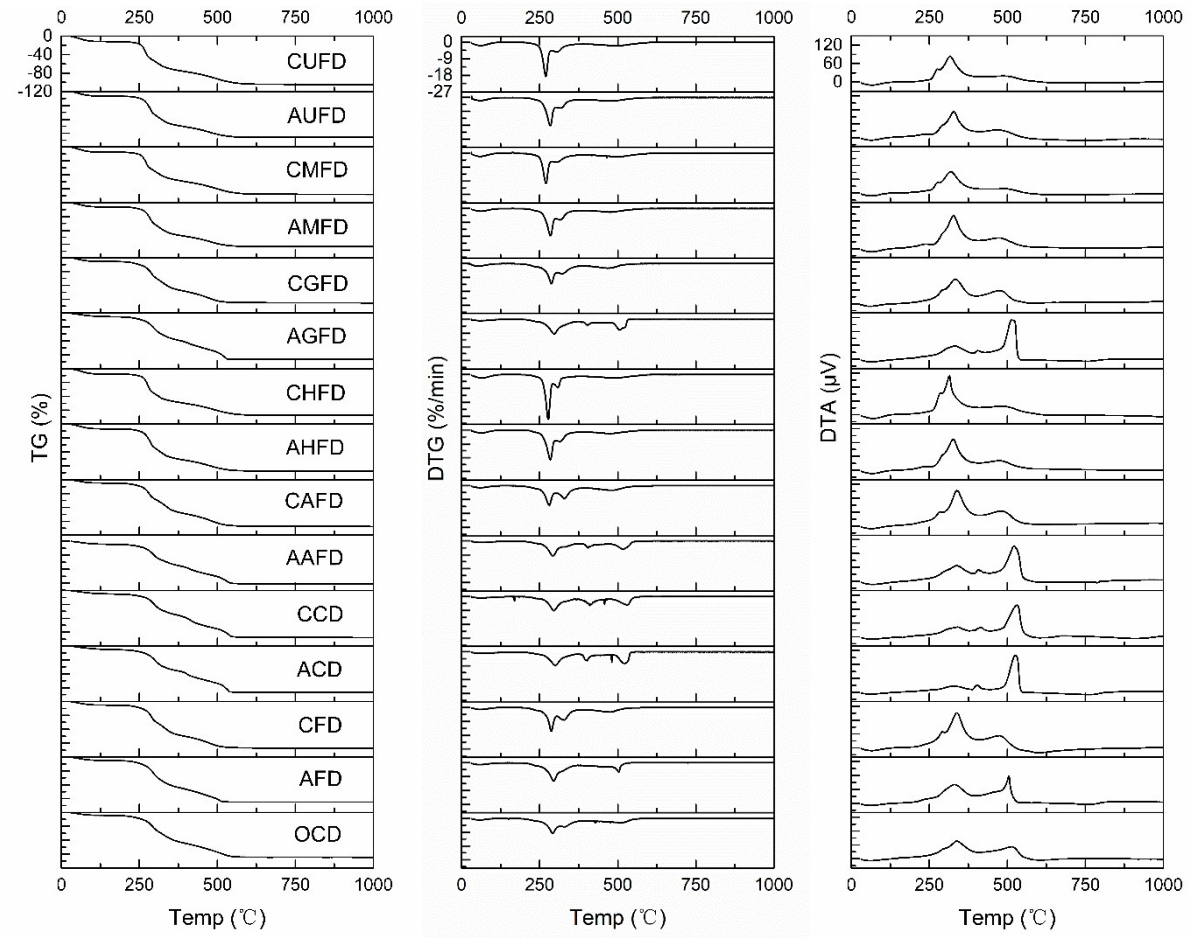

Figure 7.6 The TG/DTA curves of the residuals with different treatments.

Table 7.3 C/H/N/S/O composition with heating value calculation.

	C/H/N/S/O composition				Heating value (MJ/Kg)	
	H (%)	C (%)	N (%)	O (%)	LHV (D.B)	NHV (W.B)
OCD	9.0±0.0	53.0±0.5	2.4±0.0	35.6±0.5	19.7	7.6
ACD	9.0±0.2	52.4±0.8	2.3±0.0	36.2±1.0	19.4	4.9
AFD	8.7±0.2	51.6±0.7	2.3±0.0	37.4±0.8	19.0	8.7
AAFD	9.1±0.0	53.4±0.2	2.4±0.0	35.1±0.3	19.9	9.2
AHFD	7.9±0.1	46.0±0.7	2.8±0.1	43.3±0.8	16.4	5.5
AGFD	9.0±0.2	53.4±0.7	2.5±0.0	35.1±0.9	19.9	9.1
AMFD	8.1±0.1	47.6±0.2	2.8±0.0	41.4±0.3	17.2	5.2
AUFD	8.0±0.2	46.3±0.4	3.0±0.1	42.7±0.5	16.6	6.6
CCD	9.0±0.0	53.0±0.5	2.4±0.0	35.6±0.5	19.7	7.6
CFD	8.7±0.3	51.9±1.9	2.3±0.1	37.0±2.2	19.1	8.7
CAFD	9.1±0.1	53.3±0.7	2.6±0.0	35.0±0.7	19.9	10.6
CHFD	7.6±0.0	43.5±0.2	3.3±0.0	45.7±0.3	15.3	5.8
CGFD	8.8±0.4	53.6±2.0	2.5±0.1	35.1±2.5	20.0	10.4
CMFD	7.6±0.0	44.5±0.4	3.2±0.1	44.6±0.5	15.8	6.9
CUFD	7.9±0.0	44.7±0.0	3.5±0.0	43.9±0.0	16.0	5.3

7.4. conclusion

Initial moisture content in microalgae and cell disruption treatment were identified as two major factors for lipid extraction from *Tetradesmus obliquus* by DME method. According the results, initial moisture content below 75% was suitable for achieving an ideal raw lipid yield of >80% with a relatively high solid content of residual (> 40%). Yet just reducing moisture content was not enough, and suitable cell disruption treatment was necessary. Among five cell disruptions, extraction efficiency was heavily enhanced by heating, microwave or ultrasonic treatment with raw lipid content of 216.5 ~ 293.9 mg/g and FAMEs content of 69.9~91.0 mg/g. Both cells harvesting and disruptions had no influence on profile of the extracted FAMEs, and C14:0, C16:0, C16:1, C18:0, C18:1, C18:2 and C18:3 were mainly components. According to the optical microscope with PSD analysis, microalgae cell kept intact after all cell disruptions, but 3D-EEM showed huge amount of intracellular substances entered into liquid phase by heating, microwave and ultrasonic treatments, which demonstrated successful improvement of extraction by the three cell disruptions worked because of increasing cell wall's permeability rather than completely disrupting cells. In addition, DSC confirmed the reduction of water in residuals could be completely attributed to a removal of free water rather than bound water. After the extraction, SEM showed the cells (by heating, microwave and ultrasonic treatments) became shriveled and shrink with more folds on surface, which indicated the intracellular substance had been extracted by DME. But, DME did not cause the cell to break into debris and they remained largely intact. The TG/DTA indicated that after the lipid was completely extracted, combustion stability of residuals reduced. Besides, heating value calculation based on C/H/N/S/O analysis concluded these residuals were sufficient to be used as

solid fuel.

Reference

[1] Sun, Z., & Zhou, Z. (2019). Nature-inspired virus-assisted algal cell disruption for cost-effective biofuel production. Applied Energy, 251, 113330.

[2] Goh, B. H. H., Ong, H. C., Cheah, M. Y., Chen, W. H., Yu, K. L., & Mahlia, T. M. I. (2019). Sustainability of direct biodiesel synthesis from microalgae biomass: A critical review. Renewable and Sustainable Energy Reviews, 107, 59-74.

[3] Chen, H., Zhou, D., Luo, G., Zhang, S., & Chen, J. (2015). Macroalgae for biofuels production: Progress and perspectives. Renewable and Sustainable Energy Reviews, 47, 427-437.

[4] Arif, M., Bai, Y., Usman, M., Jalalah, M., Harraz, F. A., Al-Assiri, M. S., ... & Zhang, C. (2020). Highest accumulated microalgal lipids (polar and non-polar) for biodiesel production with advanced wastewater treatment: Role of lipidomics. Bioresource technology, 298, 122299.

[5] Ding, W., Jin, W., Zhou, X., Li, S. F., Tu, R., Han, S. F., ... & Huang, Y. (2020). Enhanced lipid extraction from the biodiesel-producing microalga Chlorella pyrenoidosa cultivated in municipal wastewater via Daphnia ingestion and digestion. Bioresource Technology, 123162.

[6] Chen, H., Wang, J., Zheng, Y., Zhan, J., He, C., & Wang, Q. (2018). Algal biofuel production coupled bioremediation of biomass power plant wastes based on Chlorella sp. C2 cultivation. Applied Energy, 211, 296-305.

[7] Menegazzo, M. L., & Fonseca, G. G. (2019). Biomass recovery and lipid extraction processes for microalgae biofuels production: a review. Renewable and Sustainable Energy Reviews, 107, 87-107.

[8] Bligh, E. G., & Dyer, W. J. (1959). A rapid method of total lipid extraction and purification. Canadian journal of biochemistry and physiology, 37(8), 911-917.

[9] Soxhlet, F. (1879). Die gewichtsanalytische bestimmung des milchfettes. Polytechnisches J, 232, 461-465.

[10] Kanda, H., Hoshino, R., Murakami, K., Zheng, Q., & Goto, M. (2020). Lipid extraction from microalgae covered with biomineralized cell walls using liquefied dimethyl ether. Fuel, 262, 116590.

[11] Araujo, G. S., Matos, L. J., Fernandes, J. O., Cartaxo, S. J., Gonçalves, L. R., Fernandes, F. A., & Farias, W. R. (2013). Extraction of lipids from microalgae by ultrasound application: prospection of the optimal extraction method. Ultrasonics sonochemistry, 20(1), 95-98.

[12] Tanzi, C. D., Vian, M. A., & Chemat, F. (2013). New procedure for extraction of algal lipids from wet biomass: A green clean and scalable process. Bioresource technology, 134, 271-275.

[13] Olmstead, I. L., Kentish, S. E., Scales, P. J., & Martin, G. J. (2013). Low solvent, low temperature method for extracting biodiesel lipids from concentrated microalgal biomass. Bioresource technology, 148, 615-619.

[14] Kanda, H., Li, P., Yoshimura, T., & Okada, S. (2013). Wet extraction of hydrocarbons from Botryococcus braunii by dimethyl ether as compared with dry extraction by hexane. Fuel, 105, 535-539.

[15] Lakshmikandan, M., Murugesan, A. G., Wang, S., Abomohra, A. E. F., Jovita, P.

A., & Kiruthiga, S. (2020). Sustainable biomass production under CO_2 conditions and effective wet microalgae lipid extraction for biodiesel production. Journal of Cleaner Production, 247, 119398.
[16] Sánchez-Bayo, A., López-Chicharro, D., Morales, V., Espada, J. J., Puyol, D., Martínez, F., ... & Rodríguez, R. (2020). Biodiesel and biogas production from Isochrysis galbana using dry and wet lipid extraction: A biorefinery approach. Renewable Energy, 146, 188-195.
[17] Ansari, F. A., Gupta, S. K., Shriwastav, A., Guldhe, A., Rawat, I., & Bux, F. (2017). Evaluation of various solvent systems for lipid extraction from wet microalgal biomass and its effects on primary metabolites of lipid-extracted biomass. Environmental Science and Pollution Research, 24(18), 15299-15307.
[18] Bauer, M. C., & Kruse, A. (2019). The use of dimethyl ether as an organic extraction solvent for biomass applications in future biorefineries: A user-oriented review. Fuel, 254, 115703.
[19] Goto, M., Kanda, H., & Machmudah, S. (2015). Extraction of carotenoids and lipids from algae by supercritical CO_2 and subcritical dimethyl ether. The journal of supercritical Fluids, 96, 245-251.
[20] Wang, Q., Oshita, K., Nitta, T., & Takaoka, M. (2020). Evaluation of a sludge-treatment process comprising lipid extraction and drying using liquefied dimethyl ether. Environmental Technology, 1-10.
[21] Tallon, S., & Fenton, K. (2010). The solubility of water in mixtures of dimethyl ether and carbon dioxide. Fluid phase equilibria, 298(1), 60-66.
[22] Subratti, A., Lalgee, L. J., & Jalsa, N. K. (2018). Liquefied dimethyl ether (DME) as a green solvent in chemical reactions: Synthesis of O-alkyl trichloroacetimidates. Sustainable Chemistry and Pharmacy, 9, 46-50.
[23] Varlet, V., Smith, F., & Augsburger, M. (2014). New trends in the kitchen: Propellants assessment of edible food aerosol sprays used on food. Food chemistry, 142, 311-317.
[24] Naito, M., Radcliffe, C., Wada, Y., Hoshino, T., Liu, X., Arai, M., & Tamura, M. (2005). A comparative study on the autoxidation of dimethyl ether (DME) comparison with diethyl ether (DEE) and diisopropyl ether (DIPE). Journal of loss prevention in the process industries, 18(4-6), 469-473.
[25] Nagappan, S., Devendran, S., Tsai, P. C., Dinakaran, S., Dahms, H. U., & Ponnusamy, V. K. (2019). Passive cell disruption lipid extraction methods of microalgae for biofuel production–a review. Fuel, 252, 699-709.
[26] Lee, A. K., Lewis, D. M., & Ashman, P. J. (2012). Disruption of microalgal cells for the extraction of lipids for biofuels: processes and specific energy requirements. Biomass and bioenergy, 46, 89-101.
[27] Goh, B. H. H., Ong, H. C., Cheah, M. Y., Chen, W. H., Yu, K. L., & Mahlia, T. M. I. (2019). Sustainability of direct biodiesel synthesis from microalgae biomass: A critical review. Renewable and Sustainable Energy Reviews, 107, 59-74.
[28] Zhang, H., Yang, J., Yu, W., Luo, S., Peng, L., Shen, X., ... & Li, Y. (2014). Mechanism of red mud combined with Fenton's reagent in sewage sludge conditioning. Water research, 59, 239-247.

[29] Huang, Y. F., & Lo, S. L. (2020). Predicting heating value of lignocellulosic biomass based on elemental analysis. Energy, 191, 116501.
[30] Orr, V. C., Plechkova, N. V., Seddon, K. R., & Rehmann, L. (2016). Disruption and wet extraction of the microalgae Chlorella vulgaris using room-temperature ionic liquids. ACS Sustainable Chemistry & Engineering, 4(2), 591-600.
[31] Feng, W., Xiong, H., Wang, W., Duan, X., Yang, T., Wu, C., ... & Wang, C. (2019). Energy consumption analysis of lipid extraction from black soldier fly biomass. Energy, 185, 1076-1085.
[32] Mouahid, A., Crampon, C., Toudji, S. A. A., & Badens, E. (2016). Effects of high water content and drying pre-treatment on supercritical CO_2 extraction from Dunaliella salina microalgae: experiments and modelling. The Journal of Supercritical Fluids, 116, 271-280.
[33] Sun, Y., Xu, C., Igou, T., Liu, P., Hu, Z., Van Ginkel, S. W., & Chen, Y. (2018). Effect of water content on [Bmim][HSO_4] assisted in-situ transesterification of wet Nannochloropsis oceanica. Applied energy, 226, 461-468.
[34] Barz, M. (2009). Sewage sludge from wastewater treatment as energy source. Journal of Renewable Energy and Smart Grid Technology, 4(1), 1-12.
[35] Spiden, E. M., Scales, P. J., Yap, B. H., Kentish, S. E., Hill, D. R., & Martin, G. J. (2015). The effects of acidic and thermal pretreatment on the mechanical rupture of two industrially relevant microalgae: Chlorella sp. and Navicula sp. Algal Research, 7, 5-10.
[36] Lee, S. Y., Cho, J. M., Chang, Y. K., & Oh, Y. K. (2017). Cell disruption and lipid extraction for microalgal biorefineries: A review. Bioresource technology, 244, 1317-1328.
[37] Günerken, E., D'Hondt, E., Eppink, M. H. M., Garcia-Gonzalez, L., Elst, K., & Wijffels, R. H. (2015). Cell disruption for microalgae biorefineries. Biotechnology advances, 33(2), 243-260.
[38] Esakkimuthu, S., Krishnamurthy, V., Wang, S., Hu, X., Swaminathan, K., & Abomohra, A. E. F. (2020). Application of p-coumaric acid for extraordinary lipid production in Tetradesmus obliquus: A sustainable approach towards enhanced biodiesel production. Renewable Energy.
[39] Islami, H. R., & Assareh, R. (2019). Effect of different iron concentrations on growth, lipid accumulation, and fatty acid profile for biodiesel production from Tetradesmus obliquus. Journal of Applied Phycology, 31(6), 3421-3432.
[40] Md Nadzir, S., Yusof, N., Nordin, N., Abdullah, H., & Kamari, A. (2019). Optimisation of carbohydrate, lipid and biomass productivity in Tetradesmus obliquus using response surface methodology. Biofuels, 1-10.
[41] Chantrasakdakul, P., Lee, K., Kim, D., Kim, S. J., & Park, K. Y. (2015). Enhancement of biogas production from anaerobic digestion of Chlorella vulgaris biomass with ultrasonic pretreatment. Sustainable Environment Research, 25(1).
[42] Lorente, E., Hapońska, M., Clavero, E., Torras, C., & Salvadó, J. (2018). Steam explosion and vibrating membrane filtration to improve the processing cost of microalgae cell disruption and fractionation. Processes, 6(4), 28.
[43] Duan, Z., Tan, X., Guo, J., Kahehu, C. W., Yang, H., Zheng, X., & Zhu, F. (2017).

Effects of biological and physical properties of microalgae on disruption induced by a low-frequency ultrasound. Journal of Applied Phycology, 29(6), 2937-2946.
[44] Rivera, E. C., Montalescot, V., Viau, M., Drouin, D., Bourseau, P., Frappart, M., ... & Couallier, E. (2018). Mechanical cell disruption of Parachlorella kessleri microalgae: Impact on lipid fraction composition. Bioresource technology, 256, 77-85.
[45] Spiden, E. M., Yap, B. H., Hill, D. R., Kentish, S. E., Scales, P. J., & Martin, G. J. (2013). Quantitative evaluation of the ease of rupture of industrially promising microalgae by high pressure homogenization. Bioresource Technology, 140, 165-171.
[46] Chen, W., Westerhoff, P., Leenheer, J. A., & Booksh, K. (2003). Fluorescence excitation− emission matrix regional integration to quantify spectra for dissolved organic matter. Environmental science & technology, 37(24), 5701-5710.
[47] Zhou, D., Zhang, C., Fu, L., Xu, L., Cui, X., Li, Q., & Crittenden, J. C. (2017). Responses of the microalga Chlorophyta sp. to bacterial quorum sensing molecules (N-acylhomoserine lactones): aromatic protein-induced self-aggregation. Environmental Science & Technology, 51(6), 3490-3498.
[48] Chen, J., Gu, B., LeBoeuf, E. J., Pan, H., & Dai, S. (2002). Spectroscopic characterization of the structural and functional properties of natural organic matter fractions. Chemosphere, 48(1), 59-68.
[49] He, D. Q., Zhang, Y. J., He, C. S., & Yu, H. Q. (2017). Changing profiles of bound water content and distribution in the activated sludge treatment by NaCl addition and pH modification. Chemosphere, 186, 702-708.
[50] Kundu, S. K., & Bhaumik, A. (2015). A triazine-based porous organic polymer: a novel heterogeneous basic organocatalyst for facile one-pot synthesis of 2-amino-4 H-chromenes. RSC Advances, 5(41), 32730-32739.
[51] Dos Santos Politi, J. R., de Matos, P. R. R., & Sales, M. J. A. (2013). Comparative study of the oxidative and thermal stability of vegetable oils to be used as lubricant bases. Journal of thermal analysis and calorimetry, 111(2), 1437-1442.
[52] Raba, D. N., Chambre, D. R., Copolovici, D. M., Moldovan, C., & Copolovici, L. O. (2018). The influence of high-temperature heating on composition and thermo-oxidative stability of the oil extracted from Arabica coffee beans. PloS one, 13(7).
[53] Huang, Y. F., & Lo, S. L. (2020). Predicting heating value of lignocellulosic biomass based on elemental analysis. Energy, 191, 116501.
[54] Awad, O. I., Mamat, R., Ibrahim, T. K., Hagos, F. Y., Noor, M. M., Yusri, I. M., & Leman, A. M. (2017). Calorific value enhancement of fusel oil by moisture removal and its effect on the performance and combustion of a spark ignition engine. Energy conversion and management, 137, 86-96.
[55] Ozyuguran, A., Akturk, A., & Yaman, S. (2018). Optimal use of condensed parameters of ultimate analysis to predict the calorific value of biomass. Fuel, 214, 640-646.

[56] Hartman, M., Svoboda, K., Pohořelý, M., & Trnka, O. (2005). Combustion of dried sewage sludge in a fluidized-bed reactor. Industrial & engineering chemistry research, 44(10), 3432-3441.

Chapter 8 Conclusion and future perspective

8.1 conclusion

The energy consumption has gradually increased, and leads to fossil fuel depletion, greenhouse gas emission, ecological deterioration and environmental pollution. Biofuels production from microalgae is a promising technique to solve this problem, due to the high lipid content in microalgae and no competing with food supply. In this study, for evaluating biofuels production efficiency of different species, several microalgae were screened by LCA with less consumption during microalgae harvesting. With clarifying the mechanism of flocculation by RSM, combination of flocculants was demonstrated to minimize dosage requirement. Then the method to optimize flocculation condition was illustrated. As for the lipid extraction, we focused on DME method because of its low cost than conventional process. Since the lipid extraction from microalgae by DME was seldom studied, we started from sludge, and the obtained results compared and instructed the research on microalgae. Considering, the cost in dewatering process, a modified DME method, can work for liquid microalgae without dewatering, was developed. Besides, cell disruption treatment was proved to significantly enhance the lipid extraction effeceicey by the DME method. The main conclusions from each chapter are presented below.

Chapter 2 using flocculation tests demonstrated $AlCl_3$ can successfully flocculate most of microalgae species with FE value above 90% by adding 30 to 115 mg/L $AlCl_3$. Achieving a FE of 85~99%, less dosage of chitosan (7.5 ~ 150 mg/L) was required by compare with $AlCl_3$, but it has a poor performance for flocculating marine species. Only marine species can be flocculated by pH adjustment (NaOH), and flocculation occurred when pH exceeds ~10.0, since it was induced by precipitation of a lot of salt. The value FE by NaOH is similar to $AlCl_3$ and chitosan, but the dosage requirement of NaOH was much higher. ACPAM flocculated least microalgae (three species) with FE above 95%, and it can be considered as an alternative for microalgae flocculation. Besides the FE and optimal dosage, the settling time, CF and CST are important were measured. The shortest settle times were observed by using ACPAM (0.5~0.6 min) while flocculation by NaOH (13 ~ 40 min) were longest. CF were varied with species and flocculants with a highest value of ~50. Similarly, CST also varied with a large interval span (7.1 ~ 410.3s), its relationship with PAM addition to improve dewaterability was established by summarizing data from numerous references. Finally, LCA was used to evaluate these species with 4 flocculants, and results showed harvesting method of CPF was suited for five species, TC for the other two and APF for last one. The LCA of TC indicated electricity demand of pre-condense step contributed the vast majority (83%~90%) of total environmental impacts, and using centrifugation to condense low cell density of microalgae was an energy-extensive process. APF cannot compete with CPF, but it can be used for marine species, for which CPF is invalid. By comparing these 8 species, *Coccomyxa sp. KJ*, *Chlorella Vulgaris* and *Tetradesmus obliquus* by

CPF have an advantage for biodiesel production with considering different lipids content of different species.

Chapter 3 investigated the flocculation performance and their mechanism of $AlCl_3$ and chitosan under various conditions of pH, salinity, and cell density. $AlCl_3$ worked better under alkaline conditions (pH 7.0–10.0), whereas chitosan was better under acidic conditions (pH 4.0–7.0). When salinity exceeded 8.4 g/L FE by chitosan decreased significantly, while its influence on $AlCl_3$ is very limited. With increasing cell density from 0.278 to 0.556 g/L optimal dosage of $AlCl_3$ increased 3.7 times, and then to a constant at ~26 g/L despite further increasing in cell density. A positive linear relationship between the optimal dosage of chitosan and cell density was found. According to RSM, [salinity][cell density] and [pH][cell density] were significant interaction effects for $AlCl_3$. And [salinity][cell density] had a significant interaction effect on the FE of chitosan. Finally, experiments indicated combination of $AlCl_3$ and chitosan enhanced flocculation performance by comparing with either flocculant alone.

Chapter 4 used RSM to investigate the flocculation performance of amphoteric flocculant (ACPAM) for harvesting microalgae. The most important factors affecting performance were identified, and then optimized to achieve an FE of ~98%. Thermal stability analyses indicated that the ACPAM was generally stable below 100°C, but crosslinking of its molecules by imidization and condensation occurred at 120°C, which resulted a decline of flocculation performance. Finally, ACPAM was compared to other two commonly used flocculants ($AlCl_3$ and chitosan) for the harvest of other two microalgal species; the results indicated that ACPAM can be widely for various microalgal species.

Chapter 5 examined the feasibility of DME as an extraction solvent for lipid production from sludge. The influencer of sludge ball size, extraction time, and DME to sludge ratio on the raw lipid yield and drying performance were studied. The lipid yield and drying performance increased with smaller sludge ball size, longer extraction time, and higher the DME/sludge ratio. From a comparison with B&D method, DME yielded lipids with higher FAMEs proportion. Difference in FAME composition was not observed between two methods. Due to FAMEs from undigested sludge have a higher proportion of unsaturated fatty acids than from digested sludge, it had superior cold flow properties. The LHV of DME-treated sludge ranged from 3.74 to 5.70 MJ/kg, and independent combustion was hence possible. Experiments proved DME can be reused at least five times for reducing the cost. Finally, the net costs of treating undigested sludge by the DME, conventional solvent extraction, and heat drying methods were 8.13, 13.28, and 19.43 $/ton, respectively. Therefore, disposing of sludge by the DME method had an economical advantage. These results were considered as comparison with microalgae.

Chapter 6 explored a novel method to extract lipids from microalgae with high water content (98%). It was achieved by using ethanol and acetone as entrainer, adding which into DME the mixture can be miscible with water, and lipid yield increased 4.0 and 6.4 times than the blank respectively. Experiments were conducted to determine suitable condition (extraction time of 30 min, 4.2 mL DME/1 mL microalgae, entrainer dosage of 8% and ethanol: acetone of 1:2). Under the condition, the modified DME method

was compared with B&D and Soxhlet methods, and results showed 26.4% of total raw lipids with 54.4% of total FAMEs in the microalgae was extracted by the DME method and FAMEs proportion by DME was highest. Finally, FTIR of extracted lipids implied the more N-H in extracted raw lipids by B&D (wet) and DME methods than others, which was confirmed by C/H/N analysis. The TG/DTA indicated the lipids by the 4 methods started to decompose from 150 ℃, and final decomposition temperature varied from 500 to 535 ℃. Since trace metals in biodiesel could cause metallic corrosion, pollution emission and engine deterioration, they were analysed by ICP. Trace metals of Fe, Ni, Cu, Zn, Sr, Ba, Mg, K and Na were detected in lipids by all methods, and high Mg was found in lipids by DME, which indicated purification was necessary for using it as vehicle fuels.

Chapter 7

By studying the effect of moisture content on lipid extraction by DME method, it's found lipid was easier to be extracted and higher residual solid content could be obtained with lower initial moisture content. The negative effect of moisture content can be attributed to the moisture competing with DME for act on the cell wall, and shielding the contact of lipids with DME. And dewatering is affected by moisture content, mainly because of DME's absorption of water is limited. Five cell disruptions (acidification, homogenization, heating, microwave and ultrasonic) with the potential to improve the DME method were examined. The results displayed acidification and homogenization were invalid for improvement of lipid extraction while heating, ultrasonic and microwave enhanced it significantly. And influence of cell disruption on profile of FAMEs was no obvious. The FAMEs by each treatment were mainly composed of C14:0, C16:0, C16:1, C18:0, C18:1, C18:2 and C18:3. The results from morphology, PSD and 3D-EEM demonstrated the microalgae of *Tetradesmus obliquus* was highly resistant to the cell disruptions and kept intact after cell disruption. The lipid extraction efficiency improved by heating, microwave and ultrasonic could be attributed to the treatments increasing the permeability of the cell wall due to thinner cell wall and larger pore size in it.

8.2 Future perspective

In this study, biodiesel production from microalgae has been investigated, mainly focusing on microalgae harvesting, dewatering, drying and lipid extraction by the DME method. One of future plan is to study the microalgae cultivation process, such as using wastewater and waste fume to cultivate it, examining pollution removal rate and cultivation condition control for microalgal growth. Usually, the waste fume containing CO_2 was emitted into atmosphere with causing environmental problem. If using the fume as carbon source for cultivating microalgae, it can reduce the pollution. And waste water contains nutrients (N/P), which can be utilized by microalgae in order to reducing cultivation cost and purifying water quality. By controlling the cultivation condition (such as N-depletion), higher lipid content or higher growth rate can be achieved. In addition, the purification method of converting lipid for biodiesel should be explored since the metals has been founded in extracted lipids. The extracted raw lipid contains

high concentration of trace metals, which restricted its using as fuel. The pointed technique to remove the metals in lipid extraction or lipid refining process should be explored. Furthermore, the mechanism of EPS effecting flocculation has not yet be well studied, and can be considered as a research point. The effect of EPS on flocculation is not clearly now, if it is possible to achieve efficiently flocculation with controlling EPS should be investigated. Besides, I plan to establish an LCA from microalgae cultivation to biodiesel production to evaluate the DME method. With the LCA, the consumption and impact on environment can be calculated, and the advantage of DME method than other methods can be further confirmed. For some microalgae species with thick and strong cell wall, common cell disruption may be failure, and by analysing the composite of the cell wall (chitin, pectin, fiber) it's possible to find a highly efficient way of cell disruption.

Appendix

Picture S1 Photo-bioreactor for cultivating microalgae.

Table S1 the component of AF-6 and ESM for cultivating microalgae species.

	AF-6[1]			ESM[2]	
$NaNO_3$	140 mg	Thiamine HCl	10 μg	$NaNO_3$	120 mg
NH_4NO_3	22 mg	Vitamin B_6	1 μg	K_2HPO_4	5 mg
$MgSO_4 \cdot 7H_2O$	30 mg	Vitamin B_{12}	1 μg	Vitamin B_{12}	1 μg
KH_2PO_4	10 mg	$Na_2EDTA \cdot 2H_2O$	5 mg	Biotin	1 μg
K_2HPO_4	5 mg	$FeCl_3 \cdot 6H_2O$	980 μg	Thiamine HCl	100 μg
$CaCl_2 \cdot 2H_2O$	10 mg	$MnCl_2 \cdot 4H_2O$	130 μg	Fe-EDTA	259 μg
Fe–citrate	2 mg	ZnSO4 · 7H2O.	110 μg	Mn-EDTA	332 μg
Citric acid	2 mg	$CoCl_2 \cdot 6H_2O$	20 μg	Tris (hydroxymethyl) aminomethane	1 g
Biotin	2 μg	$Na_2MoO_4 \cdot 2H_2O$	12.5 μg	Soil extract	25 mL
Distilled water	1000 mL			Artificial seawater 975 mL	
pH 6.6				pH 8.0	

Table S2 the component of AF-6 and ESM for cultivating microalgae species.

Species	Type	Shape	DW (g/L)	lipid content (% D.B)	Size (μm)	Cell volume (μm^3)	Surface area (μm^2)	Surface area /Surface volume (μm^{-1})	ζ-potential (mV)
Chlorella sorokiniana[3][4][5][6][7][8][9]	fresh	sphere	1.22±0.04	15~19	~3.0	14	28	2.0	-15 ~ -28
Mayamaea sp. [10]		prolate	0.51±0.02	~60	~10.0				~ -16
	marine	spheroid				131	136	1.0	
Coccomyxa sp. KJ [11][12][13]		prolate	0.66±0.03	16~24	6.0~14.0				-25 ~ -28
	fresh	spheroid				106	123	1.2	
Chlamydomonas reinhardtii [14][15][16][17]	fresh	sphere, motile	1.13±0.01	~35	~7.7	239	186	0.8	-12 ~ -20
Chlorella Vulgaris [6][14]	marine	sphere	0.83±0.14	~30	3.0~4.0	22	38	1.7	-16 ~ -30
Nannochloropsis oculate [18][19][20][21]	marine	sphere	0.64±0.01	30~35	2.6~3.1	13	26	2.1	-13 ~ -22
Tetradesmus obliquus [14][19][22][23]	fresh	prolate spheroid	0.92±0.03	12.5~35	~8.4	78	96	1.2	-8 ~ -16
Fistulifera Solaris [24][25][26][27][28]	marine	prolate spheroid	0.26±0.03	35~55	8.0~10.0	75	98	1.3	-12 ~ -15

Table S3 scenarios description and its abbreviation

Scenarios No.	1	2	3	4	5	6	7	8	9	10
	$AlCl_3$+ press filter	chitosan+ press filter	ACPAM+ press filter	pH adjustment +press filter	$AlCl_3$+ centrifugation	chitosan+ centrifugation	ACPAM+ centrifugation	pH adjustment +centrifugation	cross-flow filtration	two-step centrifugation
abbreviation	APF	CPF	KPF	SPF	AC	CC	KC	SC	CF	TC

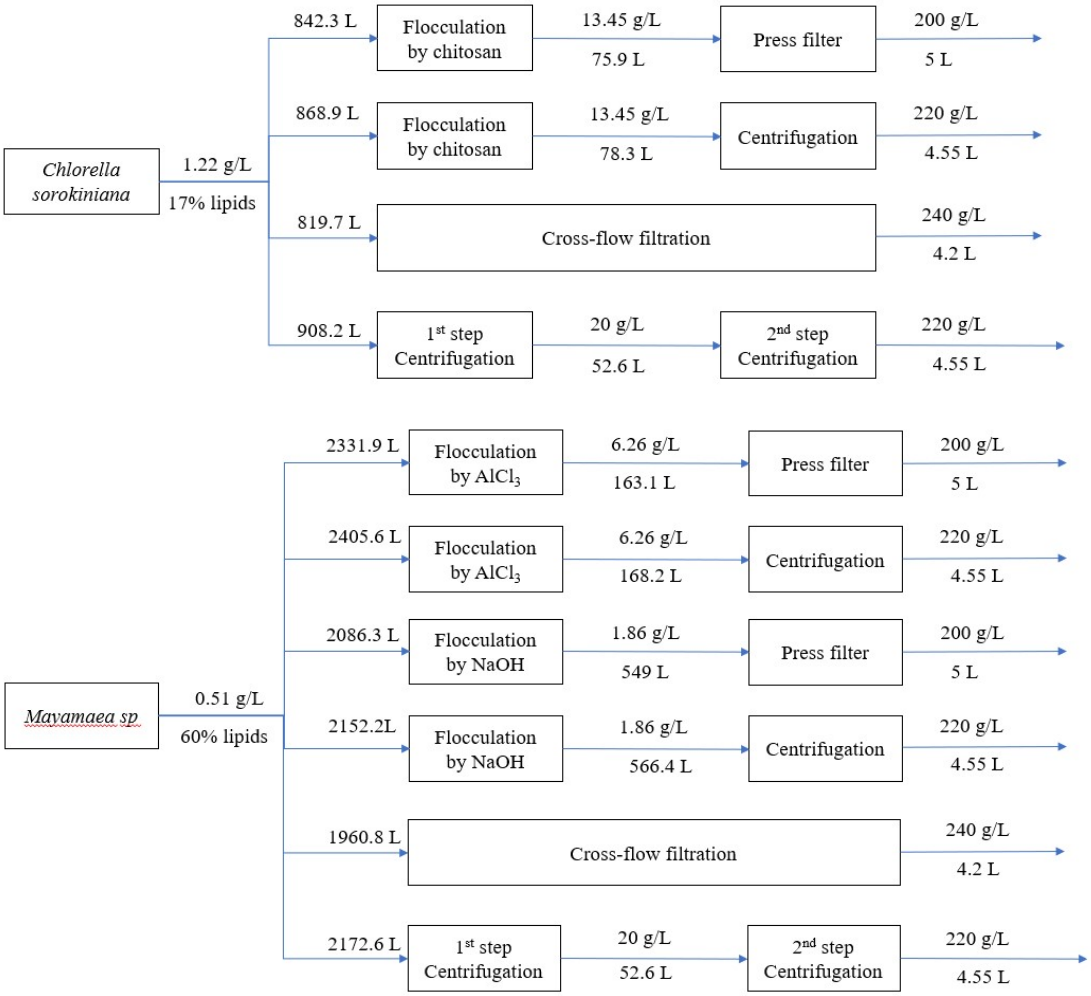
Chlorella sorokiniana
1.22 g/L
17% lipids
842.3 L
Flocculation by chitosan
13.45 g/L
75.9 L
Press filter
200 g/L
5 L
868.9 L
Flocculation by chitosan
13.45 g/L
78.3 L
Centrifugation
220 g/L
4.55 L
819.7 L
Cross-flow filtration
240 g/L
4.2 L
908.2 L
1st step Centrifugation
20 g/L
52.6 L
2nd step Centrifugation
220 g/L
4.55 L
Mayamaea sp
0.51 g/L
60% lipids
2331.9 L
Flocculation by AlCl3
6.26 g/L
163.1 L
Press filter
200 g/L
5 L
2405.6 L
Flocculation by AlCl3
6.26 g/L
168.2 L
Centrifugation
220 g/L
4.55 L
2086.3 L
Flocculation by NaOH
1.86 g/L
549 L
Press filter
200 g/L
5 L
2152.2L
Flocculation by NaOH
1.86 g/L
566.4 L
Centrifugation
220 g/L
4.55 L
1960.8 L
Cross-flow filtration
240 g/L
4.2 L
2172.6 L
1st step Centrifugation
20 g/L
52.6 L
2nd step Centrifugation
220 g/L
4.55 L

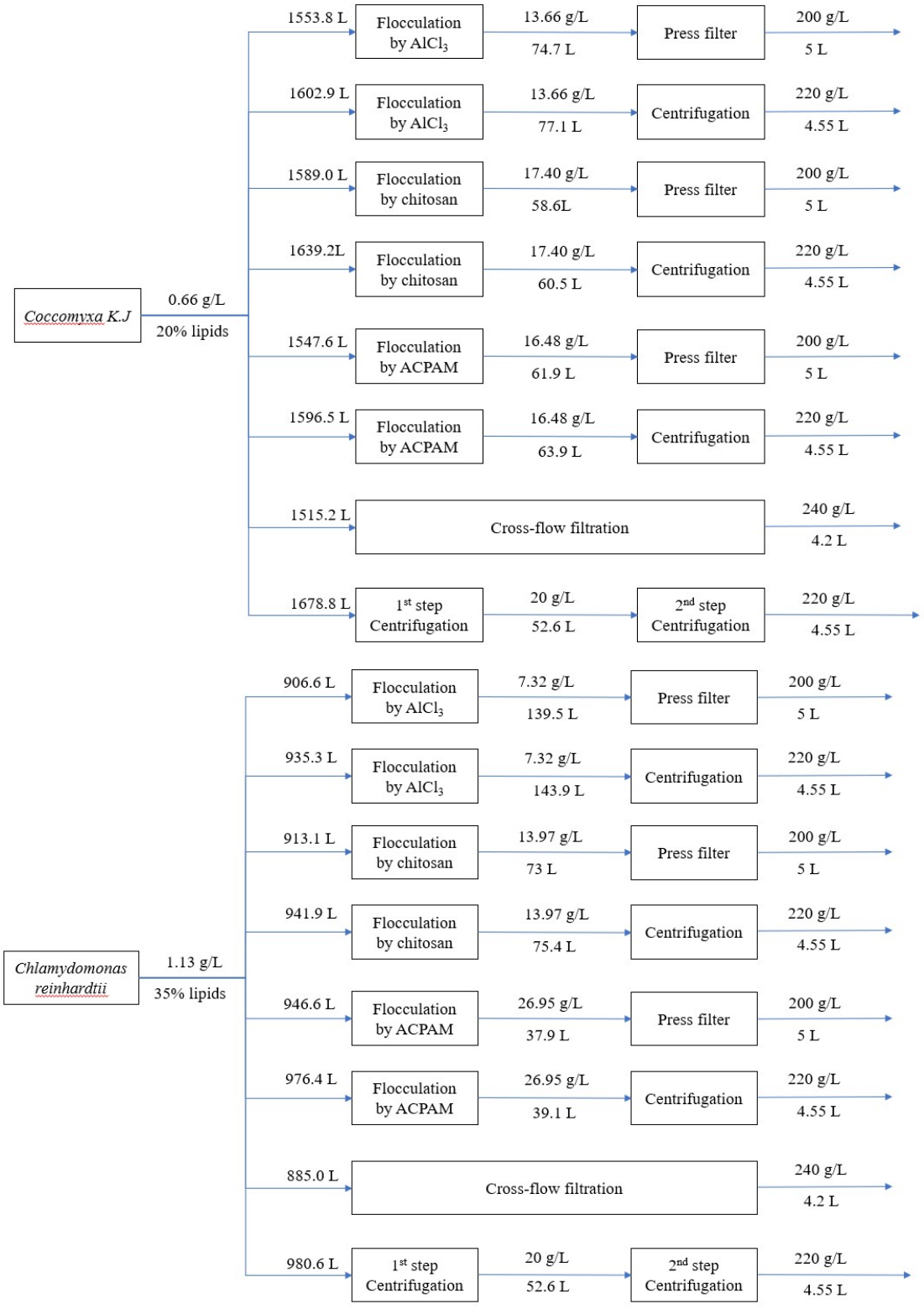
Coccomyxa K.J
0.66 g/L
20% lipids
1553.8 L
Flocculation by AlCl3
13.66 g/L
74.7 L
Press filter
200 g/L
5 L
1602.9 L
Flocculation by AlCl3
13.66 g/L
77.1 L
Centrifugation
220 g/L
4.55 L
1589.0 L
Flocculation by chitosan
17.40 g/L
58.6L
Press filter
200 g/L
5 L
1639.2L
Flocculation by chitosan
17.40 g/L
60.5 L
Centrifugation
220 g/L
4.55 L
1547.6 L
Flocculation by ACPAM
16.48 g/L
61.9 L
Press filter
200 g/L
5 L
1596.5 L
Flocculation by ACPAM
16.48 g/L
63.9 L
Centrifugation
220 g/L
4.55 L
1515.2 L
Cross-flow filtration
240 g/L
4.2 L
1678.8 L
1st step Centrifugation
20 g/L
52.6 L
2nd step Centrifugation
220 g/L
4.55 L
Chlamydomonas reinhardtii
1.13 g/L
35% lipids
906.6 L
Flocculation by AlCl3
7.32 g/L
139.5 L
Press filter
200 g/L
5 L
935.3 L
Flocculation by AlCl3
7.32 g/L
143.9 L
Centrifugation
220 g/L
4.55 L
913.1 L
Flocculation by chitosan
13.97 g/L
73 L
Press filter
200 g/L
5 L
941.9 L
Flocculation by chitosan
13.97 g/L
75.4 L
Centrifugation
220 g/L
4.55 L
946.6 L
Flocculation by ACPAM
26.95 g/L
37.9 L
Press filter
200 g/L
5 L
976.4 L
Flocculation by ACPAM
26.95 g/L
39.1 L
Centrifugation
220 g/L
4.55 L
885.0 L
Cross-flow filtration
240 g/L
4.2 L
980.6 L
1st step Centrifugation
20 g/L
52.6 L
2nd step Centrifugation
220 g/L
4.55 L

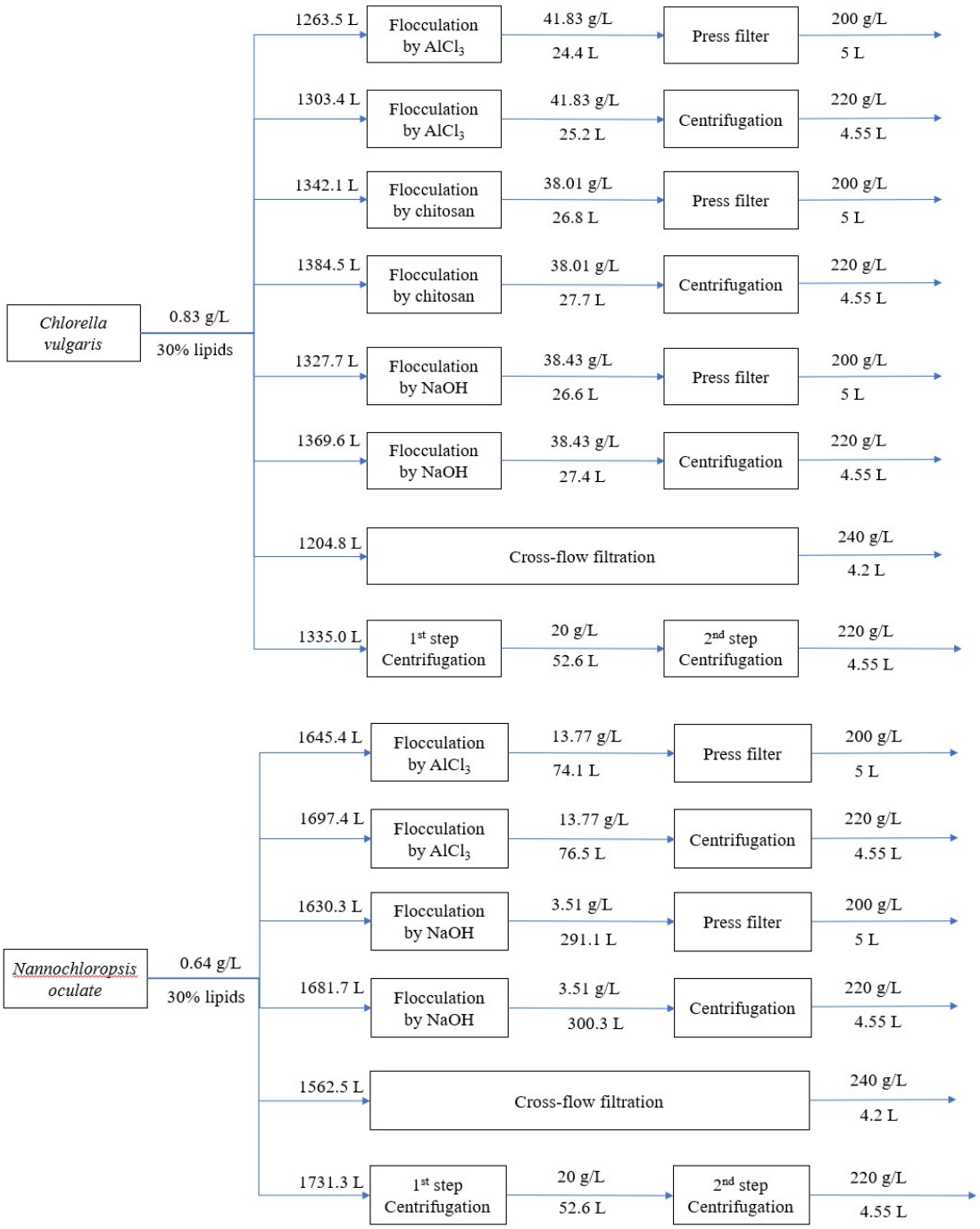
Chlorella vulgaris
0.83 g/L
30% lipids
1263.5 L
Flocculation by AlCl3
41.83 g/L
24.4 L
Press filter
200 g/L
5 L
1303.4 L
Flocculation by AlCl3
41.83 g/L
25.2 L
Centrifugation
220 g/L
4.55 L
1342.1 L
Flocculation by chitosan
38.01 g/L
26.8 L
Press filter
200 g/L
5 L
1384.5 L
Flocculation by chitosan
38.01 g/L
27.7 L
Centrifugation
220 g/L
4.55 L
1327.7 L
Flocculation by NaOH
38.43 g/L
26.6 L
Press filter
200 g/L
5 L
1369.6 L
Flocculation by NaOH
38.43 g/L
27.4 L
Centrifugation
220 g/L
4.55 L
1204.8 L
Cross-flow filtration
240 g/L
4.2 L
1335.0 L
1st step Centrifugation
20 g/L
52.6 L
2nd step Centrifugation
220 g/L
4.55 L
Nannochloropsis oculate
0.64 g/L
30% lipids
1645.4 L
Flocculation by AlCl3
13.77 g/L
74.1 L
Press filter
200 g/L
5 L
1697.4 L
Flocculation by AlCl3
13.77 g/L
76.5 L
Centrifugation
220 g/L
4.55 L
1630.3 L
Flocculation by NaOH
3.51 g/L
291.1 L
Press filter
200 g/L
5 L
1681.7 L
Flocculation by NaOH
3.51 g/L
300.3 L
Centrifugation
220 g/L
4.55 L
1562.5 L
Cross-flow filtration
240 g/L
4.2 L
1731.3 L
1st step Centrifugation
20 g/L
52.6 L
2nd step Centrifugation
220 g/L
4.55 L

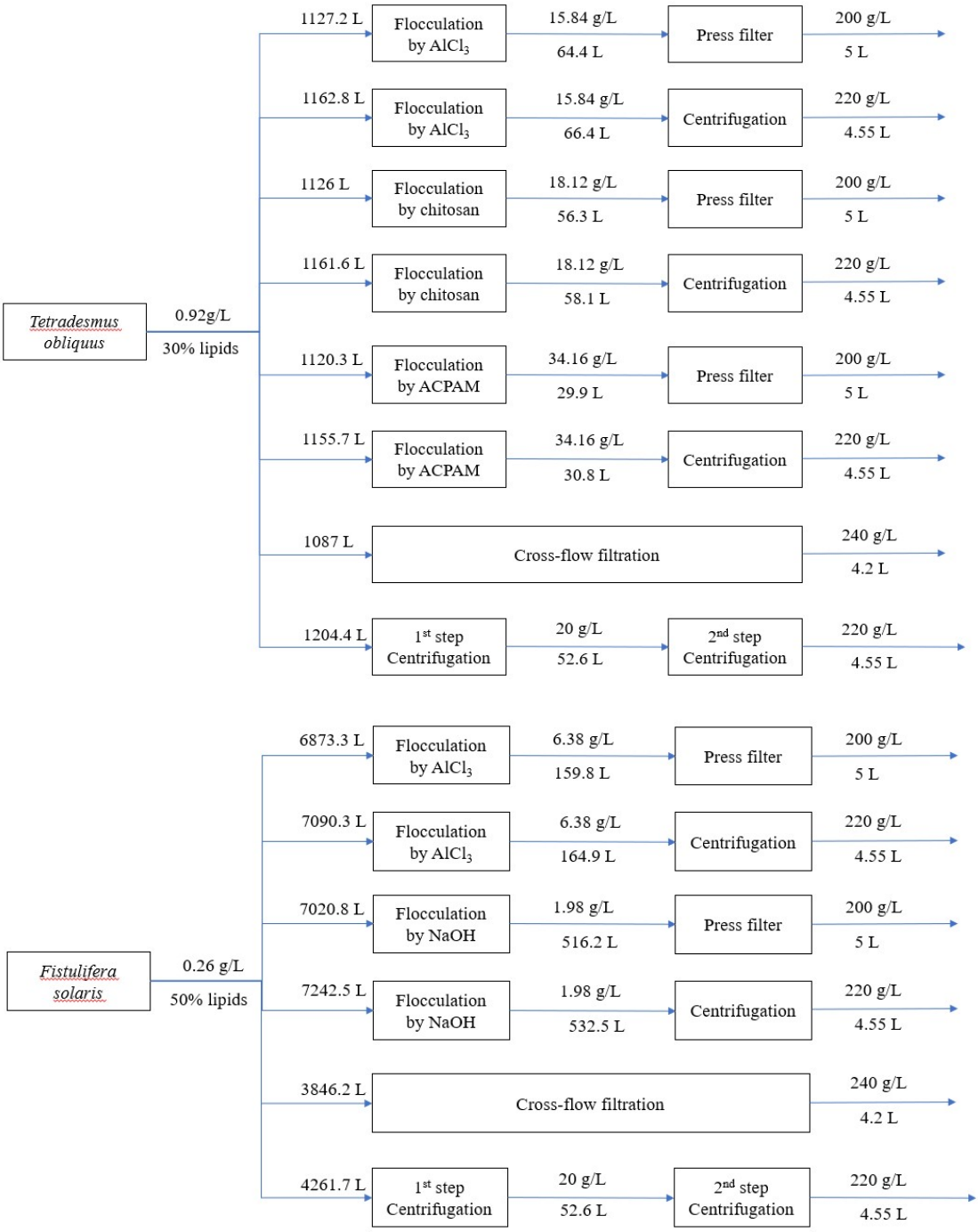

Figure S1 process value chain for lipid production from the 8 microalgae.

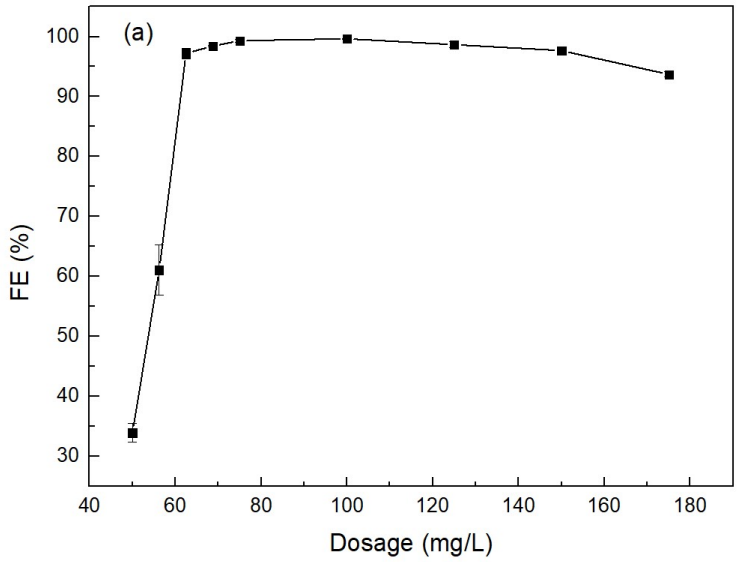
(a)
FE (%)
Dosage (mg/L)

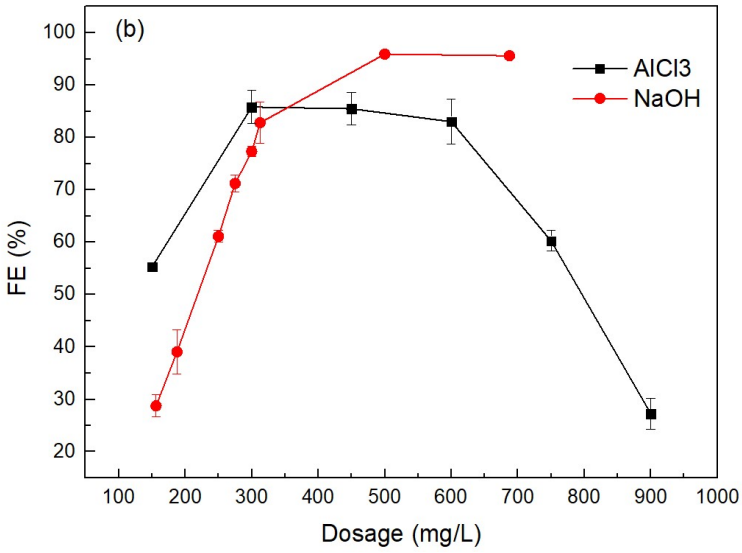
(b)
AlCl3
NaOH
FE (%)
Dosage (mg/L)

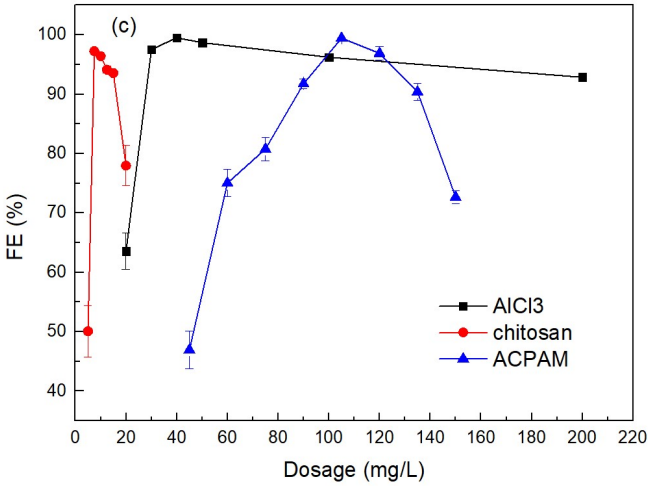
(c)
AlCl3
chitosan
ACPAM
FE (%)
Dosage (mg/L)

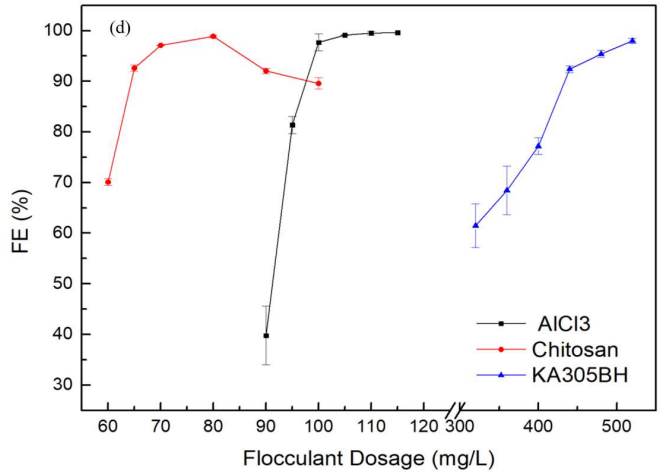
(d)
FE (%)
Flocculant Dosage (mg/L)
AlCl3
Chitosan
KA305BH

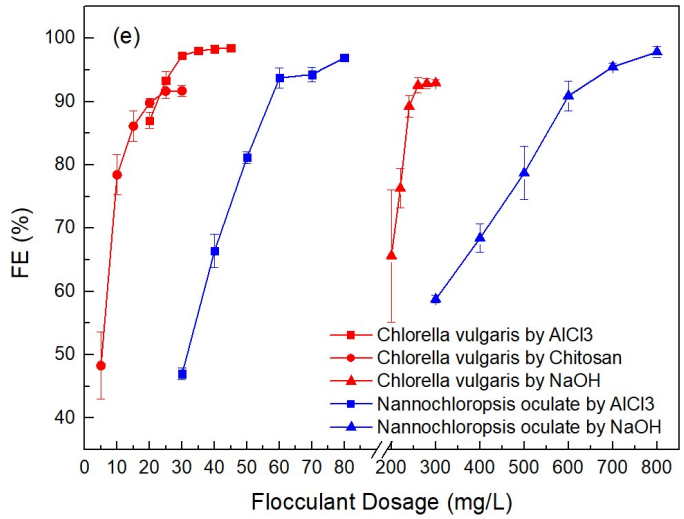
(e)
FE (%)
Flocculant Dosage (mg/L)
Chlorella vulgaris by AlCl3
Chlorella vulgaris by Chitosan
Chlorella vulgaris by NaOH
Nannochloropsis oculate by AlCl3
Nannochloropsis oculate by NaOH

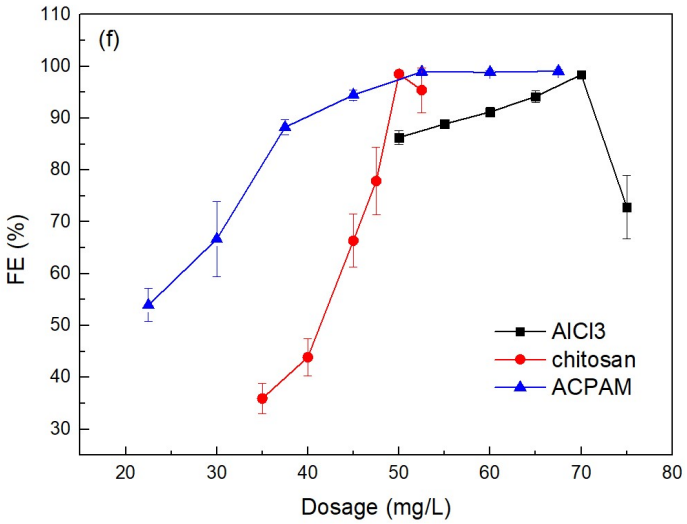
(f)
FE (%)
Dosage (mg/L)
AlCl3
chitosan
ACPAM

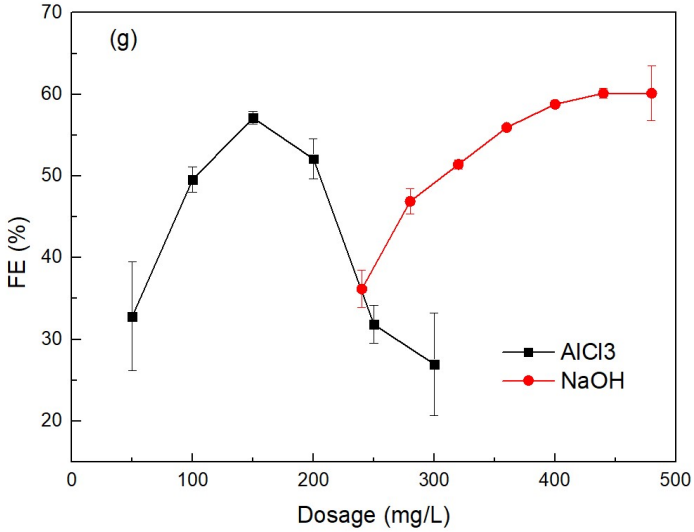

Figure S2 Flocculation of 8 species with 4 methods, a) *Chlorella sorokiniana*, b) *Mayamaea sp.*, c) *Coccomyxa sp KJ*, d) *Chlamydomonas reinhardtii*, e) *Chlorella vulgaris* and *Nannochloropsis oculate*, f) *Tetradesmus obliquus*, g) *Fistulifera solaris*.

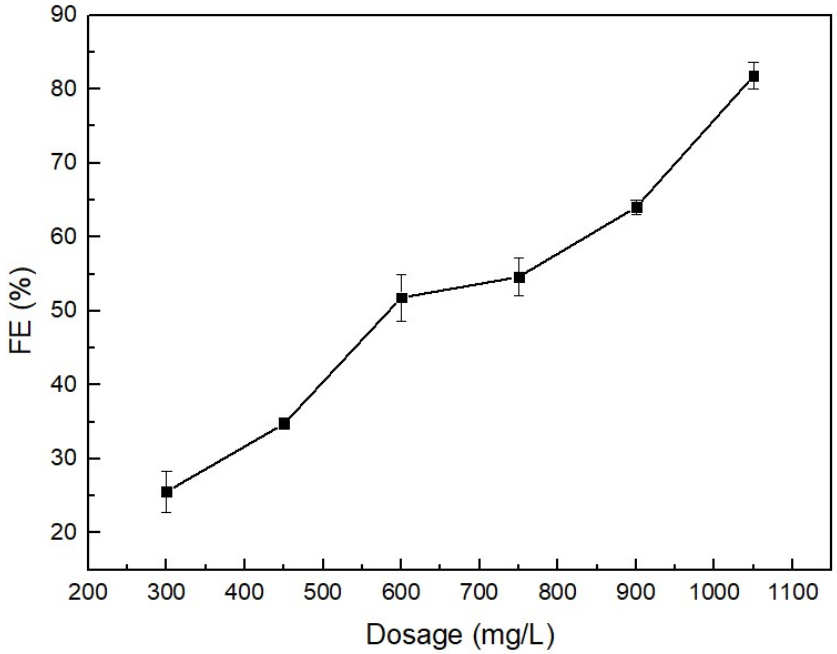

Figure S3 Flocculation of *chlorella sorokiniana* with $AlCl_3$ with pH adjustment to 4.7

Table. S4 Box-Behnken Design arrangement, results and responses for $AlCl_3$.

Run	pH	Salinity (g/L)	Cell density (g/L)	FE (%)			
				Actual value	Mean	Variance	Predicted value
1	5	0.4	0.834	15.17			
2	5	0.4	0.834	14.68			
3	5	0.4	0.834	15.29	15.0	0.32	22.45
4	5	4.4	0.556	10.14			
5	5	4.4	0.556	9.41			
6	5	4.4	0.556	9.98	9.8	0.38	6.95
7	5	4.4	1.112	13.51			
8	5	4.4	1.112	12.95			
9	5	4.4	1.112	12.39	13.0	0.56	10.15
10	5	8.4	0.834	10.80			
11	5	8.4	0.834	11.35			
12	5	8.4	0.834	10.74	11.0	0.34	9.26
13	7	0.4	0.556	96.35			
14	7	0.4	0.556	97.08			
15	7	0.4	0.556	97.65	97.0	0.65	92.52
16	7	0.4	1.112	96.07			
17	7	0.4	1.112	95.51			
18	7	0.4	1.112	95.67	95.8	0.29	91.15
19	7	4.4	0.834	95.45			
20	7	4.4	0.834	94.78			
21	7	4.4	0.834	95.87	95.4	0.55	93.88
22	7	4.4	0.834	93.57			
23	7	4.4	0.834	93.26			
24	7	4.4	0.834	93.57	93.5	0.18	93.88
25	7	4.4	0.834	94.11			
26	7	4.4	0.834	93.39			
27	7	4.4	0.834	90.96	92.8	1.65	93.88
28	7	8.4	0.556	92.54			
29	7	8.4	0.556	92.70			
30	7	8.4	0.556	91.81	92.4	0.47	96.95
31	7	8.4	1.112	49.52			
32	7	8.4	1.112	52.17			
33	7	8.4	1.112	56.14	52.6	3.33	57.12
34	9	0.4	0.834	88.17			
35	9	0.4	0.834	90.17			
36	9	0.4	0.834	88.65	89.0	1.04	90.7
37	9	4.4	0.556	93.76			
38	9	4.4	0.556	94.65			

39	9	4.4	0.556	95.38	94.6	0.81	97.4
40	9	4.4	1.112	51.20			
41	9	4.4	1.112	49.36			
42	9	4.4	1.112	49.72	50.1	0.98	52.99
43	9	8.4	0.834	82.10			
44	9	8.4	0.834	81.61			
45	9	8.4	0.834	81.43	81.7	0.35	74.31

Table. S5 Box-Behnken Design arrangement, results and responses for Chitosan.

Run	pH	Salinity (g/L)	Cell density (g/L)	FE (%)			
				Actual value	Mean	Variance	Predicted value
1	5	0.4	0.834	96.84			
2	5	0.4	0.834	97.15			
3	5	0.4	0.834	97.15	97.0	0.18	99.18
4	5	4.4	0.556	89.46			
5	5	4.4	0.556	90.75			
6	5	4.4	0.556	91.89	90.7	1.22	93.97
7	5	4.4	1.112	98.06			
8	5	4.4	1.112	97.50			
9	5	4.4	1.112	97.76	97.8	0.28	95.92
10	5	8.4	0.834	96.91			
11	5	8.4	0.834	95.75			
12	5	8.4	0.834	94.60	95.8	1.16	92.2
13	7	0.4	0.556	94.81			
14	7	0.4	0.556	94.32			
15	7	0.4	0.556	94.65	94.6	0.25	89.19
16	7	0.4	1.112	87.97			
17	7	0.4	1.112	82.41			
18	7	0.4	1.112	86.89	85.8	2.95	85.48
19	7	4.4	0.834	93.63			
20	7	4.4	0.834	93.87			
21	7	4.4	0.834	94.24	93.9	0.31	93.76
22	7	4.4	0.834	93.75			
23	7	4.4	0.834	93.51			
24	7	4.4	0.834	95.39	94.2	1.02	93.76
25	7	4.4	0.834	93.99			
26	7	4.4	0.834	92.29			
27	7	4.4	0.834	93.20	93.2	0.85	93.76
28	7	8.4	0.556	78.67			
29	7	8.4	0.556	78.91			
30	7	8.4	0.556	80.86	79.5	1.20	79.76

31	7	8.4	1.112	79.25			
32	7	8.4	1.112	79.70			
33	7	8.4	1.112	80.01	79.7	0.38	85.06
34	9	0.4	0.834	2.37			
35	9	0.4	0.834	2.61			
36	9	0.4	0.834	2.31	2.4	0.16	5.98
37	9	4.4	0.556	2.51			
38	9	4.4	0.556	2.27			
39	9	4.4	0.556	1.62	2.1	0.46	3.98
40	9	4.4	1.112	6.83			
41	9	4.4	1.112	6.48			
42	9	4.4	1.112	7.34	6.9	0.43	3.61
43	9	8.4	0.834	5.76			
44	9	8.4	0.834	4.49			
45	9	8.4	0.834	5.46	5.2	0.66	3.1

Table. S6 Central composite design arrangement, results and responses for $AlCl_3$+Chitosan dual flocculation at pH 5.0, salinity of 0.4 g/L and cell density of 0.417 g/L.

Run	chitosan (mg/L)	$AlCl_3$ (mg/L)	FE (%)			
			Actual value	Mean	Variance	Predicted value
1	0.076	15.0	78.71			
2	0.076	15.0	76.56			
3	0.076	15.0	81.18	78.8	2.31	83.14
4	0.20	6.0	88.28			
5	0.20	6.0	87.20			
6	0.20	6.0	87.74	87.7	0.54	84.04
7	0.20	24.0	94.41			
8	0.20	24.0	93.44			
9	0.20	24.0	94.30	94.1	0.53	90.6
10	0.50	2.3	89.14			
11	0.50	2.3	88.71			
12	0.50	2.3	85.59	87.8	1.94	89.74
13	0.50	15.0	97.31			
14	0.50	15.0	96.99			
15	0.50	15.0	97.10	97.1	0.16	96.39
16	0.50	15.0	96.56			
17	0.50	15.0	96.34			
18	0.50	15.0	96.34	96.4	0.13	96.39

19	0.50	15.0	95.48			
20	0.50	15.0	95.59			
21	0.50	15.0	95.81	95.6	0.17	96.39
22	0.50	27.7	94.30			
23	0.50	27.7	94.62			
24	0.50	27.7	95.48	94.8	0.61	96.37
25	0.80	6.0	91.61			
26	0.80	6.0	90.22			
27	0.80	6.0	91.94	91.3	0.91	91.21
28	0.80	24.0	94.95			
29	0.80	24.0	93.87			
30	0.80	24.0	92.69	93.8	1.13	94.04
31	0.92	15.0	90.65			
32	0.92	15.0	91.61			
33	0.92	15.0	92.15	91.5	0.76	90.64

Table. S7 Central composite design arrangement, results and responses for $AlCl_3$+Chitosan dual flocculation at pH 7.0, salinity of 4.4 g/L and cell density of 0.556 g/L.

Run	chitosan (mg/L)	$AlCl_3$ (mg/L)	FE (%)			
			Actual value	Mean	Variance	Predicted value
1	0.22	9.0	97.87			
2	0.22	9.0	96.42			
3	0.22	9.0	97.36	97.2	0.74	92.7
4	0.38	4.5	80.5			
5	0.38	4.5	75.75			
6	0.38	4.5	82.42	79.6	3.43	84.41
7	0.38	13.5	98.12			
8	0.38	13.5	97.44			
9	0.38	13.5	97.53	97.7	0.37	100.23
10	0.75	2.6	92.07			
11	0.75	2.6	90.45			
12	0.75	2.6	91.3	91.3	0.81	87.94
13	0.75	9.0	97.87			
14	0.75	9.0	98.55			
15	0.75	9.0	97.53	98.0	0.52	98.56
16	0.75	9.0	99.06			
17	0.75	9.0	98.89			
18	0.75	9.0	99.32	99.1	0.22	98.56
19	0.75	9.0	98.29			
20	0.75	9.0	98.81			
21	0.75	9.0	98.72	98.6	0.28	98.56
22	0.75	15.4	97.27			
23	0.75	15.4	98.81			
24	0.75	15.4	98.55	98.2	0.82	98.15
25	1.13	4.5	95.48			
26	1.13	4.5	95.65			
27	1.13	4.5	96.59	95.9	0.60	96.77
28	1.13	13.5	96.85			
29	1.13	13.5	97.53			
30	1.13	13.5	96.16	96.8	0.69	95.39
31	1.28	9.0	96.33			
32	1.28	9.0	97.44			
33	1.28	9.0	96.93	96.9	0.56	98.02

Table. S8 Central composite design arrangement, results and responses for $AlCl_3$+Chitosan dual flocculation at pH 9.0, salinity of 8.4 g/L and cell density of 0.695 g/L.

Run	chitosan (mg/L)	$AlCl_3$ (mg/L)	FE (%)			
			Actual value	Mean	Variance	Predicted value
1	0.38	9.0	75.42			
2	0.38	9.0	80.08			
3	0.38	9.0	80.53	78.7	2.83	72.75
4	1.00	3.6	16.11			
5	1.00	3.6	15.95			
6	1.00	3.6	14.89	15.7	0.66	26.91
7	1.00	14.4	91.76			
8	1.00	14.4	90.08			
9	1.00	14.4	92.06	91.3	1.07	91.08
10	2.50	1.4	12.14			
11	2.50	1.4	9.85			
12	2.50	1.4	10.92	11.0	1.15	-1.68
13	2.50	9.0	69.16			
14	2.50	9.0	72.52			
15	2.50	9.0	72.29	71.3	1.88	71.24
16	2.50	9.0	71.15			
17	2.50	9.0	72.14			
18	2.50	9.0	70.92	71.4	0.65	71.24
19	2.50	9.0	73.05			
20	2.50	9.0	69.54			
21	2.50	9.0	70.38	71.0	1.83	71.24
22	2.50	16.6	86.03			
23	2.50	16.6	87.71			
24	2.50	16.6	90.08	87.9	2.03	91.52
25	4.00	3.6	14.96			
26	4.00	3.6	14.89			
27	4.00	3.6	14.43	14.8	0.29	24.05
28	4.00	14.4	93.74			
29	4.00	14.4	92.82			
30	4.00	14.4	95.11	93.9	1.15	91.7
31	4.60	9.0	71.53			
32	4.60	9.0	74.58			
33	4.60	9.0	76.79	74.3	2.64	71.16

Table.S9 Analysis of variance for RSM by $AlCl_3$+Chitosan dual-flocculation.

		Low-level					Medium-level					High-level				
Source	DF	Adj SS	Adj MS	T-Value	F-Value	P-Value	Adj SS	Adj MS	T-Value	F-Value	P-Value	Adj SS	Adj MS	T-Value	F-Value	P-Value
Model	5	694.7	138.9		20.55	<0.0001	760.3	152.1		17.90	<0.0001	29345.2	5869.0		115.68	<0.0001
Linear	2	300.6	150.3		22.23	<0.0001	398.0	199.0		23.42	<0.0001	26070.7	13035.4		256.93	<0.0001
Chitosan	1	168.5	168.5	4.99	24.92	<0.0001	85.0	85.0	3.16	10.00	0.0038	7.6	7.6	-0.39	0.15	0.7025
$AlCl_3$	1	132.1	132.1	4.42	19.54	0.0001	313.0	313.0	6.07	36.84	<0.0001	26063.2	26063.2	22.67	513.7	<0.0001
Square	2	383.6	191.8		28.37	<0.0001	140.5	70.2		8.27	0.0016	3265.3	1632.7		32.18	<0.0001
chitosan*chitosan	1	382.2	382.2	-7.52	56.53	<0.0001	43.4	43.4	-2.26	5.11	0.0321	2.2	2.2	0.21	0.04	0.8382
$AlCl_3$*$AlCl_3$	1	47.2	47.1	-2.64	6.97	0.0136	128.9	128.9	-3.90	15.18	0.0006	2933.9	2933.9	-7.60	57.83	<0.0001
2-Way Interaction	1	10.4	10.4		1.54	0.2248	221.9	221.9		26.11	<0.0001	9.1	9.1		0.18	0.6756
chitosan*$AlCl_3$	1	10.4	10.4	-1.24	1.54	0.2248	221.9	221.9	-5.11	26.11	<0.0001	9.1	9.1	0.42	0.18	0.6756
Fitted Equation		FE(%)= 67.65+66.79[chitosan]+1.051[$AlCl_3$]-52.78[chitosan]^2-0.02060[$AlCl_3$]^2-0.345[chitosan][$AlCl_3$]					FE(%)= 67.65+66.79[chitosan]+1.051[$AlCl_3$]-52.78[chitosan]^2-0.02060[$AlCl_3$]^2-0.345[chitosan][$AlCl_3$]					FE(%)= -15.90-2.13[chitosan]+13.96[$AlCl_3$]+0.159[chitosan]^2-0.4513[$AlCl_3$]^2+0.107[chitosan][$AlCl_3$]				

Table S10 The component of AF-6 for cultivating *Coccomyxa sp. KJ*

Item	**Content**	**Item**	**Content**
$NaNO_3$	14 mg	Thiamine HCl	1 μg
NH_4NO_3	2.2 mg	Vitamin B_6	0.1 μg
$MgSO_4 \cdot 7H_2O$	3 mg	Vitamin B_{12}	0.1 μg
KH_2PO_4	1 mg	$Na_2EDTA \cdot 2H_2O$	0.5 mg
K_2HPO_4	0.5 mg	$FeCl_3 \cdot 6H_2O$	98 μg
$CaCl_2 \cdot 2H_2O$	1 mg	$MnCl_2 \cdot 4H_2O$	13 μg
Fe–citrate	0.2 mg	ZnSO4 · 7H2O.	11 μg
Citric acid	0.2 mg	$CoCl_2 \cdot 6H_2O$	2 μg
Biotin	0.2 μg	$Na_2MoO_4 \cdot 2H_2O$	1.25 μg
Distilled water	99.5 mL		
pH 6.6			

Table S11 Experimental design and results of the steepest ascent

Run	ω1 (rpm)	pH	dosage (mg/L)	Flocculation activity (%)
1	200	8.5	10	15.2
2	250	9.0	15	50
3	300	9.5	20	74.3
4	350	10.0	25	95.6
5	400	10.5	30	94.8
6	450	11.0	35	69.4

Table S12 Experimental result of Box-Behnken design and its predicted value

Run	pH	Dosage (mg/L)	ω1 (rpm)	Flocculation activity (%)	
				Actual result	Predicted value
1	10.0(0)	35(+1)	450(+1)	73.6±2.3	77.1
2	9.0(-1)	35(+1)	350(0)	90.8±1.0	90.2
3	10.0(0)	15(-1)	250(-1)	48.6±2.1	42.3
4	10.0(0)	25(0)	350(0)	92.2	93.9
5	11.0(+1)	25(0)	450(+1)	91.9±0.7	88.5
6	11.0(+1)	35(+1)	350(0)	90.9±0.8	90.2
7	10.0(0)	25(0)	350(0)	93.1	93.9
8	10.0(0)	25(0)	350(0)	96.0	93.9
9	11.0(+1)	25(0)	250(-1)	72.2±3.7	78.3
10	10.0(0)	25(0)	350(0)	95.6	93.9
11	9.0(-1)	15(-1)	350(0)	62.4±4.6	65.6
12	11.0(+1)	15(-1)	350(0)	62.0±2.6	65.6
13	10.0(0)	35(+1)	250(-1)	84.6±1.4	82.3
14	9.0(-1)	25(0)	250(-1)	75.8±0.9	78.3
15	10.0(0)	15(-1)	450(+1)	68.4±1.2	67.9
16	10.0(0)	25(0)	450(+1)	88.1±0.6	88.5
17	10.0(0)	25(0)	350(0)	98.0	93.9

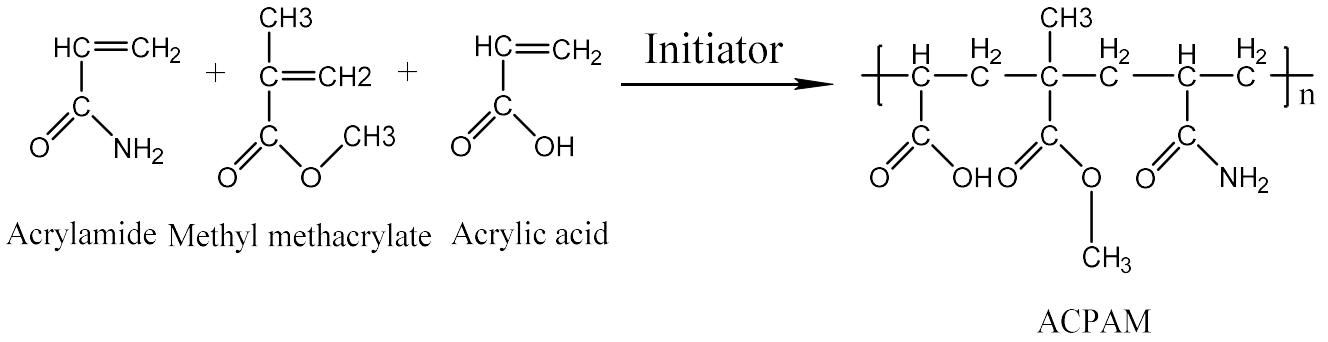

Figure S4 Polyreaction pathways for the ACPAM

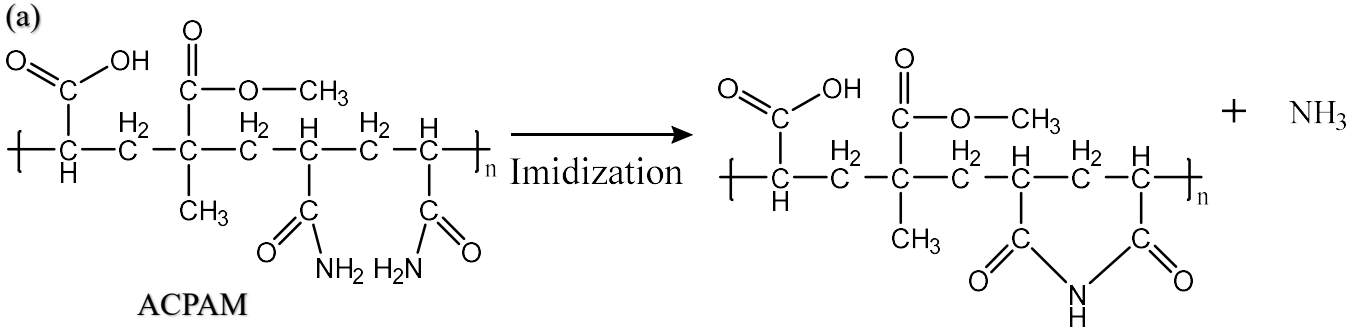

(b)

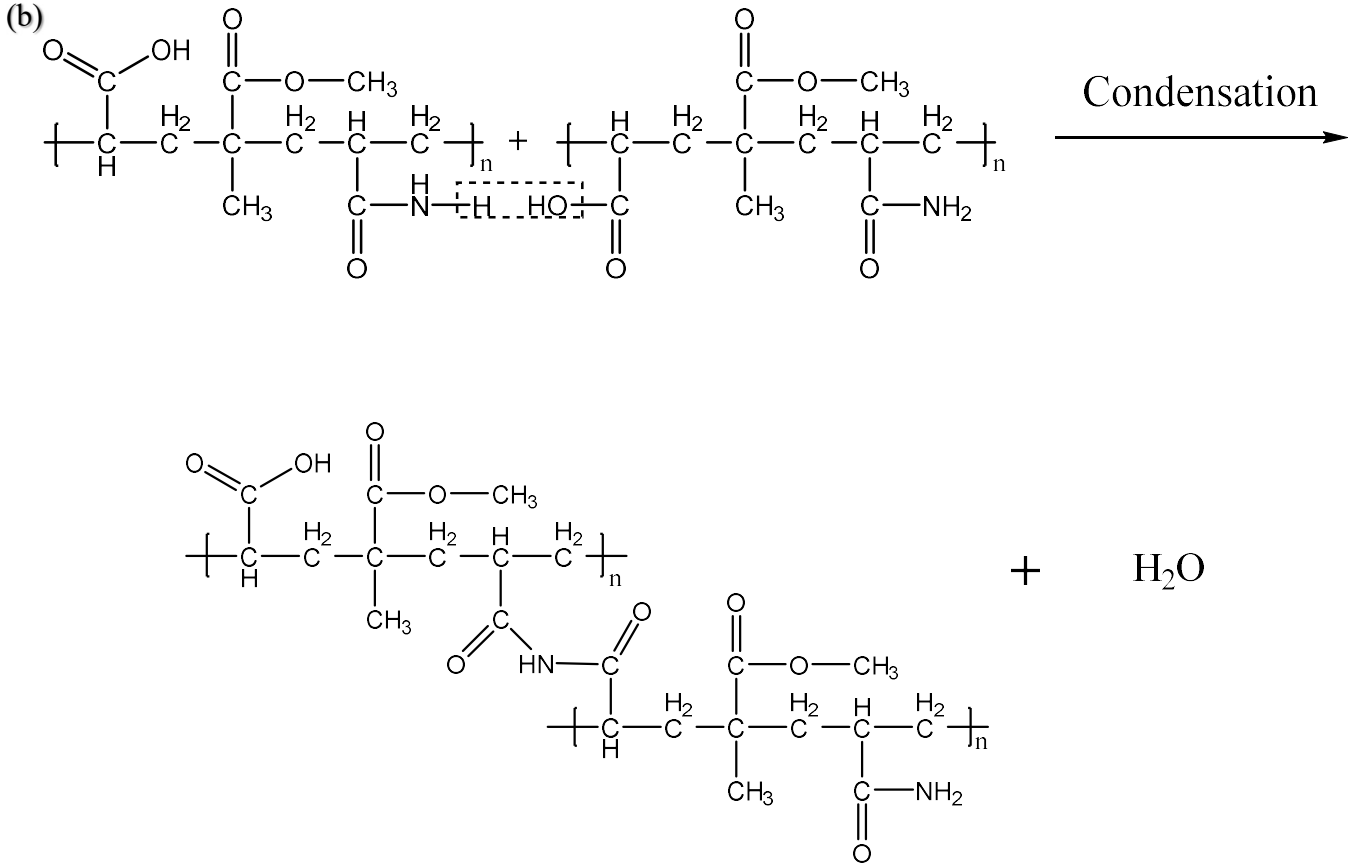

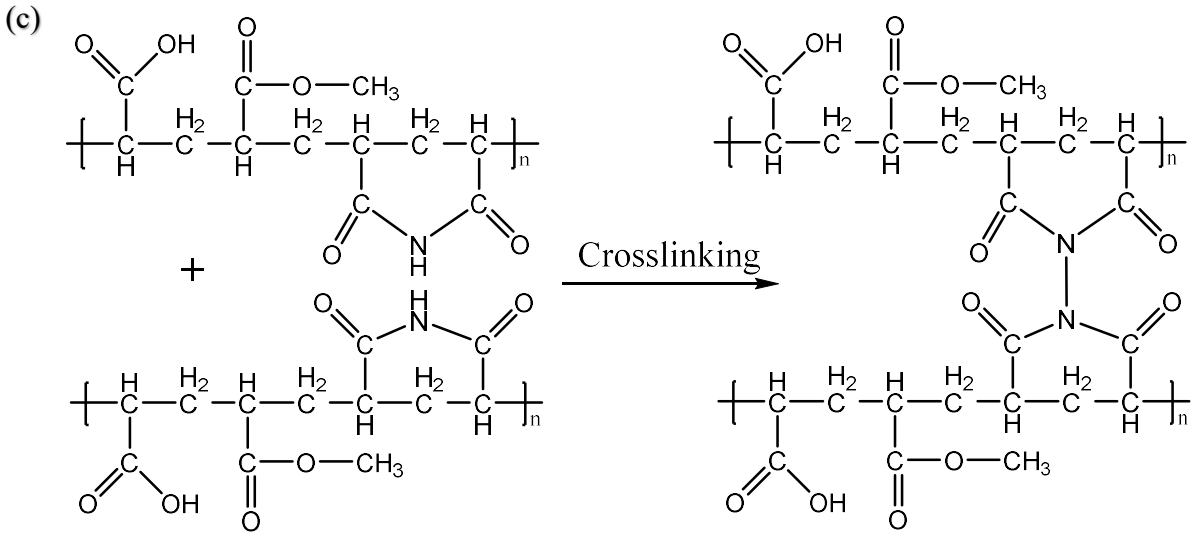

Figure S5 Transformation pathways of the ACPAM during heating treatment, a) imidization, b) condensation and c) crosslinking.

1.1 Mass balance

Figure S6 shows the mass composition before and after treatment of 1 g of dewatered sludge. For each group of columns, the first column shows the initial value and the second column shows the value after treatment by the DME or B&D method.

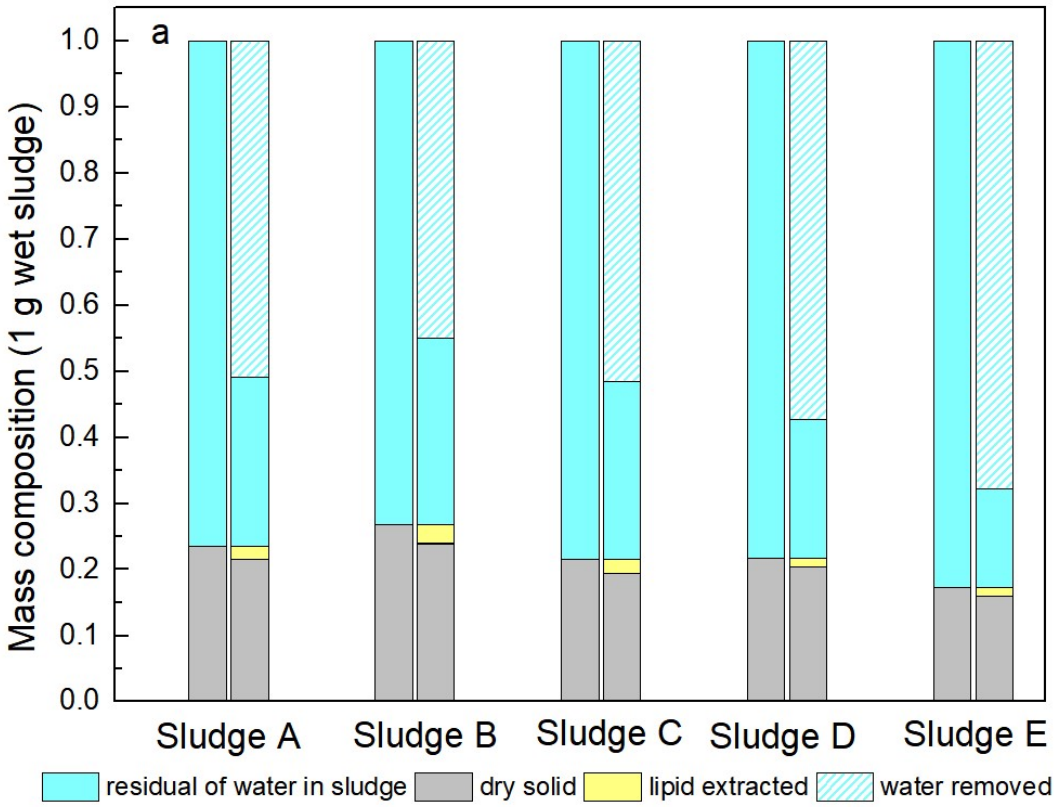

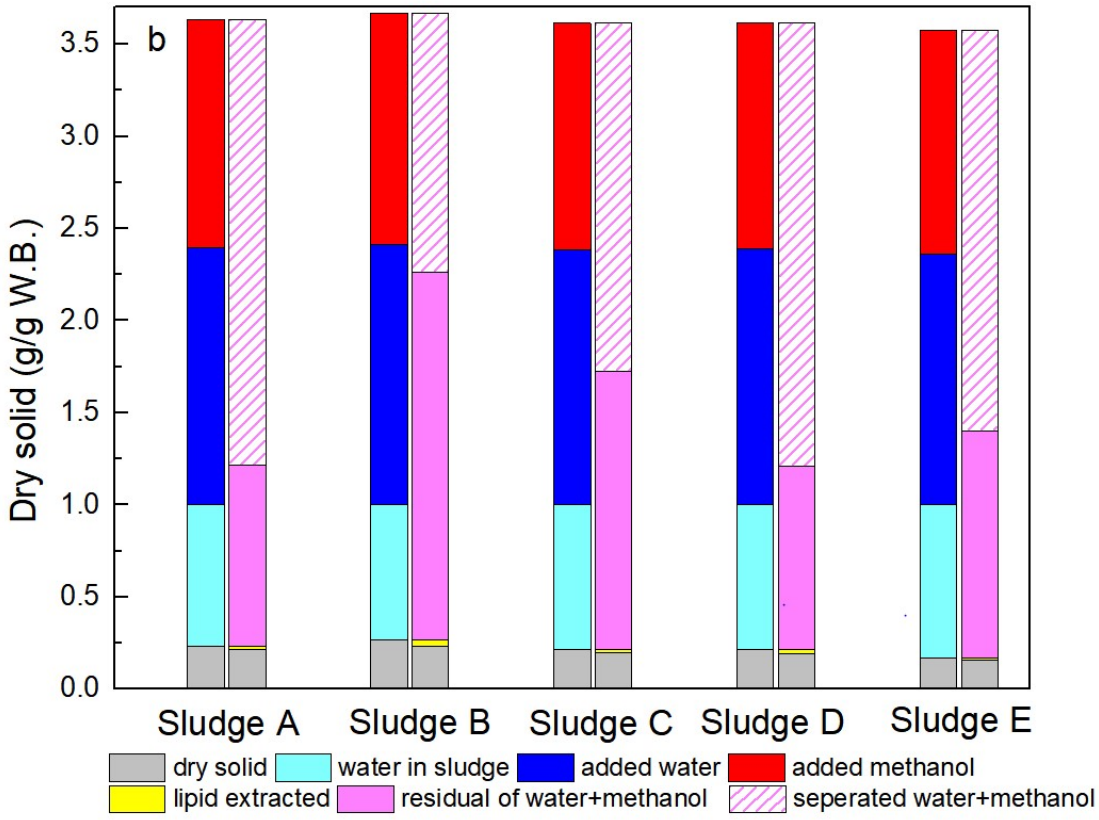

Figure S6. Mass composition of sludge before and after treatment by the (a) DME and (b) B&D methods.

1.2 Cost of lipid extraction by the DME method

The only energy requirement in the DME method is the electrical power used by the compressor to liquefy DME gas, so energy consumption is proportional to the amount of DME liquefied. The energy consumption E (kJ/kg) of treating 1 kg of sludge can be calculated by Eq. (1):

$$\mathrm{E} = E_c \times \eta_s \qquad (1)$$

where E_c (kJ/kg) indicates the energy consumed to liquefy 1 kg of DME, and η_s (kg/kg) is the DME to sludge ratio.

According to the original process (Kanda *et al.*, 2008), the water content of coal can be reduced from 66.7% to 30.2% using the DME method with a η_c of 7.4 kg/kg. The energy E_l (kJ/kg) required to remove 1 kg of water from wet coal in this process is 1,109 kJ/kg-water. Thus, the E_c can be calculated by the following equations:

$$M_{water\ removed} = m_0 - m_1 \qquad (2)$$

$$m_0 = \omega_0 \times M \qquad (3)$$

$$m_1 = \frac{\mathrm{M}\times(1-\omega_0)}{(1-\omega_1)} \times \omega_1 \qquad (4)$$

$$E_1 \times M_{water,removed} = E_c \times M \times \eta_c \quad (5)$$

Where $M_{water\ removed}$ (kg) is the mass of water removed, m_0 (kg) and m_1 (kg) are the weight of water before and after drying, ω_0 (%) and ω_1 (%) are the water contents before and after drying, and M (kg) is the biosolid mass.
The value of E_c is calculated as 78.4 kJ/kg-DME according to Eqs. (2)–(3).

1.3 Cost of sludge drying by the conventional heat-drying method
First, from the water content ω_0 (%) of the original biosolid cake, the water content ω_1 (%) of the dried biosolid cake, the mass flux M' (kg/h) of the original biosolid cake, and the mass flux X (kg-water/h) of removed water are calculated by Eq. (6):

$$X = \mathrm{M}' \times \frac{(\omega_0 - \omega_1)}{(1 - \omega_1)} \quad (6)$$

Next, the flux of heat Q (kJ/h) required to remove water flux X from biosolid cake by the rotary dryer is calculated. Using the thermal capacity coefficient H_a (kJ/(m^3•h•°C) of the rotary dryer, the log-mean temperature difference Δt (°C) between the biosolid and heating media, and the mass flux of removed water per drying chamber volume S_v (kg-water/(m^3•h)), Q (kJ/h) can be calculated by Eq. (7):

$$Q = H_a \cdot \Delta\mathrm{t} \cdot \mathrm{X}/S_v \quad (7)$$

The log-mean temperature difference can be calculated by Eq. (8):

$$\Delta\mathrm{t} = \frac{(\mathrm{T}_1 - \mathrm{t}_1) - (\mathrm{T}_2 - \mathrm{t}_2)}{2.3 \cdot \log(\frac{\mathrm{T}_1 - \mathrm{t}_1}{\mathrm{T}_2 - \mathrm{t}_2})} \quad (8)$$

Where T_1 is the temperature of the heating air introduced into the dryer, T_2 is the temperature of exhaust air, and t_1 and t_2 are the temperatures of the biosolid cake before and after drying.

Finally, using the mass flux M' and the flux of heat Q calculated by Eq. (7), the energy E_s (kJ/kg sludge cake) necessary to dry 1 kg of sludge cake is given by Eq. (9):

$$\mathrm{E_s} = \mathrm{Q}/\mathrm{M}' = H_a \times \frac{\Delta\mathrm{t}}{S_v} \times \frac{(\omega_0 - \omega_1)}{(1 - \omega_1)} \quad (9)$$

Table S13. The component of ESM for cultivating *Nannochloropsis oculate*.

Items	Content
$NaNO_3$	120 mg/L
K_2HPO_4	5 mg/L
Vitamin B_{12}	1 μg/L
Biotin	1 μg/L
Thiamine HCl	100 μg/L
Fe-EDTA	259 μg/L
Mn-EDTA	332 μg/L
Tris (hydroxymethyl) aminomethane	1 g/L
Soil extract	25 mL/L
Artificial seawater (33.4 g salts per liter)	975 mL/L
pH 8.0	

Table S14. The Elemental composition of extracted raw lipids by the 4 methods.

	H (%)	C (%)	N (%)	O (%)
Soxhlet extraction (HE)	10.44±1.09	68.76±8.17	0.11±0.01	20.69±4.76
DME	11.59±0.50	71.09±2.70	0.23±0.06	17.09±1.59
B&D (dry)	9.87±2.01	65.52±8.10	0.09±0.03	24.52±4.82
B&D (wet)	12.30±0.34	76.21±2.22	0.13±0.01	11.36±1.30

Key Constraints Factors: DME can not mix with liquid microalgae without entrainer.

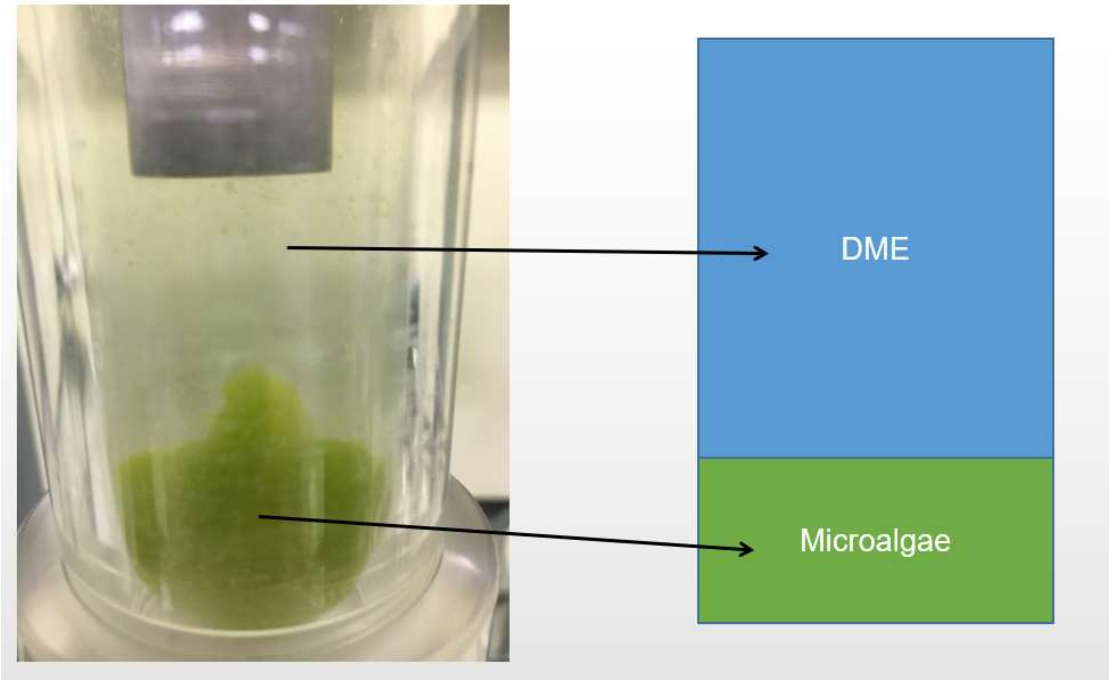

Picture S2. Illustration for DME extraction without entrainer.

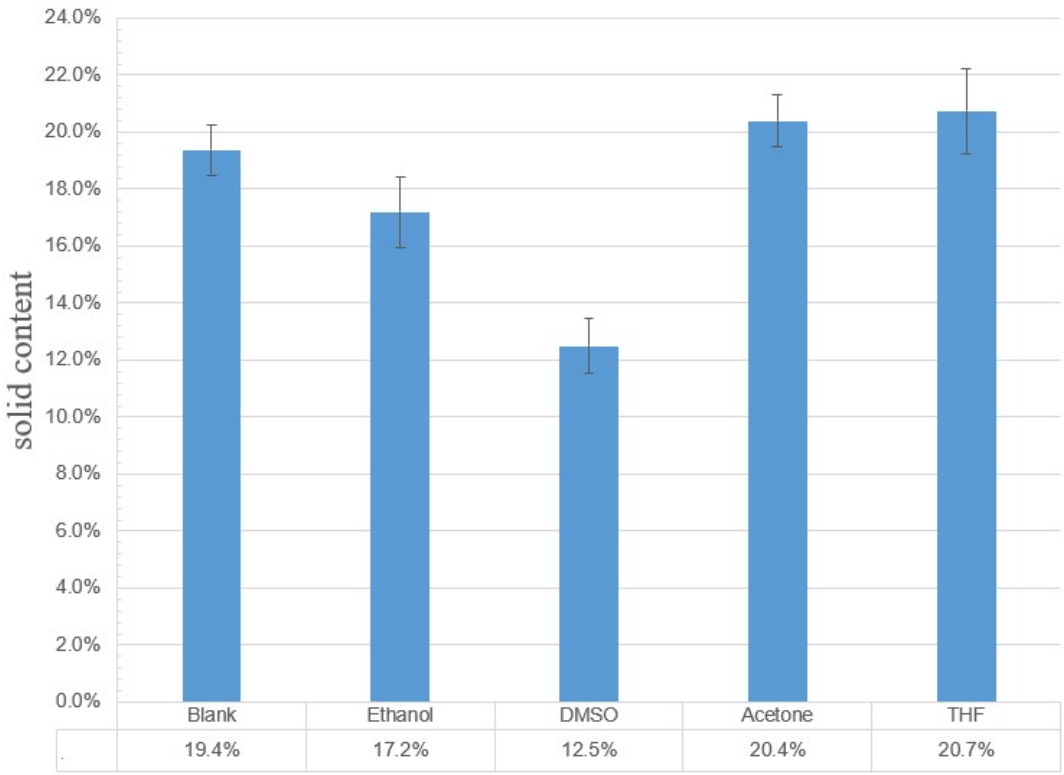

Figure S7. Solid content of microalgae after lipid extraction by DME with 4 kinds of additive agents added.

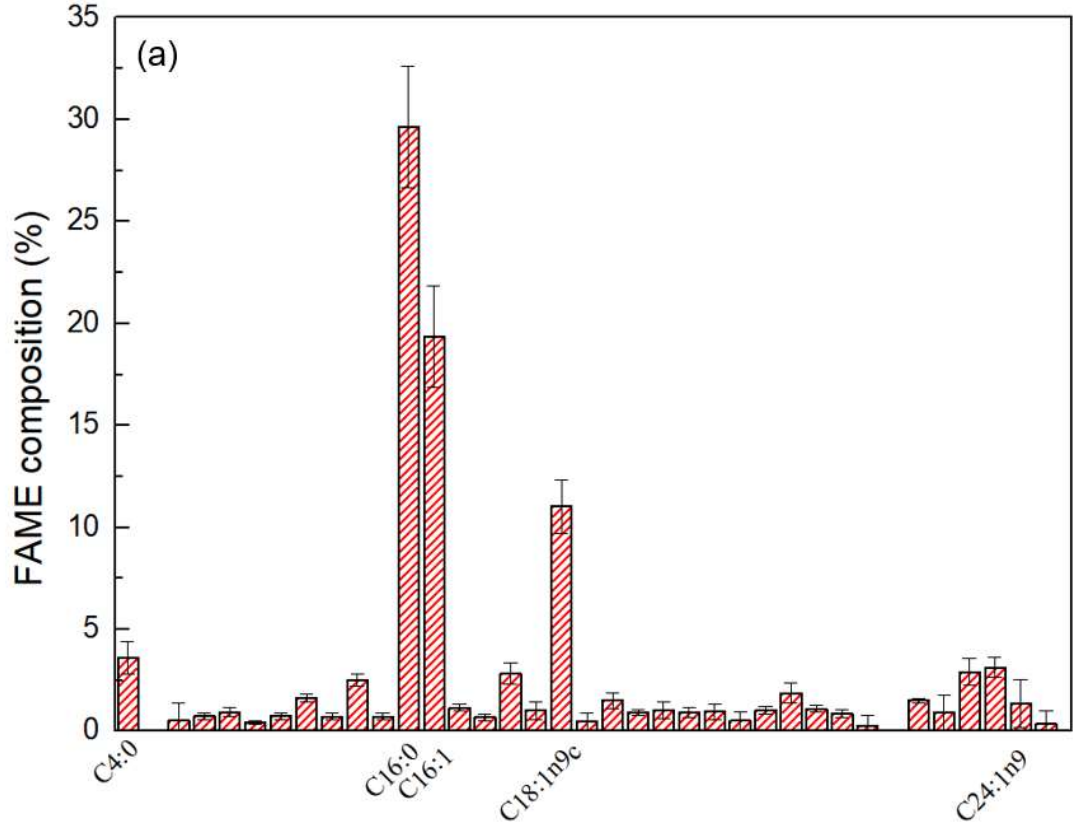
(a)
FAME composition (%)
35
30
25
20
15
10
5
0
C4:0
C16:0
C16:1
C18:1n9c
C24:1n9

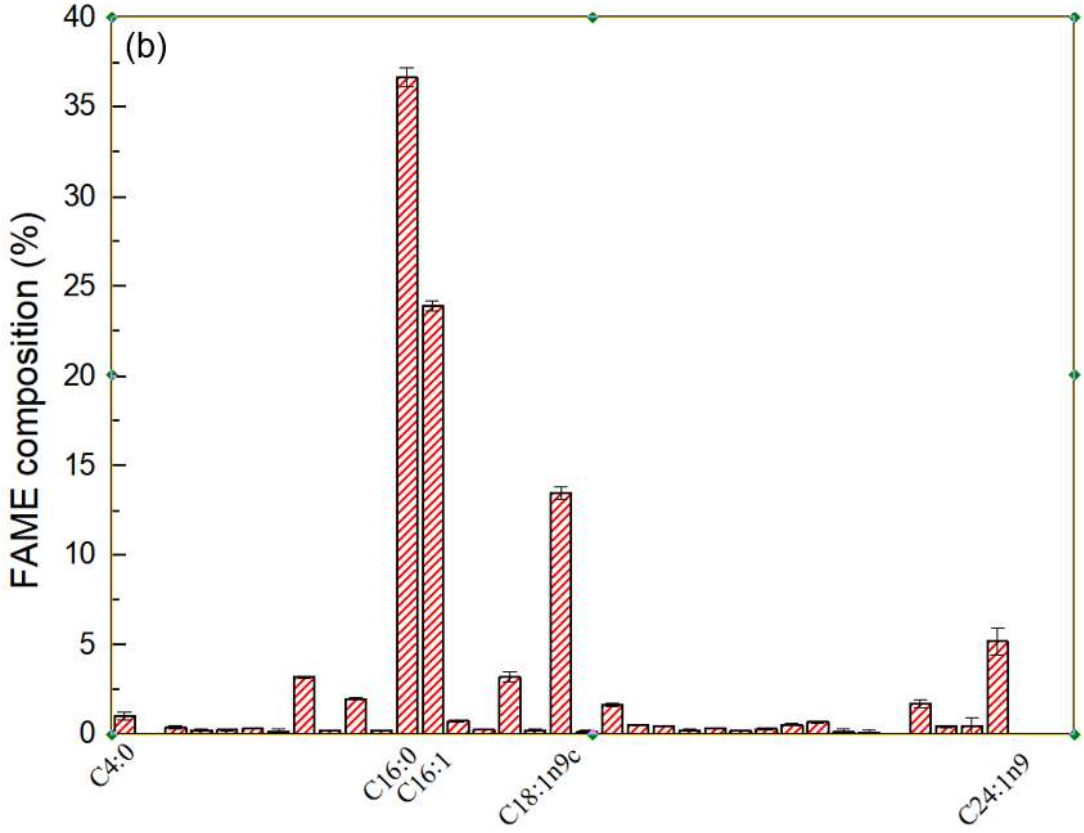
(b)
FAME composition (%)
40
35
30
25
20
15
10
5
0
C4:0
C16:0
C16:1
C18:1n9c
C24:1n9

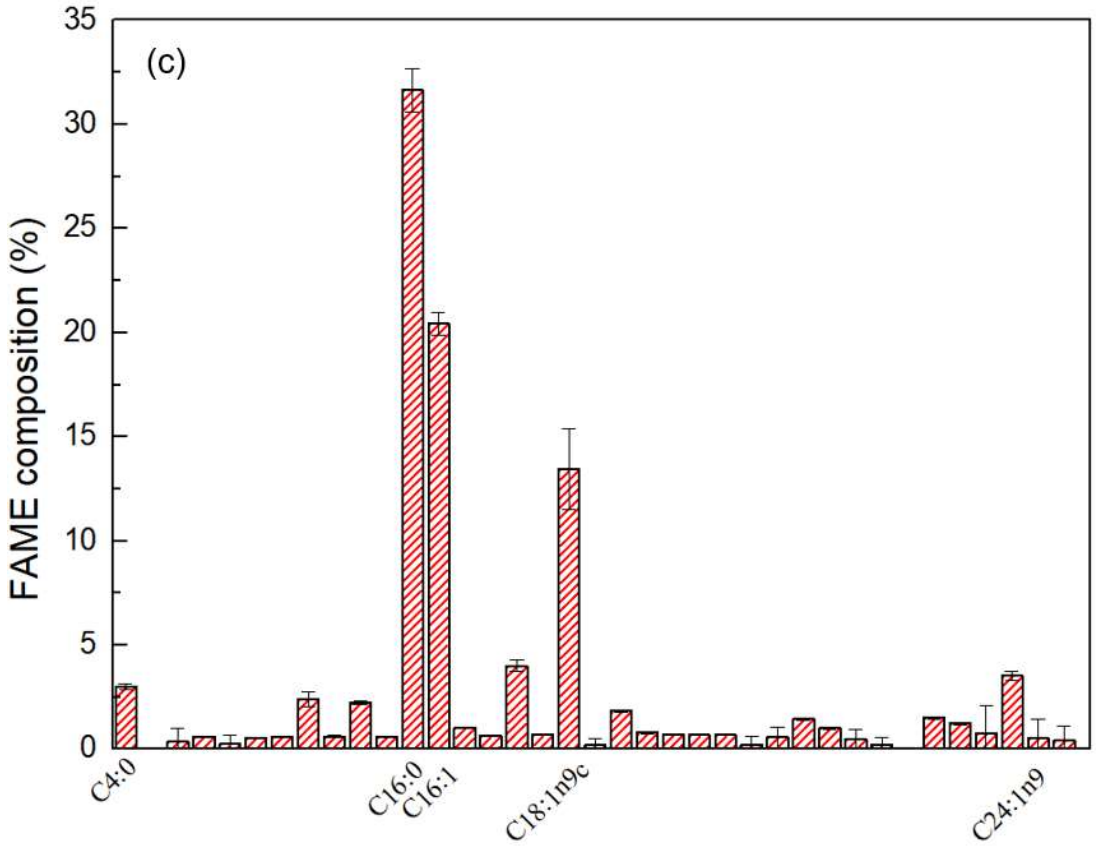
(c)
FAME composition (%)
35
30
25
20
15
10
5
0
C4:0
C16:0
C16:1
C18:1n9c
C24:1n9

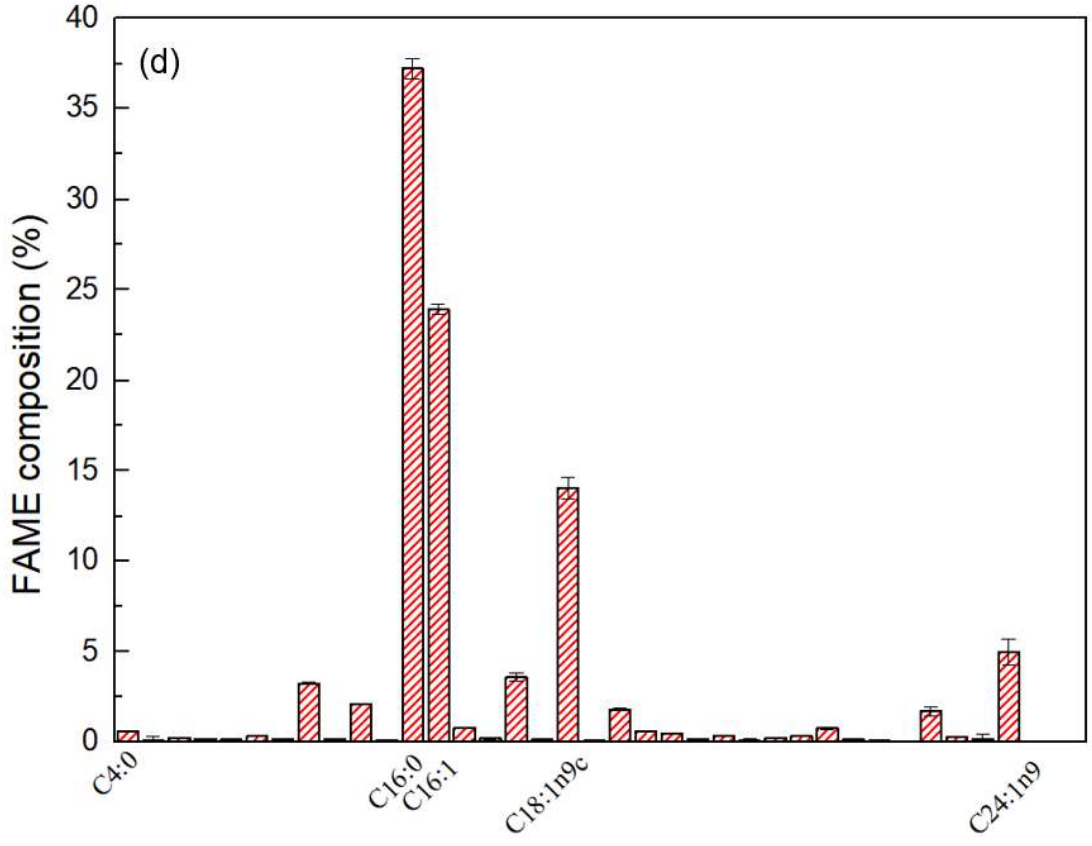
(d)
FAME composition (%)
40
35
30
25
20
15
10
5
0
C4:0
C16:0
C16:1
C18:1n9c
C24:1n9

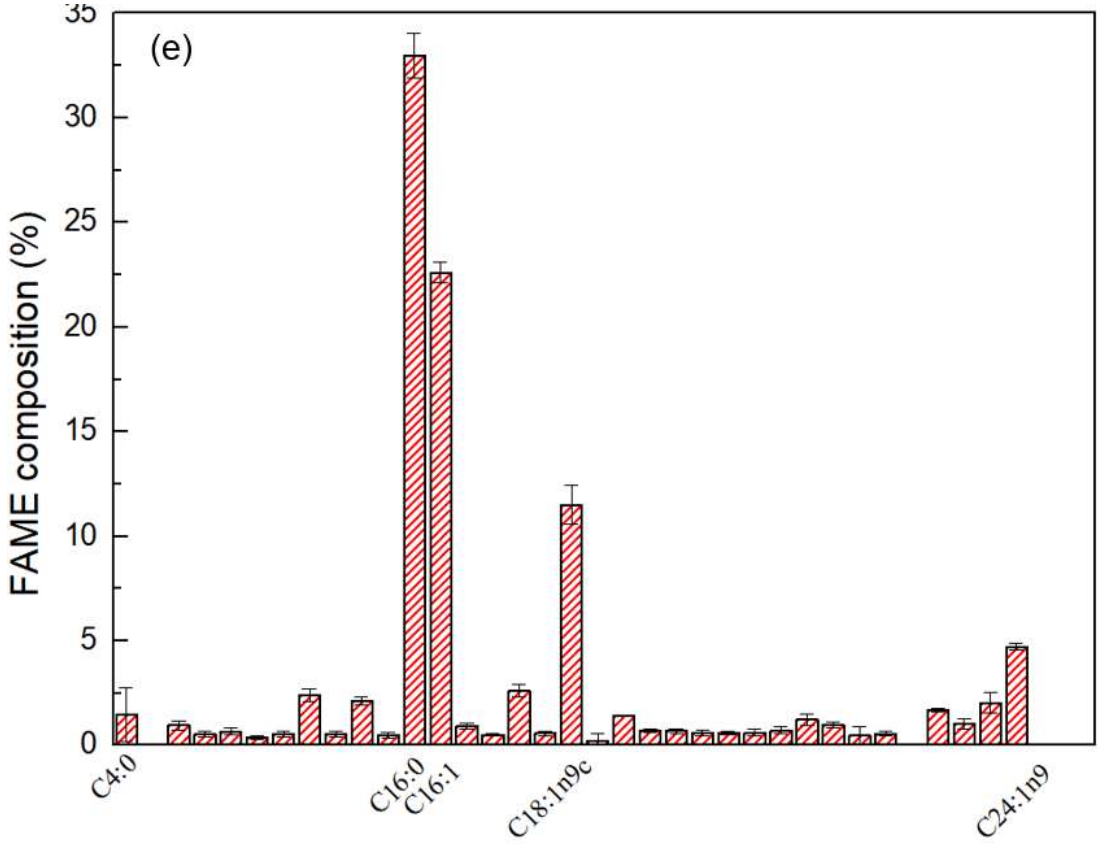

Figure S8. FAMEs composition of extracted lipid with 4 kinds of additive agents added, a) blank, b) ethanol, c) DMSO, d) acetone, e) THF.

Table S15 The component of AF-6 for cultivating *Tetradesmus obliquus*

Item	Content	Item	Content
$NaNO_3$	14 mg	**Thiamine HCl**	1 μg
NH_4NO_3	2.2 mg	**Vitamin B_6**	0.1 μg
$MgSO_4 \cdot 7H_2O$	3 mg	**Vitamin B_{12}**	0.1 μg
KH_2PO_4	1 mg	**$Na_2EDTA \cdot 2H_2O$**	0.5 mg
K_2HPO_4	0.5 mg	**$FeCl_3 \cdot 6H_2O$**	98 μg
$CaCl_2 \cdot 2H_2O$	1 mg	**$MnCl_2 \cdot 4H_2O$**	13 μg
Fe–citrate	0.2 mg	**ZnSO4 · 7H2O.**	11 μg
Citric acid	0.2 mg	**$CoCl_2 \cdot 6H_2O$**	2 μg
Biotin	0.2 μg	**$Na_2MoO_4 \cdot 2H_2O$**	1.25 μg
Distilled water	99.5 mL		
pH 6.6			

Table S16 Experimental results and fitted model results of raw lipids extraction and dewatering performance in study of moisture content

Extraction time (min)	Initial moisture content (%)	DME dosage (ml/g)	Raw lipids yield (%)		Solid content (%)	
			Experimental value	Predicted value	Experimental value	Predicted value
20	85	75	69.2±1.3	69.9	17.9±1.4	14.9
20	65	175	81.3±4.0	81.0	46.7±0.0	46.6
20	75	125	74.7±0.9	74.0	34.5±1.8	34.7
20	75	175	77.0±1.6	76.8	37.1±1.8	38.3
20	65	125	78.1±0.6	78.2	47.9±1.4	44.5
20	85	125	71.7±1.5	71.8	19.9±0.2	19.3
20	75	75	71.9±0.3	72.0	28.6±2.0	31.8
20	85	175	74.4±1.9	74.4	24.2±1.0	24.4
20	65	75	76.0±0.3	76.1	40.8±1.6	43.1
40	65	175	84.7±0.8	86.0	49.6±1.5	50.1
40	75	125	77.7±1.7	78.2	38.1±2.4	37.9
40	85	75	73.8±3.1	73.2	17.9±0.4	17.7
40	85	125	75.8±1.9	75.8	21.0±2.8	22.7
40	75	175	81.6±3.2	81.6	43.5±2.9	42.0
40	75	75	76.8±1.9	75.6	34.0±0.5	34.4
40	65	125	82.9±0.8	82.6	47.5±1.2	47.6
40	65	75	79.5±3.2	79.8	47.8±2.1	45.6
40	85	175	79.0±2.8	79.1	27.0±1.4	28.3

60	65	175	90.7±2.8	89.8	51.0±2.7	51.9
60	75	125	80.9±2.0	81.2	38.0±1.8	39.4
60	85	75	75.4±1.3	75.3	16.1±0.3	18.7
60	75	175	84.7±2.9	85.2	47.2±1.3	44.0
60	65	125	86.1±2.4	85.7	45.5±2.8	48.8
60	85	125	78.1±3.3	78.5	26.9±1.6	24.3
60	75	75	77.2±1.3	77.9	36.8±1.6	35.3
60	85	175	83.1±4.0	82.5	29.8±3.4	30.4
60	65	75	82.4±0.8	82.4	47.9±8.2	46.4

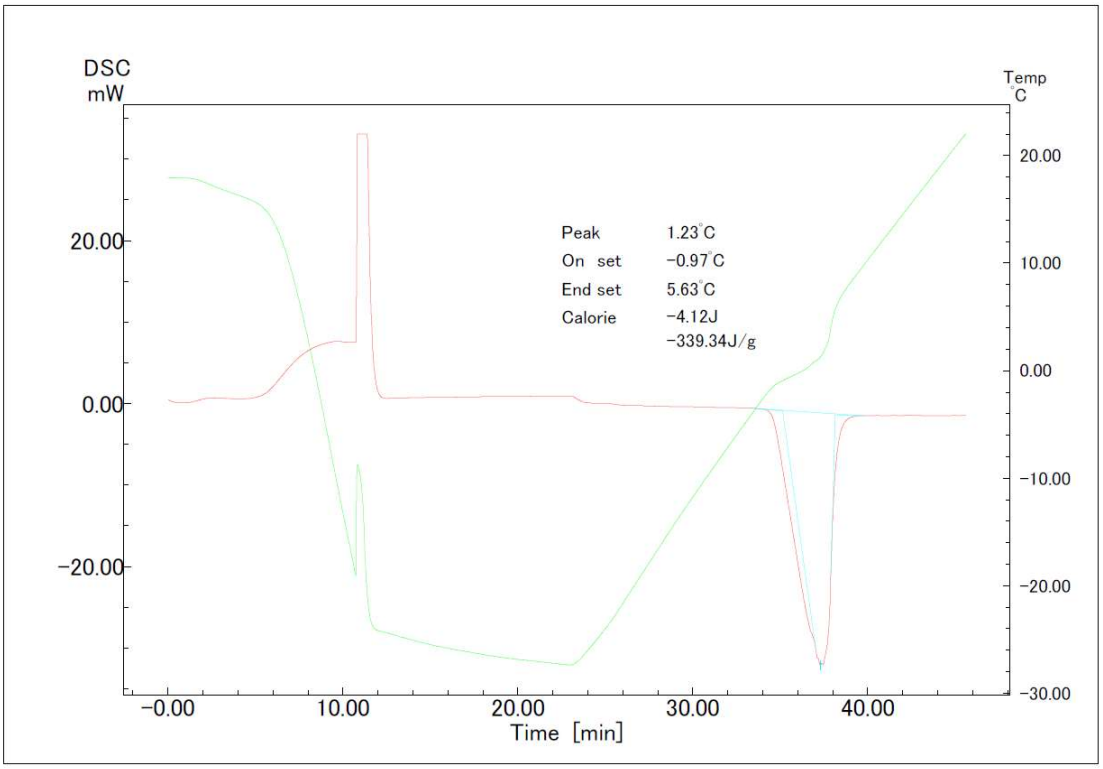

Figure S9. DSC curve of pure water for calculating free and bound water.

Reference

[1] Kato, S. (1982). Laboratory culture and morphology of Colacium vesiculosum Ehrb.(Euglenophyceae). Jpn. J. Phycol., 30, 63-67.

[2] Tsuzuki, M., Okada, K., Isoda, H., Hirano, M., Odaka, T., Saijo, H., ... & Fujiwara, S. (2019). Physiological Properties of Photoautotrophic Microalgae and Cyanobacteria Relevant to Industrial Biomass Production. Marine Biotechnology, 21(3), 406-415.

[3] De Souza Leite, L., Hoffmann, M. T., & Daniel, L. A. (2019). Coagulation and dissolved air flotation as a harvesting method for microalgae cultivated in wastewater. Journal of Water Process Engineering, 32, 100947.

[4] Lopez-Exposito, P., Campano, C., van de Ven, T. G., Negro, C., & Blanco, A. (2019). Microalgae harvesting with the novel flocculant hairy cationic nanocrystalline cellulose. Colloids and Surfaces B: Biointerfaces, 178, 329-336.

[5] De Souza Leite, L., Daniel, L. A., Pivokonsky, M., Novotna, K., Branyikova, I., & Branyik, T. (2019). Interference of model wastewater components with flocculation of Chlorella sorokiniana induced by calcium phosphate precipitates. Bioresource technology, 286, 121352.

[6] Cheng, Y. S., Zheng, Y., Labavitch, J. M., & VanderGheynst, J. S. (2011). The impact of cell wall carbohydrate composition on the chitosan flocculation of Chlorella. Process Biochemistry, 46(10), 1927-1933.

[7] Gerulová, K., Bartošová, A., Blinová, L., Bártová, K., Dománková, M., Garaiová, Z., & Palcut, M. (2018). Magnetic Fe_3O_4-polyethyleneimine nanocomposites for efficient harvesting of Chlorella zofingiensis, Chlorella vulgaris, Chlorella sorokiniana, Chlorella ellipsoidea and Botryococcus braunii. Algal research, 33, 165-172.

[8] Toscano, L., Ogden, K. L., Ogden, G., Cervantes, L., Steichen, S. A., Brown, C., ... & Brown, J. K. (2018). Harvesting the Microalga Chlorella sorokiniana by Fungal-Assisted Pelletization. Journal of Biobased Materials and Bioenergy, 12(6), 493-505.

[9] Zhang, X., Jiang, Z., Li, M., Zhang, X., Wang, G., Chou, A., ... & Zuo, Y. Y. (2014). Rapid spectrophotometric method for determining surface free energy of microalgal cells. Analytical chemistry, 86(17), 8751-8756.

[10] Miranda, A. A., Shaikh, S. M., Sarode, P. R., & Desai, P. V. (2012). Carbon Nanoparticle Toxicity to marine algae Navicula longa and Isochrysis galbana.

[11] Darienko, T., Gustavs, L., Eggert, A., Wolf, W., & Pröschold, T. (2015). Evaluating the species boundaries of green microalgae (Coccomyxa, Trebouxiophyceae, Chlorophyta) using integrative taxonomy and DNA barcoding with further implications for the species identification in environmental samples. PloS one, 10(6).

[12] Maltsev, Y., Maltseva, I., Maltseva, S., Kociolek, J. P., & Kulikovskiy, M. (2019). Fatty acid content and profile of the novel strain of Coccomyxa elongata (Trebouxiophyceae, Chlorophyta) cultivated at reduced nitrogen and phosphorus concentrations. Journal of phycology, 55(5), 1154-1165.

[13] Allen, J. W., DiRusso, C. C., & Black, P. N. (2015). Triacylglycerol synthesis

during nitrogen stress involves the prokaryotic lipid synthesis pathway and acyl chain remodeling in the microalgae Coccomyxa subellipsoidea. Algal Research, 10, 110-120.
[14] Chen, Q., Fan, Q., Zhang, Z., Mei, Y., & Wang, H. (2018). Effective in situ harvest of microalgae with bacterial cellulose produced by Gluconacetobacter xylinus. Algal research, 35, 349-354.
[15] Gerde, J. A., Yao, L., Lio, J., Wen, Z., & Wang, T. (2014). Microalgae flocculation: impact of flocculant type, algae species and cell concentration. Algal research, 3, 30-35.
[16] Delrue, F., Imbert, Y., Fleury, G., Peltier, G., & Sassi, J. F. (2015). Using coagulation–flocculation to harvest Chlamydomonas reinhardtii: coagulant and flocculant efficiencies, and reuse of the liquid phase as growth medium. Algal research, 9, 283-290.
[17] Slaveykova, V. I., Li, M., Worms, I. A., & Liu, W. (2020). When environmental chemistry meets ecotoxicology: Bioavailability of inorganic nanoparticles to phytoplankton. CHIMIA International Journal for Chemistry, 74(3), 115-121.
[18] Prochazkova, G., Safarik, I., & Branyik, T. (2013). Harvesting microalgae with microwave synthesized magnetic microparticles. Bioresource technology, 130, 472-477.
[19] Kurniawati, H. A., Ismadji, S., & Liu, J. C. (2014). Microalgae harvesting by flotation using natural saponin and chitosan. Bioresource technology, 166, 429-434.
[20] Fayad, N., Yehya, T., Audonnet, F., & Vial, C. (2017). Harvesting of microalgae Chlorella vulgaris using electro-coagulation-flocculation in the batch mode. Algal research, 25, 1-11.
[21] Gojkovic, Z., Shchukarev, A., Ramstedt, M., & Funk, C. (2020). Cryogenic X-ray photoelectron spectroscopy determines surface composition of algal cells and gives insights into their spontaneous sedimentation. Algal Research, 47, 101836.
[22] Roy, M., & Mohanty, K. (2020). Valorization of waste eggshell-derived bioflocculant for harvesting T. obliquus: Process optimization, kinetic studies and recyclability of the spent medium for circular bioeconomy. Bioresource Technology, 123205.
[23] Jung, J. Y., Lee, H., Shin, W. S., Sung, M. G., Kwon, J. H., & Yang, J. W. (2015). Utilization of seawater for cost-effective cultivation and harvesting of Scenedesmus obliquus. Bioprocess and biosystems engineering, 38(3), 449-455.
[24] Grassi, G., Gabellieri, E., Cioni, P., Paccagnini, E., Faleri, C., Lupetti, P., ... & Morelli, E. (2020). Interplay between extracellular polymeric substances (EPS) from a marine diatom and model nanoplastic through eco-corona formation. Science of The Total Environment, 138457.
[25] Tanaka, T., Yabuuchi, T., Maeda, Y., Nojima, D., Matsumoto, M., & Yoshino, T. (2017). Production of eicosapentaenoic acid by high cell density cultivation of the marine oleaginous diatom Fistulifera solaris. Bioresource technology, 245, 567-572.
[26] Cvjetinovic, J., Salimon, A. I., Novoselova, M. V., Sapozhnikov, P. V., Shirshin,

E. A., Yashchenok, A. M., ... & Gorin, D. A. (2020). Photoacoustic and Fluorescence Lifetime Imaging of Diatoms. Photoacoustics, 100171.
[27] Liang, Y., Maeda, Y., Yoshino, T., Matsumoto, M., & Tanaka, T. (2014). Profiling of fatty acid methyl esters from the oleaginous diatom Fistulifera sp. strain JPCC DA0580 under nutrition-sufficient and-deficient conditions. Journal of applied phycology, 26(6), 2295-2302.
[28] Matsumoto, M., Sugiyama, H., Maeda, Y., Sato, R., Tanaka, T., & Matsunaga, T. (2010). Marine diatom, Navicula sp. strain JPCC DA0580 and marine green alga, Chlorella sp. strain NKG400014 as potential sources for biodiesel production. Applied biochemistry and biotechnology, 161(1-8), 483-490.
[29] Kätkä, K. (2013). Laboratory Testing Methods for Centrifugal Sludge Dewatering Processes.
[30] Wang, H. F., Wang, H. J., Hu, H., & Zeng, R. J. (2017). Applying rheological analysis to understand the mechanism of polyacrylamide (PAM) conditioning for sewage sludge dewatering. RSC advances, 7(48), 30274-30282.
[31] Zhang, Y. (2017). Evaluating the dewaterability of waste activated sludge via iron dosing and forward osmosis membrane filtration.
[32] Cole, A. I., & Singer, P. C. (1985). Conditioning of anaerobically digested sludge. Journal of Environmental Engineering, 111(4), 501-510.
[33] Yuan, H. P., Cheng, X. B., Chen, S. P., Zhu, N. W., & Zhou, Z. Y. (2011). New sludge pretreatment method to improve dewaterability of waste activated sludge. Bioresource technology, 102(10), 5659-5664.
[34] Zhao, S., & Gao, B. (2016). Application of Enteromorpha as a new kind of coagulant aid in municipal sludge treatment. Desalination and Water Treatment, 57(17), 7988-7998.
[35] Kurade, M. B., Murugesan, K., Selvam, A., Yu, S. M., & Wong, J. W. (2016). Sludge conditioning using biogenic flocculant produced by Acidithiobacillus ferrooxidans for enhancement in dewaterability. Bioresource technology, 217, 179-185.
[36] Bi, D., Guo, X., Cai, Z., Yu, Z., Wang, D., & Wang, Y. (2015). Enhanced dewaterability of waste-activated sludge by combined cationic polyacrylamide and magnetic field pretreatment. Environmental technology, 36(4), 455-462.
[37] Chen, Q., & Wang, Y. (2015). Influence of single-and dual-flocculant conditioning on the geometric morphology and internal structure of activated sludge. Powder technology, 270, 1-9.
[38] Kurade, M. B., Murugesan, K., Selvam, A., Yu, S. M., & Wong, J. W. (2014). Ferric biogenic flocculant produced by Acidithiobacillus ferrooxidans enable rapid dewaterability of municipal sewage sludge: a comparison with commercial cationic polymer. International Biodeterioration & Biodegradation, 96, 105-111.
[39] Fu, J., & Cai, W. (2007). Application of a well-designed cationic polyelectrolyte for activated sludge dewatering. Journal of Chemical Engineering of Japan, 40(12), 1113-1120.
[40] Feng, J., Wang, Y. L., & Yang, M. L. (2011). Impacts of flocculation conditioning on dewaterability and physicochemical properties of anaerobic digested sludge

(ADS) flocs. Acta Scientiae Circumstantiae, 31(7), 1421-1430.
[41] Lau, S. W., Sen, T. K., Chua, H. B., & Ang, H. M. (2017). Conditioning of synthetic sludge and anaerobically digested sludge using chitosan, organic polyelectrolytes and inorganic metal cations to enhance sludge dewaterability. Water, Air, & Soil Pollution, 228(9), 358.
[42] Dong, Y. J., Wang, Y. L., & Feng, J. (2011). Rheological and fractal characteristics of unconditioned and conditioned water treatment residuals. Water research, 45(13), 3871-3882.
[43] Mu, D. & Xu, H. & Xiao, Feng & Wang, D. & Duan, J.. (2016). Effects of conditionings on sludge dewaterability for water treatment residuals. 10. 5447-5452. 10.12030/j.cjee.201505138.
[44] Mamais, D., Tzimas, A., Efthimiadou, A., Kissandrakis, J., & Andreadakis, A. (2009). Evaluation of different sludge mechanical dewatering technologies. Journal of Residuals Science and Technology, 6(1), 27-34.
[45] Chuan-jun, Z. . (2013). Study on Pre-treatment Technology of Urban Sludge Anaerobic Digestion. (02), 59-62.
[46] Li, Y. Y.; He, W. L.; Deng, B.; Li, B. Study on the Conditioning of Sludge by Using Ultrasonic Combined with Macromolecule Flocculants. Ind. Water Treat. 2015, 35, 57–60.
[47] Liu L R, Lou Y Q, Peng L S, et al. Study on screening and optimization of municipal sludge deep dewatering conditioners[J]. Environmental Engineering, 2014,(S1):65-69.
[48] WANG Wei,LIU Xing.The Selection of Sludge Dewatering Agent Used in Municipal Wastewater Treatment Plant[J].GuangZhou Chemical Industry and Technology,2011,39(23):119-121.
[49] Meng W J, Li J, Zhang J H, et al. Chemical conditioning of municipal sludge based on enhanced dewatering by plate-frame pressure filtration [J]. China Water & Wastewater, 215,31(9).
[50] CHEN Jing, CHEN Shicai, Xu Jianhua, Wang Jin, Hong Juemin, Pretreatment of sludge from water treatment plant using polyacrylamide. China Water & Wastewater 2004, 20(9): 37-39.
[51] Li Jing, Hu Wenrong, Pei Haiyan, Application of the flocculant, chitosan, to the treatment of citric acid wastewater sludge[J];Industrial Water Treatment;2008-08.
[52] Dun, M.-N & Hu, W.-R & Pei, H.-Y & Li, J.. (2009). Application of chitosan in conditioning of activated sludge and digested sludge. Wuhan Ligong Daxue Xuebao/Journal of Wuhan University of Technology. 31. 86-91. 10.3963/j.issn.1671-4431.2009.06.022.
[53] LI Yuying , DENG Bin , WANG Junchao.Experiment on sludge conditioning by using cationic guar gum and PAM[J].Chemical Industry and Engineering Progress,2013(9):2253-2257.
[54] Wu, C. C., Huang, C., & Lee, D. J. (1997). Effects of polymer dosage on alum sludge dewatering characteristics and physical properties. Colloids and Surfaces A: Physicochemical and Engineering Aspects, 122(1-3), 89-96.
[55] Novak, J. T., Prendeville, J. F., & Sherrard, J. H. (1988). Mixing intensity and

polymer performance in sludge dewatering. Journal of Environmental Engineering, 114(1), 190-198.
[56] Yan, W. L., Wang, Y. L., & Chen, Y. J. (2013). Effect of conditioning by PAM polymers with different charges on the structural and characteristic evolutions of water treatment residuals. Water research, 47(17), 6445-6456.
[57] Wang, N., Zhang, W., Cao, B., Yang, P., Cui, F., & Wang, D. (2018). Advanced anaerobic digested sludge dewaterability enhancement using sludge based activated carbon (SBAC) in combination with organic polymers. Chemical Engineering Journal, 350, 660-672.
[58] Jin, H., Cho, J., Okayama, T., & Li, J. (2014). Optimum Amount of Addition of the Polymer Flocculant in Papermaking Wastewater Treatment. SEN-I GAKKAISHI, 70(5), 96-99.

Acknowledgments

It has been almost 4 years since I first came to Japan. Time flied, the day when I first arrived at Kansai airport seem to be yesterday. The day was also slow, I cannot wait for a sunrise. The future will definitely come to be past, but the past will be eternal. So, where to start. Sometimes, I discovered names one by one in experimental notebook, folder of PC, pictures, diary or just one paper in the drawer. Some are the classmates still in the lab, some of them has graduated, some of them I heard their name but never meet, some of them I don't know who they are. I wonder if a situation will come to be true, maybe 10 years, maybe 50 years or even 100 years later, someone may discover my trace with same consideration. Even though I always persuade myself the having been existed should be perpetual, I still eager to have more time for interacting with the world. The four years is not a short period of time, I meted peoples who I should meet or met adventitiously, of course I missed someone unexpectedly. Things happens day by day with one by one, trivial but impressive. I'm grateful to the peoples and things, no matter bringing positive or negative substance for me with my remaining precious.

Professor Takaoka is my supervisor. Thank you for accepting me into Takaoka Laboratory, and I really enjoyed those days in the Lab. Thank you for giving this chance and supporting my PhD research. It's still impressive that you went to the hospital to visit me. May the joy and happiness around you today and always.

I meted Professor Oshita 4 years ago, and thank you for guiding and helping me a lot. I think you spent a lot of time to support my study and revise my paper. Professor Oshita is usually very busy, so we have to discuss at weekend even at evening sometimes. So, I hope you can rest more. I remember I received New year postcard from you, which is the best souvenir for me. You taught me a lot, and thank for everything you did for me. I sincerely wish you happiness, cheerfulness and success.

I also like to thank Professor Fujimori and Professor Kusakabe. Thank you for your help. And Mr. Shiota also help me a lot especially on my experiments with instrument operation. Thank you so much. I'd like to express my sincerely thanks to secretaries of our laboratory Mrs. Osawa and Mrs. Yamamoto. I hope we would meet again after my graduation. Wish you good luck and good health.

Thank METAWATER company and their staffs. Thank you for providing me with the internship opportunity. Thank J-POWER company for supplying two microalgae.

Thank you, my colleagues and my friends. We play games together. We go shopping together. We barbecue together. We have dinner together. Together we learn and grow, together we enjoy the life, and together we can reach our goals. You brought me joy. I would like to express my hope for happiness and good future. Good luck and great success in your coming days.

Next, I want to thank my family. Thank you for your support to my whole life.

Finally, I would like to thank the Japanese and Chinese governments for providing the scholarship to support my doctoral course.

Kyoto city has left me many good memories. Uji Bridge, Daikichiyama observation deck, Arashiyama, Katsura river, these places where I often walk. Thank you.